THE DEVELOPMENT OF CHEMICALLY MODIFIED ELECTRODES

FOR ELECTROCATALYSIS

by

Josef Emilio Przeworski (B.Sc., A.R.C.S.)

A thesis submitted for the degree of Doctor of
Philosophy of the University of London and for
the Diploma of Membership of Imperial College

Department of Chemistry
Imperial College
London SW7 2AY

October 1984

ABSTRACT

Chemically modified electrodes are electrodes which have been deliberately coated with foreign molecules to give some specific functionality to the electrode surface. Their use in electrocatalysis is achieved by redox centres immobilised within the coat which can react with solution species and be regenerated by the electrode, thus leading to mediated electron transfer.

To date, the majority of redox centres incorporated in electrode coats have been one-electron couples. This means that their use as electrocatalysts in organic reactions will result in the formation of radical species which will initiate many reactions besides that intended. Therefore, described in this thesis is work on the development of chemically modified electrodes containing two-electron couples. The palladium (II/0) and nickel (II/0) couples are of main interest due to their wide use in catalysis of organic reactions.

There is a general introduction to the field of chemically modified electrodes and to catalysis by palladium and nickel complexes. After this, theories and experimental techniques used are discussed. Included are descriptions of the theories developed for the analysis of modified electrodes and the techniques needed for rigorous non-aqueous electrochemistry.

Palladium and nickel complexes are electrochemically investigated in solution with most analysis being done on phosphine complexes of both the two and zero oxidation states. These metals are then incorporated into synthesised styrene based polymers containing complexing isocyanide or phosphine ligands. Coats of these polymers, with and without the metal species, are examined electrochemically and for catalysis. After the need for a conducting polymer backbone is introduced, conducting polymer films of pyrrole, furan and thiophene are investigated. These

films are formed by the electropolymerisation of the monomeric species
through the two and five positions. The development of phosphine
derivatives of these monomers, their attempted electropolymerisation
and metal incorporation is described.

ACKNOWLEDGEMENTS

To my parents

CONTENTS

FIGURES

TABLES

1. INTRODUCTION

1.1. Chemically Modified Electrodes

A chemically modified electrode is an electrode which has been deliberately coated with a stable film. A chemical is immobilised on the electrode surface so that the electrode displays the chemical, electrochemical, optical and other properties of the immobilised species. In the literature these types of electrode are referred to as chemically modified, derivatised, functionalised, electrostatically trapped or polymer coated.

The most interesting of immobilised chemicals are those which are electrochemically reactive and hence, directly or indirectly, exchange electrons with the electrode surface leading to oxidation/reduction of the species. These coats can be designed to catalyse or block specific reactions giving high selectivity and sensitivity to the electrode surface.

Modified electrodes for electrocatalysis result from the immobilised redox couple, rather than the electrode, reacting with solution species and then being regenerated by the electrode, leading to 'mediated' electron transfer (see figure 1.1). This is a process which first involves electron transfer between the conductor and the modifier. Then, reaction between the modifier and the solution species can take place, either at the surface of the modifying film, or inside the film in which reactant, as well as electrons, move between modifier and solution. Therefore, the rate can be limited not only by the electrocatalytic reaction but also by the diffusion of solution species or by the propagation of electrons, through the film.

Electrode   Coating   Electrolyte
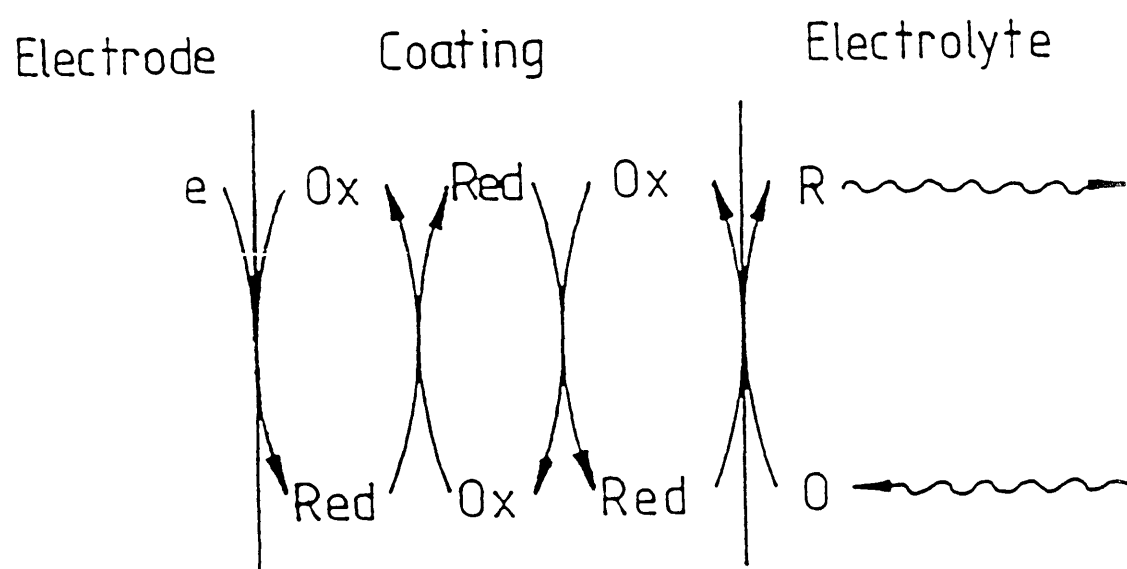
Figure 1.1. Mediated electron transfer in a modified electrode.

1.1.1. <u>History</u>

This area of research was started in 1973 with the publication
of work by Lane and Hubbard[1,2] on the chemisorption of olefins on
platinum electrode surfaces. Chelates connected to the electrode surface,
through an olefinic side chain, allowed the selective, irreversible
adsorption of metals at the electrode surface. However, the first
synthesised electrode coat, leading to the term chemically modified
electrodes, was designed by Murray and co-workers[3] in 1975. This was
the covalent attachment of several ligands (amine, pyridine and ethylene-
diamine) on tin oxide electrodes via organosilane linkages. At the same
time Miller and co-workers[4] covalently bonded an amino acid to a
graphite electrode to give a 'chiral' electrode.

Work on modified electrodes rapidly accelerated in the late seventies.
Many reviews have been published including those by Heineman and Kissinger[5],
Snell and Keenan[6], Murray[7], Diaz[8] and Albery and Hillman[9]; the
most recent is by Murray[10] and contains 363 references.

Most of the early publications are on methods of coating the electrodes
and characterisation of the films formed. More recently, there has been
greater emphasis on designing electrodes for specific applications and in
understanding the complex kinetics of the electron transfer processes in
the coat.

1.1.2. <u>Preparation</u>

Methods of coating electrodes have become quite diverse. Originally
[1,2], species were chemisorbed but these coats were not stable or repro-
ducible. Another early method used was covalent bonding of species to
metal oxides via organosilane linkages[3,8,11]. Direct covalent bonding
to pyrolytic graphite electrodes of dihydroquinone[12], 4-aminomethyl-
pyridine[13,14] and other compounds[15,16] was also developed. However,

these methods required delicate surface synthesis in very dry conditions, gave only monolayer coverages, and although the resulting electrodes were durable they tended to retard reaction rates of solution reactants. Due to these reasons the above methods have been superseded.

Species can be adsorbed on electrode surfaces by dipping the electrode in a required coating solution (dip coating), by dropping a small amount of solution on the electrode and allowing the solvent to evaporate (drop coating) or by dropping a small amount of solution on a rapidly spinning electrode (spin coating). The coat is held on the electrode surface by a combination of chemisorption and low solubility in the contacting solution. These methods are used for polymer[17-21] and porphyrin/ phthalocyanine[22-25] films, resulting in multilayers, up to ca. 10^5 monolayer equivalents, on the electrode. The disadvantages of these methods are the lack of precise control over the number of layers coated and that the resulting coats are relatively uneven.

Polymer coats can also be formed by the electrode initiating polymerisation of solution monomers which then grow polymeric films on the electrode. For this method to succeed the polymer formed has to be conducting as otherwise electrode passivation occurs and film growth is halted. Monomers such as anilines[26], pyrrole[27], thiophene[28] and furan[29] have been used. This method gives the most control over coverage and produces very even films.

Finally, plasma discharge polymerisation has been used to grow polymeric films on electrodes by radical initiation[30,31]. However, this method requires sophisticated equipment.

1.1.3. Characterisation

Characterisation of coats has been by electrochemical and spectroscopic techniques. The main electrochemical technique used is cyclic

voltammetry, which is discussed in chapter 2, though chronoamperometry and chronocoulometry[32] have also been used. Differential pulse voltammetry[22,33] and AC voltammetry[34] have been applied to coats of monolayer, or less, coverage.

Development of spectroscopic analysis has been comprehensive with scanning electron microscopy[21,26,35], absorption spectroscopy[36,37], secondary ion mass spectroscopy[38,39], multiple reflection infrared[40,41], laser Raman[42,43], X-ray photoelectron spectroscopy[44,45], electron spin resonance spectroscopy[101,102] and Auger[46,103] being applied to modified electrodes.

1.1.4. Applications

Applications of modified electrodes are increasing in number as novel coats are developed. Electrocatalysis, by redox species, is the main area of interest. However, their investigation for protecting semiconductor electrodes[47-49], making photoactive electrodes for photogalvanics[50,51], electrosynthesis of chiral compounds[4,52,53] and biological systems[54-56] is widespread. More recently the development of modified electrodes for electrochromics[57,58] and of bilayer modified electrodes giving semi-conductor like behaviour[59-61] has opened new areas of interest. Also, their application in battery storage systems and as electroanalytical sensors can be envisaged in the near future.

Murray[62], and Zak and Kuwana[63] have written general articles on chemically modified electrodes for electrocatalysis. In electrocatalysis the main area investigated has been O_2 reduction mainly by metallo-porphyrin[64,65] or metallo-phthalocyanine[66,67] coats, though polymeric quinones[68] and polymeric viologens[69,70] have also been used. This includes some interesting work by Collman and co-workers[25,71,72] who synthesised a cofacial metallo-porphyrin which would reduce oxygen to

water. Another large area of interest is the oxidation of NADH[73,74] (the reduced form of nicotinamide adenine dinucleotide) by immobilised biological mediators. This is of interest because the NAD/NADH couple is extensively used by enzymes in biological systems.

The use of chemically modified electrodes for electrocatalysis of organic reactions has been rather limited with only a few examples having been published. The first by Miller and co-workers[20] was the electrocatalytic reduction of organic dihalides by polynitrostyrene coated electrodes. The reaction was carried out on a preparative scale and was quite successful with a turnover of each catalytic centre of about 10^4. A similar reaction was also achieved by Rocklin and Murray[75], and Elliott and Marrese[76] using metallo-porphyrin coated electrodes.

Samuels and Mayer[77] developed a polymer which encapsulated a Ru (IV/II) couple. The Ru (IV) could be used as an oxidant and be regenerated electrochemically. One of the reactions investigated was the oxidation of isopropanol to acetone. However, the polymer lacked long term stability and only small currents were passed even with large reactant concentrations. Isopropanol has also been oxidised to acetone by photo-excited quinone derivatives chemically bound to an electrode[78].

Kinetic models have been developed both by Albery and Hillman[9], and by Andrieux, Dumas-Bouchiat and Savéant[79] for the catalysis of electrochemical reactions at redox polymer modified electrodes. These will be discussed in chapter 2.

As one can see, chemical modification of electrode surfaces has opened new avenues for developments in the field of electrochemistry. Their use in electrocatalysis, combining the advantages of normal homogeneous catalysis and heterogeneous electrocatalysis is exciting, and is the main theme of this thesis.

1.2. Catalysis

Catalysis of organic reactions by transition metal complexes is well known. In some cases the reactions result in the catalysing metal complex changing oxidation state and hence needing to be regenerated. At present this regeneration is normally achieved by other chemical reagents but these could be replaced by an electrode. In homogeneous catalysis the regeneration by electrochemistry would be difficult due to the transport of solution species to the electrode, though electrochemistry has been used to prolong catalytic activity[80]. However, polymer supported catalysts have several advantages (see later) and these could be coated on an electrode. This modified electrode could undergo organic reactions and be regenerated by the electrode, leading to electrocatalysis.

Although many metals perform these redox catalysis reactions, palladium and nickel have been of main interest in this work.

1.2.1. Palladium Complexes

Catalytic reactions involving palladium are extensive[81-83]. These include a number where Pd(II) is reduced to Pd(0). However, due to the relative ease of the reoxidation of Pd(0) catalytic activity can still be maintained. This is applied industrially in the Wacker process by which ethylene is converted into acetaldehyde. In this process Cu(II) is used to regenerate the catalyst leading to a reaction scheme:

$$C_2H_4 + PdCl_2 + H_2O \longrightarrow CH_3CHO + Pd^O + 2\ HCl$$

$$Pd^O + 2\ CuCl_2 \longrightarrow PdCl_2 + 2\ CuCl$$

$$2\ CuCl + 2\ HCl + \tfrac{1}{2}\ O_2 \longrightarrow 2CuCl_2 + H_2O$$
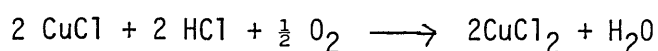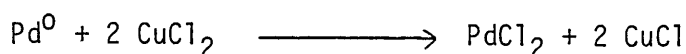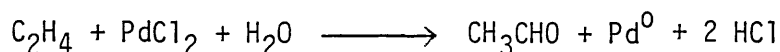
Therefore, the overall reaction is:

$$C_2H_4 + \tfrac{1}{2}O_2 \longrightarrow CH_3CHO$$
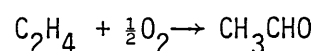
The stereochemistry of this reaction has been of great interest in the literature[84,85] (see figure 1.2).

This is only one of many ethylene reactions catalysed by palladium (II) complexes[86]. In the above reaction, if the solvent is acetic acid one gets vinyl acetate[87,88] and if the solvent is an alcohol[89] then ethers and acetals are produced. Vinyl chloride is produced in very polar solvents[90,91] such as formamide of N-methylacetamide while in less polar solvents, like benzonitrile, oligomerisation occurs.

Another very important series of reactions is the coupling of two hydrocarbons[81]:

$$2RH + PdCl_2 \longrightarrow R\text{-}R + 2HCl + Pd$$
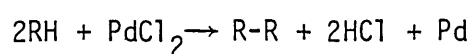
Again Pd(II) can be regenerated by Cu(II). A large number of variations of this reaction are also known. It is similar to the Heck reaction[92,93] which uses organomercury compounds:

$$2ArHgCl + PdCl_2 \longrightarrow Ar\text{-}Ar + 2HgCl_2 + Pd$$
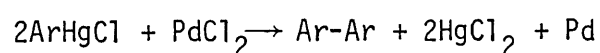
or in the presence of vinyl compounds one gets:

$$PdCl_4^{2-} + C_2H_4 \rightleftharpoons \left[Cl-Pd \begin{matrix} Cl \\ \\ Cl \end{matrix} - \| \begin{matrix} CH_2 \\ CH_2 \end{matrix} \right]^- + Cl^-$$

$$\left[Cl-Pd \begin{matrix} Cl \\ \\ Cl \end{matrix} - \| \begin{matrix} CH_2 \\ CH_2 \end{matrix} \right]^- + H_2O \rightleftharpoons Cl-Pd \begin{matrix} Cl \\ \\ OH_2 \end{matrix} - \| \begin{matrix} CH_2 \\ CH_2 \end{matrix} + Cl^-$$

$$Cl-Pd \begin{matrix} Cl \\ \\ OH_2 \end{matrix} - \| \begin{matrix} CH_2 \\ CH_2 \end{matrix} + H_2O \rightleftharpoons Cl-\overset{-}{Pd} \begin{matrix} Cl \\ \\ OH_2 \end{matrix} -CH_2CH_2\overset{+}{O}H_2$$

$$Cl-\overset{-}{Pd} \begin{matrix} Cl \\ \\ OH_2 \end{matrix} -CH_2CH_2\overset{+}{O}H_2 + H_2O \rightleftharpoons \left[Cl-Pd \begin{matrix} Cl \\ \\ OH_2 \end{matrix} -CH_2CH_2OH \right]^- + H_3O^+$$

$$\left[Cl-Pd \begin{matrix} Cl \\ \\ OH_2 \end{matrix} -CH_2CH_2OH \right]^- \xrightarrow{slow} \begin{matrix} Cl \\ \diagdown \\ H_2O \diagup \end{matrix} Pd-CH_2CH_2OH + Cl^-$$

$$\begin{matrix} Cl \\ \diagdown \\ H_2O \diagup \end{matrix} Pd-CH_2CH_2OH \xrightarrow{fast} H_2O-Pd \begin{matrix} Cl \\ \\ \\ H \end{matrix} - \| \begin{matrix} CHOH \\ \\ CH_2 \end{matrix}$$

$$H_2O-Pd \begin{matrix} Cl \\ \\ \\ H \end{matrix} - \| \begin{matrix} CHOH \\ \\ CH_2 \end{matrix} \longrightarrow CH_3CHO + HCl + Pd^{(0)} + H_2O$$

Figure 1.2(a). The mechanism for the palladium (II) catalysed oxidation of ethylene in water (the Wacker Process).
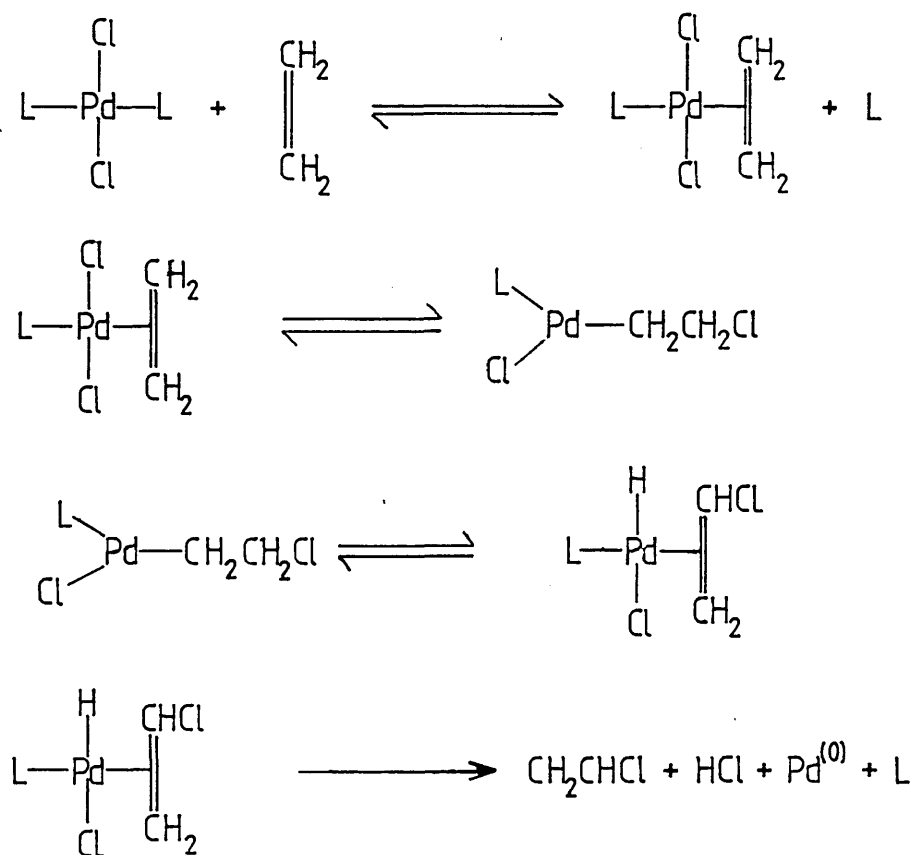
Figure 1.2(b). The mechanism for the palladium (II) catalysed chloride substitution of ethylene, to form vinyl chloride. A non-aqueous variation of the Wacker Process (L = neutral ligand or just solvent).

$$ArHgCl + PdCl_2 \longrightarrow ArPdCl + HgCl_2$$

$$\downarrow +C_2H_4$$

$$ArCH_2CH_2Cl + HgCl_2 + Pd$$

or

$$ArHgCl + PdCl_2 \longrightarrow ArPdCl + HgCl_2$$

$$\downarrow +CH_2 =\!\!=\!\! CHCH(R)OH$$

$$ArCH_2CH_2COR + HgCl_2 + HCl + Pd$$
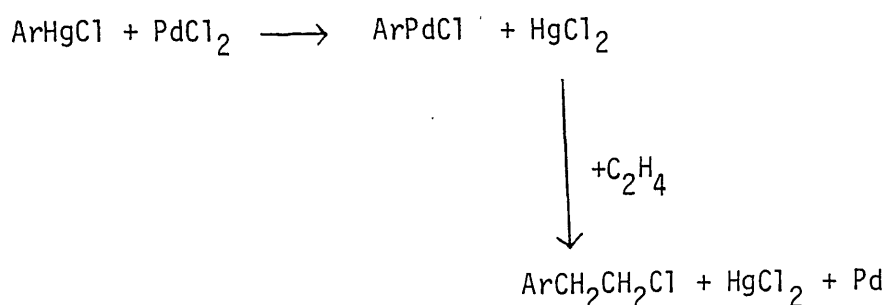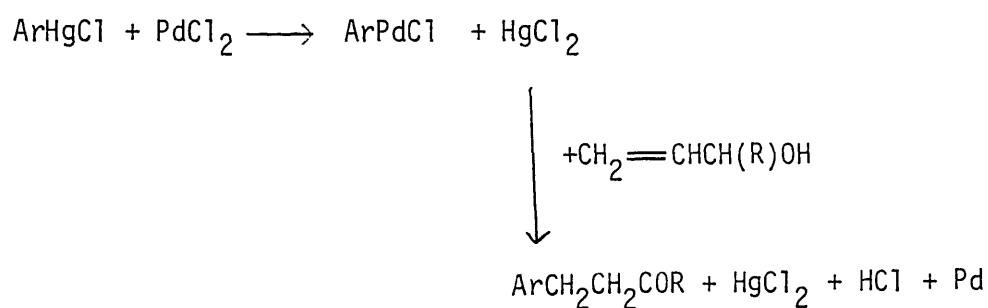
In all the above reactions Pd(II) is reduced to Pd(0) and can be regenerated using Cu(II). Under the right conditions, this reoxidation could be done electrochemically.

1.2.2. Nickel Complexes

Nickel complexes, though not as extensively as palladium, are also used in organic synthesis and some reactions involve changes in oxidation state[94]. The main reaction of interest is the coupling of organic halides in which nickel (0) complexes are used in stoichiometric amounts. This can either be a one step process when coupling like molecules

$$2RX + Ni(0) \longrightarrow R\text{-}R + NiX_2$$
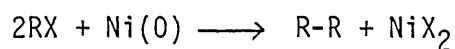
or in two steps when coupling dissimilar molecules

$$RX + Ni(0) \longrightarrow R-Ni-X \xrightarrow{R'X} R-R' + NiX_2$$
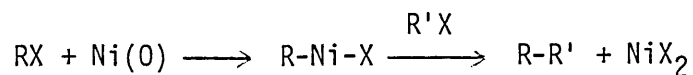
Originally $Ni(CO)_4$ complexes were used but $Ni(PPh_3)_4$ is now preferred as it is less toxic and no carbonylation can occur. This reaction is used for a wide range of R groups including

$$2PhX \longrightarrow Ph-Ph \tag{95}$$

(96)

and

$$2CH_2X_2 \longrightarrow CH_2 = CH_2 \tag{97}$$
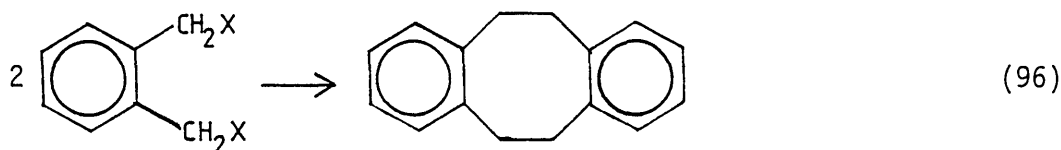
Stoichiometric amounts of the Ni(0) complex are needed in these reactions. However, if coated on an electrode the Ni(0) complex could be regenerated electrochemically leading to electrocatalysis.

Above, known reactions which could be made electrocatalytic by using modified electrodes containing palladium and nickel species have been discussed. However, there is also the possibility of new reactions, not yet envisaged, where intermediate organometallic complexes, formed in a modified electrode coat, could be oxidised or reduced to give a different product than usually observed.

1.2.3. Polymer Supported Catalysts

There has been great interest in polymer supported catalysis with several reviews having been written including those by Gates[98] and Pittman[99] and references therein. Three major classes of polymer supports exist. The first class includes highly cross-linked resin beads of large surface area. The catalyst sits near the surface where it can be wetted by solvent and hence reached by reactants. The second type are lightly cross-linked polymers which swell, allowing diffusion of solvent and reactants into their internal volume. This gives a much higher capacity for catalyst sites. There is no sharp dividing line between these two categories but the third is more definable; that is soluble polymer supports.

It is the second class of lightly cross-linked polymer supports which is of interest to modified electrodes. An example is a polymeric styrene resin with 1-2% divinylbenzene cross-linking agent. This type of polymer support coated on an electrode would be stable and allow diffusion of reactants to, and products away from, the catalytic sites.

The advantages of homogeneous catalysts are high selectivity and high activity, under relatively mild conditions, as every molecule of the catalyst can react. The advantages of heterogeneous catalysts are durability and that they are easily separated from the reaction solution. Polymer supported catalysts combine the advantages of both homogeneous and heterogeneous catalysts while avoiding their disadvantages.

Palladium and nickel complexes have been incorporated into several polymer supports and this will be discussed further in chapter 5. One example is some very interesting work by Arai and Yashiro[100] who used a palladium dichloride polymer supported catalyst for the oxidation of ethylene (see 1.2.1). Also bound to the polymer were quinone groups which were used to regenerate the Pd(II) catalytic species. Thus the general reaction scheme was:

$$PdCl_2 + C_2H_4 + H_2O \longrightarrow Pd^O + 2HCl + CH_3CHO$$
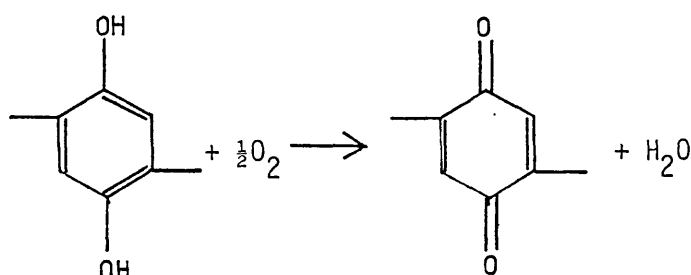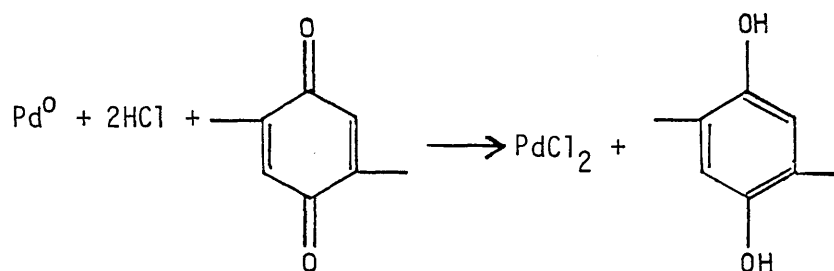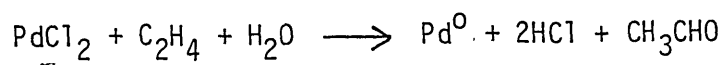
In this scheme the reoxidation of the hydroquinone to quinone was found to be the rate-determining step. With a modified electrode the regeneration of Pd(II) would be electrochemical.

1.3. Organisation and Aim of this Thesis

As discussed earlier (in section 1.1) the use of modified electrodes for electrocatalysis of organic reactions has been rather limited. To prevent the formation of radical species, which would initiate many reactions besides that intended, two electron redox centres should be incorporated in the electrode coat. The palladium (II/0) and nickel (II/0) redox couples are ideal for this as their use in organic reaction catalysis is very extensive (see section 1.2).

Therefore, in this work, the development of electrodes coated with polymers containing mainly the palladium (II/0) or nickel (II/0) redox couples is presented. These metal redox centres are complexed in polymers through phosphine or isocyanide ligands as these bond in both oxidation states.

In this introduction a general appraisal of the ever-widening field of chemically modified electrodes, a description of palladium and nickel

redox catalysis and a discussion of polymer supported catalysis has been given. In chapter 2 the theories for rotating disc and ring-disc electrodes, analysis of current voltage curves, cyclic voltammetry, and for the kinetics of catalysis, by redox centres, at modified electrodes, are given. Also, the derivation of Koutecky-Levich equations for possible pre-equilibria to electrode reactions is presented. Chapter 3 describes the apparatus and techniques used, including purifications of gases, solvents and supporting electrolytes.

Before polymer incorporation of the metal ions, their electrochemistry had to be known. Thus work is presented, in chapter 4, on the synthesis and the solution electrochemistry of metal complexes which are later incorporated into polymers. Also, some catalysis investigations are discussed. Then, in chapter 5, there is a description of the synthesis of various styrene based polymers with their metal incorporation, coating on electrodes (pre- and post-metal incorporation), electrochemistry and use in catalysis being discussed.

In chapter 6, after the need for conducting polymers is introduced, the results of the electropolymerisation of pyrrole, furan and thiophene and the analysis of their coats are given. The synthesis of phosphine derivatives of these monomers, their electrochemistry and metal complexation are described.

To prevent interrupting the flow of this thesis, experimental details of the synthetic work presented has been placed in appendices to each chapter.

2. THEORY

2.1. The Rotating Disc and Rotating Ring-Disc Electrodes

For reproducible electrode kinetic measurements a forced pattern of convection has to be imposed on the solution, giving a time independent diffusion layer of calculable thickness and hence controllable mass transfer. Otherwise, stray convections due to thermal gradients and mechanical shock cause changes in the diffusion layer thickness, thus giving variable results. Several electrode systems have been developed which satisfy this requirement and the rotating disc electrode (RDE) is one of the most popular.

The RDE consists of a disc of the electrode material of interest surrounded by a coplanar insulating mantle (see figure 2.1a). The hydro-dynamics of this system have been defined[104] and the equations solved. The coordinate system and fluid velocity vector components are shown in figure 2.2. It is important to note that the velocity in the z-direction is only dependent on z.

The RDE draws up solution from beneath it and flings it out laterally (see figure 2.3a). The lack of dependence of the velocity in the z-direction on the radial and angular coordinates means that the surface of the disc is uniformly accessible to solution species. Close to the electrode the solution rotates with the disc (see figure 2.3b) resulting in a stagnant layer in which diffusion is the only means of transport. This diffusion layer thickness is of the order of 10^{-5} - 10^{-4} m and is given by

$$Z_D = 0.643 \ W^{-1/2} \ \nu^{1/6} \ D^{1/3} \tag{2.1}$$

Figure 2.1. (a) A rotating disc electrode (RDE);
(b) A rotating ring-disc electrode (RRDE).

Insulating mantle

Electroactive disc (Area~0,4 cm²)

Disc

Insulating gap

Ring

(a)   (b)
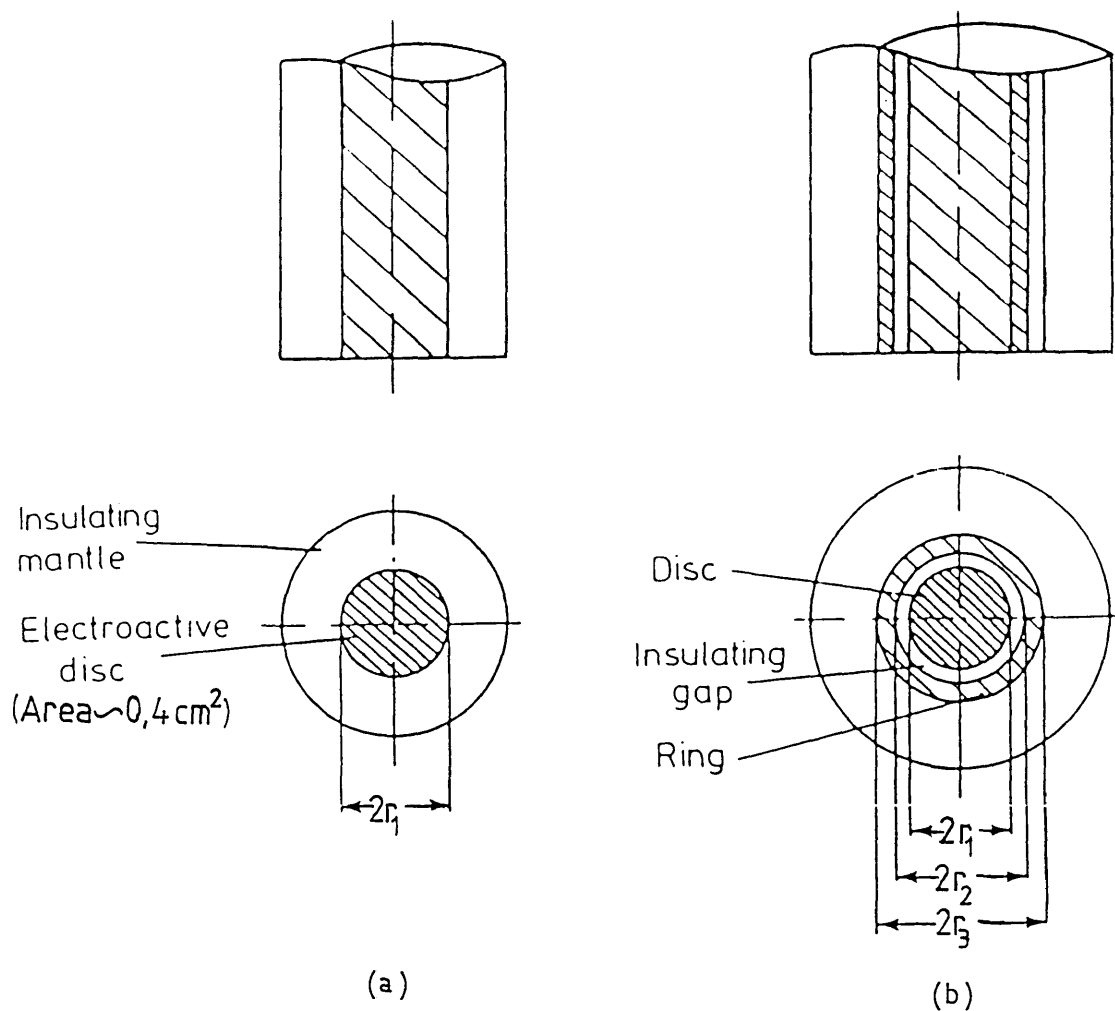
Figure 2.2. Co-ordinate system and fluid velocity vector components for the RDE.
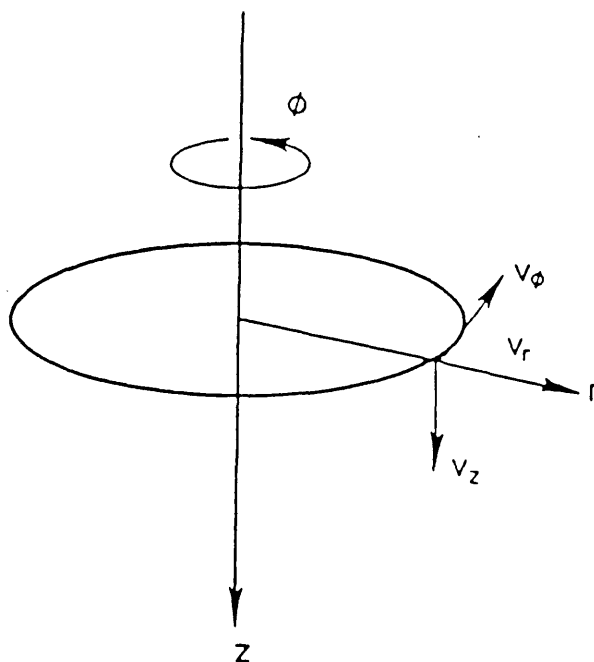
Figure 2.3. Schematic representation of the fluid flow at a RDE.

(a)

(b)
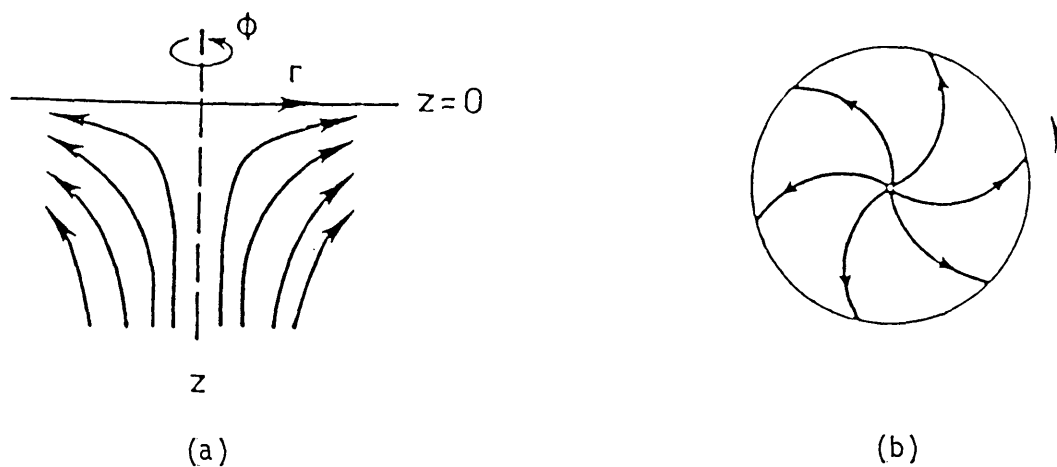
Figure 2.4. Schematic polarogram for the oxidation of an electro-active species at a RDE. Schematic concentration profiles are shown.
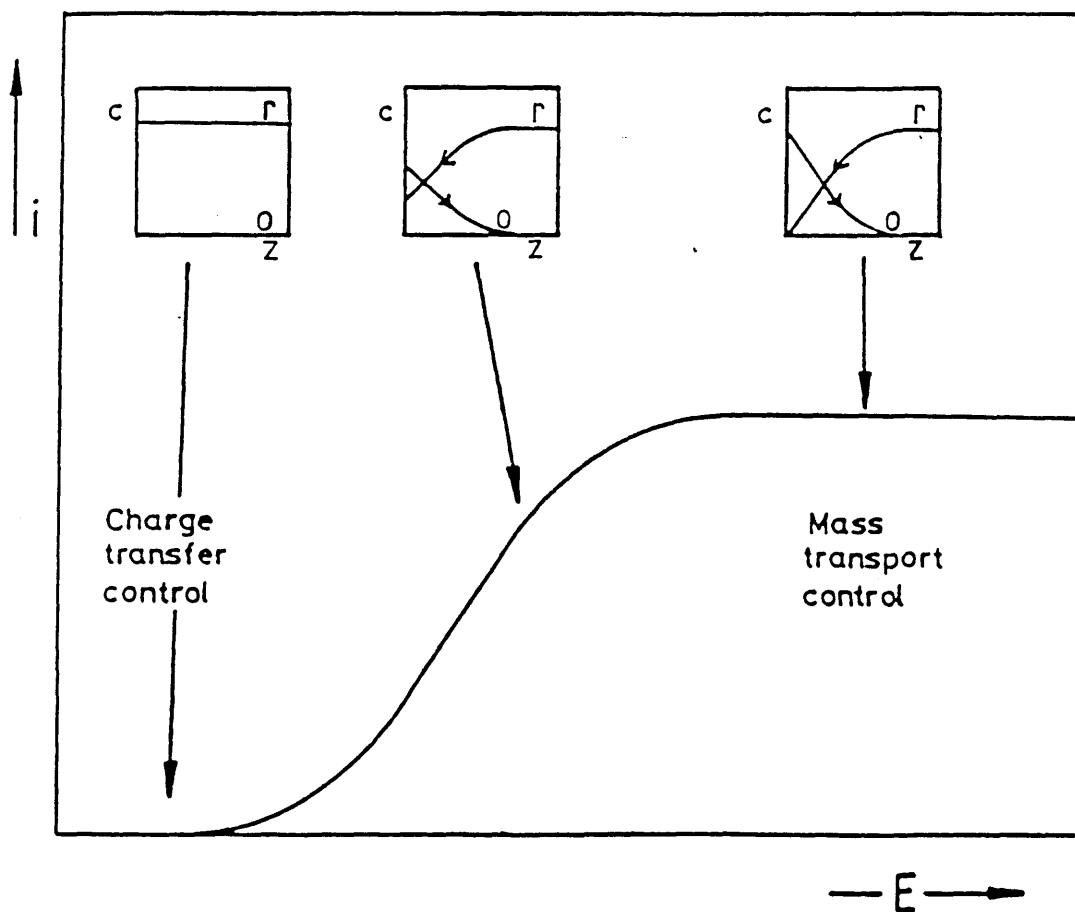
where

Z_D is the diffusion layer thickness (cm),

W is the rotation speed (Hz),

ν is the kinematic viscosity ($cm^2 \; s^{-1}$), and

D is the diffusion coefficient ($cm^2 \; s^{-1}$).

Further out from the electrode convection prevails and the solution is well stirred.

At a RDE as one sweeps the potential the electrode reaction changes from a charge transfer controlled region, where charge transfer is slow and only a small fraction of the species supplied to the electrode react, to a mass transfer controlled region, where every species reaching the electrode reacts (see figure 2.4).

The concentration profile when in the mass transport region is shown in figure 2.5. Under these conditions the limiting current can be given by

$$i_L = nFAc_\infty k_D'$$ (2.2)

where

i_L is the limiting current (A),

n is the number of electrons in the electrode reaction,

F is the Faraday constant ($C \; mol^{-1}$),

A is the area of the electrode (cm^2),

c_∞ is the bulk concentration of the reacting species ($mol \; cm^{-3}$), and

k_D' is the mass transfer rate constant ($cm \; s^{-1}$)
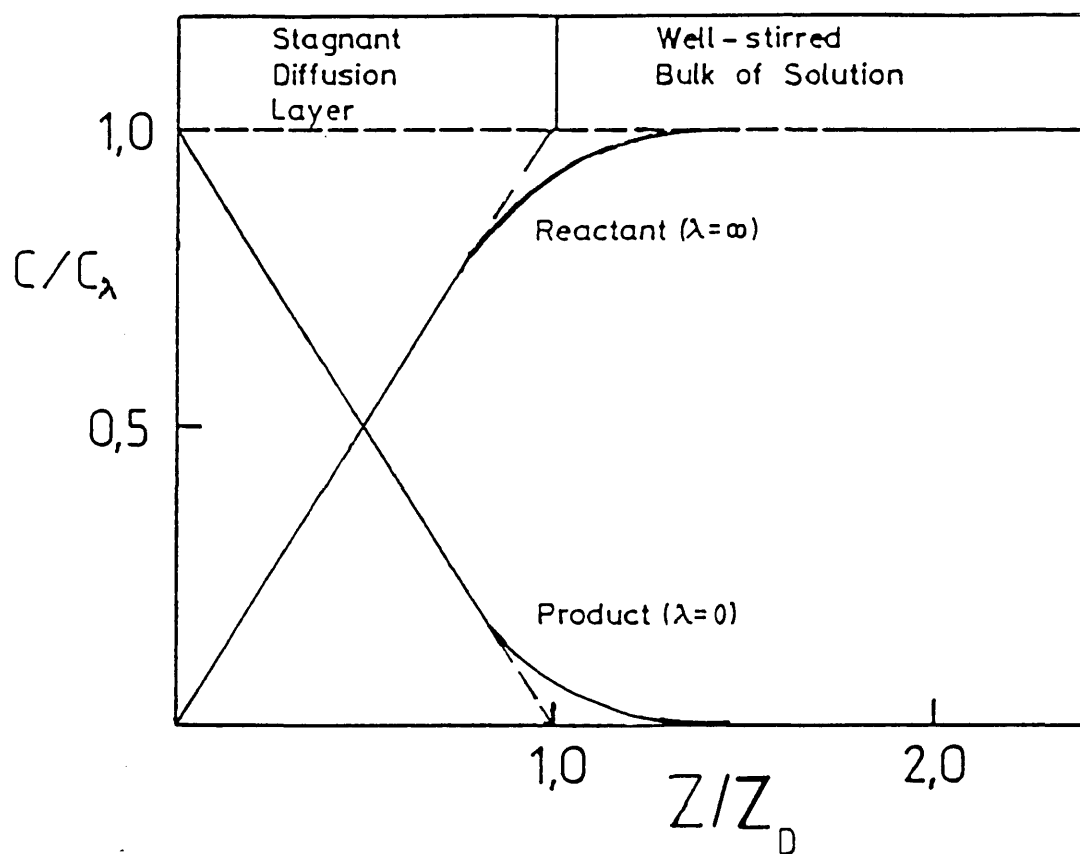
Figure 2.5. Variation of concentration with distance from a RDE, when current is mass transport controlled.

The mass transfer rate constant is given by

$$k_D' = \frac{D}{Z_D} \tag{2.3}$$

Therefore combining equations 2.1, 2.2 and 2.3 the mass transport limiting current is given by

$$i_L = 1.554 \text{ } nFAc_\infty \text{ } D^{2/3} \text{ } \nu^{-1/6} \text{ } W^{1/2} \tag{2.4}$$

Thus, plotting the limiting current versus the square root of the rotation speed (the Levich Plot) gives a straight line through the origin.

However, if there is another step, which is mass transfer independent, near the electrode surface, in series with the transport step, a lower limiting current than the Levich predicted limiting current may be observed. If the additional step is given the rate constant $k_?'$ the overall electrochemical rate (k') is given by

$$\frac{1}{k'} = \frac{1}{k_D'} + \frac{1}{k_?'} \tag{2.5}$$

where the smaller of $k_?'$ and k_D' is rate-determining. This results in the limiting current being given by

$$\frac{nFAc_\infty}{i_L} = \frac{0.643 \; D^{-2/3} \; \nu^{1/6}}{W^{1/2}} + \frac{1}{k'_?} \tag{2.6}$$

Therefore a plot of i_L^{-1} versus $W^{-1/2}$ (the Koutecky-Levich Plot[105]) gives a straight line with an intercept of $(nFAc_\infty k'_?)^{-1}$.

It should be noted that for all the above to apply one must use sufficient excess supporting electrolyte to prevent non-uniform current distribution.

The idea of a concentric ring around the RDE, to give a rotating ring-disc electrode (RRDE), was devised by Frumkin and Nekrasov[106]. This coplanar ring is separated from the disc by an insulating gap (see figure 2.1b). Looking at the flow with a RDE/RRDE (see figure 2.3a) one can see that the ring is ideal as a downstream monitor of the disc electrode reaction. Thus, A is converted to B at the disc electrode and B is then carried downstream to the ring. Then at the ring, B is converted to C, which may or may not be the same as A, in a mass transfer limited manner.

Disc $A \pm ne^- \rightarrow B$
Ring $B \pm me^- \rightarrow C$
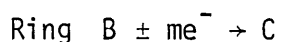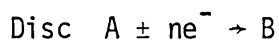
The transport properties of this system can be calculated leading to a mathematical treatment of the ring current[107]. The concentration

profile of B at the electrode is shown in figure 2.6. It should be stressed that the concentration of B at the ring electrode and in the bulk solution is zero. The fraction of B reaching the ring electrode is called the collection efficiency (N_0) and, if C is the same as A, is given by

$$N_0 = \frac{-i_R}{i_D} \qquad (2.7)$$

where

i_R is the ring electrode current, and

i_D is the disc electrode current.

The minus sign is because the same reaction, but in different directions, is occurring at the two electrodes. The collection efficiency, of a RRDE, can be calculated[108,109] as a function of only the three radii (see figure 2.1b) and is independent of the rotation speed[109].

For the majority of redox systems (e.g. Ferri/Ferrocyanide) the calculated collection efficiency and the experimentally found collection efficiency will agree. However, if, for example, product B of the disc reaction is unstable and decomposes, then the experimentally found collection efficiency will be less than the theoretical value. This discrepancy can be used to calculate the rate of decomposition of B.

Wide applications have been developed for the RRDE[107], from the detection of intermediates generated at the disc electrode to the more complex study of transients for the investigation of the mechanism of electrode reactions.
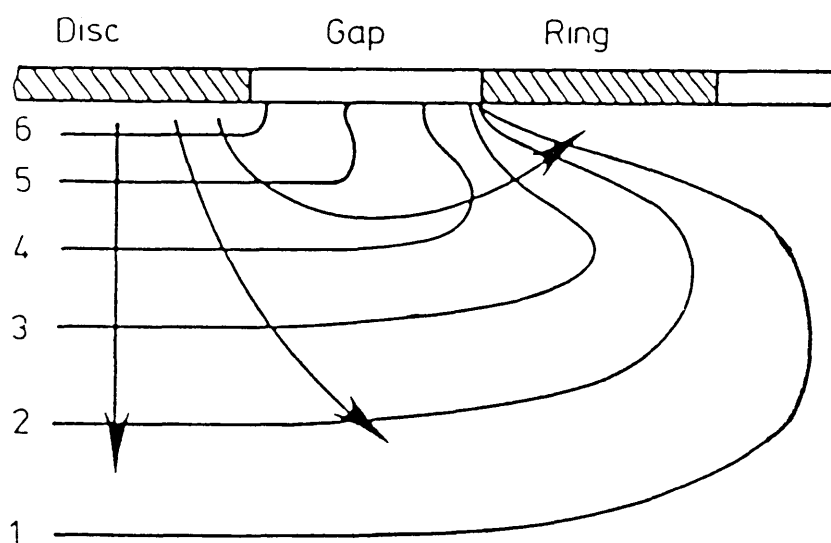
Figure 2.6.   Schematic concentration profile for a
               species (B) generated at the disc and
               destroyed at the ring of a RRDE.

The RDE and RRDE have been used to study many systems including semiconductor electrodes[110,111], transparent electrodes[112,113], perovskite electrodes[114,115] and chemically modified electrodes[54,116].

2.2. Analysis of Current Voltage Curves

In section 2.1 electrochemistry at a rotating disc electrode was introduced and a general current voltage curve for an electrochemical reaction R - ne → O shown in figure 2.4. As discussed earlier, this shows two different regions where current is either charge transfer or mass transfer controlled.

A general expression can be derived[50,133] for current voltage curves for the reaction

$$A + ne^- \; \underset{k'_{-1}}{\overset{k'_1}{\rightleftharpoons}} \; B$$
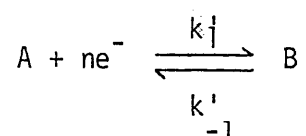
taking into account both the forward and back reactions. In the steady state, the flux, j, is given by

$$j = k'_1 [A]_0 - k'_{-1} [B]_0 \qquad\qquad (2.8)$$

$$= k'_{D,A} ([A]_\infty - [A]_0) \qquad\qquad (2.9)$$

$$= k'_{D,B} ([B]_0 - [B]_\infty) \qquad\qquad (2.10)$$

where

$k'_{D,X}$ is the mass transfer rate constant for species X(X = A or B),

$[X]_\infty$ is the bulk concentration of species X,

and $[X]_0$ is the electrode surface concentration of species X.

For a RDE, from equations 2.1 and 2.3

$$k'_{D,X} = \frac{D_X}{Z_D} = 1.554 \ D_X^{2/3} \ \nu^{-1/6} \ W^{1/2} \tag{2.11}$$

The limiting fluxes of A and B, j_A and j_B, are given by:

$$j_A = k'_{D,A}[A]_\infty \tag{2.12}$$

and

$$j_B = -k'_{D,B}[B]_\infty \tag{2.13}$$

Eliminating the four concentrations in the above equations (2.8 to 2.13) one gets

$$j = \frac{1}{k'_{D,A}} \left[k'_1(j_A - j) - k'_{-1}(j - j_B) \left(\frac{D_A}{D_B} \right)^{2/3} \right] \tag{2.14}$$

The heterogeneous rate constants are given by:

$$k_1' = k_0' \exp\left(-\frac{\alpha(E - E')F}{RT}\right) \tag{2.15}$$

and

$$k_{-1}' = k_0' \exp\left(\frac{(n - \alpha)(E - E')F}{RT}\right) \tag{2.16}$$

where

k_0' is the value of the electrochemical rate constant (k') at

E = E'. As the potential is at the formal electrode

potential the electrochemical rate constant for the

oxidation reaction equals that for the reduction, both

being equal to k_0',

α is the cathodic transfer coefficient,

E is any given electrode potential,

E' is the formal electrode potential, and

n is the number of electrons for the couple.

Substituting equations 2.15 and 2.16 into equation 2.14 and rearranging, one gets

$$\frac{k_{D,A}'}{k_0'}\left(\exp\left(\frac{\alpha(E-E')F}{RT}\right)\right) = \left(\frac{j_A}{j} - 1\right) + \left(\frac{j_B}{j} - 1\right)\left(\frac{D_A}{D_B}\right)^{2/3}\exp\left(\frac{n(E-E')F}{RT}\right) \tag{2.17}$$

Limiting currents are given by:

$$i_0 = nFAj_B \qquad (2.18)$$

and

$$i_R = nFAj_A \qquad (2.19)$$

where it must be remembered that j_A corresponds to a flux of electrons from the electrode to the solution, which means that i_R, the limiting reduction current, will be negative.

i_0 is the limiting oxidation current (positive), and

A is the area of the electrode.

Converting fluxes into currents in equation 2.17 and taking logs, gives the general expression

$$\ln\left(\frac{k'_{D,A}}{k'_0}\right) + \frac{\alpha(E - E')F}{RT} =$$

$$\ln\left[\left(\frac{i_R}{i} - 1\right) + \left(\frac{i_0}{i} - 1\right)\left(\frac{D_A}{D_B}\right)^{2/3} \exp\left(\frac{n(E - E')F}{RT}\right)\right] \qquad (2.20)$$

where

> i is the current at any given potential E (reduction currents
> being negative).

With an irreversible system E must be well removed from E' for a finite current to pass. This means one of the two additive terms, in the logarithm, on the right side of equation 2.20, will dominate. For a reduction E << E' and the left hand term will dominate while for an oxidation E >> E' and the right hand term will dominate. For both cases equation 2.20 simplifies to the usual Tafel equations corrected for mass transport where for a reduction:

$$\ln\left(\frac{i_L}{i} - 1\right) = \ln\left(\frac{k_D'}{k_0'}\right) + \frac{\alpha(E - E')F}{RT} \qquad (2.21a)$$

and for an oxidation:

$$\ln\left(\frac{i_L}{i} - 1\right) = \ln\left(\frac{k_D'}{k_0'}\right) - \frac{\beta(E - E')F}{RT} \qquad (2.21b)$$

where

> i_L is the mass transport limited current, and
>
> α and β are the cathodic and anodic transfer coefficients
> respectively. (As the reaction is irreversible $\alpha + \beta$
> does not have to equal n).

Therefore a plot of $\ln[(i_L/i) - 1]$ vs E will give α or β from the slope and k_0' from the intercept.

For reversible systems $k_0' \gg k_{D,A}'$ thus making the left hand side of equation 2.20 very large and negative. Therefore, the exponential of the right hand side can be equated to zero, giving:

$$\left(\frac{i_R}{i} - 1\right) + \left(\frac{i_0}{i} - 1\right)\left(\frac{D_A}{D_B}\right)^{2/3} \exp \frac{n(E - E')F}{RT} = 0 \qquad (2.22)$$

Thus

$$\ln\left(\frac{i - i_R}{i_0 - i}\right) = \frac{n(E - E')F}{RT} + \frac{2}{3}\ln\left(\frac{D_A}{D_B}\right) \qquad (2.23)$$

One can see that in equation 2.23 the kinetic terms α and k_0' have disappeared as the electrode reaction is very fast and controlled by the thermodynamics. Thus the parameters n and E' can be obtained because the ions, at the electrode surface, are in equilibrium and thus obey the Nernst law. For many systems $D_A \sim D_B$ is a good approximation. Therefore, E = E' when $i - i_R = i_0 - i$, i.e. when $i = \frac{1}{2}(i_0 + i_R)$ which occurs at the half wave potential. Therefore,

$$E' = E_{\frac{1}{2}} \qquad (2.24)$$

is a good approximation.

For quasi-reversible systems the full equation 2.20 has to
be used to analyse the current voltage curves. Here it can be pos-
sible to extract k_o', α and E' though values will be less accurate.

2.3. Cyclic Voltammetry

In this electrochemical technique the potential of a stationary
working electrode is swept in a saw-tooth manner as shown in figure
2.7. The current for any electrochemical oxidations or reductions
is measured for each cycle and plotted with respect to potential.
The increase in the electrochemical rate constant as the potential
is swept and the decrease in the concentration of unreacted species,
at the electrode as the reaction proceeds, leads to a maximum in
the current (peak height) for the electrochemical reaction (see
figure 2.8a).

For solution species this technique is a simple method of
investigating electrode reaction products or intermediates, as any-
thing generated at the stationary electrode is still present during
the rest of the potential cycle, and thus, if electroactive, can be
detected.

For reversible electrochemistry (e.g. Ferro/Ferricyanide, see
figure 2.9) one observes an oxidation and a reduction peak. For
rapid kinetics of the electrode reaction the two peaks are separated by 60mV
at the standard electrode potential (E') but for slower kinetics the
peaks separate. However, the standard electrode potential can still
be obtained from the mean of the two peak potentials ($E_{p,A}$, $E_{p,C}$).

For solution species one observes peak height being proportional
to the square root of sweep rate.
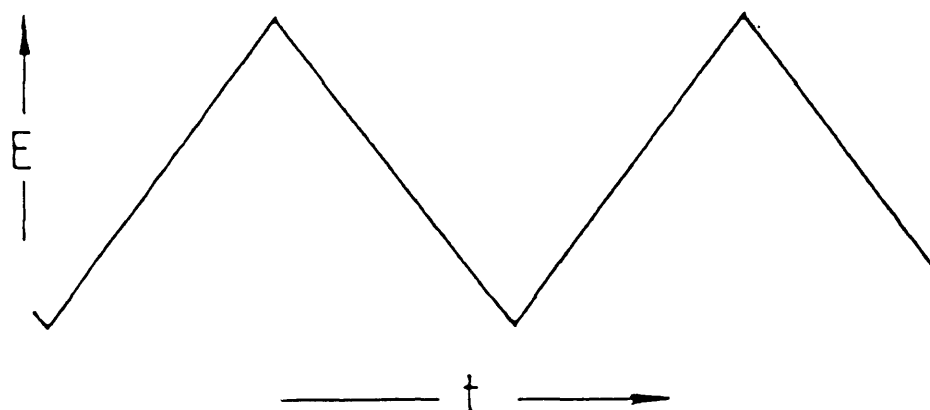
Figure 2.7. Variation of potential with time during cyclic voltammetry.

(a)

$E_{P,A}$

$i_{P,A}$

i

E

E'

$i_p \propto v^{1/2}$

(v = Sweep Rate)

$\left(E_{P,A} - E_{P,C} = 60mV\right)$

$i_{P,C}$

$E_{P,C}$

(b)

$E_{P,A}$

$i_{P,A}$

Q

(Q = Total Charge
Passed)

i

E

E'_{SURF}

$i_p \propto v$

$i_{P,C}$

$E_{P,C}$
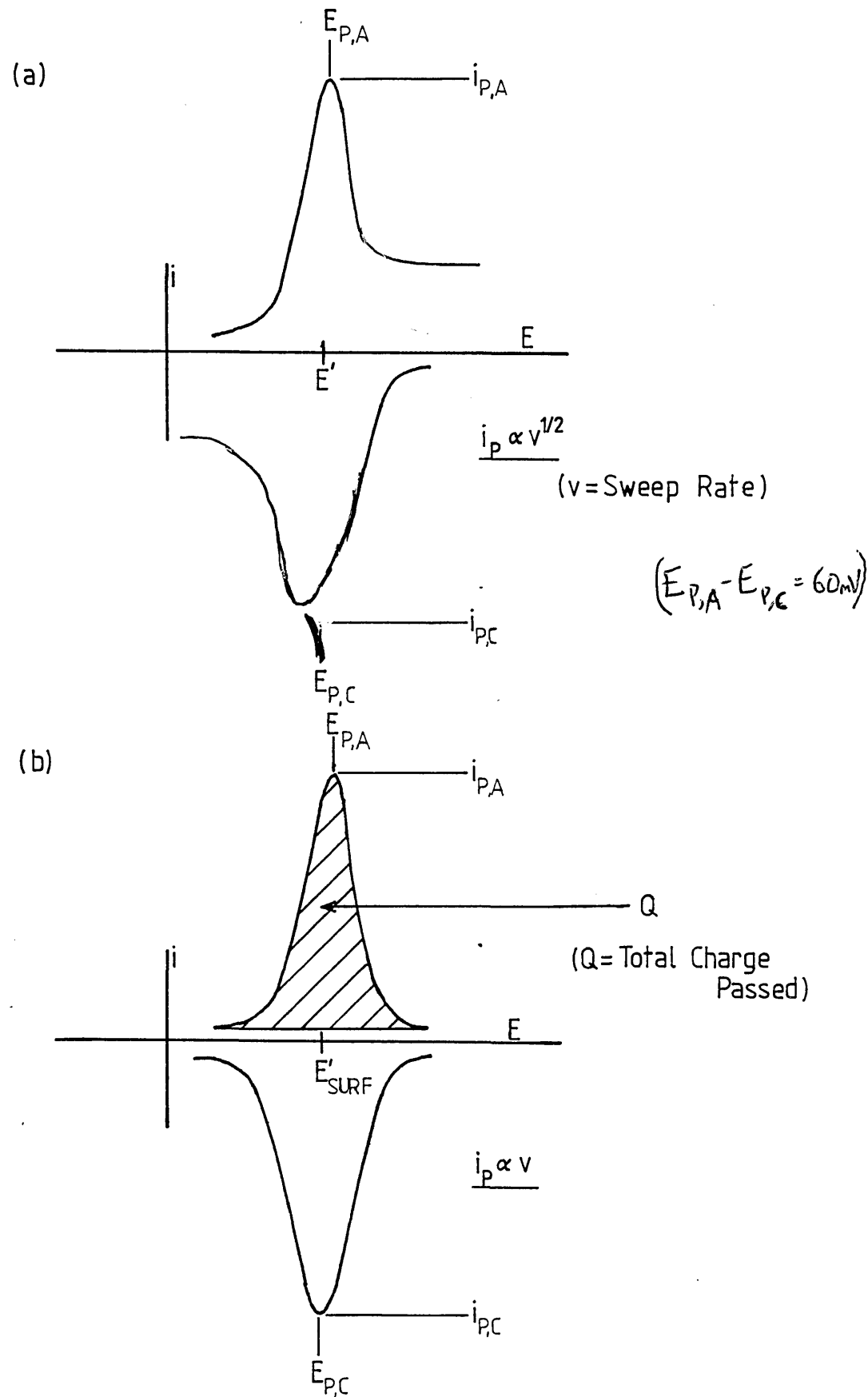
Figure 2.8. Schematic, reversible cyclic voltammograms for (a) solution redox species and (b) redox species coated on an electrode (assuming complete reaction of the coat during each cycle).
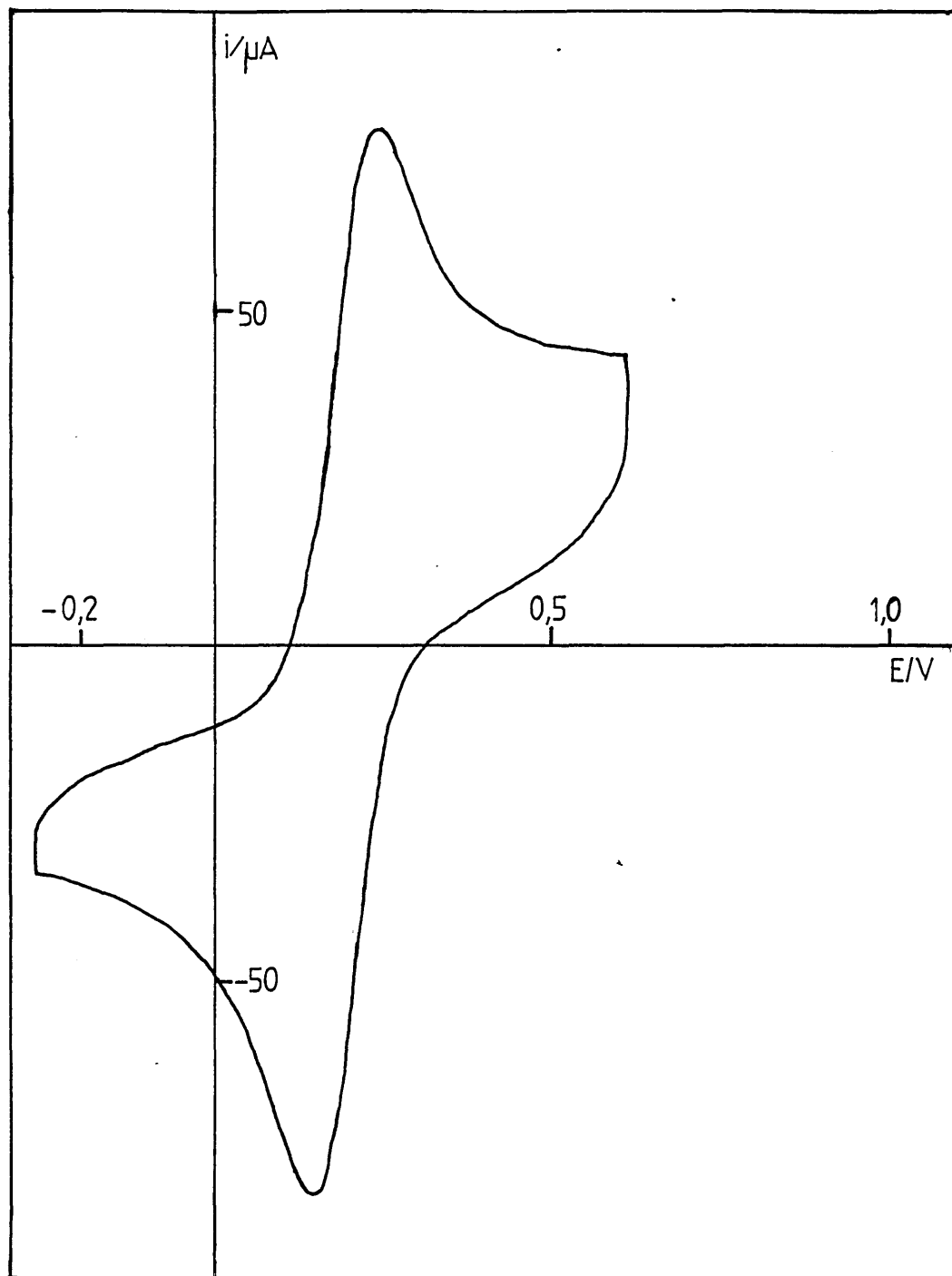
Figure 2.9. Reversible, cyclic voltammogram for the Ferro/Ferricyanide redox couple.

It should be noted that, in cyclic voltammetry of more complicated systems, a wave can sometimes be observed rather than the expected peak. This indicates a constant production of the electroactive species at the electrode. An example of this is a pre-equilibrium

$$A + B \rightleftharpoons C$$
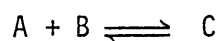
where C is the electroactive species and as it reacts at the electrode, A and B react to produce more C. Therefore the concentration of C does not decrease and the current is limited by the kinetics of the pre-equilibrium reaction. An example of this is observed in section 4.2.2. A theoretical analysis of these types of more complicated systems has been published by Nicholson and Shain[117,118].

For reversible redox centres anchored on an electrode, as in a modified electrode, peaks in current with respect to potential are also observed (see figure 2.8b) as again there is only a fixed amount of electroactive species present to react at the electrode. However, here the peak height varies linearly with sweep rate and the electrode can be stationary or rotating.

The area of the peak gives the total amount of charge necessary to oxidise/reduce the electroactive centres in the coat. Therefore, the total number of electroactive centres can be calculated and, with knowledge of the chemical composition of the coat, its thickness can be estimated (see figure 2.8b).

However, the above assumes the sweep rate is slow enough and the kinetics of charge transfer fast enough for complete reaction of the coat during each cycle. If this is not the case then the kinetics of the charge transfer process become diffusive in nature and the peak height reverts to square root dependence on sweep rate.

As with solution species, simple one electron transfers with rapid kinetics, at these immobilised redox centres, give coincident oxidation and reduction peaks at $E = E'_{SURF}$. However, if the kinetics are slow or the sweep rate too fast then the peaks will separate. In these cases the standard potential E'_{SURF} can be obtained from the average of the peak potentials.

Detailed theoretical analysis for the shape of cyclic voltammograms of different types of modified electrode have been published by Laviron and coworkers[119,120].

Potential step experiments are also used for analysis of modified electrodes and this is discussed in section 2.4.2.

2.4. Theoretical Description of Chemically Modified Electrodes

As discussed in chapter 1, the use of chemically modified electrodes for electrocatalysis is one of the major motivations for the increasing interest in this field. A theoretical description for the behaviour of modified electrodes is necessary to understand the processes present in the coat and to find where the reactions occur. Thus, one can find the rate-limiting processes and design modified electrodes to maximise efficiency.

Some important early theoretical papers were published by Anson[121], Savéant[122] and Murray[62,75]. More recently, two

comprehensive theoretical descriptions have been presented by Andrieux, Dumas-Bouchiat and Savéant[79] and by Albery and Hillman[9]. These present very similar mathematical treatments, though with different notation, and come to conclusions in good agreement. In the discussion below the Albery/Hillman notation is adopted as this seems to give a more logical view.

The processes taking place at a modified electrode, in an electrochemical reaction, are shown in figure 2.10. The redox couple A,B is present throughout the coat and the modified electrode is reducing solution species Y to Z. This reaction can occur at the layer/solution interface with rate constant k" or Y can diffuse into the coat and then the reaction takes place in the layer with rate constant k. Two diffusion processes are important which are the diffusion of electrons (D_e) from the electrode to meet the Y species, and the diffusion of Y (D_Y) in the layer itself.

Using the Albery/Hillman method one introduces an electrochemical rate constant for a modified electrode (k'_{ME}) which relates the flux of electrons at the electrode (j_0) to the concentration of Y in the solution at the layer/solution interface (y_s), i.e.

$$j_0 = k'_{ME} \, y_s \tag{2.25}$$

As stated by many authors[50,75,123], k'_{ME} can be obtained from the intercept of a Koutecky-Levich plot for a rotating disc electrode (see section 2.4.1).
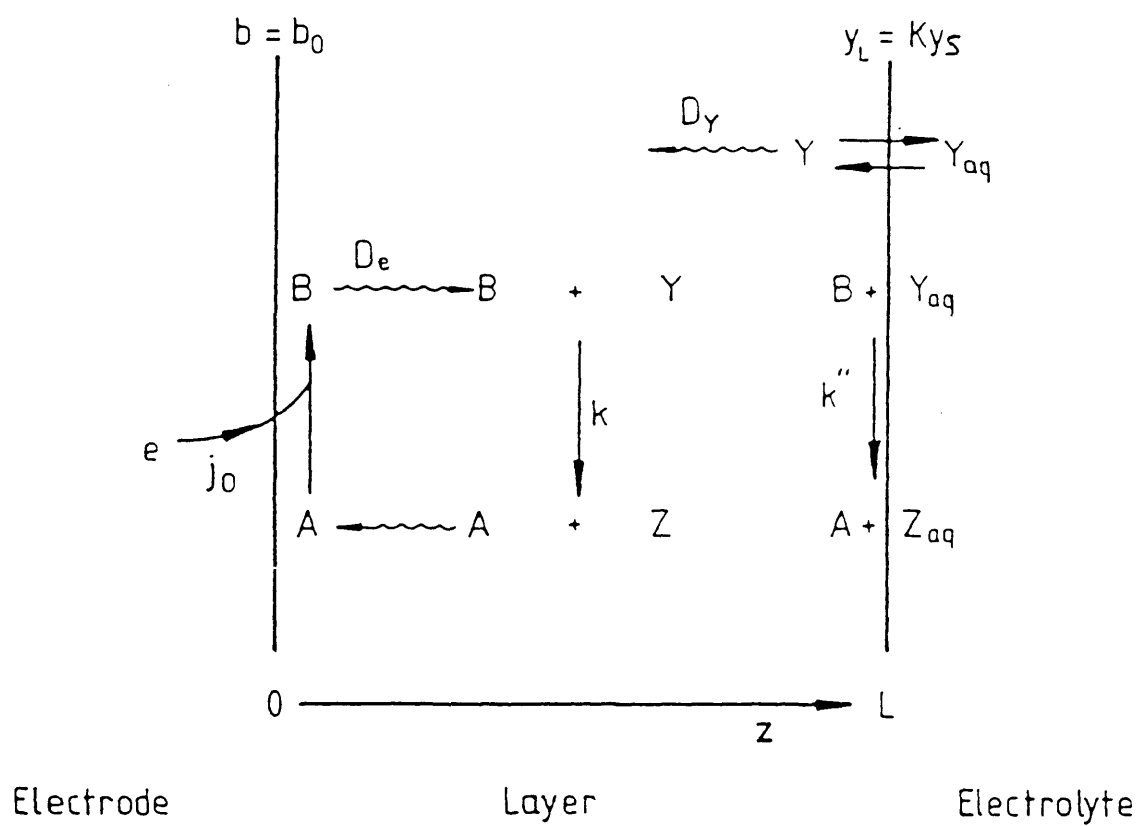
Figure 2.10. General kinetic model for a modified electrode.

Equations describing the transport of charge and the transport and kinetics of Y in the layer can be integrated[9] to give two approximate solutions for k'_{ME} depending on the relative sizes of $D_e b_0$ and $D_Y K y_s$. Here b_0 is the concentration of B at the electrode surface, which is fixed by the potential, and $K y_s$ is the partitioning of Y from the solution into the layer, for which it is assumed there is no kinetic barrier.

The two solutions are:

for $D_e b_0 \gg D_Y K y_s$ (i.e. electrons penetrate across the layer more easily than Y).

then

$$\frac{1}{k'_{ME}} = \frac{y_s L}{D_e b_0} + \frac{1}{k''b_0 + kb_0 K X_L \tanh(L/X_L)} \qquad (2.26)$$

| transport of e across the layer | surface reaction | layer reaction |

and

for $D_e b_0 \ll D_y K y_s$ (i.e. Y penetrates across the layer more easily than electrons).

then

$$\frac{1}{k'_{ME}} = \frac{L}{KD_Y} + \frac{k'' \tanh(L/X_0) + kKX_0}{kKX_0 b_0 [k'' + kKX_0 \tanh(L/X_0)]} \qquad (2.27)$$

<div style="text-align:center">
transport of Y   surface   layer
across the layer   reaction   reaction
</div>

where

    L   is the thickness of the coat,

    X_L is the average distance Y will diffuse in the layer before being destroyed by reaction with B and is given by

$$X_L = (D_Y/kb_L)^{\frac{1}{2}} \qquad (2.28)$$

    where b_L is the concentration of B at the layer/solution interface,

    X_0 is the average distance an electron diffuses before reacting with Y and is given by:

$$X_0 = (D_e/ky_0)^{\frac{1}{2}} \qquad (2.29)$$

    where y_0 is the concentration of Y at the electrode surface, and all other terms have been defined earlier.

There is a third solution for k'_{ME} when

$$D_e b_0 \sim D_Y K y_s$$

where if X_0 or X_L is less than L then the reaction is transport controlled by the supply of electrons, from the electrode, and the supply of Y, from the electrolyte. Here

$$\frac{1}{k'_{ME}} = \frac{L}{D_Y K + D_e b_0/y_s}$$ (2.30)

From the above results five locations of the reaction can be distinguished (see figure 2.11):-

(i)   At the electrolyte/coat interface, labelled S for surface,

(ii)   Throughout the layer over the distance L, labelled L for layer,

(iii) In the layer close to the electrolyte interface over the distance X_L, labelled L/S for layer/surface,

(iv)   In the layer close to the electrode surface over the distance X_0, labelled L/E for layer/electrode, and

(v)   In a zone somewhere in the middle of the layer, labelled L/RZ for layer/reaction zone.

Albery and Hillman[9] constructed a diagram (their figure 10) which shows the five different locations of reaction as a function of only three ratios ℓ/KL, X_0/L and X_L/L. Here ℓ is the distance within which a molecule, in the electrolyte, close to the surface, can react ($\sim 10^{-7}$ cm); it relates the surface reaction rate constant

Eqn. (2.27), $X_0 > X_L$

$$\frac{L}{KD_Y} \quad + \quad \frac{KX_0 + l \tanh (L/X_0)}{kKb_0 X_0 [l + KX_0 \tanh (L/X_0)]}$$

$X_0 < L$ $X_0 > L$

$$\frac{L}{KD_Y} + \frac{1}{kKb_0 X_0} \quad L/E$$

$l < KX_0$ $l > KX_0$

$$\frac{L}{KD_Y + D_e b_0/y_s} \quad L/RZ$$

$$\frac{1}{kKb_0 L} \quad L$$

$$\frac{Ly_s}{D_e b_0} + \frac{1}{k b_0 l} \quad S$$

$$\frac{Ly_s}{D_e b_0} + \frac{1}{kKb_0 X_L} \quad L/S$$

$l < KX_L$ $l > KX_L$

$X_L < L$ $X_L > L$

$$\frac{Ly_s}{D_e b_0} \quad + \quad \frac{1}{k b_0 [l + KX_L \tanh (L/X_L)]}$$

Eqn. (2.26), $X_L < X_0$
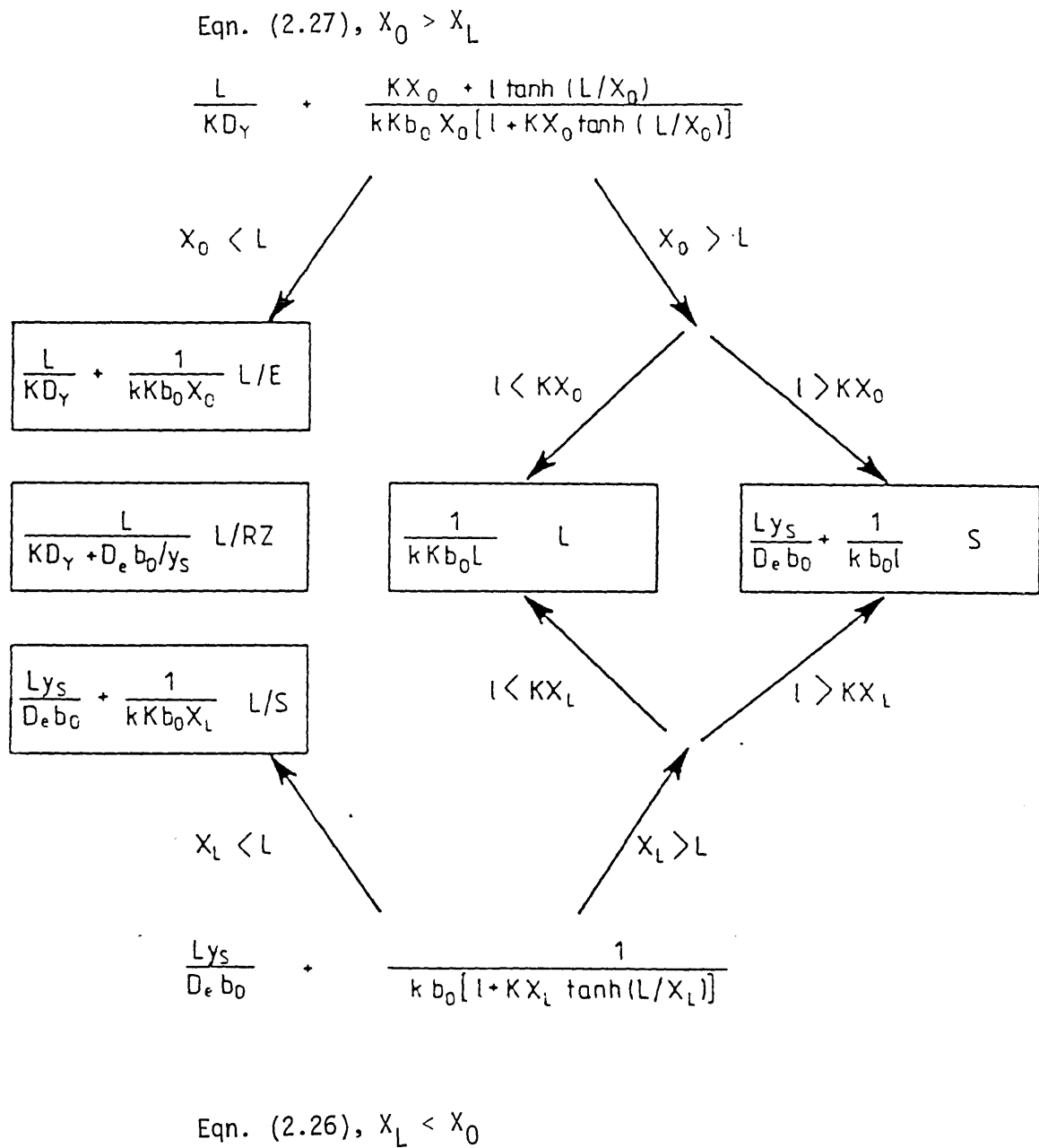
Figure 2.11. Derivation of simplified forms of equations 2.26 and 2.27 for the different cases.

(k") to the layer reaction rate constant (k) by

$$k" = k\ell \qquad\qquad (2.31)$$

assuming the same free energy of activation for both $B + Y \rightarrow A + Z$ reactions.

Although at first glance one may be tempted to pass over the diagram, leaving it for the stouter of heart, on further inspection one can see that it shows eight different cases of where the reaction occurs, its rate-limiting process and how these change as a function of the three parameters. The eight cases are given in table 2.1 where the first term indicates where the reaction occurs (see above) and the second term gives the rate-limiting process where transport limiting is indicated by either

t_e - transport of electrons across the layer, or

t_Y - transport of Y across the layer.

and kinetic limiting is indicated by either

k" - the surface reaction rate constant, or

k - the layer reaction rate constant.

The approximate values of k'_{ME}, in these regions, are also given in table 2.1 though it must be stressed that near any boundaries between different cases, in the diagram, the more complicated expressions (equations 2.26 and 2.27) must be used.

Table 2.1:   The Eight Different Cases for Reaction in a Modified

Electrode, Including the Results for k'_{ME}.

Case	k'_{ME}
S-k"	$k"b_0$
S-t_e	$D_e b_0 / L y_S$
L/S-k	$K(kb_0 D_Y)^{\frac{1}{2}}$
L/S-t_e	$D_e b_0 / L y_S$
L-k	$KkLb_0$
L/RZ-$t_e t_Y$	$\dfrac{D_e b_0}{L y_S} + \dfrac{KD_Y}{L}$
L/E-k	$Kb_0 (D_e k / y_S)^{\frac{1}{2}}$
L/E-t_Y	KD_Y / L

2.4.1. Distinguishing the Possible Mechanisms for a Modified Electrode

As can be seen from equations 2.26, 2.27 and 2.30, any system can be characterised by eight variables $\ell(=k''/k)$, K, D_Y, D_e, k, b_o, y_s and L where ℓ, K, D_Y, D_e and k are fixed for any system.

One can vary b_o by varying the potential of the electrode. Dependence of k'_{ME} on b_o can be seen, for the different cases, in table 2.1 but it should be noted that changing b_o one can change k'_{ME} (i.e. move from one case to another).

Varying L, one can optimise the thickness of the coat to give the best efficiency (i.e. optimise k'_{ME}). Optimum conditions are given in table 2.2 where in the first three positions it is best to aim for a layer reaction with L adjusted to give sufficient space for reaction but not so thick as to impede the transport. In all other instances it is best to aim for a surface reaction, reducing L so that the transport of electrons through the layer is efficient.

Using a rotating disc electrode y_s can easily be varied by changes in rotation speed. Looking at the k'_{ME} expressions for the different cases in table 2.1 and at equation 2.25, one can see that for cases S-k'', L/S-k, L-k and L/E-t$_Y$ one observes first order dependence of the flux of electrons (proportional to current) on y_s. Therefore a second step has been introduced in series with mass transport i.e.

$$Y_\infty \underset{k'_D}{\overset{k'_D}{\rightleftarrows}} Y_s \xrightarrow{k'_{ME}} Z$$
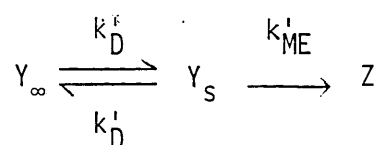
Table 2.2: Criteria for L for Optimum Performance of Modified Electrodes.

Conditions	Optimum Case	Conditions for L	k'_{ME}
$D_e b_0 \gg K D_\gamma y_S$ (i) $\quad$ $KX_L > \ell$	L/S-k	$X_L < L < X_0^2/X_L = D_e/kKX_L y_S$	$kKX_L b_0$
$D_e b_0 \simeq K D_\gamma y_S$ (ii) $\quad$ $KX_0 \simeq KX_L > \ell$	?	$L \simeq X_0 \simeq X_L$	$kKX_0^{\frac{1}{2}} X_L^{\frac{1}{2}} b_0$
$D_e b_0 \ll K D_\gamma y_S$ (iii) $\quad$ $KX_0 < \ell$	L/E-k	$X_0 < L < X_L^2/X_0 = D_\gamma/kb_0 X_0$	$kKX_0 b_0$
All others	S-k"	$L < D_e/k'' y_S$	$k'' b_0$

where $X_0 + (D_e/kKy_0)^{\frac{1}{2}}$ and $X_L = (D_\gamma/kb_L)^{\frac{1}{2}}$; (i) $X_0^2 \gg X_L^2$; (ii) $X_0^2 \simeq X_L^2$; (iii) $X_0^2 \ll X_L^2$.

and hence, as discussed in section 2.1, current can be described by a Koutecky-Levich equation (see equations 2.5 and 2.6).

$$\frac{n\,FA\,y_\infty}{i} = \frac{1}{k_D^{\,\iota}} + \frac{1}{k_{ME}^{\,\iota}} \qquad (2.32)$$

where now a plot of $1/i$ vs $1/W^{\frac{1}{2}}$ will have an intercept which will give $k_{ME}^{\,\iota}$.

For cases $L/S\text{-}t_e$ and $S\text{-}t_e$ the flux of electrons becomes independent of y_S and hence current will be independent of rotation speed.

For the L/RZ case Andrieux, Dumas-Bouchiat and Savéant[79] find

$$\frac{n\,FA\,y_\infty}{i} = \frac{1}{k_D^{\,\iota}\left(1 + \dfrac{D_e b_0}{D_\gamma K\,y_\infty}\right)} + \frac{L}{D_\gamma K + D_e b_0/y_\infty} \qquad (2.33)$$

where now a plot of $1/i$ vs $1/W^{\frac{1}{2}}$ will give $k_{ME}^{\,\iota}$ from the intercept (as $y_S = y_\infty$ when $W = \infty$, i.e. at the intercept) but the slope will be less than expected for a Koutecky-Levich plot. They also find that for the L/E-k case the current can be described by

$$\left(\frac{n\,FA\,y_\infty}{i}\right)^2 = \frac{n\,FA\,y_\infty}{k_D^{\,\iota}\,i} + \left(\frac{1}{k_{ME}^{\,\iota\iota}}\right)^2 \qquad (2.34)$$

where

$$k_{ME}^{"} = Kb_0 \left(\frac{D_e k}{y_\infty} \right)^{\frac{1}{2}}$$ (2.35)

which is the expression for $k_{ME}^{'}$ with y_s replaced by y_∞. Thus, the square root of the intercept of a i^{-2} vs $i^{-1} W^{-\frac{1}{2}}$ plot will give $k_{ME}^{"}$.

Therefore a rotating disc electrode goes part of the way to distinguish between the eight different cases in table 2.1.

The S-k", L/S-k, L-k and L/E-t_y cases can be further differentiated by varying b_0 and L (see above) while the S-t_e and L/S-t_e can be separated by first lowering y_∞ so that S-t_e would become S-k" and L/S-t_e would become L/S-k which can then be divided by varying b_0. Table 2.3 shows the diagnosis to distinguish the different mechanisms for modified electrodes.

Andrieux, Dumas-Bouchiat and Savéant[79] discuss the possibility of a second wave as one sweeps the potential further, so that Y can be reduced by the electrode without the catalyst and use this as another diagnostic tool. However, this assumes the reaction Y → Z will occur at the bare electrode which may not be true.

It has been wisely pointed out[9] that if the observed current is less than 10% of the calculated limiting value for Y then variations in rotation speed will make little difference to y_s and experimental error will mask any results. If this is found, then assuming $y_s = y_\infty$ and varying the bulk concentration of Y (i.e. y_∞) can be used for mechanistic distinction.

Table 2.3:   Diagnosis of the Mechanism for Modified Electrodes

```
┌──────────────┐
│ Is i         │        ┌─────┐          S-t_e ⎤  difficult to
│ independent  │──────▶ │ Yes │──────▶   or    ⎥→ distinguish but
│ of W?        │        └─────┘          L/S-t_e⎦  can be done
└──────┬───────┘                                   (see text).
       │
       ▼
   ┌──────┐
   │  No  │
   └──┬───┘
      │
      ▼
┌──────────────────┐                  ┌──────────────┐
│ Is Koutecky-     │      ┌─────┐     │ Is plot of   │      ┌─────┐
│ Levich           │─────▶│ No  │────▶│ eqn. 2.34    │─────▶│ Yes │─▶ L/E-k
│ plot linear?     │      └─────┘     │ linear?      │      └─────┘
└────────┬─────────┘                  └──────┬───────┘
         │                                   │
         ▼                                   ▼
      ┌──────┐                           ┌──────┐
      │ Yes  │                           │  No  │
      └──┬───┘                           └──┬───┘
         │                                  ▼
         │                          ┌────────────────┐
         │                          │ Questionable   │
         │                          │ results!       │
         │                          └────────────────┘
         ▼
┌─────────────────────┐
│ Is gradient         │       ┌──────────────────┐
│ given by            │──────▶│ No, it's smaller │──────▶ L/RZ-t_e t_y
│ (1.55 nF            │       └──────────────────┘
│ Ay_∞ D^{2/3} ν^{-1/6})^{-1} │
└──────────┬──────────┘
           │
           ▼
        ┌──────┐
        │ Yes  │─────▶   S-k"      L/S-k      L-k      L/E-t_y
        └──────┘
```

	S-k"	L/S-k	L-k	L/E-t_y
Order w.r.t. b_0	1	$\frac{1}{2}$	1	0
Order w.r.t. L	0	0	1	-1
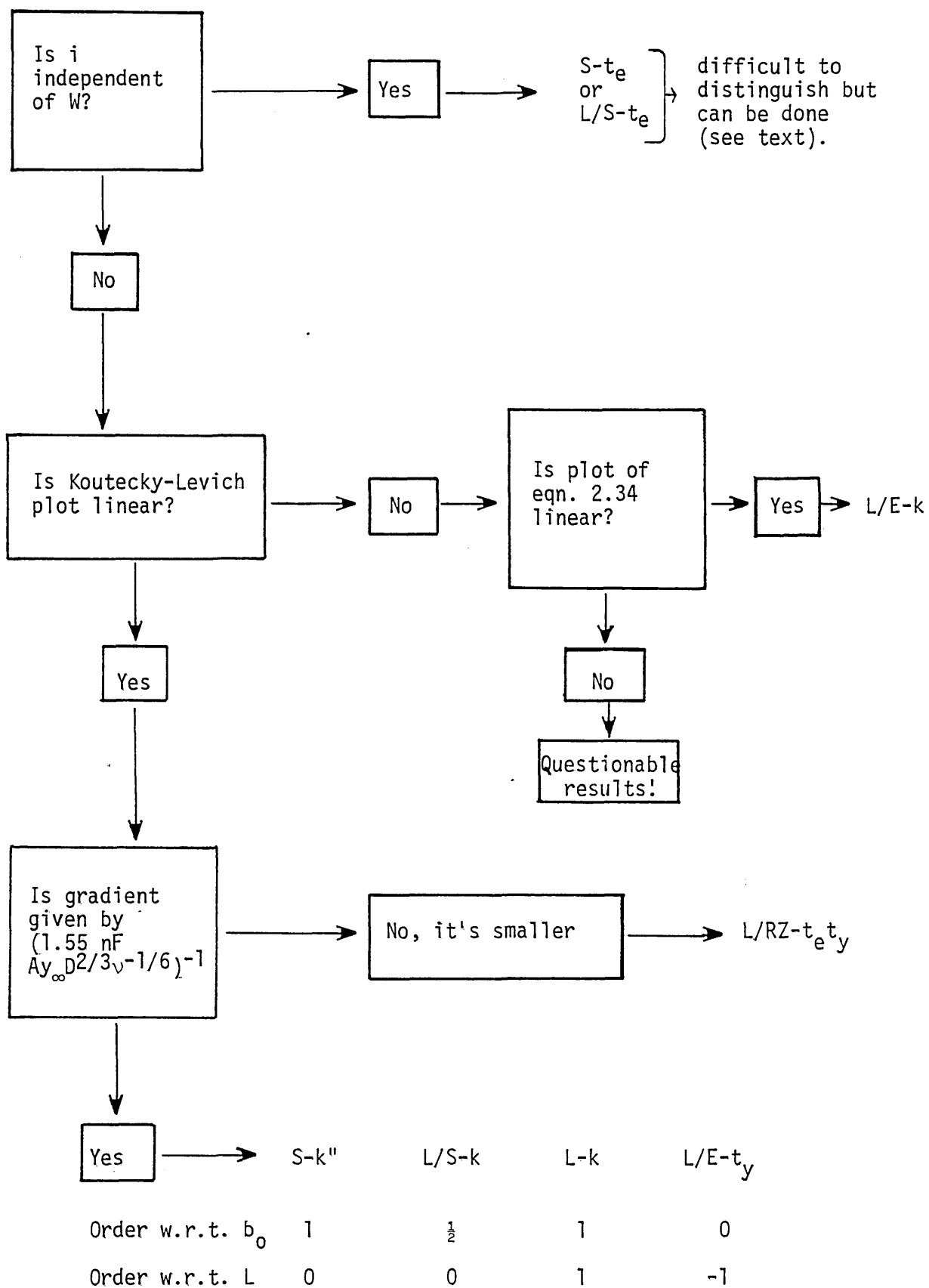
2.4.2. Potential Step Experiments

Potential step experiments can be used to analyse the kinetics of the A/B system (see figure 2.10) without the complication of a Faradaic reaction with species $Y \rightarrow Z^{(124)}$. Therefore, one is looking at the changing of the charge in the coat and the rate and mechanism of electron transport. Many systems have been analysed using this method[21,36,37,125-127] and three main rate-limiting processes have been found. These are:-

(i)   the electron exchange itself, i.e. $A + B \rightarrow B + A$,

(ii) if A and B are far away, polymer motion to bring A and B in close proximity,

(iii) if there is a change in charge in the A/B reaction, the movement of counter ions to balance this charge.

Case (iii) can be distinguished from the other two by seeing if the transient response varies with the size of the counter ion. It is important to differentiate this case as here, the diffusion coefficient measured will not be D_e, the diffusion coefficient for the transport of electrons through the layer in the steady state.

Distinguishing between (i) and (ii) is harder but Murray has shown[128] that it can be done using arguments based on the measured rate of A/B exchange in solution, the concentration of redox centres in the coat and the polymer structure.

2.4.3. Addendum

During the preparation of this thesis Albery and Hillman published[230] a more complete theoretical treatment of the transport

and kinetics in modified electrodes. In this treatment they consider the added possibility of the solution species, Y, diffusing through the coat and reacting at the electrode surface with rate constant k_E'.

With this extra possibility included, the solutions for k_{ME}' become

if $D_e b_o \gg D_Y K y_s$

$$k_{ME}' = \cfrac{1}{\cfrac{y_s L}{D_e b_o} + \cfrac{1}{k''b_o + kKb_o X_L \tanh(L/X_L)}} +$$

$$\qquad\quad \underset{\substack{\text{transport of e} \\ \text{across the} \\ \text{layer}}}{\uparrow} \qquad\qquad \underset{\substack{\text{surface} \\ \text{reaction}}}{\uparrow} \quad \underset{\substack{\text{layer} \\ \text{reaction}}}{\uparrow}$$

$$\cfrac{K \mathrm{sech}(L/X_L)}{\cfrac{L}{D_Y} + \cfrac{1}{k_{ME}'}} \tag{2.26A}$$

$$\underset{\substack{\text{transport of Y} \\ \text{across the} \\ \text{layer}}}{\uparrow} \qquad \underset{\substack{\text{electrode} \\ \text{reaction}}}{\uparrow}$$

and

$$\text{if } D_e b_0 \ll D_Y K y_s$$

$$k'_{ME} = \cfrac{kKb_0X_0 \left[\cfrac{k'' + kKX_0 \tanh(L/X_0)}{k''\tanh(L/X_0) + kKX_0} \right] + k'_E K}{1 + (L/D_Y)(k'_E + kb_0X_0)} \qquad (2.27A)$$

with labels:

layer reaction, surface reaction, electrode reaction (pointing to the three terms), and transport of Y across the layer (pointing to the denominator).

If the electrode reaction is negligible then these equations revert to those previously presented (i.e. 2.26 and 2.27).

Considering the possibility of the reaction of Y at the electrode gives a sixth possible location for reaction with a modified electrode. This possibility is labelled E for electrode. Two processes can be rate-limiting for this electrode reaction. These are the diffusion of Y through the coat (t_Y) and the reaction of Y at the electrode (rate constant k'_E). Therefore, two extra cases for k'_{ME} can be added to the previous eight (see table 2.1) and a more complete collection is shown in table 2.4.

Table 2.4: A More Complete Table for the Different Possible Cases
for Reaction in a Modified Electrode. The Results of
k'_{ME} for these Cases are also Given.

Case	k'_{ME}
S-k"	$k''b_0$
S-t_e	$D_e b_0 / L y_S$
L/S-k	$K(kb_0 D_\gamma)^{\frac{1}{2}}$
L/S-t_e	$D_e b_0 / L y_S$
L-k	$KkLb_0$
L/RZ-$t_e t_\gamma$	$\dfrac{D_e b_0}{L y_S} + \dfrac{K D_\gamma}{L}$
L/E-k	$Kb_0(D_e k/y_S)^{\frac{1}{2}}$
L/E-t_γ	$K D_\gamma / L$
E-k'_E	Kk'_E
E-t_γ	$\dfrac{K D_\gamma}{L}$

2.5. The Derivation of Koutecky-Levich Equations for Possible Pre-equilibria to Electrochemical Reactions at a RDE

If, for an electrochemical reaction at a RDE, there is a pre-equilibrium in series with the transport process, Koutecky-Levich dependence will result (see section 2.1)[211].

To distinguish between three possible pre-equilibria of ligand exchange

$$A + B \rightleftharpoons C + D \qquad \text{(where C is electroactive)}$$

ligand association

$$A + B \rightleftharpoons E \qquad \text{(where E is electroactive)}$$

and a more complex ligand exchange

$$A + B \rightleftharpoons F + 2D \qquad \text{(where F is electroactive)}$$
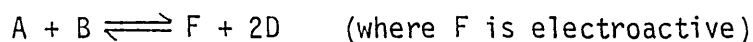
the Koutecky-Levich equations for these processes are derived below. One would expect that the ligand exchange mechanisms would result in some dependence on the concentration of D while the ligand association mechanism would not. Therefore, the processes could be distinguished.

SCHEME I: The formation of an electroactive species C by a simple ligand exchange

In solution

$$A + B \underset{k_{-I}}{\overset{k_I}{\rightleftharpoons}} C + D \qquad (1)$$

$$K_I = \frac{k_I}{k_{-I}} = \frac{[C][D]}{[A][B]}$$

Let $c_A = [A]$

$c_B = [B]$

$c_C = [C]$

and $c_D = [D]$

Experiments are arranged so that c_B and $c_D > 10 \, c_A$ and therefore c_B and c_D can be regarded as constant throughout the solution, including at the electrode.

Considering the case where all C reaching the electrode immediately reacts and A does not react, equilibrium (1) will be in balance in the bulk solution, but close to the electrode it will be perturbed. This is because as C is being removed more A will react to maintain the equilibrium constant. It is assumed that the distance over which the equilibrium

is perturbed is much smaller than the diffusion layer. The conditions under which this assumption is valid are discussed with equation 2.47.

Thus the problem can be separated into two parts; firstly the description of the concentrations very close to the electrode in the reaction layer which is given a thickness Z_R. Secondly, there is the description of the transport from the bulk solution to the outside of the reaction layer.

Combining Fick's second law and normal homogeneous kinetics one gets for A in the reaction layer

$$\frac{dc_A}{dt} = D_A \frac{d^2 c_A}{dz^2} - k_I c_A c_B + k_{-I} c_C c_D$$

where z is the distance from the electrode.

In the steady state, at the electrode, diffusion balances the formation and decomposition of A, i.e.

$$\frac{dc_A}{dt} = 0$$

Hence

$$D_A \frac{d^2 c_A}{dz^2} = k_I c_A c_B - k_{-I} c_C c_D \qquad (2.36)$$

where D_A = the diffusion coefficient of A.

Similarly for C

$$D_C \frac{d^2 c_C}{dz^2} = -k_I c_A c_B + k_{-I} c_C c_D \qquad (2.37)$$

At the electrode where $z = 0$

$$c_C = 0 \quad \text{as C is destroyed on the electrode.}$$

and

$$\frac{dc_A}{dz} = 0 \quad \text{as A does not react on the electrode.}$$

At a distance $z > Z_R$, just outside the reaction layer

$$c_A \text{ is defined as } c_{A,R}$$

and as equilibrium (1) is in balance

$$c_C = \frac{k_I c_A c_B}{k_{-I} c_D}$$

Let y describe the breakdown of the equilibrium between A and C, so that

$$y = \frac{k_I \, c_A \, c_B}{k_{-I} \, c_D} - c_C = \frac{K_I \, c_A \, c_B}{c_D} - c_C \qquad (2.38)$$

Then, at equilibrium $y = 0$, but close to the electrode where $c_C = 0$

$$y_0 = \frac{K_I \, c_{A,0} \, c_{B,0}}{c_{D,0}} = \frac{K_I \, c_{A,0} \, c_B}{c_D} \qquad (2.39)$$

as c_B and $c_D \gg c_A$. Equation 2.38 gives

$$k_I \, c_A \, c_B - k_{-I} \, c_C \, c_D = k_{-I} \, c_D \, y$$

Substituting in equations 2.36 and 2.37 gives

$$\frac{D_A \, d^2 c_A}{dz^2} = k_{-I} \, y \, c_D \qquad (2.40)$$

and

$$D_C \frac{d^2 c_C}{dz^2} = -k_{-I} \, y \, c_D \tag{2.41}$$

Multiplying equation 2.40 by $\dfrac{K_I \, c_B}{D_A \, c_D}$ gives,

$$\frac{K_I \, c_B}{c_D} \frac{d^2 c_A}{dz^2} = \frac{K_I \, k_{-I} \, y \, c_B}{D_A} \tag{2.42}$$

and equation 2.41 by $1/D_C$ gives,

$$\frac{d^2 c_C}{dz^2} = \frac{-k_{-I} \, y \, c_D}{D_C} \tag{2.43}$$

As K_I, c_B and c_D are independent of z, equation 2.42 can be written

$$\frac{d^2 (K_I c_A c_B / c_D)}{dz^2} = \frac{K_I k_{-I} \, y \, c_B}{D_A} \tag{2.44}$$

Subtracting equation 2.43 from equation 2.44 gives,

$$\frac{d^2((K_I c_A c_B / c_D) - c_C)}{dz^2} = \frac{d^2 y}{dz^2} = \left(\frac{K_I c_B}{D_A c_D} + \frac{1}{D_C} \right) k_{-I} c_D y \qquad (2.45)$$

As $\dfrac{K_I c_B}{c_D} \simeq \dfrac{c_C}{c_A}$ and $c_A \gg c_C$, $\quad \dfrac{K_I c_B}{c_D} \ll 1$, and assuming that $D_A \sim D_C$

equation 2.45 can be approximated to

$$\frac{d^2 y}{dz^2} = \frac{k_{-I} c_D y}{D_C}$$

Integrating with boundary conditions

when $z = 0$ $\quad y = y_0 = \dfrac{K_I \, c_{A,0} \, c_B}{c_D}$

and as $z \to \infty$ $\quad y \to 0$

gives

$$y = y_0 \exp\left(-\frac{z}{z_R}\right) \qquad (2.46)$$

where

$$z_R = \left(\frac{D_C}{k_{-I}\, c_D}\right)^{\frac{1}{2}} \qquad (2.47)$$

As discussed at the beginning of this section, for this analysis to be valid $z_R < z_D$ (the diffusion layer thickness). Using equation 2.47 and reasonable values for D_C ($\sim 10^{-6}$ cm^{2}s^{-1}), c_D (0.01 mol dm^{-3}) and z_D (10^{-5} m) one can see that for $z_R < z_D$, k_{-I} must be greater than 10^4 dm^3 mol^{-1} s^{-1}.

The distance z_R is the distance over which the species C, once formed, has a chance to diffuse before it encounters a D species and is turned back to A and B. Because of the exponential term in equation 2.46 when $z > z_R$, y rapidly falls to zero (i.e. the equilibrium comes into balance).

From equation 2.38, the limiting flux of C at the electrode surface is given by

$$j_L = D_C\left(\frac{dc_C}{dz}\right)_{z\,=\,0} = -\,D_C\left(\frac{dy}{dz}\right)_{z\,=\,0}$$

Then using equation 2.46,

$$j_L = \frac{D_C y_0}{Z_R} = \frac{D_C K_I c_{A,0} c_B}{Z_R c_D}$$

Therefore

$$j_L = k_R' c_{A,0} \tag{2.48}$$

where

$$k_R' = \frac{D_C K_I c_B}{c_D Z_R} = \frac{D_C K_I c_B}{c_D} \left(\frac{k_{-I} c_D}{D_C} \right)^{\frac{1}{2}}$$

Thus

$$k_R' = \left(\frac{K_I k_I D_C}{c_D} \right)^{\frac{1}{2}} c_B \tag{2.49}$$

As $c_A \gg c_C$ it is the reaction of A + B which supplies C for the electrode reaction and, as $c_B \gg c_A$, the flux is related to A's transport through the diffusion layer. Therefore, the limiting flux (j_L) when the electrode removes all C produced is given by

$$j_L = \frac{D_A (c_{A,\infty} - c_{A,R})}{Z_D} \tag{2.50}$$

and since $\left(\dfrac{dc_A}{dz} \right)_{z=0} = 0$ and Z_r is small, $c_{A,0} \simeq c_{A,R}$.

Therefore combining equations 2.48 and 2.50

$$j_L = \frac{D_A}{Z_D} \left(c_{A,\infty} - \frac{j_L}{k_R'} \right)$$

$$\Rightarrow \quad j_L \left(1 + \frac{D_A}{Z_D k_R'} \right) = \frac{D_A c_{A,\infty}}{Z_D}$$

$$\Rightarrow \quad \frac{1}{j_L} = \frac{1}{(D_A/Z_D) c_{A,\infty}} + \frac{1}{k_R' c_{A,\infty}} = \frac{1}{c_{A,\infty}} \left(\frac{1}{k_D'} + \frac{1}{k_R'} \right)$$

As

$$i_L = n\,FA\,j_L \quad \text{(see sections 2.1 and 2.2)}$$

$$\Rightarrow \quad \frac{n\,FA}{i_L} = \frac{1}{[A]} \left(\frac{1}{k_D'} + \frac{1}{k_R'} \right) \tag{2.51}$$

where

$$k_R' = (K_I k_I D_C)^{\frac{1}{2}} [B][D]^{-\frac{1}{2}} \tag{2.52}$$

and

$$k_D' = 1.554\, D_A^{2/3}\, \nu^{-1/6}\, W^{1/2} \tag{2.53}$$

Equation 2.51 is the Koutecky-Levich equation for this system with k_D' describing the mass transport control of the current and k_R' describing the homogeneous kinetic control of the current. Concentration profiles for A, B, C and D for this system are shown in figure 2.12.

SCHEME II.   The formation of an electroactive species E

by ligand association

In solution
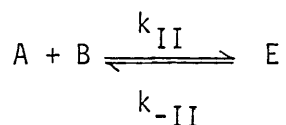
$$A + B \underset{k_{-II}}{\overset{k_{II}}{\rightleftharpoons}} E$$

$$K_{II} = \frac{k_{II}}{k_{-II}} = \frac{[E]}{[A][B]}$$

Following the same procedure as for scheme I, one gets the same Koutecky-Levich equation

$$\frac{n\,FA}{i_L} = \frac{1}{[A]}\left(\frac{1}{k_D'} + \frac{1}{k_R'}\right)$$

(2.51)
above

Figure 2.12. Concentration profiles for the reduction of a species C formed by the equilibrium A + B $\rightleftharpoons$ C + D. The discontinuities on the y-axis show differences in an order of magnitude between the concentration of the various species.
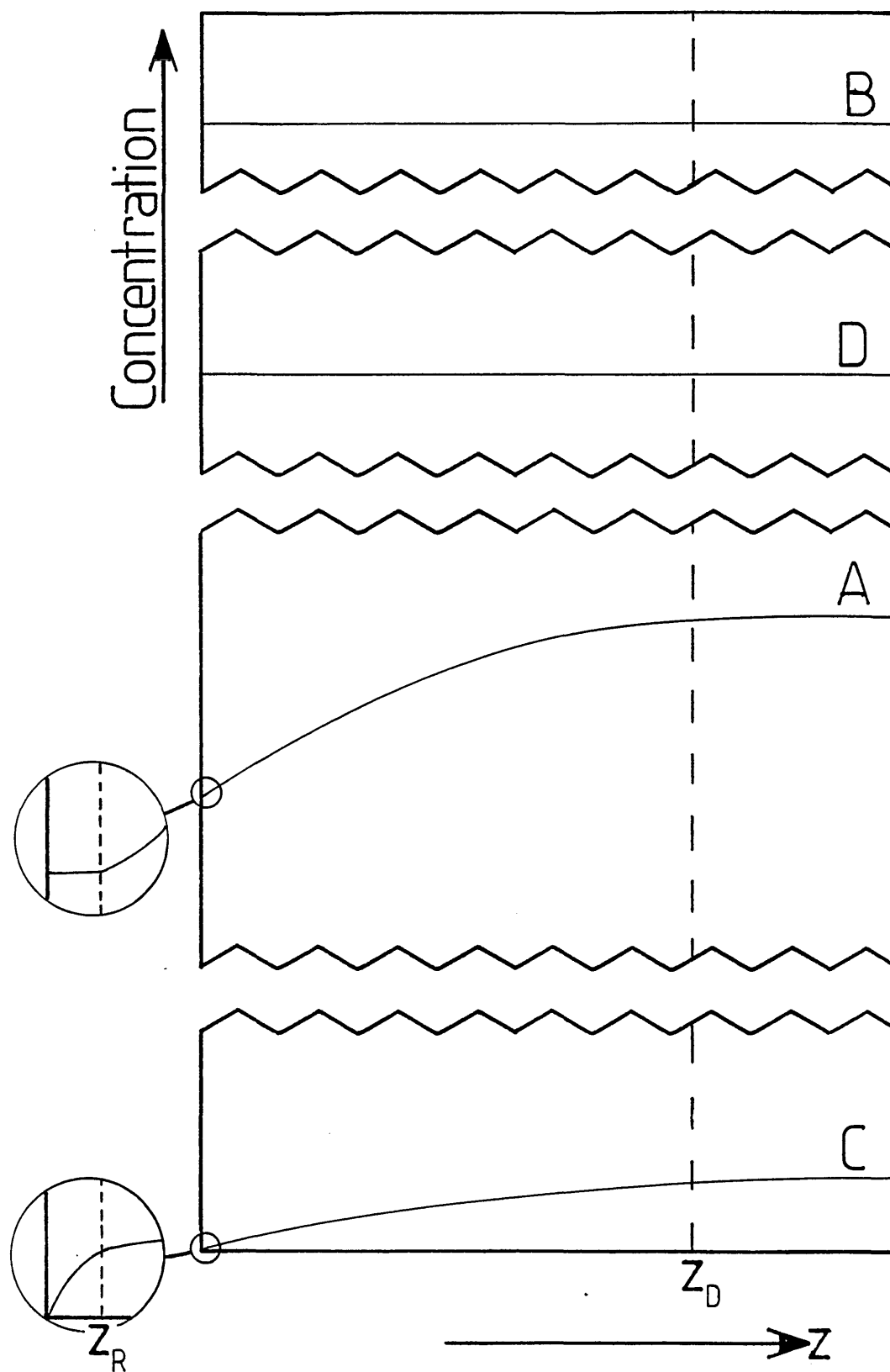
but here

$$k_R' = (K_{II} \, k_{II} \, D_E)^{\frac{1}{2}} [B]$$

(2.54)

while, naturally, k_D' is the same as in equation 2.53.

SCHEME III. The formation of an electroactive species F by a
more complex ligand exchange (than SCHEME I).

In solution
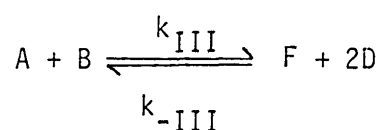
$$A + B \xrightleftharpoons[k_{-III}]{k_{III}} F + 2D$$

$$K_{III} = \frac{k_{III}}{k_{-III}} = \frac{[F][D]^2}{[A][B]}$$

Following the same procedure as SCHEME I, one gets the same Koutecky-
Levich equation

$$\frac{n\,FA}{i_L} = \frac{1}{[A]}\left(\frac{1}{k_D'} + \frac{1}{k_R'}\right)$$

(2.51)
above

but here

$$k_R' = (K_{III} \, k_{III} \, D_F)^{\frac{1}{2}} \, [B][D]^{-1}$$ (2.55)

and k_D' is the same as in equation 2.53.

Therefore, as expected, the different dependence on the concentration of D (equations 2.52, 2.54 and 2.55) can be used to distinguish between the three pre-equilibria.

These results are used in chapter 4 to investigate the electrochemical reduction of $Pd(PPh_3)_2Cl_2$ in chloroform. This reduction needs excess triphenylphosphine ligands and is shown to be preceded by an equilibrium which can be

(i) $Pd(PPh_3)_2Cl_2 + PPh_3 \rightleftharpoons (Pd(PPh_3)_3Cl_2)$
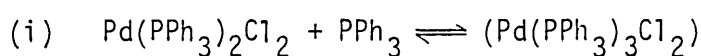
   with $Pd(PPh_3)_3Cl_2$ being reduced at the electrode,

(ii) $Pd(PPh_3)_2Cl_2 + PPh_3 \rightleftharpoons (Pd(PPh_3)_3Cl)^+ + Cl^-$
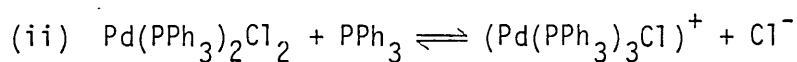
   with $(Pd(PPh_3)_3Cl)^+$ being reduced at the electrode,

or

(iii) $Pd(PPh_3)_2Cl_2 + PPh_3 \rightleftharpoons (Pd(PPh_3)_3)^{2+} + 2Cl^-$
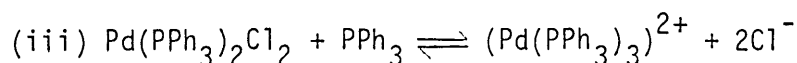
   with $(Pd(PPh_3)_3)^{2+}$ being reduced at the electrode.

Therefore in the above analysis one can simply substitute

$$A = Pd(PPh_3)_2Cl_2$$

$$B = PPh_3$$

$$C = (Pd(PPh_3)_3Cl)^+$$

$$D = Cl^-$$

$$E = (Pd(PPh_3)_3Cl_2)$$

and $$F = (Pd(PPh_3)_3)^{2+}$$
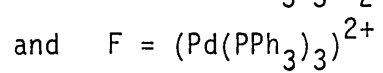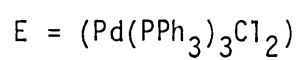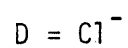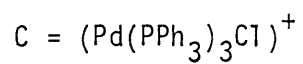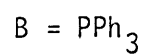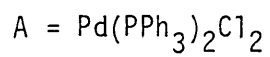
3. EXPERIMENTAL

3.1. Electrodes

A three electrode system consisting of a working electrode (some-
times two, disc and ring), a reference electrode and a counter electrode
was used.

3.1.1. Working Electrodes

These were either rotating disc or rotating ring-disc electrodes
(see figure 2.1). The insulating materials used were araldite for
aqueous electrochemistry and Kel-F or Teflon for non-aqueous electro-
chemistry. Several electrode materials were used including platinum
(Johnson Matthey Ltd.), gold (Johnson Matthey Ltd.) and glassy carbon
(Fluorocarbon).

The electrodes were mechanically polished using a rotating polishing
disc, covered with 25 μm alumina lubricated with glycerol, across which
the electrode was swept. This was repeated with 6 μm and 3 μm diamond
lapping compound. Then the electrodes were hand polished using a slurry
of 1 μm alumina, in doubly distilled water, applied with cotton wool.

The platinum and gold electrodes were hand polished with a 0.3 μm
alumina slurry to give a mirror finish, before each experiment. Platinum
electrodes were sometimes further cleaned electrochemically. This in-
volved evolving hydrogen (-0.3 V w.r.t. S.C.E.) and oxygen (+1.3 V w.r.t.
S.C.E.) in 50 mM sulphuric acid, for a few minutes. This was complete
when the standard cyclic voltammogram of platinum in acid, including
well defined hydrogen adsorption peaks, was obtained.

Glassy carbon electrodes were hand polished with a Cerirouge slurry,
in doubly distilled water, before use. Although there are several papers

in the literature[129-131] on electrochemical cleaning of glassy carbon electrodes, this was found to be unneccessary.

3.1.2. Reference Electrodes

For aqueous electrochemistry a home-made saturated calomel electrode (S.C.E.) was used. Its potential was regularly checked against a commercial (Radiometer) electrode and found to agree within 1 mV.

For non-aqueous electrochemistry the saturated calomel electrode is unsatisfactory as ill-defined junction potentials would be set up between the two different electrolytes[132]. Also, KCl and water would leak into the purified/dried organic solvent. Therefore, a silver-silver ion (Ag/Ag$^+$) electrode was used. This comprised of a silver wire dipping into a 0.01 mol dm^{-3} silver nitrate (or silver perchlorate) solution. This solution was made of the solvent being used in the cell plus the same supporting electrolyte in the same concentration (see figure 3.1). This electrode, when not in use, was stored dipping into a similar solution as it contained, in an air tight vessel, in the dark. The solution was periodically changed and the silver wire cleaned by abrasion. This electrode has a potential of +0.681 V with respect to the standard hydrogen electrode (+0.437 V w.r.t. S.C.E.).

3.1.3. Counter Electrodes

These were made of platinum gauze and were regularly cleaned in a concentrated nitric/sulphuric acid (1:1) mixture.

3.2. Rotation System and Cell Assembly

The rotation system (Oxford Electrodes) consisted of a bearing block with an axially mounted motor supported by two vertical pillars,

Araldite

Silver wire

rubber
policeman

Solution containing 0.01 M
$AgNO_3$ (or $AgClO_4$) (solvent
is the same as in the electro-
chemical cell and contains the
same supporting electrolyte,
in the same concentration).

glass
frit
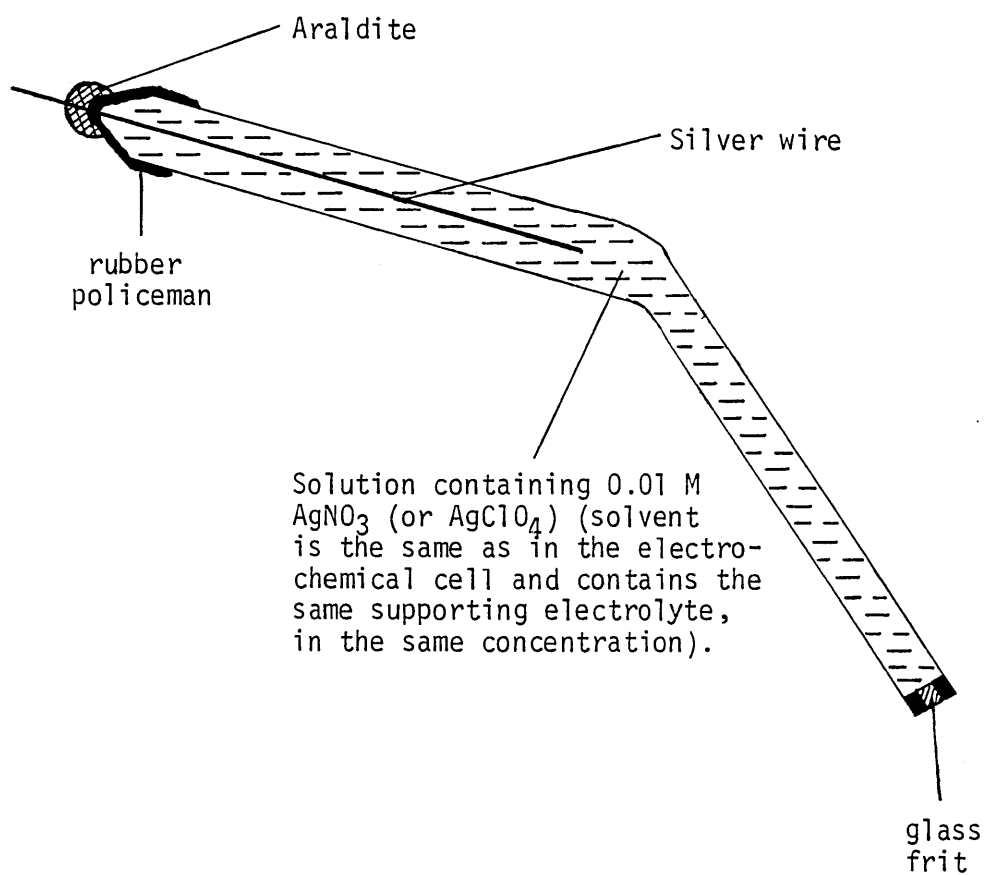
Figure 3.1. Schematic representation of an Ag/Ag^+
reference electrode.

such that the unit could be raised and lowered. The motor controller had

a feed-back system which gave a digital read-out of the rotation speed.

The electrodes were attached to the bearing block via a screw thread contact

to the disc and a taper fitted contact to the ring. Inside the bearing

were sealed mercury contacts which lead to sockets on the outside (see

figure 3.2).

Two similar cell assemblies were employed. For aqueous electro-

chemistry, a glass cell (see figure 3.3a) with an internal volume of

approximately 125 cm^3 was used. This had an outer jacket through which

thermostatted water was pumped to maintain the contents at $25^{o}C$. A side

arm carried the counter electrode which was separated from the bulk solu-

tion by a porous frit. This was to prevent contamination by the products

of the counter electrode reaction. A small jet at the bottom of the cell

was used as a nitrogen inlet to deoxygenate the solution. A teflon cell

lid was fitted with holes for the working and reference electrodes.

For non-aqueous electrochemistry, where stringent purifications are

necessary, a similar but smaller cell (see figure 3.3b) was used. This

had an internal volume of about 25 cm^3, so minimising the amount of solvent

and background electrolyte needed. As the cell was smaller a second side arm

was fitted for the reference electrode and, in addition to the inlet for

solution deoxygenation, there was another gas inlet above the solution so

that a blanket of dry/deoxygenated argon could be maintained.

3.3. Electronics and Circuitry

Circuits were assembled by connecting modular electronic units.

These modular units were based on the operational amplifier (see figure

3.4) and consisted of a triangular wave generator (see figure 3.5), a dual

input potentiostat (see figure 3.6), a dual input galvanostat (see

figure 3.7), voltage sources, an inverter, a subtractor, a summing inverter and
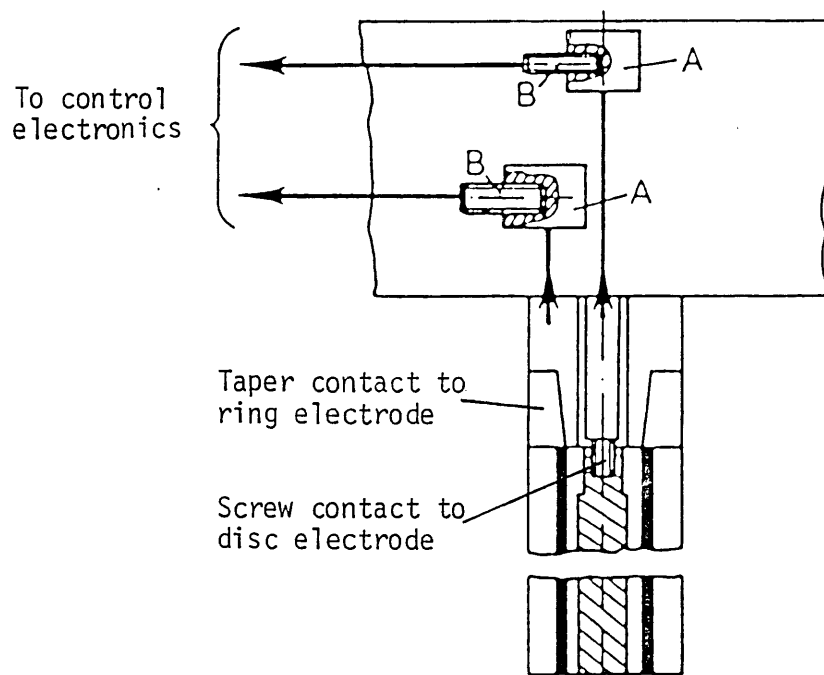
Figure 3.2. Schematic representation of electrode contact
system; the screw and taper contacts to the
disc and ring, respectively, lead to sealed
mercury contacts (A) and then via screws (B),
on the outside of the bearing block, to the
control electronics.

Figure 3.3.   Electrochemical cells: (a) for aqueous solutions;
              (b) Mini-cell for non-aqueous solutions.
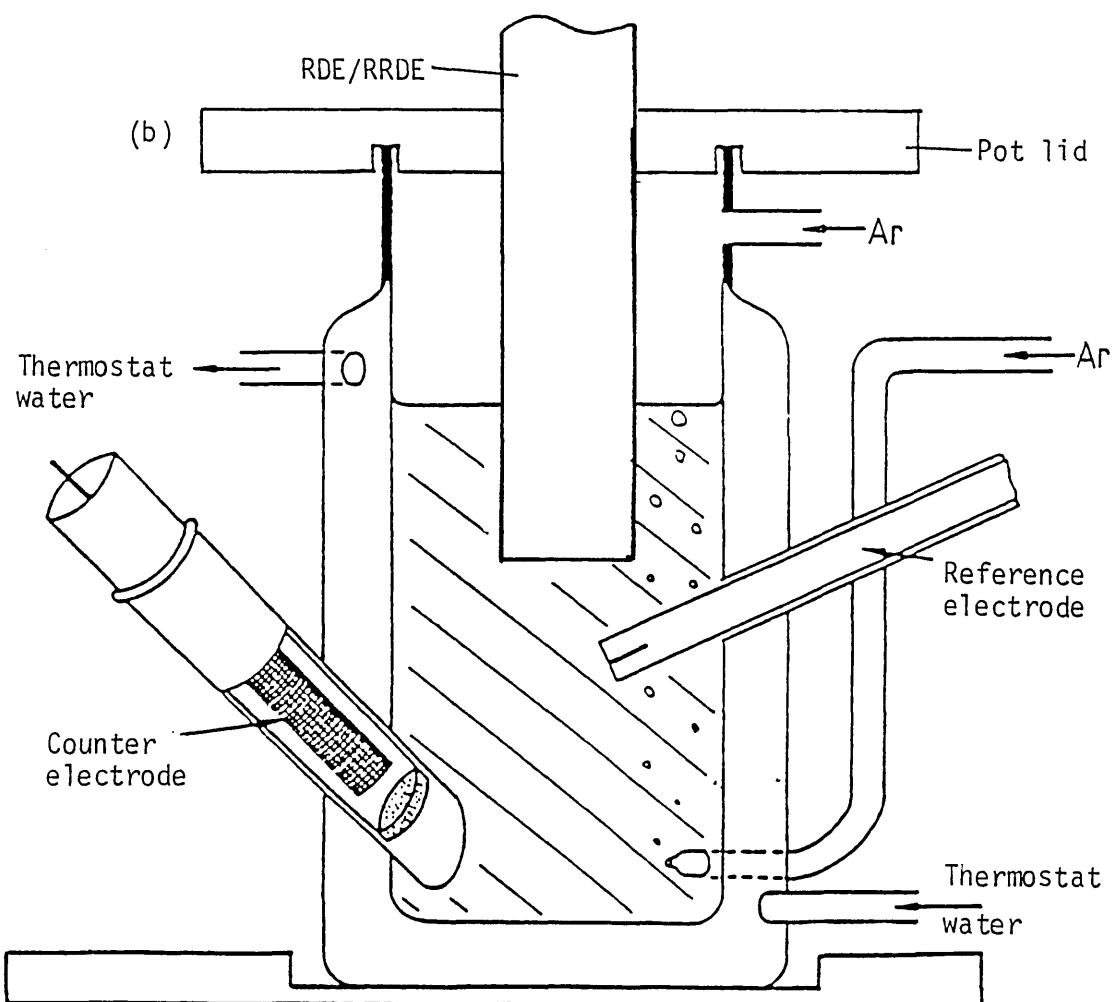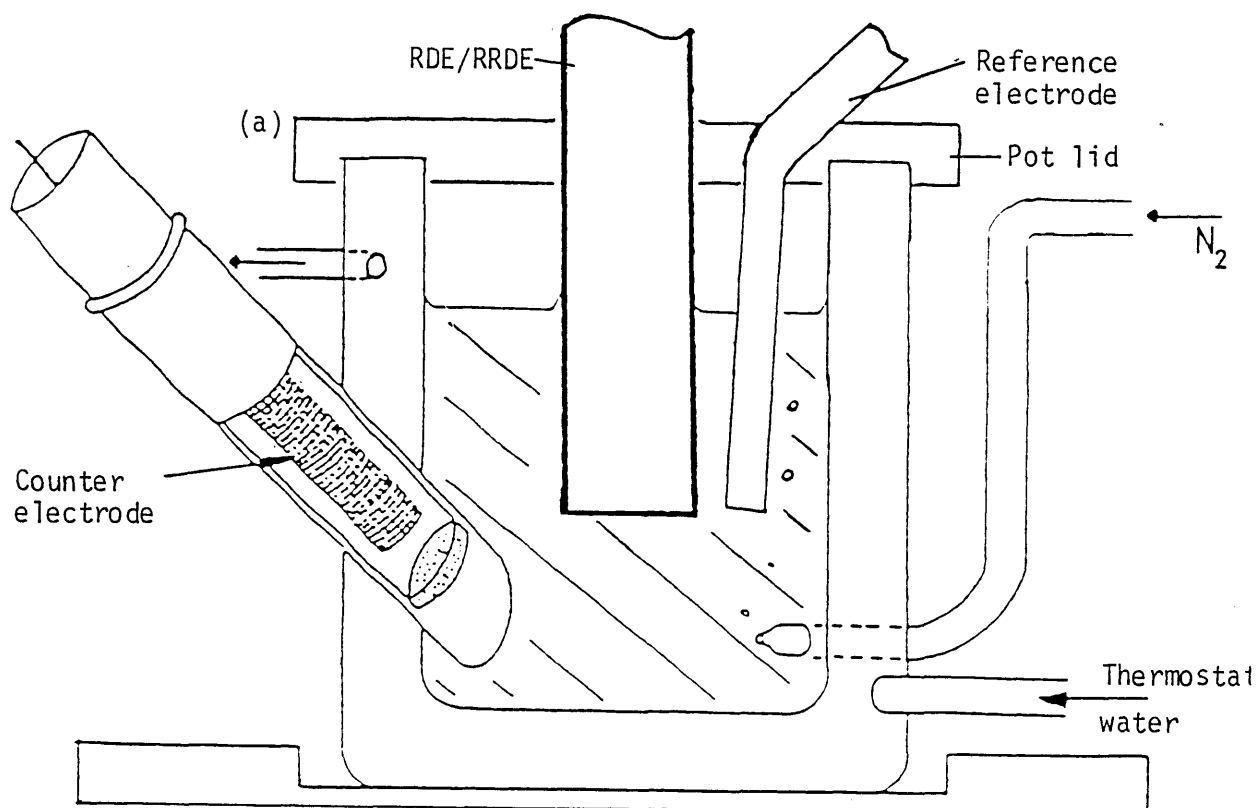
Figure 3.4. Schematic operational amplifier.
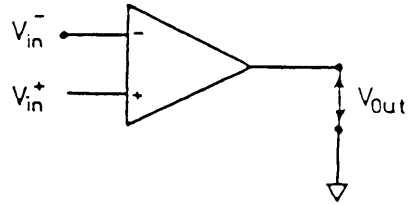
Figure 3.5. Triangular wave generator[133].
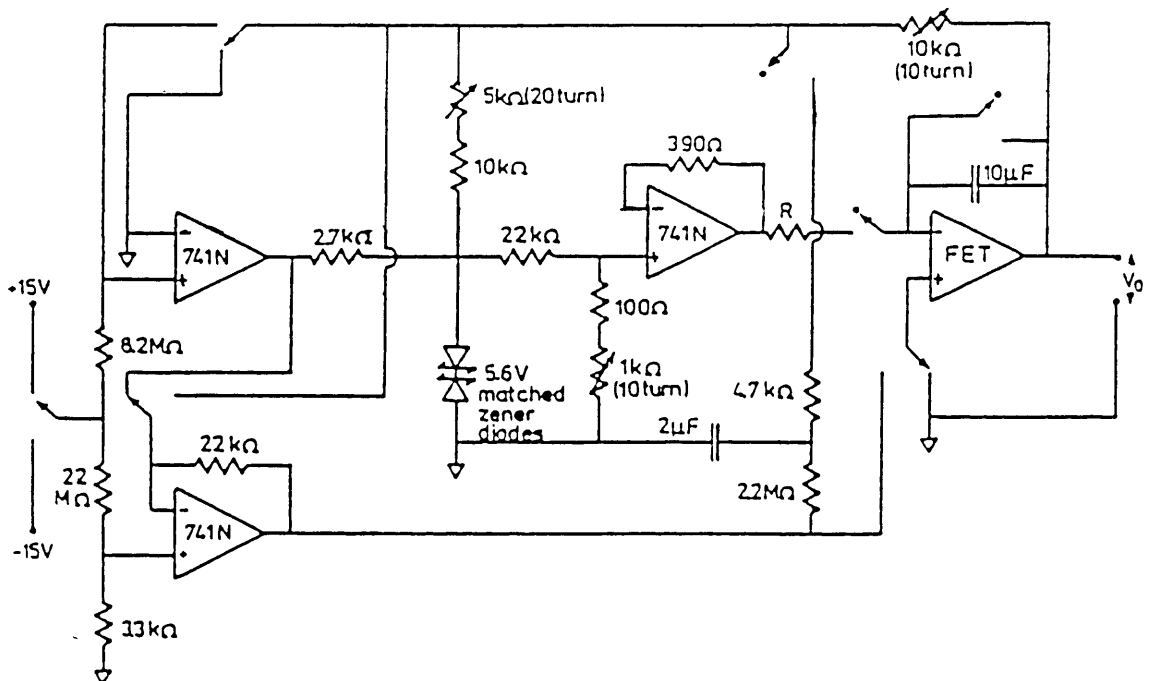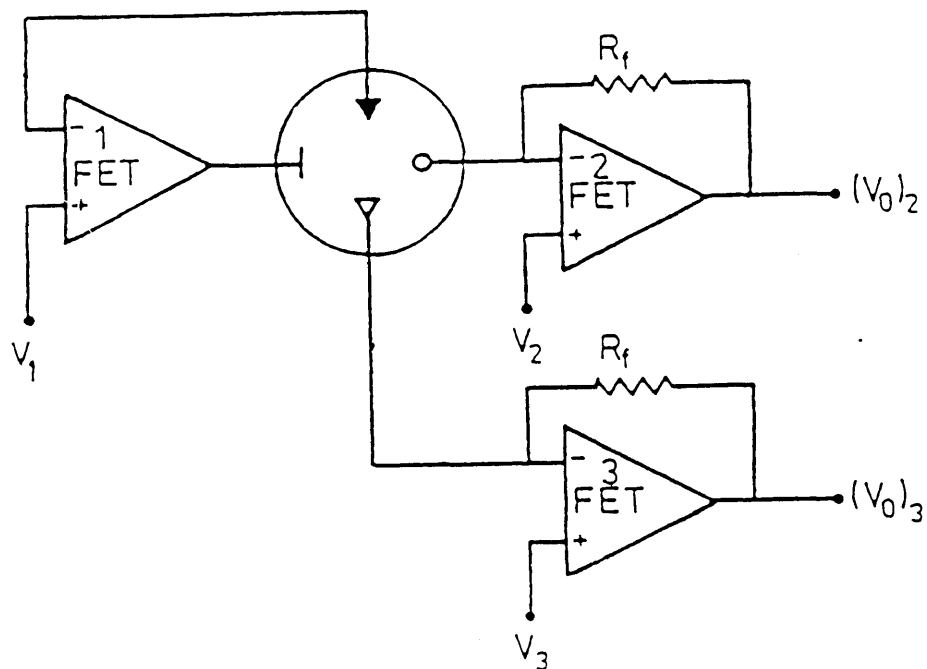
Figure 3.6. Potentiostat module for independent control of
two working electrodes ($R_f/k\Omega$ = 1,10 or 100)
($\dashv$ = counter electrode, $\rightarrow$ = reference electrode,
$\prec$ = disc electrode and O = ring electrode).
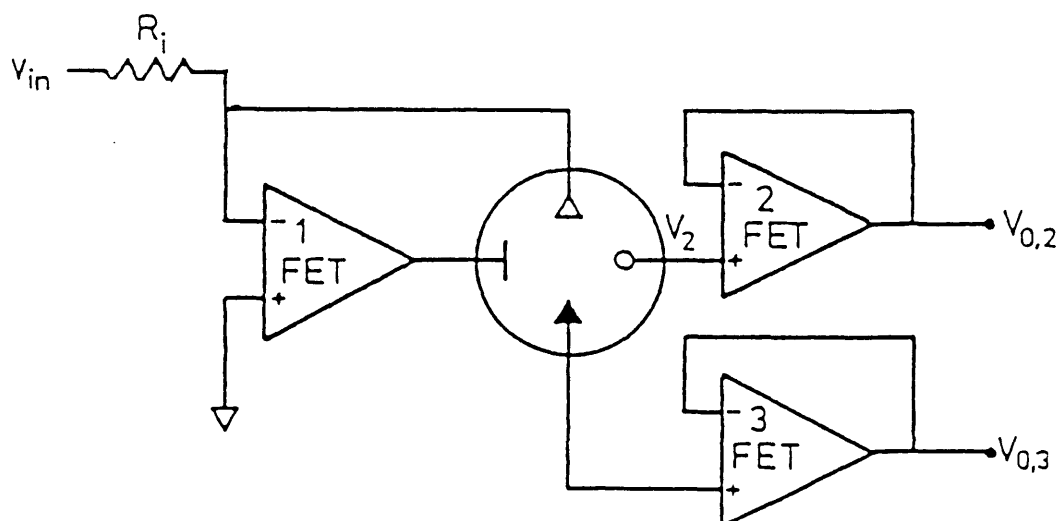
Figure 3.7. Galvanostat module, allowing control of the
current passing through one working electrode
and of the potential of the other.

several voltage followers (see figure 3.8 a-e). As these modular units and the operational amplifiers have been described several times elsewhere[133,134] no more details will be given.

The main circuit used is that in figure 3.9. In this circuit the potential of the working electrode (the disc) is controlled with respect to the reference electrode, without drawing any current from the reference electrode. The current is passed through the counter electrode. The output voltage from the potentiostat consists of the input voltage plus the current being passed in the cell multiplied by the measuring resistor (R_M). The input voltage is subtracted out by the subtractor, giving an output proportional to the current.

For a ring-disc electrode a more complicated circuit is necessary (see figure 3.10) with additional units for the control of the ring potential, which is done in a similar manner as for the disc.

Commercial instruments used included a digital voltmeter (Fluke 8000A), an x-y-t recorder (Bryans 29000 or 60000) and a digital storage oscilloscope (Gould OS4000 or OS4001). A Research Machines 380z microcomputer interfaced for electrochemistry was used for some experiments and a BBC microcomputer was used for data analysis.

3.4. Deoxygenation Systems

3.4.1. Aqueous

Aqueous solutions were deoxygenated with white spot nitrogen for twenty minutes before use. To remove any traces of oxygen, this nitrogen was first passed through three Dreschel bottles containing an aqueous caustic solution of anthraquinone-2-sulphonate in contact with amalgamated zinc. The gas was then passed through purified water to remove any anthraquinone compound and to presaturate the gas.

Figure 3.8. Modular electronic units
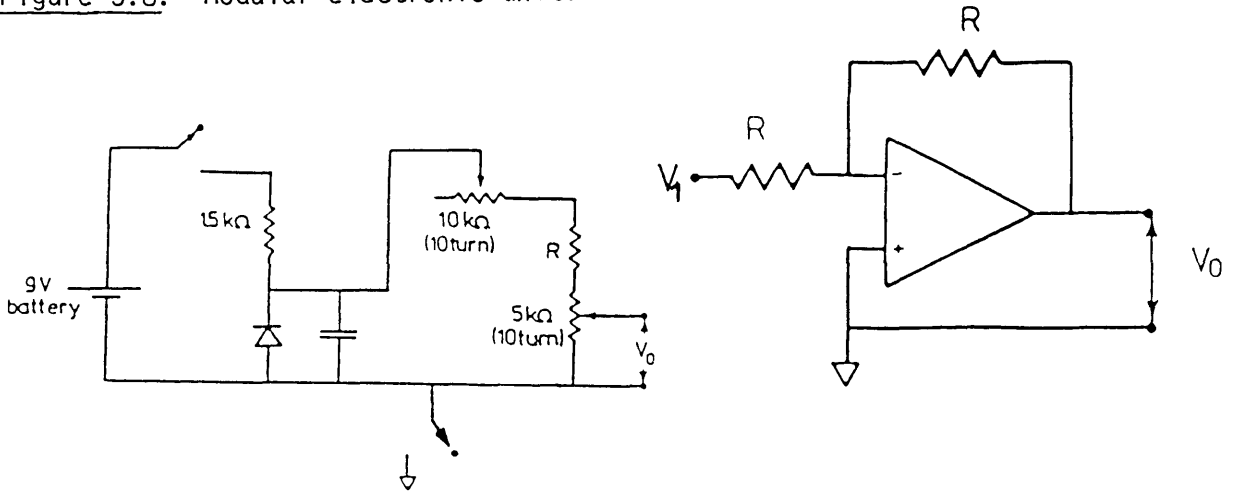
(a) Voltage source;
    R = 0, V_0(max) = ±5 V
    R = 22 kΩ, V_0(max) = ± 1 V

(b) Inverter;

$V_0 = -V_1$
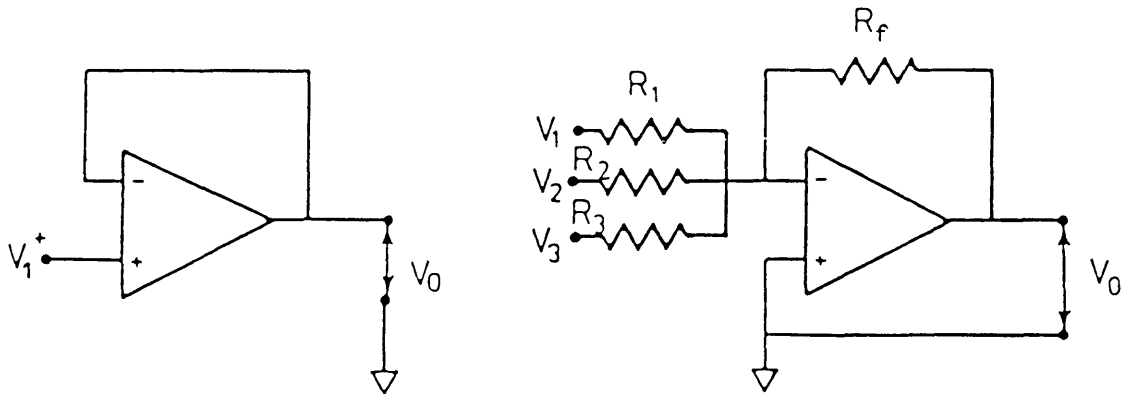
(c) Voltage follower;

$V_0 = V_1$.

(d) Summing inverter;

$$V_0 = -R_f \left(\frac{V_1}{R_1} + \frac{V_2}{R_2} + \frac{V_3}{R_3} \right)$$
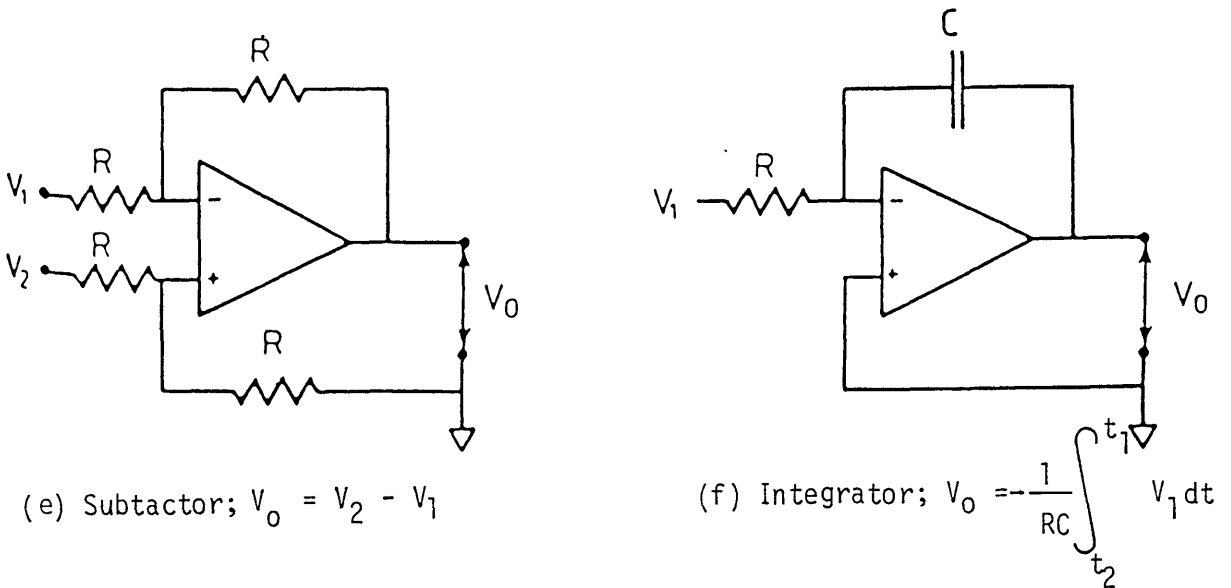
(e) Subtactor; $V_0 = V_2 - V_1$

(f) Integrator; $V_0 = -\frac{1}{RC} \int_{t_2}^{t_1} V_1 dt$

Figure 3.9. Block diagram of a circuit for potentiostatic disc electrochemistry.
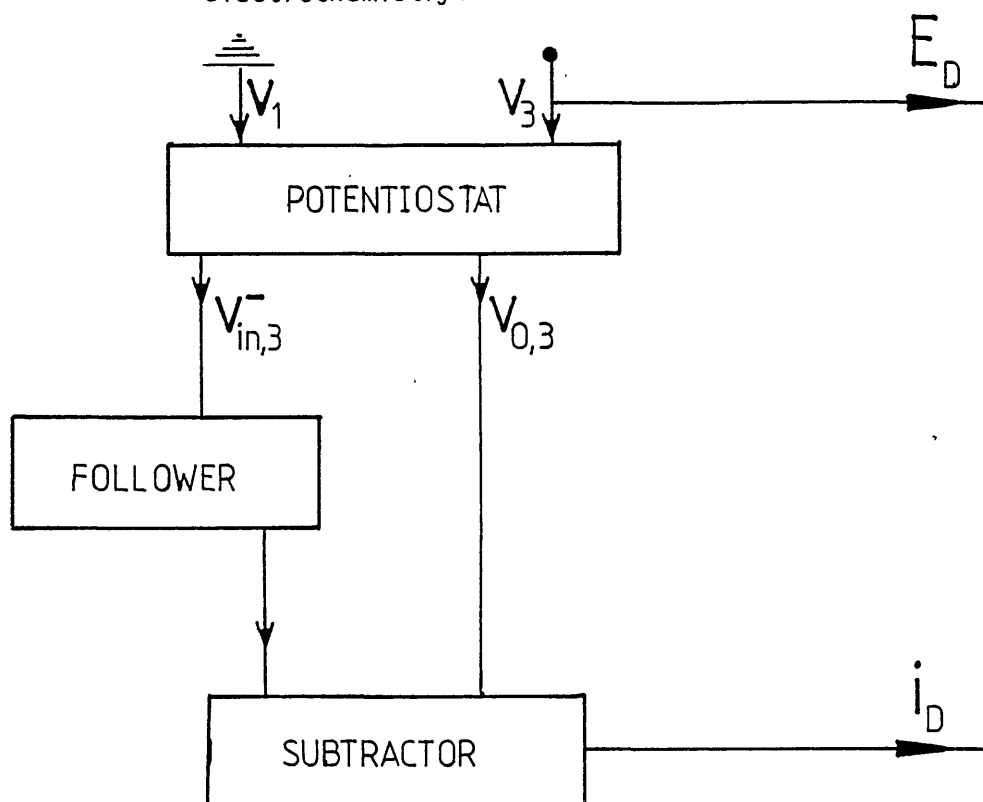
Figure 3.10. Block diagram of a circuit for potentiostatic ring-disc electrochemistry.
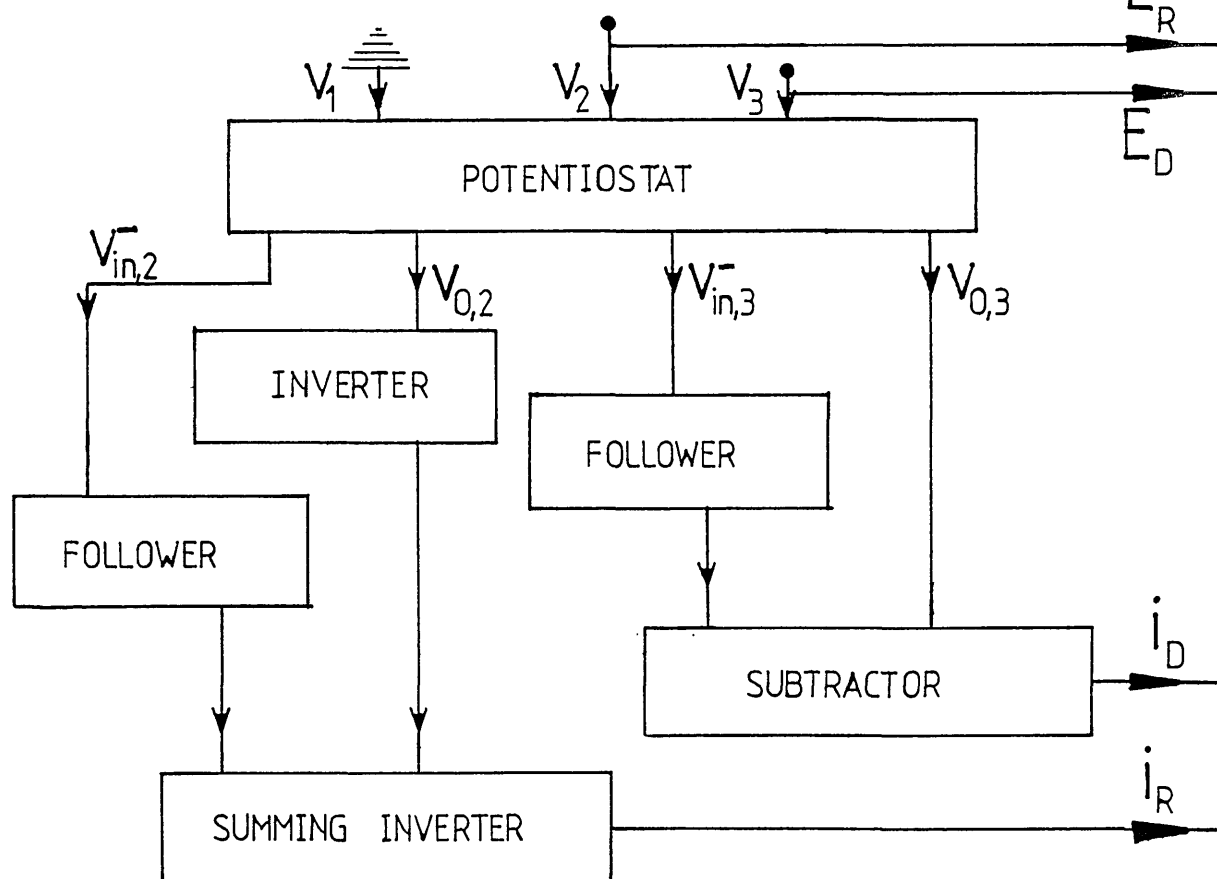
3.4.2. Non-aqueous

Non-aqueous solutions were deoxygenated with high purity (99.99%) argon for twenty minutes before use. This argon was purified by passing through calcium hydride for drying, down a chromium oxide/silica deoxygenating/drying column and then through two Dreschel bottles containing purified organic solvent, over activated molecular sieves, to presaturate the gas with the solvent being used. This gas presaturation is especially important with volatile solvents (e.g. chloroform) as otherwise evaporation of solvent in the electrochemical cell would occur rapidly, resulting in changes in concentration.

The deoxygenating/drying column was prepared by dissolving chromium trioxide (20 g) in distilled water (500 cm^3). Merck 7733 silica gel (400 g) was added and the mixture stirred for 30 minutes. This was then filtered and the solid dried for 12 hours at 120°C, under vacuum. This impregnated gel was then transferred to the column and heated in a stream of O$_2$ at 500°C for 30 minutes. Then, argon was passed through for 5 minutes followed by carbon monoxide for 15 minutes above 350°C. This was exchanged for high purity argon and the column was allowed to cool. Once used, these columns could be reactivated by following the above procedure from heating in a stream of O$_2$.

3.5. Solvent Purification

All solvents used for electrochemistry were purified and the following methods were found to be satisfactory,

Water

This was either de-ionised and then twice distilled or passed through a Millipore Milli-Q filter system.

Acetonitrile (Bp. 81.6°C)

Fisons dried, distilled acetonitrile was refluxed for two hours over calcium hydride (1% weight/volume) and then was fractionally distilled It could then be stored over activated 3 Å molecular sieves[135] under dry argon. If reagent grade acetonitrile is used, a much longer purification procedure is necessary[136].

Chloroform (Bp. 61°C)

This was dried over anhydrous calcium chloride for 24 hours and then fractionally distilled.

Dimethylsulphoxide (Bp. 189.0°C)

The best method found was by Mann[137]. This involved slowly freezing 80% of the batch. After discarding the liquid, the solid was melted, benzene (50 cm^3/dm^3) added and the mixture distilled to remove water. The remaining dimethylsulphoxide was rapidly distilled under vacuum and could be stored over activated 4 Å molecular sieves[138] under dry argon.

Ethanol (Bp. 78.3°C)

Absolute alcohol was treated with magnesium metal (activated by iodine) followed by fractional distillation.

The chloroform, dimethylsulphoxide and the absolute alcohol were obtained from B.D.H. Ltd. (AnalaR grade).

3.6. Supporting Electrolytes

Supporting electrolytes were used in 0.1 mol dm^{-3} concentration when the electroactive species being investigated was present in about

0.001 mol dm^{-3} concentration. They are added to carry the current in the bulk of the solution, hence minimising 'iR drop' and ensuring that the potential drop at the electrode is confined to the Helmholtz layer and does not spread out into the diffuse layer.

In aqueous solutions, depending on the required ions and pH, potassium chloride, potassium sulphate, hydrochloric acid, sulphuric acid and potassium hydroxide were used as supporting electrolytes. AnalaR reagents, from B.D.H. Ltd., were used without the need for further purification.

However, for non-aqueous solvents, the supporting electrolytes needed to be purified and dried. Several supporting electrolytes were used and their purifications are given.

Tetraethylammonium Perchlorate (TEAP, Et$_4$NClO$_4$)

Recrystallised three times from water. Dried under vacuum at 100°C.

Tetraethylammonium Tetrafluoroborate (TEAT, Et$_4$NBF$_4$)

Recrystallised three times from methanol-petroleum ether (Bp. $30-40^{\circ}$C). Dried under vacuum at 50°C.

Tetra-n-Butylammonium Perchlorate (TBAP, Bu$_4$NClO$_4$)

Recrystallised three times from ethyl acetate-petroleum ether (Bp. $40-60^{\circ}$C). Dried under vacuum at 100°C.

Tetra-n-Butylammonium Tetrafluoroborate (TBAT, Bu$_4$NBF$_4$)

Recrystallised three times from ethyl acetate-petroleum ether (Bp. $40-60^{\circ}$C). Dried under vacuum at 50°C.

Tetraethylammonium Chloride (TEAC, Et$_4$NCl)

Recrystallised three times from chloroform-ether. Dried under vacuum at 140°C.

All these tetra-alkylammonium salts were obtained from Fluka (Purum grade).

Lithium perchlorate (LiClO$_4$) and sodium tetrafluoroborate (NaBF$_4$), obtained from Aldrich, were also used on occasion. The only purification necessary for these was drying under vacuum. These inorganic supporting electrolytes gave smaller background currents in the positive potential region while the tetra-alkylammonium salts were better in the negative potential region.

3.7. Miscellaneous

All glassware was soaked in Decon 90 (BDH Ltd.), rinsed several times with purified water and dried in an oven.

Molecular sieves were activated at 300°C under a dry nitrogen (liquid nitrogen vapour) atmosphere immediately before use.

A number of experiments involved air sensitive or moisture sensitive materials. These were undertaken in a dry box under a high purity argon (99.99%) atmosphere.

All chemicals and solvents used for electrochemistry were purified, while for syntheses reagent grade chemicals were used unless otherwise stated.

All chemical preparations were analysed by microanalysis, mass spectroscopy, infra-red and NMR (60 MHz unless otherwise stated).

3.7.1. General Purifications

Triphenylphosphine

This was recrystallised twice from methanol and dried under vacuum. It was then stored under dry argon in the dark.

Pyrrole

This was distilled (Bp. 131°C) and stored over activated sieves (3 Å), under argon, in the dark.

Thiophene

This was distilled (Bp. 84°C) and stored under argon.

Furan

This was distilled (Bp. 32°C) and stored under argon at 5°C.

3-Bromothiophene and 3-Bromofuran

These compounds were stored at 0°C and used without any purification.

4. SOLUTION ELECTROCHEMISTRY

4.1. Introduction

Before investigating modified electrodes containing palladium and nickel redox centres it was felt that proper characterisation of the solution electrochemistry of these couples would be useful. Therefore, in this chapter, the investigation of the aqueous and non-aqueous electrochemistry of palladium and nickel complexes is presented. These results can later be used to identify redox reactions in polymer coated electrodes.

Some catalysis by solution species was also investigated and these results are presented in section 4.4.

In this work a number of complexes had to be synthesised and the experimental details of these syntheses are given in section 4.5, rather than interrupting the rest of the chapter.

Electrochemical investigation, in this chapter, was generally done on a rotating disc or rotating ring–disc electrode giving current voltage curves (see section 2.1). Unless otherwise stated in the text, the electrodes were rotated at 10 Hz and the potential, of the working electrode, was swept at 10 mV s^{-1}. Some cyclic voltammetry (see section 2.3) at stationary electrodes was also done and here the potential, of the working electrode, was swept at either 100 or 250 mV s^{-1}.

Exact conditions for the electrochemical experiments are given on the figures referred to in the text. This is to prevent unnecessary repetition in the text.

4.2. Solution Electrochemistry of Palladium Complexes

4.2.1. Aqueous Solutions

An aqueous solution of K_2PdCl_4 (1 mM), with KCl (0.1 M) supporting electrolyte, was investigated electrochemically using a glassy carbon rotating disc electrode (RDE). To minimise oxygen or hydrogen adsorption glassy carbon was chosen in preference to platinum. The electrode was rotated at 10 Hz and the potential swept at 10 mV s^{-1} to give a current voltage curve as shown in figure 4.1. The main feature is the reduction wave ($E_{\frac{1}{2}}$ = +0.26V vs SCE) due to palladium plating.

$$PdCl_4^{2-} \longrightarrow Pd_{(metal)} + 4Cl^-$$
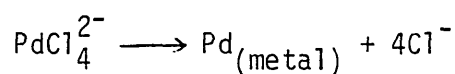
The palladium metal coat can be seen visually and it cannot be electrochemically stripped due to the noble nature of palladium metal.

Looking at the current voltage curve (see figure 4.1) one can also see an anodic peak (E_p = +0.6 V vs SCE), due to oxygen adsorption on the plated palladium metal, and a cathodic peak (E_p = -0.2 V vs SCE) from oxygen stripping. There is also a hydrogen adsorption peak (E_p = -0.7 V vs SCE) and its stripping peaks (E_p = -0.25 V and -0.35 V vs SCE).

Unlike clean glassy carbon (see figure 4.2) a palladium plated electrode shows these hydrogen and oxygen adsorption/stripping peaks in plain aqueous supporting electrolyte (see figure 4.3).

Therefore, one can see that palladium (II) reduction occurs, under these conditions, at $E_{\frac{1}{2}}$ = +0.26 V vs SCE, to give a palladium metal coat. This metal coat can be verified visually and by observing
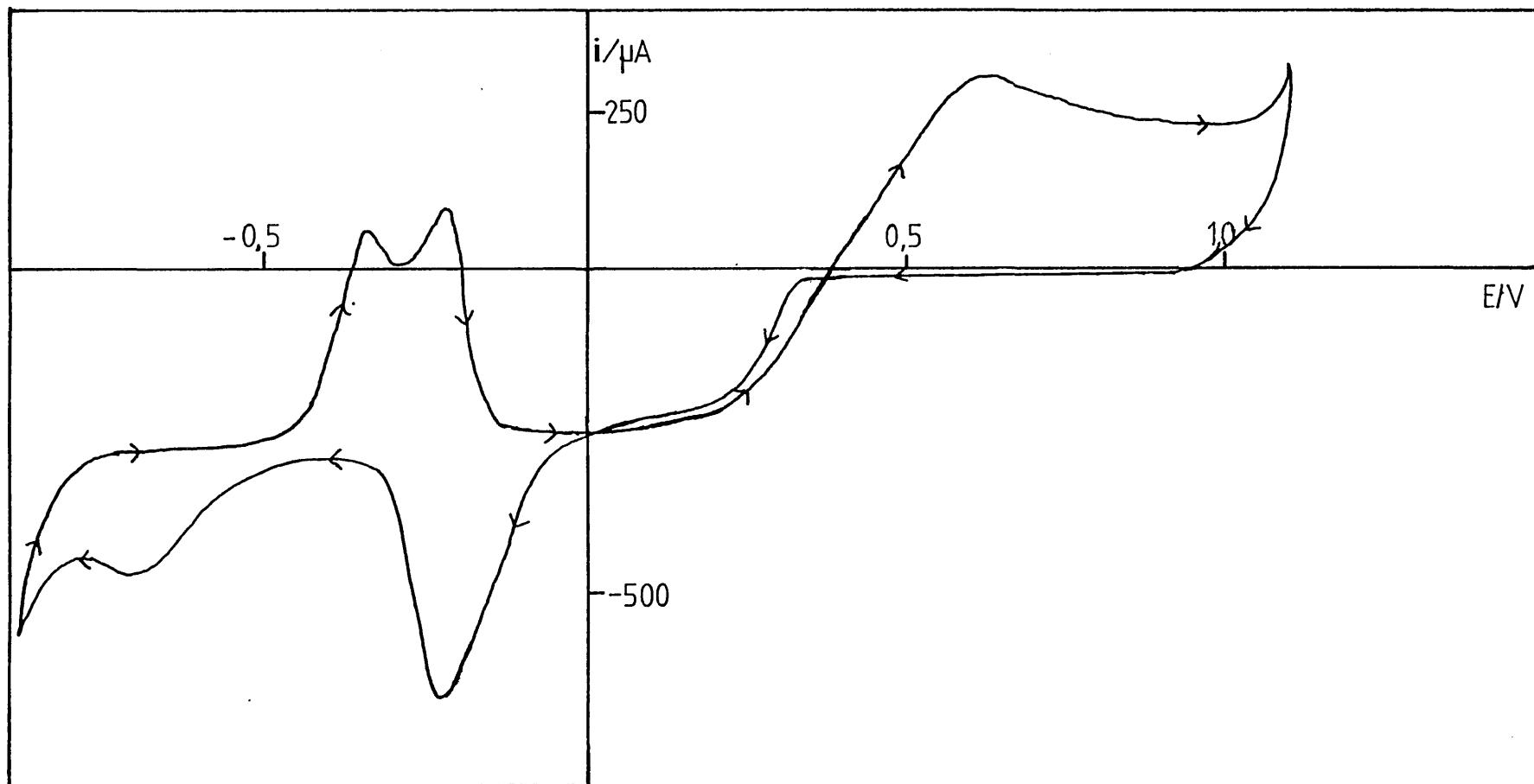
Figure 4.1. Current voltage curve for the reduction of K_2PdCl_4 at a RDE.
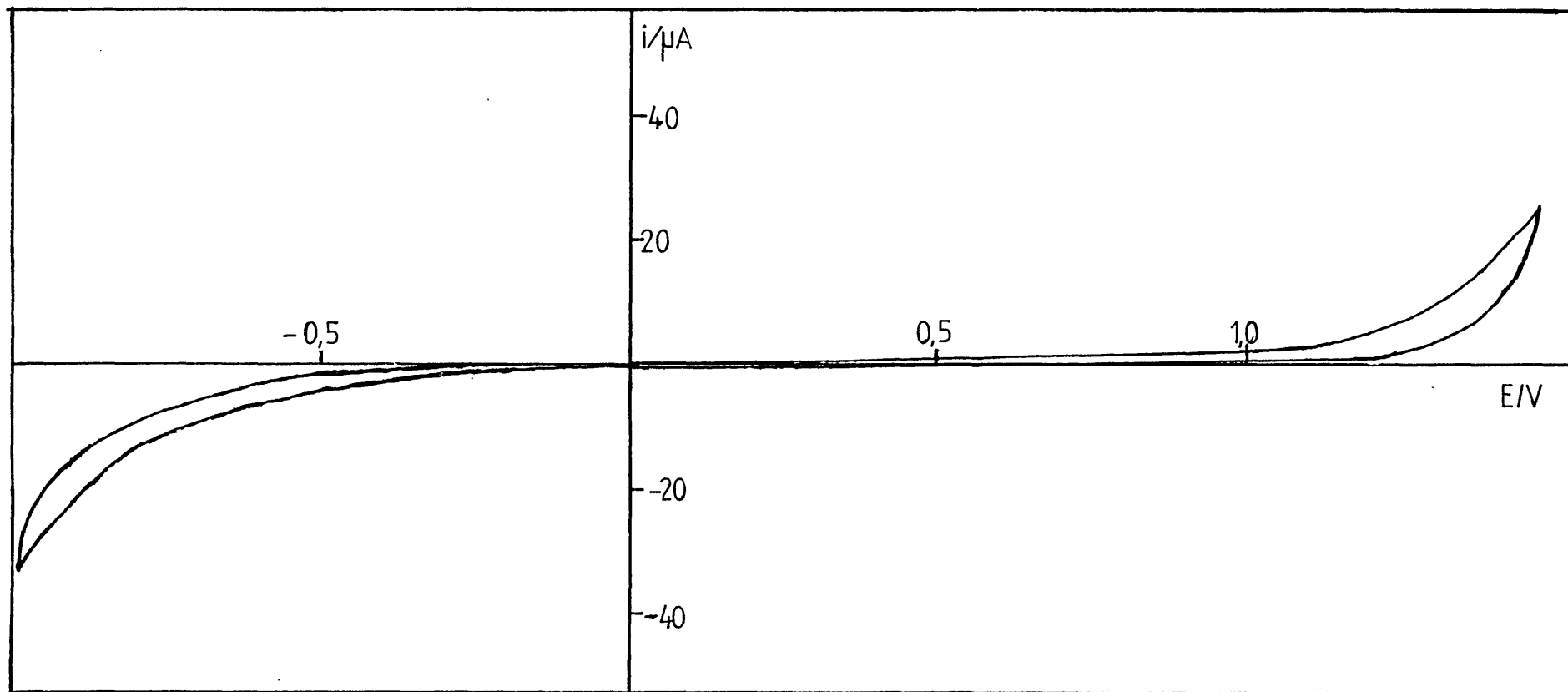
Figure 4.2. Current voltage curve for a clean glassy carbon RDE in aqueous 0.1 M KCl (W = 10 Hz, v (sweep rate) = 10 mV s^{-1}).
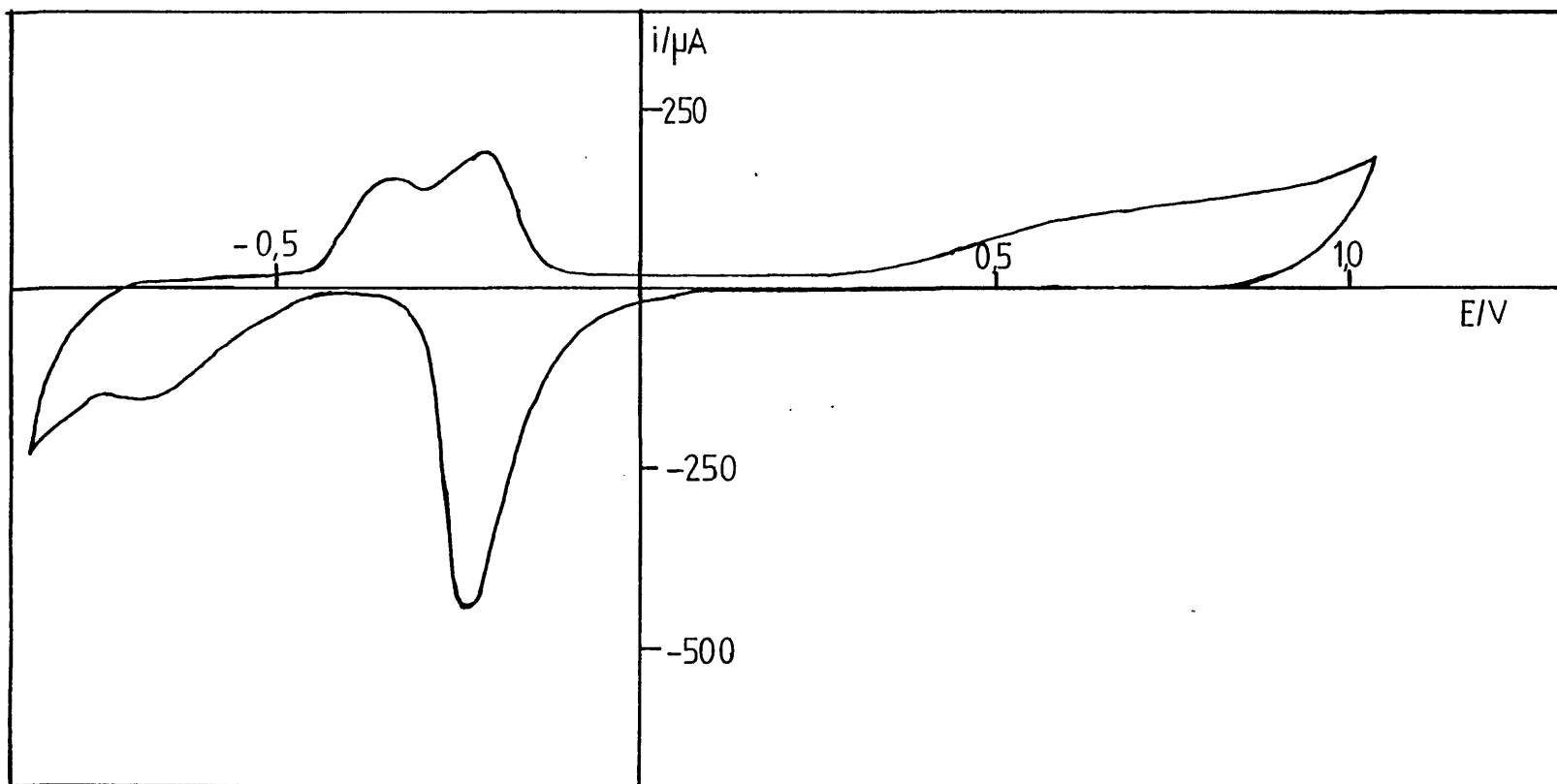
Figure 4.3. Current voltage curve for a palladium plated glassy carbon RDE in aqueous 0.1 M KCl (W = 10 Hz, v = 10 mV s⁻¹).

the oxygen and hydrogen adsorption/stripping peaks. When visual inspection is inconclusive, the oxygen and hydrogen adsorption/stripping peaks can be used to identify plated palladium metal.

4.2.2. Non-Aqueous Solutions

For polymer coated electrodes (see chapter 5) it was found necessary to use non-aqueous solvents and so electrochemical investigation of palladium solution species in non-aqueous conditions was pursued.

4.2.2.1. Electrochemistry of Pd(MeCN)$_2$Cl$_2$

Electrochemical reduction of Pd(MeCN)$_2$Cl$_2$ was tried as a method of incorporating palladium species into polymer coated electrodes (see chapter 5). Therefore, its solution electrochemistry was investigated.

Similar experiments, as with the aqueous solutions, were carried out on Pd(MeCN)$_2$Cl$_2$ (0.5 mM, synthesis in section 4.5) in acetonitrile (+ 0.1 M TBAT supporting electrolyte) with a glassy carbon RDE. One irreversible cathodic wave ($E_{\frac{1}{2}}$ = -2.0 V vs Ag/Ag$^+$, see figure 4.4), due to palladium plating, was observed. There was no other electrochemical activity, within solvent limits, due to the non-aqueous, anaerobic conditions.

4.2.2.2. Reversible Electrochemistry of the Palladium (II/0) Couple

One of the aims of this work was to produce a palladium incorporated polymer which would undergo reversible electrochemistry (i.e. Pd(II/0)). Phosphine ligand containing polymers were one type chosen to be investigated (see chapter 5) as these ligands are known to form stable complexes in both oxidation states.

Figure 4.4. Current voltage curve for the reduction of $Pd(MeCN)_2Cl_2$
(W = 10 Hz, v = 10·mV s^{-1}).
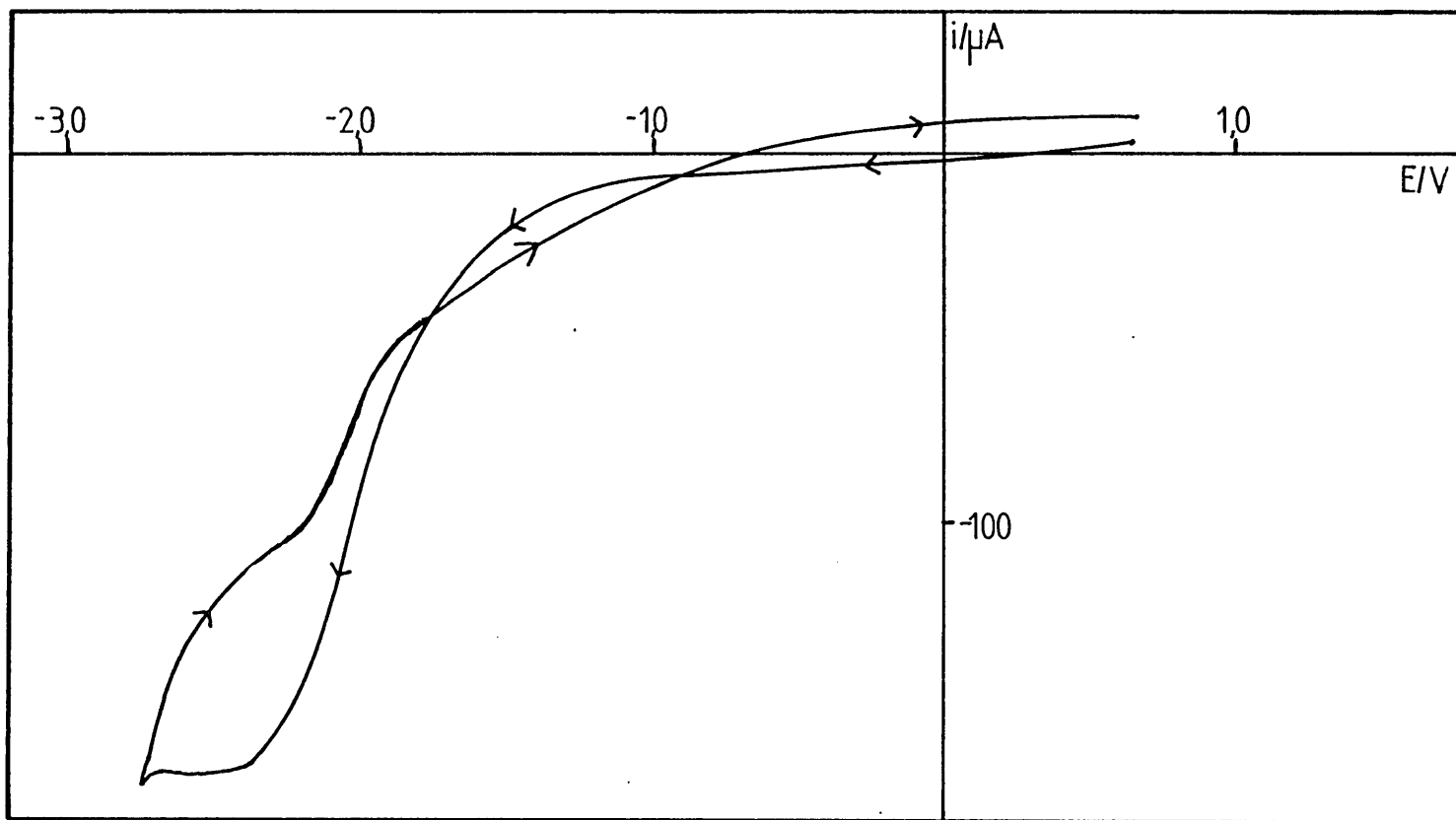
To aid the identification of the electrochemical couples in these polymers it was decided to investigate the solution electrochemistry of similar species. Mechanistic investigation of the solution electrochemistry of these species could also assist in deducing the mechanisms of similar reactions in polymer coats.

Therefore, $Pd(PPh_3)_2Cl_2$ was synthesised (see section 4.5) and a reaction of the form

$$Pd(PPh_3)_2Cl_2 + 2PPh_3 \rightarrow Pd(PPh_3)_4 + 2Cl^-$$
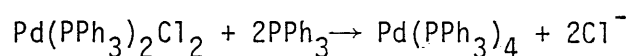
was envisaged.

Initially, for electrochemical investigations, a non-coordinating solvent was chosen to prevent possible ligand exchange

$$Pd(PPh_3)_2Cl_2 + S \rightleftharpoons Pd(PPh_3)SCl_2 + PPh_3$$
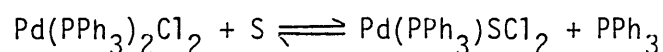
(where S = solvent).

Chloroform was found suitable. Using a platinum RDE chloroform, with TEAP (0.1 M) supporting electrolyte, gives solvent limits of +1.4 V and -1.8 V vs SCE (a saturated calomel reference electrode was used as an Ag/Ag^+ reference electrode was impractical due to the low solubility of silver salts in chloroform).

4.2.2.3. Electrochemistry of Triphenylphosphine

If in the electrochemical reduction of $Pd(PPh_3)_2Cl_2$, $Pd(PPh_3)_4$ is to be produced excess triphenylphosphine will be needed in solution. Therefore, to see how the presence of triphenylphosphine will affect potential limits, its electrochemistry was investigated.

Investigating triphenylphosphine (10 mM) in chloroform (+0.1 M TEAP) with a platinum RDE (rotating at 10 Hz, potential being swept at 10 mV s^{-1}) one observes phosphine oxidation ($E_{\frac{1}{2}}$ = +0.61 V vs SCE) which also tends to poison the electrode. Cyclic voltammetric analysis, at a platinum electrode, shows the expected three peaks (see figure 4.5) for phosphine anodic electrochemistry. These have been explained[139] as an oxidation (Peak 1)

$$PPh_3 \longrightarrow PPh_3^{\cdot+} + e^- \text{ at } E_p = +0.85 \text{ V vs SCE}$$

followed by a reduction (Peak 2)

$$PPh_3H^{+\cdot} + e^- \longrightarrow PPh_3 + \tfrac{1}{2}H_2 \text{ at } E_p = -0.25 \text{ V vs SCE}$$
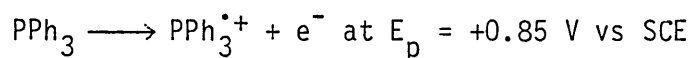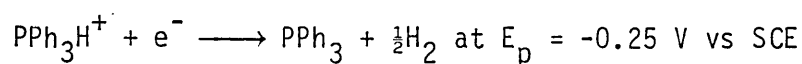
and, in the presence of PPh_3, the hydrogen thus formed can be oxidised (Peak 3)

$$\tfrac{1}{2}H_2 \longrightarrow H^+ + e^- \text{ at } E_p = +0.14 \text{ V vs SCE}$$
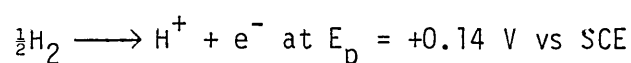
Figure 4.5. Cyclic voltammetric behaviour of triphenylphosphine in chloroform (+0.1 M TEAP) (v = 250 mV s^{-1}).
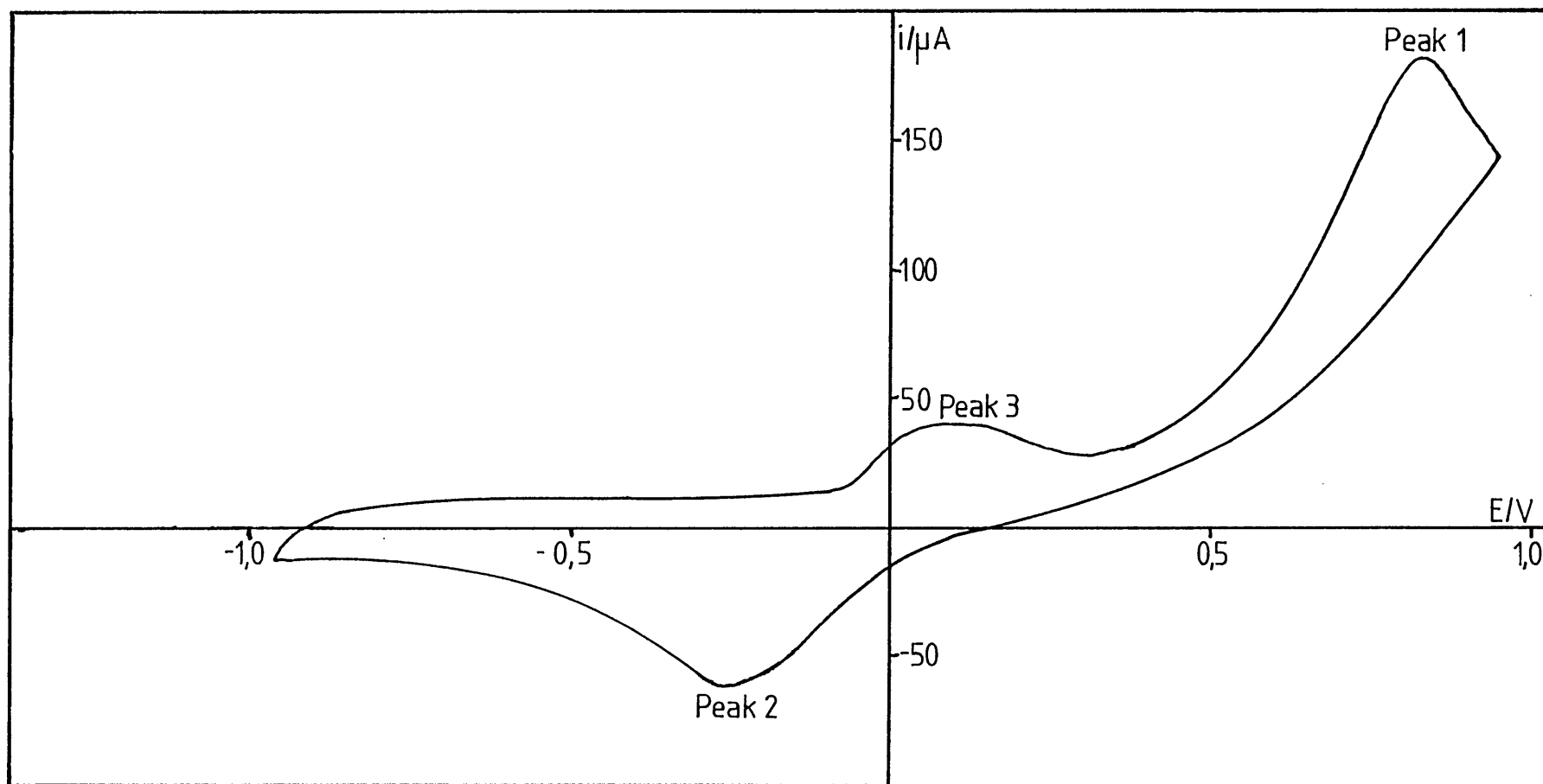
The PPh_3H^+ species is formed by the reaction of $PPh_3^{\cdot+}$ with traces of water

$$PPh_3^{\cdot+} + H_2O \longrightarrow PPh_3O + 2H^+ + e^-$$

and then

$$PPh_3 + H^+ \longrightarrow PPh_3H^+$$
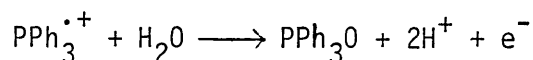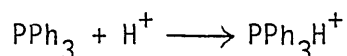
This explanation which was for acetonitrile, dimethylformamide and methanol solutions is quite reasonable considering the results presented and seems applicable to the above chloroform solution.

Due to this phosphine activity chloroform solutions, containing triphenylphosphine, were not investigated above +0.4 V vs SCE.

Similar investigations in acetonitrile (+ 0.1 M TBAT), with added triphenylphosphine (1 mM) gave peak 1 at +0.88 V vs Ag/Ag^+, peak 2 at -0.59 V vs Ag/Ag^+ and peak 3 at -0.30 V vs Ag/Ag^+.

4.2.2.4. <u>Electrochemistry of Pd$(PPh_3)_2Cl_2$ and Pd$(PPh_3)_4$ in Chloroform</u>
<u>Solutions</u>

Although a great deal of work has been done on palladium plating[140], reversible electrochemical analysis of palladium complexes has been very limited with only some recent interest in Russian journals[141,142].

In a chloroform solution of $Pd(PPh_3)_2Cl_2$ (4 mM), with TEAP (0.2 M)
supporting electrolyte, no electrochemistry, on a platinum RDE, was
observed within the solvent limits. However on the addition of triphenyl-
phosphine (40 mM) a reduction wave ($E_{\frac{1}{2}}$ = -0.52 V vs SCE), which is not
present in the absence of $Pd(PPh_3)_2Cl_2$, was observed (see figure 4.6).
Rotation speed dependence analysis of this wave gave a curved Levich
plot with a non-zero intercept (see figure 4.7) and linear Koutecky-
Levich dependence (see figure 4.8). As discussed in section 2.1, this
indicates that the current is not transport controlled. Therefore, for
the reduction of $Pd(PPh_3)_2Cl_2$, there is some process occurring in series
with the electrochemical reaction which is transport independent.

Cyclic voltammetric analysis, at a platinum electrode, of this
system gave a reduction wave, rather than an expected peak, at
$E_{\frac{1}{2}}$ = -0.50 V vs SCE and a reverse oxidation peak at E_p = +0.05 V vs SCE
(see figure 4.9). This oxidation peak is the regeneration of the
$Pd(PPh_3)_2X_2$ species from $Pd(PPh_3)_4$ formed by the reduction.

Therefore, using a platinum/platinum rotating ring disc electrode
(RRDE), the disc was held at -0.65Vvs SCE (a potential at which one
has limiting current) so that a fixed amount of $Pd(PPh_3)_4$ is generated.
The ring potential was then swept anodically (at 10 mV s^{-1}) and an
oxidation wave was observed ($E_{\frac{1}{2}}$ = -0.02 V vs SCE). Within experimental
error, the collection efficiency (see section 2.1) was the theoretical
value. This indicates two properties of the disc's reaction product.
Firstly, it is stable and does not react with solution species and
secondly, it does not need to undergo any solution chemistry before
being reoxidised, electrochemically, at the ring.

To ensure that the above oxidation was that of $Pd(PPh_3)_4$, this
complex was synthesised (see section 4.5) and investigated electrochemically

Figure 4.6. Current voltage curve for the reduction of $Pd(PPh_3)_2Cl_2$ in the presence of excess PPh_3 ($W = 10$ Hz, $v = 10$ mV s^{-1}).
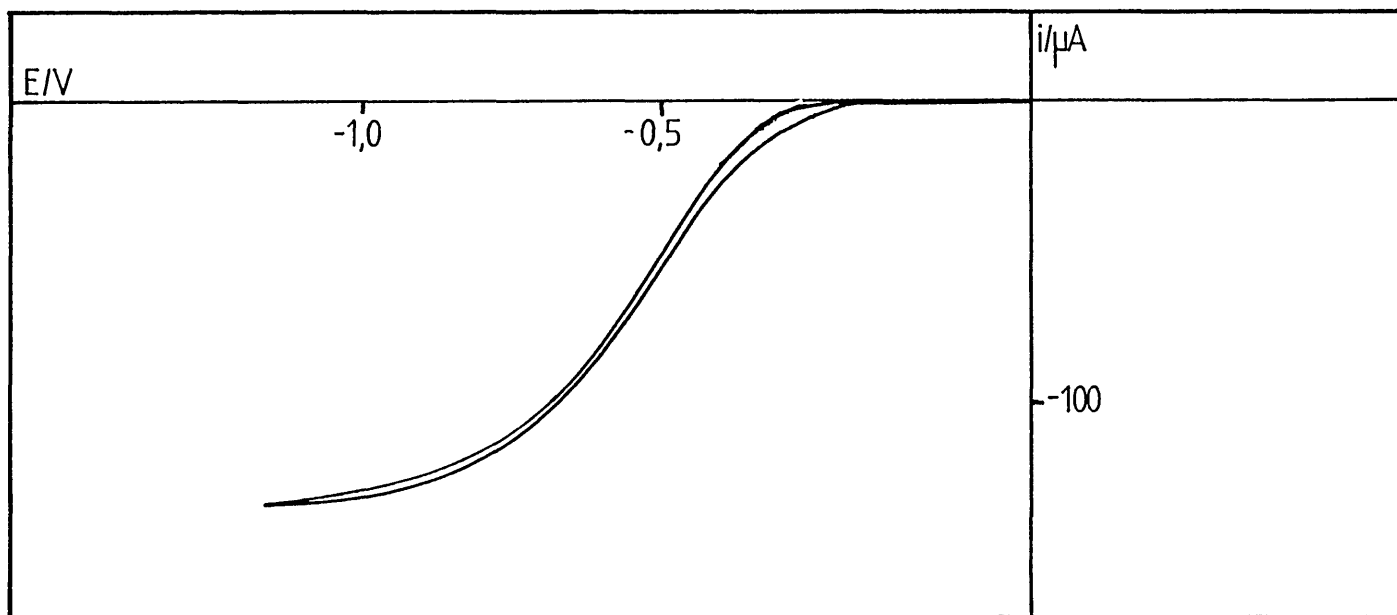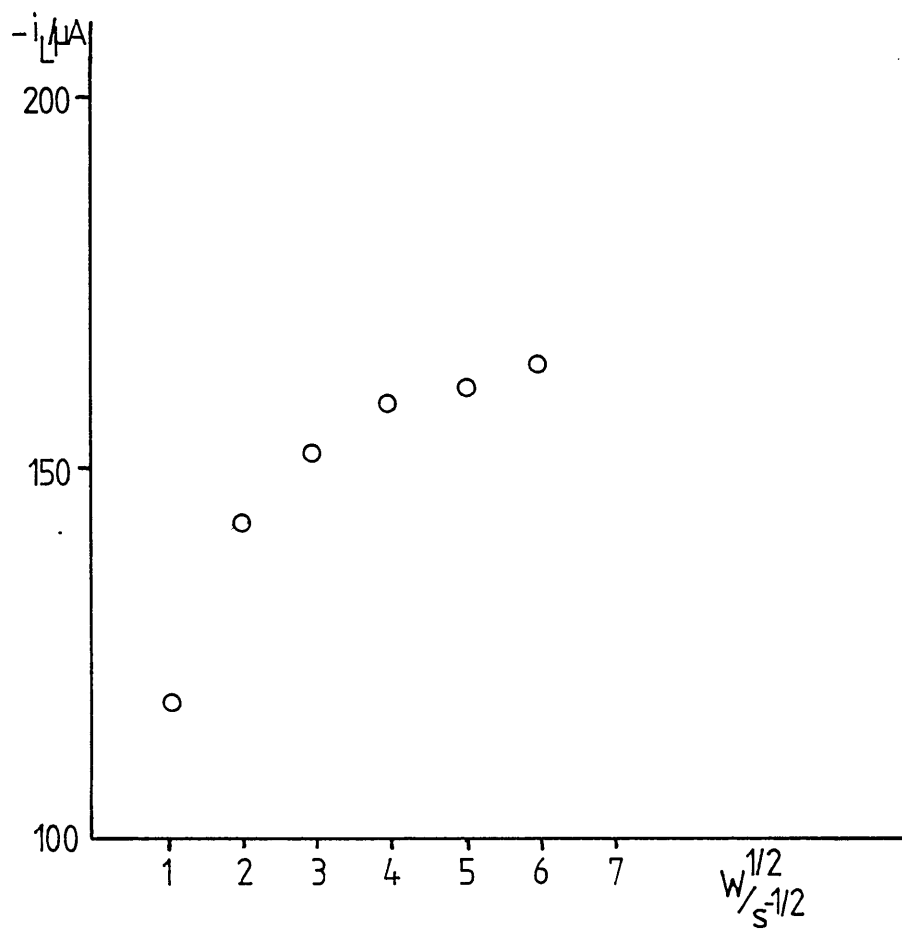
Figure 4.7. Levich plot for the reduction of $Pd(PPh_3)_2Cl_2$ in the presence of excess PPh_3 (see figure 4.6).

Figure 4.8. Koutecky-Levich plot for the reduction of $Pd(PPh_3)_2Cl_2$ in the presence of excess PPh_3 (see figure 4.6).
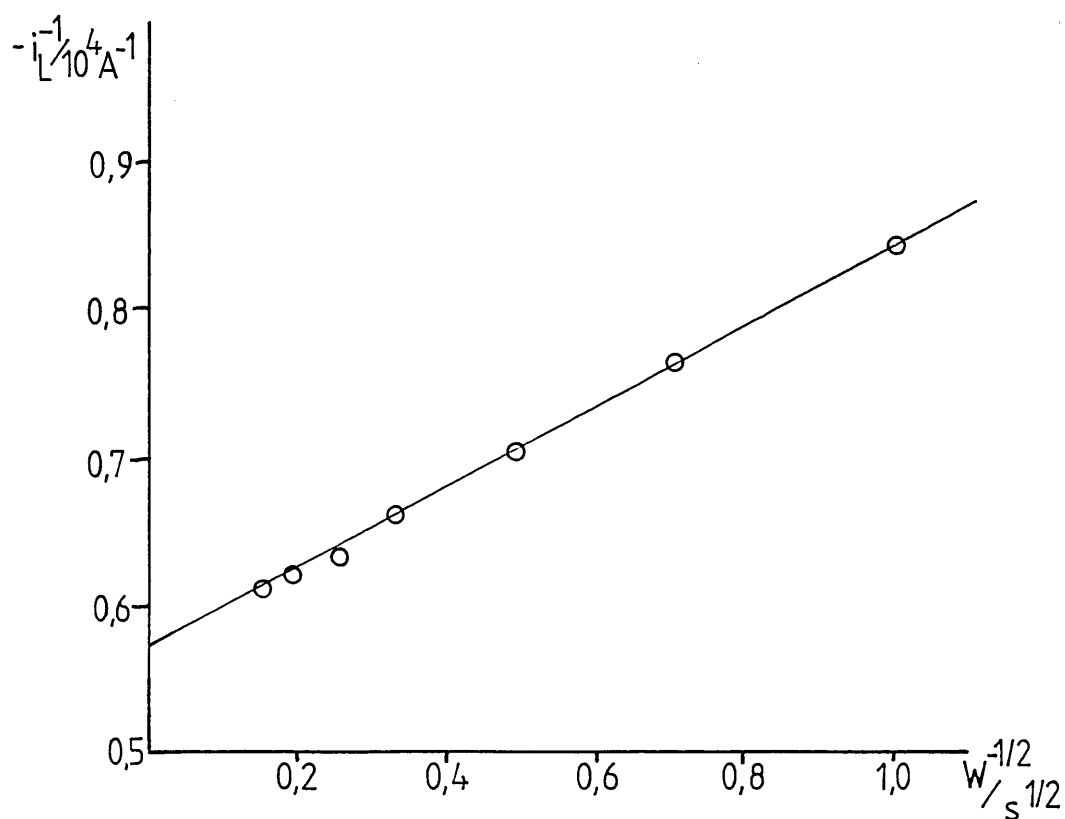
Figure 4.9. Cyclic voltammogram of $Pd(PPh_3)_2Cl_2$, with excess PPh_3, in chloroform ($v = 100$ mV s^{-1}).
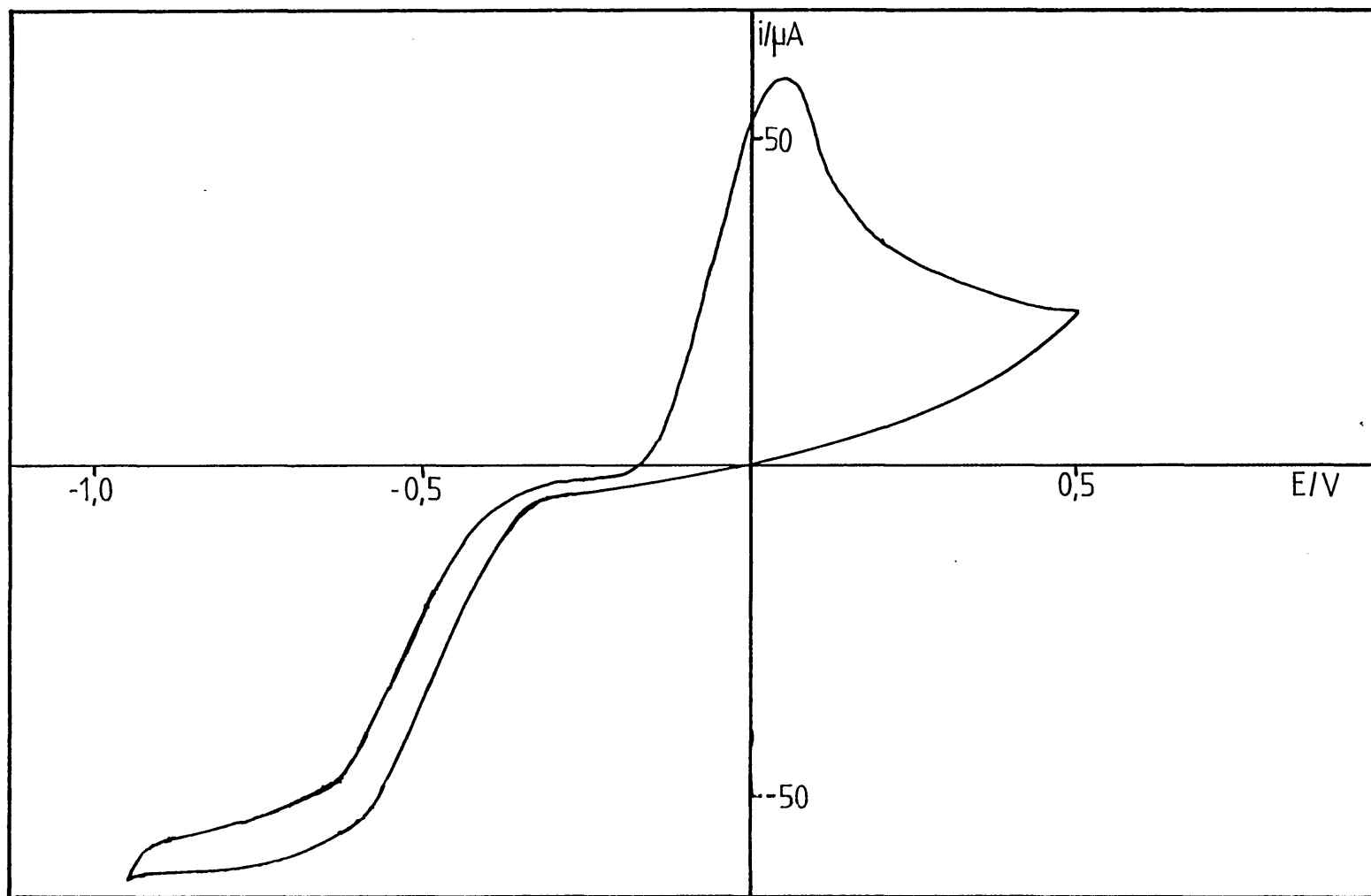
in chloroform (+ 0.1 M TEAP). At a platinum RDE an oxidation wave

was observed at $E_{\frac{1}{2}}$ = -0.02 V vs SCE (see figure 4.10) which showed

Levich dependence (see figure 4.11) on rotation speed, indicating

a transport controlled electrochemical reaction. Using a platinum/

platinum RRDE, now holding the disc potential at +0.2 V vs SCE (the

top of the oxidation wave) and sweeping the ring potential cathodically

(at 10 mV s^{-1}) a reduction wave was observed at $E_{\frac{1}{2}}$ = -0.52 V vs SCE.

However, this time, the collection efficiency was well below the

theoretical value and dependent on the rotation speed. This indicates

that the disc's oxidation product either needs to undergo some solution

reaction before it can be reduced or is unstable and is decomposing

in solution.

Thus, from the above results one can see that in excess triphenyl-

phosphine $Pd(PPh_3)_2Cl_2$ can be reduced electrochemically to $Pd(PPh_3)_4$

and $Pd(PPh_3)_4$ can be oxidised to $Pd(PPh_3)_2X_2$. The mechanism of this

couple was investigated further and this is discussed in the next

section.

4.2.2.5. Study of the Mechanism of the $Pd(PPh_3)_2Cl_2/Pd(PPh_3)_4$ Couple

To help in the determination of the mechanism for this couple,

the solution chemistry of $Pd(PPh_3)_4$ and $Pd(PPh_3)_2Cl_2$ complexes was

sought in the literature.

Initially, looking at $Pd(PPh_3)_4$, spectroscopic analysis of

benzene solutions[143] has shown complete dissociation

$$Pd(PPh_3)_4 \rightleftharpoons Pd(PPh_3)_3 + PPh_3$$
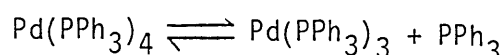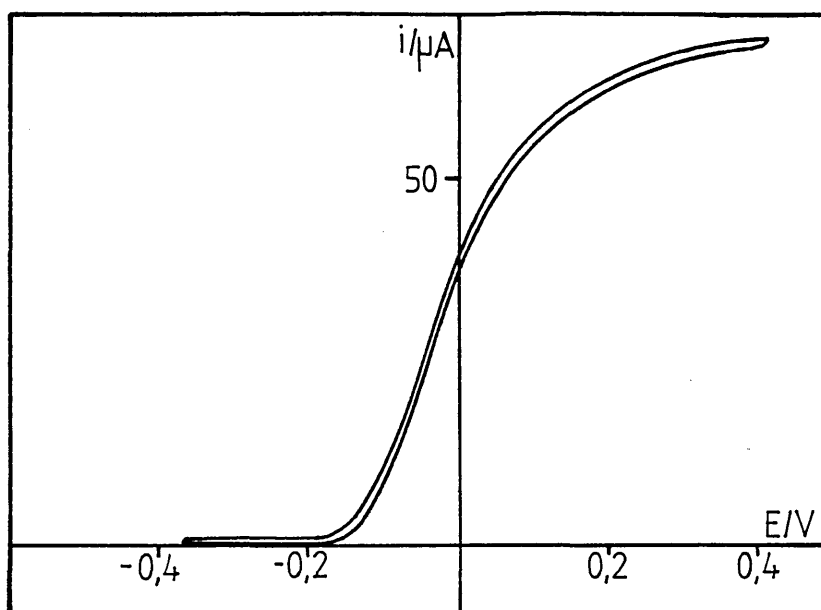
Figure 4.10. Current voltage curve for the oxidation of $Pd(PPh_3)_4$ (W = 10 Hz, v = 10 mV s^{-1}).

Figure 4.11. Levich plot for the oxidation of $Pd(PPh_3)_4$ (see figure 4.10).
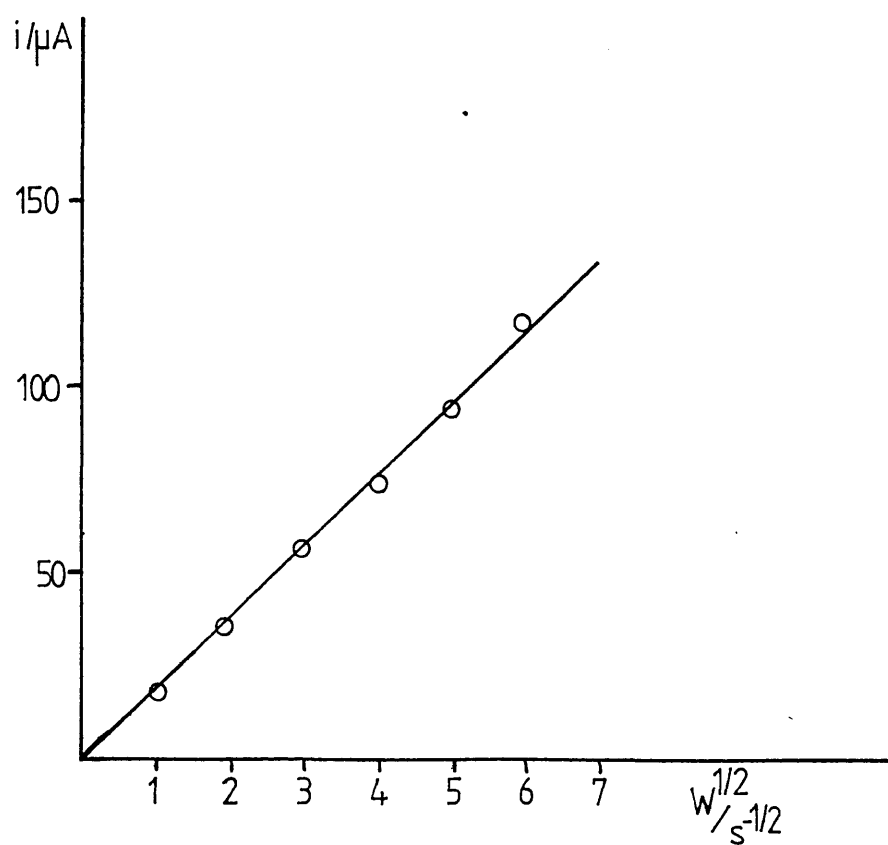
and even with 1 M triphenylphosphine present in solution, $Pd(PPh_3)_4$ could not be detected. This indicates that the equilibrium constant must be greater than 10 mol dm^{-3}.

This paper[143] also looks at the possibility of further dissociation

$$\text{i.e. } Pd(PPh_3)_3 \rightleftharpoons Pd(PPh_3)_2 + PPh_3$$
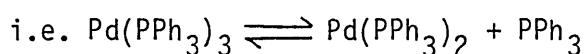
and found that this equilibrium was not detectable which indicates an equilibrium constant less than 10^{-6} mol dm^{-3}.

Dissociation of $Pd(PPh_3)_4$ and $Pt(PPh_3)_4$, in solution, has been widely reported in the literature[144,145]. Assuming similar behaviour in the above electrochemical solutions, one can postulate that $Pd(PPh_3)_3$ is the major palladium species with less than 1% $Pd(PPh_3)_4$ or $Pd(PPh_3)_2$ being present.

Moving to the solution chemistry of $Pd(PPh_3)_2Cl_2$, it is interesting to note that for its electrochemical reduction (at $E_{\frac{1}{2}}$ = -0.52 V vs SCE in chloroform) excess triphenylphosphine was needed to be present. It was also noted that, at a platinum RDE, the limiting reduction current increased with increasing triphenylphosphine concentration, while the half wave potential remained constant.

Looking at the solution chemistry of $Pd(PPh_3)_2Cl_2$, great interest has been shown[146,147,148] in its cis-trans isomerisation. This isomerisation is catalysed by trace amounts of free triphenylphosphine. The mechanism of this process has been fully discussed in a review published by Anderson and Cross[149]. The cis-trans isomerisation goes via a 5-coordinate trigonal bipyramidal transition state. This transition state can pseudo-rotate to form a square-pyramidal

intermediate. It is suggested that regarding this configuration as an intermediate, rather than a transition state, is not unreasonable as vacant sites (in the octahedral positions) are almost certainly solvated[150,151,152], whereas trigonal bipyramidal complexes are not, at the cost of some energy (see figure 4.12). Polar solvents form ionic intermediates which result from the displacement of the axial ligand (see figure 4.12A). The overall isomerisation profile is shown in figure 4.13, where the intermediate

(Point C)
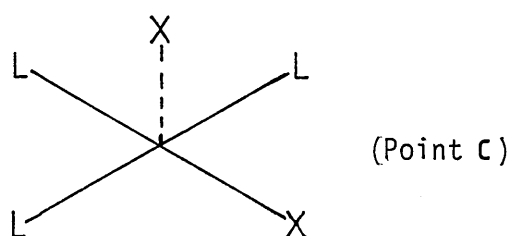
can either be dissociated to give ionic species $(Pd(PPh_3)_3X)^+$, associated to give a pentavalent $(Pd(PPh_3)_3X_2)$ species or something between the two.

Looking at the solution chemistry of $Pd(PPh_3)_4$ and $Pd(PPh_3)_2Cl_2$, a scheme of squares, for the above electrochemical behaviour, is proposed in figure 4.14. It has already been discussed that at point (dz), on the scheme of squares, the equilibrium is completely to the left, with $Pd(PPh_3)_3$ being the species present in solution.

Investigating the electrochemical oxidation of $Pd(PPh_3)_3$ $(Pd(PPh_3)_4$ dissociated in solution) a straightforward two electron wave, showing Levich dependence, has been described above. Also, theoretical collection efficiencies, for $Pd(PPh_3)_3$ generated at the disc, were observed.

Tafel analysis (see equation 2.21) of the observed oxidation current voltage curve (e.g. figure 4.10) gives the expected straight line plot (see figure 4.15). From the slope one gets a value
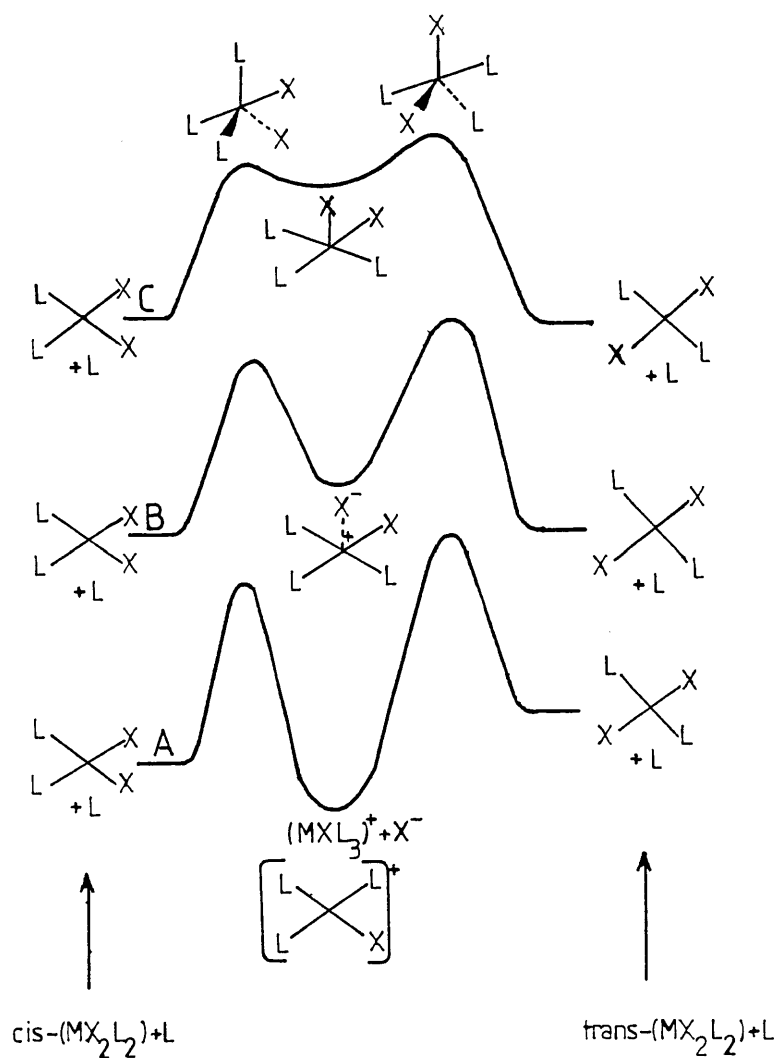
Figure 4.12.   Reaction profiles of L-catalysed cis-trans
               isomerisations of MX_2L_2 (where M = Pd^{2+},
               X = Cl^- and L = PPh_3). A: polar solvent,
               favouring the formation of ionic inter-
               mediates. B: intermediate polarity solvent
               allowing ion-pair formation. C: non-polar
               solvent with 5-coordinate intermediates.
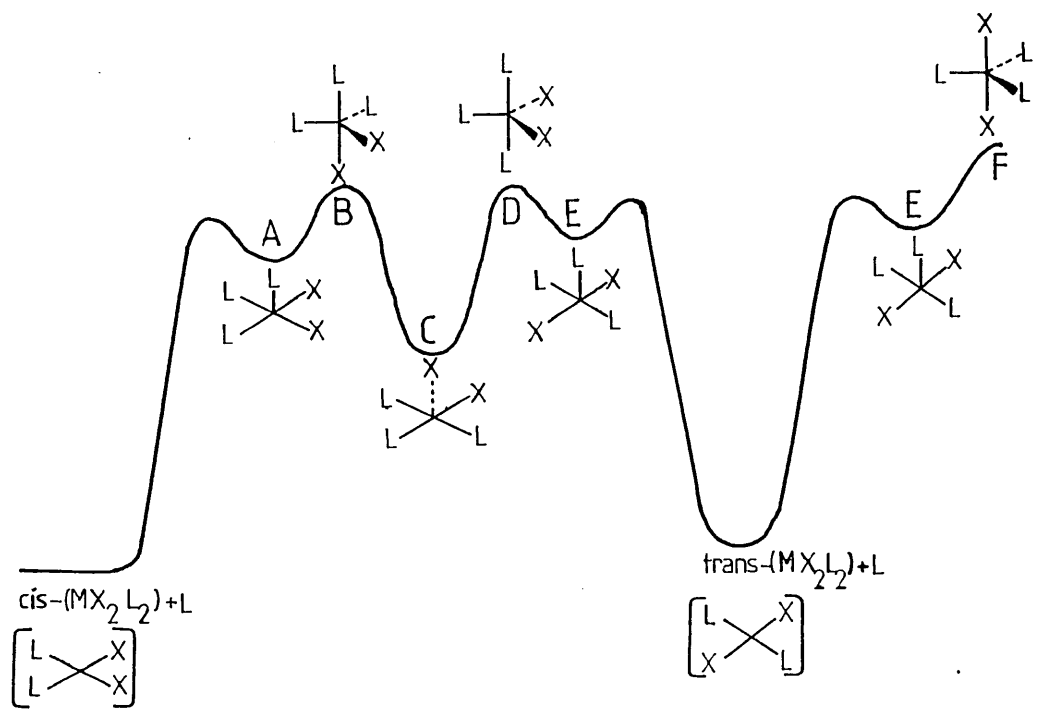
Figure 4.13. Overall profile for the isomerisation of MX_2L_2. No significance should be attached to the relative energies of intermediates or transition states, except that C is probably of lower energy than the others. The nature of C depends on the solvent (see figure 4.12).

Figure 4.14. (See overleaf).

$$\xrightarrow{+PPh_3} \qquad \xrightarrow{-Cl^-} \qquad \xrightarrow{-Cl^-} \qquad \xrightarrow{+PPh_3}$$

$$Pd(PPh_3)_2Cl_2 \underset{}{\overset{(ax)}{\rightleftharpoons}} Pd(PPh_3)_3Cl_2 \underset{}{\overset{(bx)}{\rightleftharpoons}} Pd(PPh_3)_3Cl^+ \underset{}{\overset{(cx)}{\rightleftharpoons}} Pd(PPh_3)_3^{2+} \underset{}{\overset{(dx)}{\rightleftharpoons}} Pd(PPh_3)_4^{2+}$$

$$-e \quad (1) \qquad (2) \qquad (3) \qquad (4) \qquad (5) \quad +e$$

$$Pd(PPh_3)_2Cl_2^- \underset{}{\overset{(ay)}{\rightleftharpoons}} Pd(PPh_3)_3Cl_2^- \underset{}{\overset{(by)}{\rightleftharpoons}} Pd(PPh_3)_3Cl \underset{}{\overset{(cy)}{\rightleftharpoons}} Pd(PPh_3)_3^+ \underset{}{\overset{(dy)}{\rightleftharpoons}} Pd(PPh_3)_4^+$$

$$-e \quad (i) \qquad (ii) \qquad (iii) \qquad (iv) \qquad (v) \quad +e$$

$$Pd(PPh_3)_2Cl_2^{2-} \underset{}{\overset{(az)}{\rightleftharpoons}} Pd(PPh_3)_3Cl_2^{2-} \underset{}{\overset{(bz)}{\rightleftharpoons}} Pd(PPh_3)_3Cl^- \underset{}{\overset{(cz)}{\rightleftharpoons}} Pd(PPh_3)_3 \underset{}{\overset{(dz)}{\rightleftharpoons}} Pd(PPh_3)_4$$

$$\xleftarrow{-PPh_3} \qquad \xleftarrow{+Cl^-} \qquad \xleftarrow{+Cl^-} \qquad \xleftarrow{-PPh_3}$$
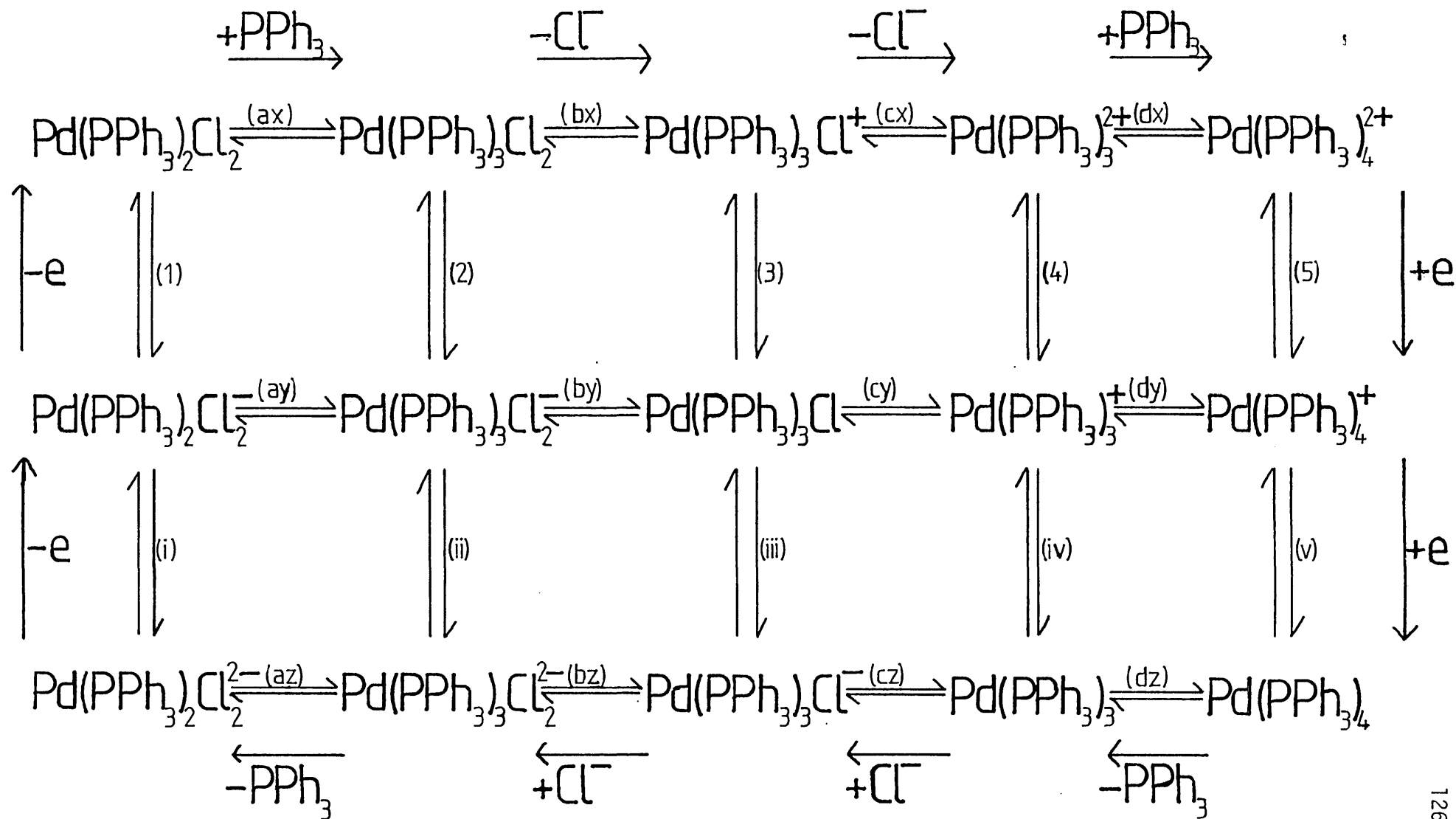
Figure 4.14. The scheme of squares for the $Pd(PPh_3)_2Cl_2/Pd(PPh_3)_4$ redox couple. This shows the possible routes by which $Pd(PPh_3)_2Cl_2$ is reduced to $Pd(PPh_3)_4$ and by which $Pd(PPh_3)_4$ is oxidised to $Pd(PPh_3)_2Cl_2$. Verticle equilibria (i.e. (1)-(5) and (i) → (v)) are electron transfers while horizontal equilibria (i.e. ax - dz) are either loss or gain of ligands. The horizontal axis shows both Cl^- and PPh_3 ligand equilibria, as to separate these would require the use of a third axis hence giving a scheme of cubes, which would be very complicated. As only a two-dimensional diagram is presented, certain equilibria, which can be assumed to be unimportant for this system, have been omitted.
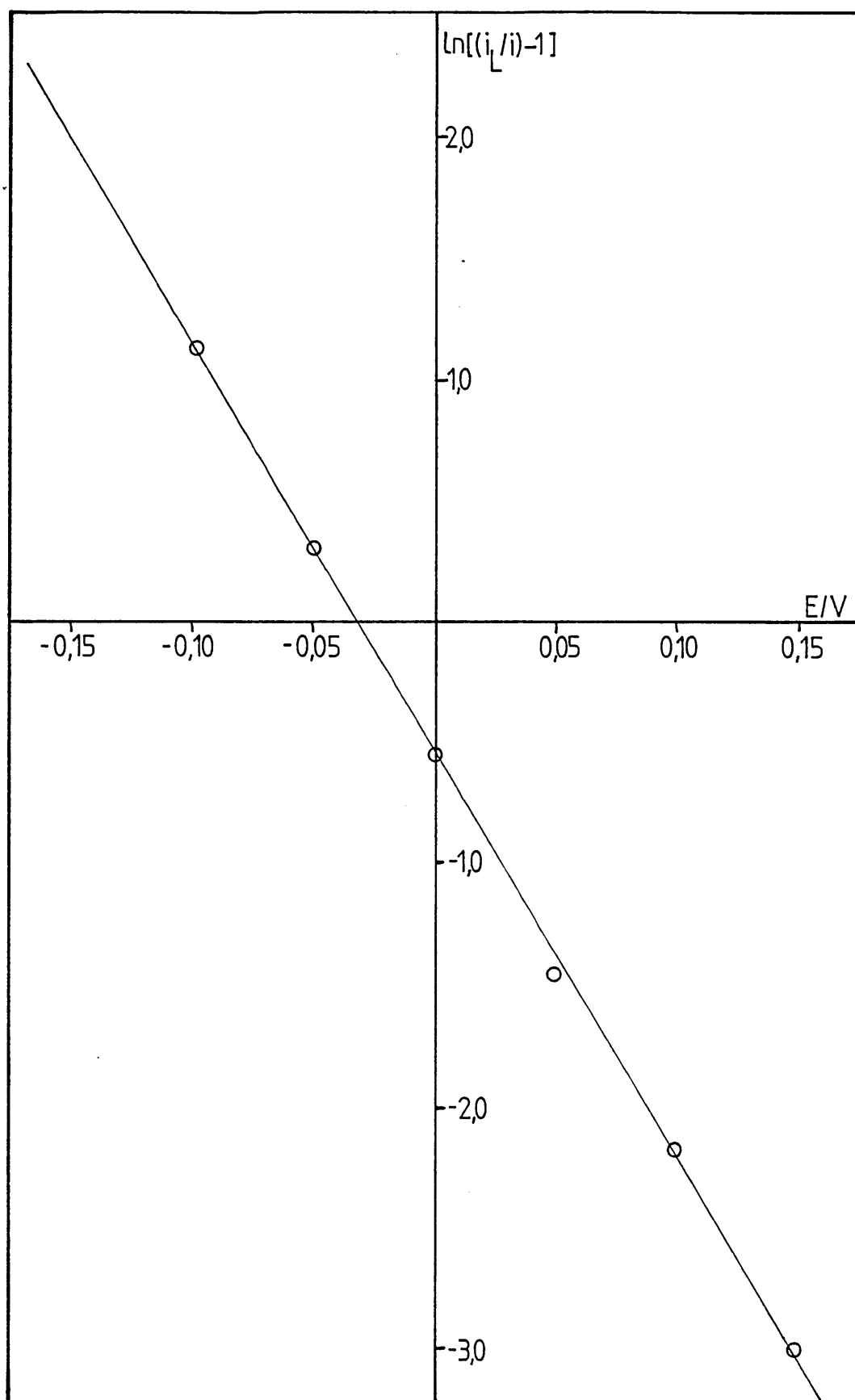
Figure 4.15. Tafel plot for the oxidation of $Pd(PPh_3)_3$.

for the oxidative transfer coefficient of 0.42 ($\pm$ 0.05), indicating

the first electron transfer is rate-limiting. Therefore, looking

at the scheme of squares, one of positions (i) - (v) is the transition

state for the electrochemical oxidation of $Pd(PPh_3)_3$. The formal

electrode potential for the couple is unknown and as the cyclic voltam-

mogram's peaks are so far apart (see figure 4.9) it cannot be estimated.

However, taking it as the half-way point between the oxidation and

reduction peaks (i.e. $E_\frac{1}{2} = -0.23$ V vs SCE), one gets a value for the

electrochemical rate constant

$$k'_{E_\frac{1}{2}} \sim 5 \times 10^{-5} \text{ cm s}^{-1}$$

which is quite sluggish.

It was also observed that the transport limited current, for

the oxidation of $Pd(PPh_3)_3$, did not vary with varying concentrations

of PPh_3 or Cl^-. The lack of dependence on triphenylphosphine con-

centration supports the above discussion that $Pd(PPh_3)_3$ is the only

palladium species present with less than 1% $Pd(PPh_3)_4$ or $Pd(PPh_3)_2$

being formed.

The first electron transfer being rate determining and the lack

of dependence on chloride anion concentration indicates that the

transition state for the oxidation of $Pd(PPh_3)_3$ (i.e. $Pd(PPh_3)_4$ in

solution) is at point (iv) on the scheme of squares (see figure 4.14).

Moving on to consider the solution electrochemistry of $Pd(PPh_3)_2Cl_2$,

the evidence presented in section 4.2.2.4. shows that the reduction of

$Pd(PPh_3)_2Cl_2$ is complicated, giving Koutecky-Levich rotation speed

dependence, less than theoretical collection efficiencies, a wave rather than a peak during cyclic voltammetry and limiting reduction currents dependent on the bulk triphenylphosphine concentration. This behaviour indicates some pre-equilibrium process before reduction can occur.

Tafel analyses of the reduction waves from figures 4.17-19 give linear plots (e.g. figure 4.16), from the slope of which one gets a value for the reduction transfer coefficient of 0.39 (± 0.06). This indicates that the first electron transfer is rate-limiting.

Considering the limiting current's dependence on triphenyl-phosphine concentration and the first electron transfer being rate-limiting, one can propose that the transition state for the reduction of $Pd(PPh_3)_2Cl_2$ is at either points (2), (3) or (4) on the scheme of squares (see figure 4.14).

One can regard these possible mechanisms as an electrochemical reduction preceded by an equilibrium reaction where, if point (2) is the transition state, the pre-equilibrium is

$$Pd(PPh_3)_2Cl_2 + PPh_3 \rightleftharpoons Pd(PPh_3)_3Cl_2 \qquad (A)$$
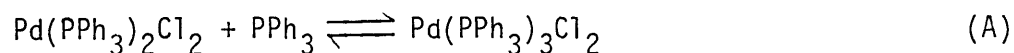
if point (3) is the transition state, the pre-equilibrium is

$$Pd(PPh_3)_2Cl_2 + PPh_3 \rightleftharpoons [Pd(PPh_3)_3Cl]^+ + Cl^- \qquad (B)$$
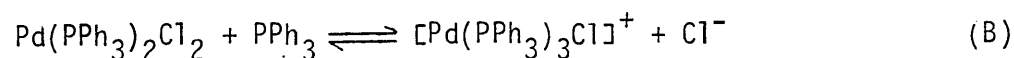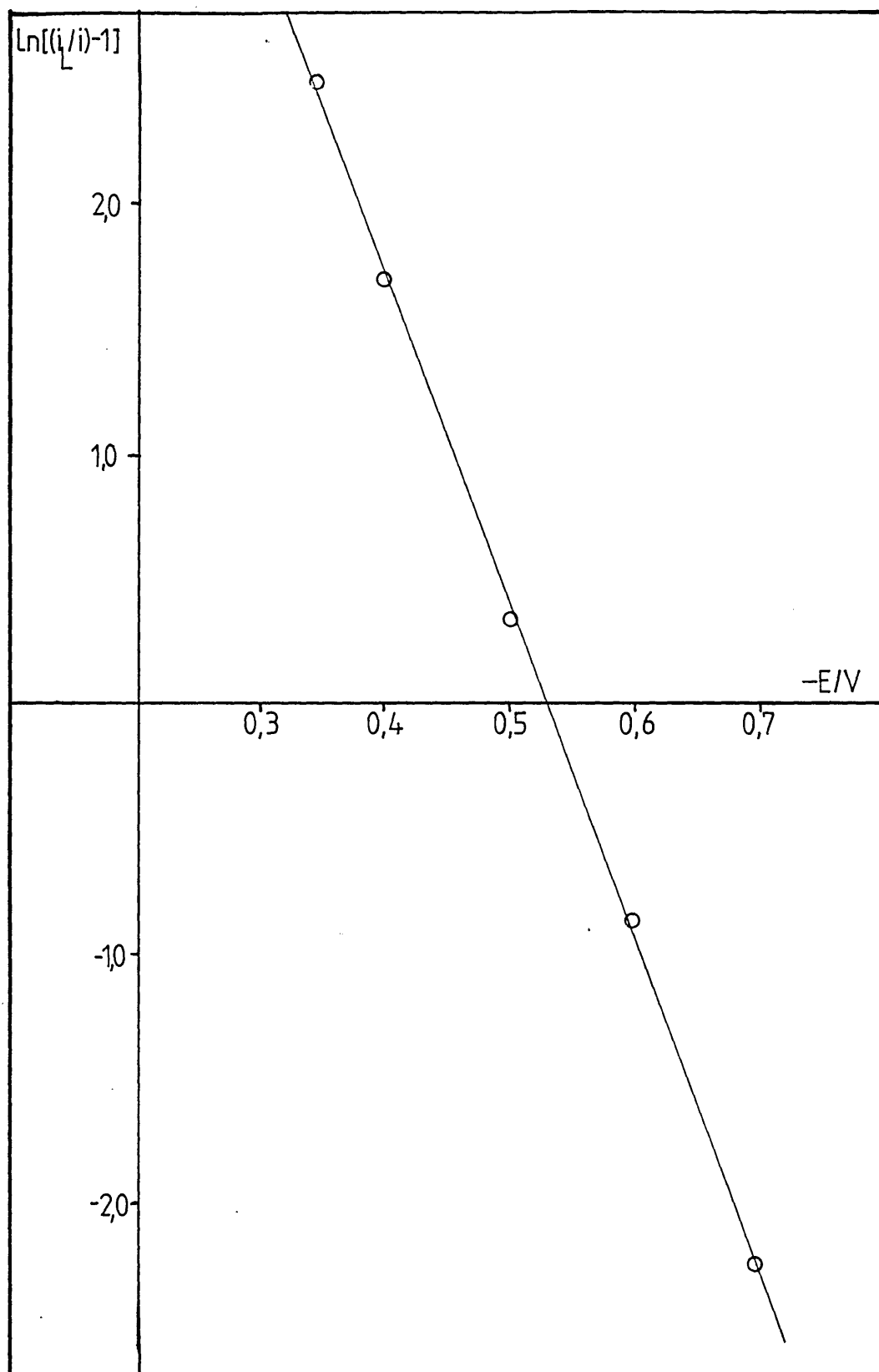
Figure 4.16. Tafel plot for the reduction of $Pd(PPh_3)_2Cl_2$ in the presence of excess PPh_3 and TEAC.

and if point (4) is the transition state, the pre-equilibrium is

$$Pd(PPh_3)_2Cl_2 + PPh_3 \rightleftharpoons [Pd(PPh_3)_3]^{2+} + 2Cl^- \qquad (C)$$
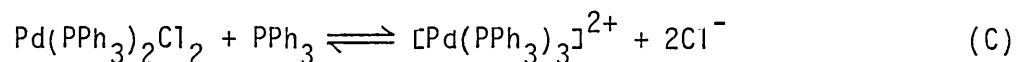
Theoretical analysis of these possibilities was developed (see section 2.5) and it gave a general Koutecky-Levich equation

$$\frac{nFA}{i_L} = \frac{1}{[Pd(PPh_3)_2Cl_2]} \left[\frac{1}{k'_D} + \frac{1}{k'_R} \right]$$

where for pre-equilibrium (A) $k'_R \propto [PPh_3]$ only,

for pre-equilibrium (B) $k'_R \propto [PPh_3]$ and $[Cl^-]^{-\frac{1}{2}}$,

and for pre-equilibrium (C) $k'_R \propto [PPh_3]$ and $[Cl^-]^{-1}$.

Therefore, a series of rotation speed dependence experiments were done, at a platinum RDE, to obtain a set of Koutecky-Levich plots. Chloroform (+ 0.2 M TEAP supporting electrolyte) solutions of $Pd(PPh_3)_2Cl_2$ (2 mM), with varying concentrations of tetraethylammonium chloride (TEAC) and triphenylphosphine (see table 4.1) were used. It should be noted that there was always a minimum bulk concentration (20 mM) of both TEAC and PPh_3 so that any generated by the electrode reaction would not appreciably change the bulk concentrations or concentrations at the electrode surface.

Table 4.1: Typical Results for the Slope and Intercept of Koutecky-Levich Plots for the Reduction of $Pd(PPh_3)_2Cl_2$ with Various Concentrations of PPh_3 and TEAC.

$[Pd(PPh_3)_2Cl_2]$ /mmol dm^{-3}	$[PPh_3]$ /mmol dm^{-3}	$[TEAC]$ /mmol dm^{-3}	K-L Slope /10^4 A^{-1} $s^{-\frac{1}{2}}$	K-L Intercept /10^4 A^{-1}
1.0	60	20	1.11	6.56
2.0	60	20	0.56	3.28
2.0	80	20	0.55	2.52
2.0	130	20	0.53	1.66
2.0	150	20	0.55	1.50
2.0	200	20	0.53	1.08
2.0	300	20	0.56	0.81
2.0	300	40	0.54	1.15
2.0	300	60	0.55	1.36
2.0	300	80	0.54	1.41
2.0	300	100	0.55	1.52

From equations 2.51 and 2.53 one can see that a Koutecky-Levich plot (i_L^{-1} vs $W^{-\frac{1}{2}}$) should give a straight line of

$$\text{slope} = (1.554 \, nFA[Pd(PPh_3)_2Cl_2]D_{(Pd(PPh_3)_2Cl_2)}^{2/3} \, \nu^{-1/6})^{-1}$$

and

$$\text{intercept} = (nFA[Pd(PPh_3)_2Cl_2]k'_R)^{-1}$$

where for pre-equilibrium (A) (see equation 2.54):

$$k'_R = (K_A k_A D_{(Pd(PPh_3)_3Cl_2)})^{\frac{1}{2}} [PPh_3]$$

hence intercept α $[PPh_3]^{-1}$

for pre-equilibrium (B) (see equation 2.52):

$$k'_R = (K_B k_B D_{(Pd(PPh_3)_3Cl^+)})^{\frac{1}{2}}[PPh_3][Cl^-]^{-\frac{1}{2}}$$

hence intercept α $[PPh_3]^{-1}$ and $[Cl^-]^{\frac{1}{2}}$

and for pre-equilibrium (C) (see equation 2.55):

$$k'_R = (K_C k_C^D {}_{(Pd(PPh_3)_3{}^{2+})})^{\frac{1}{2}} [PPh_3][Cl^-]^{-1}$$

hence intercept α $[PPh_3]^{-1}$ and $[Cl^-]$

Thus, the dependence of the intercept on the concentrations of PPh_3 and TEAC will indicate which of the pre-equilibria is applicable and hence where the transition state occurs on the scheme of squares.

A series of typical results are given in table 4.1, where the slope and intercept of Koutecky-Levich plots, for a range of PPh_3 and TEAC concentrations, are presented. A selection of actual Koutecky-Levich plots are given in figures 4.17, 4.18 and 4.19. One can see that the slope is independent of the concentrations of PPh_3 and TEAC but does vary with the concentration of $Pd(PPh_3)_2Cl_2$. This is as predicted by the above theory.

Looking at the intercepts one can see that they vary with both the PPh_3 and TEAC concentrations. A plot of ln(intercept) vs ln$[PPh_3]$, at a fixed TEAC concentration, gives a good straight line (see figure 4.20) of slope -0.92 (i.e. -1) which fits in well with the above theory. The Koutecky-Levich intercept also increases with increasing TEAC concentration. A plot of ln(intercept) vs ln[TEAC] (see figure 4.21) gives an approximate straight line of slope +0.4 ± 0.2 (i.e. 0.5). The error in this value is probably
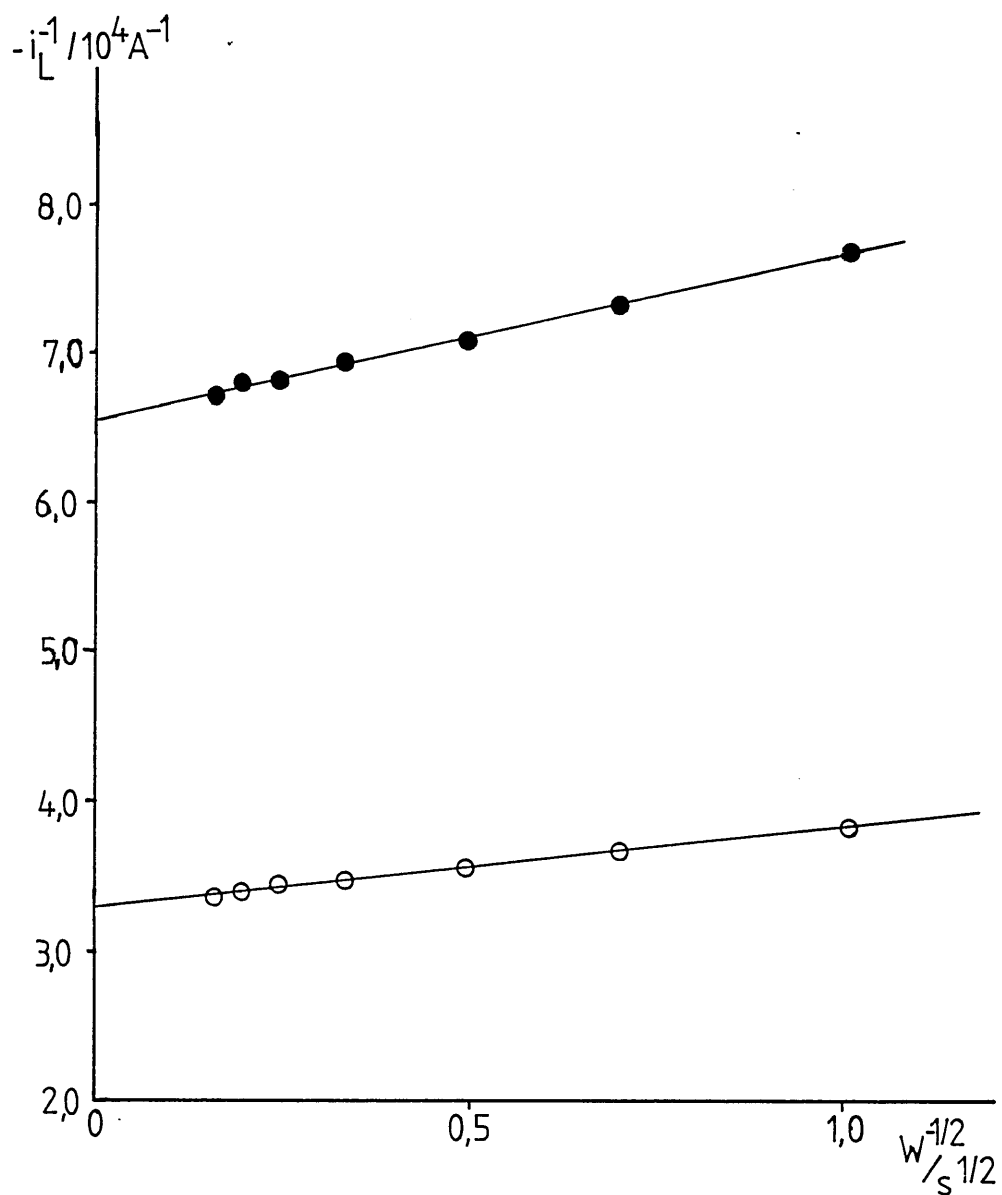
Figure 4.17. Koutecky-Levich plots for the reduction of
$Pd(PPh_3)_2Cl_2$ with various concentrations of
$Pd(PPh_3)_2Cl_2$. $[PPh_3] = 60$ mmol dm^{-3}; $[TEAC] =$
20 mmol dm^{-3}; $[Pd(PPh_3)_2Cl_2] = \bullet$ 1.0, $\circ$ 2.0
mmol dm^{-3}.
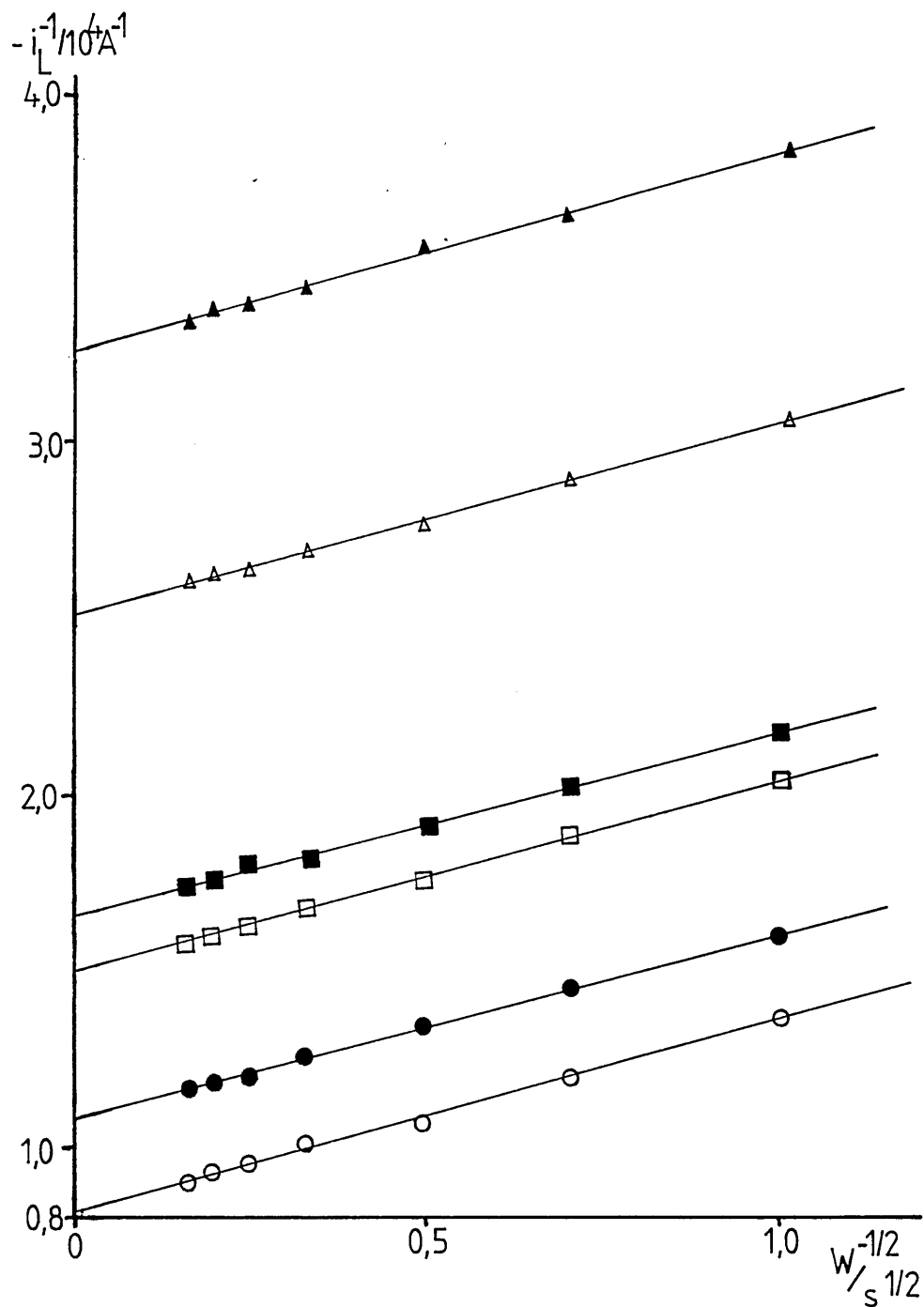
Figure 4.18. Koutecky-Levich plots for the reduction of $Pd(PPh_3)_2Cl_2$ with various concentrations of PPh_3. $[Pd(PPh_3)_2Cl_2] = 2.0$ mmol dm^{-3}; $[TEAC] = 20$ mmol dm^{-3}; $[PPh_3] = $ ▲ 60, △ 80, ■ 130, □ 150, ● 200, ○ 300 mmol dm^{-3}.
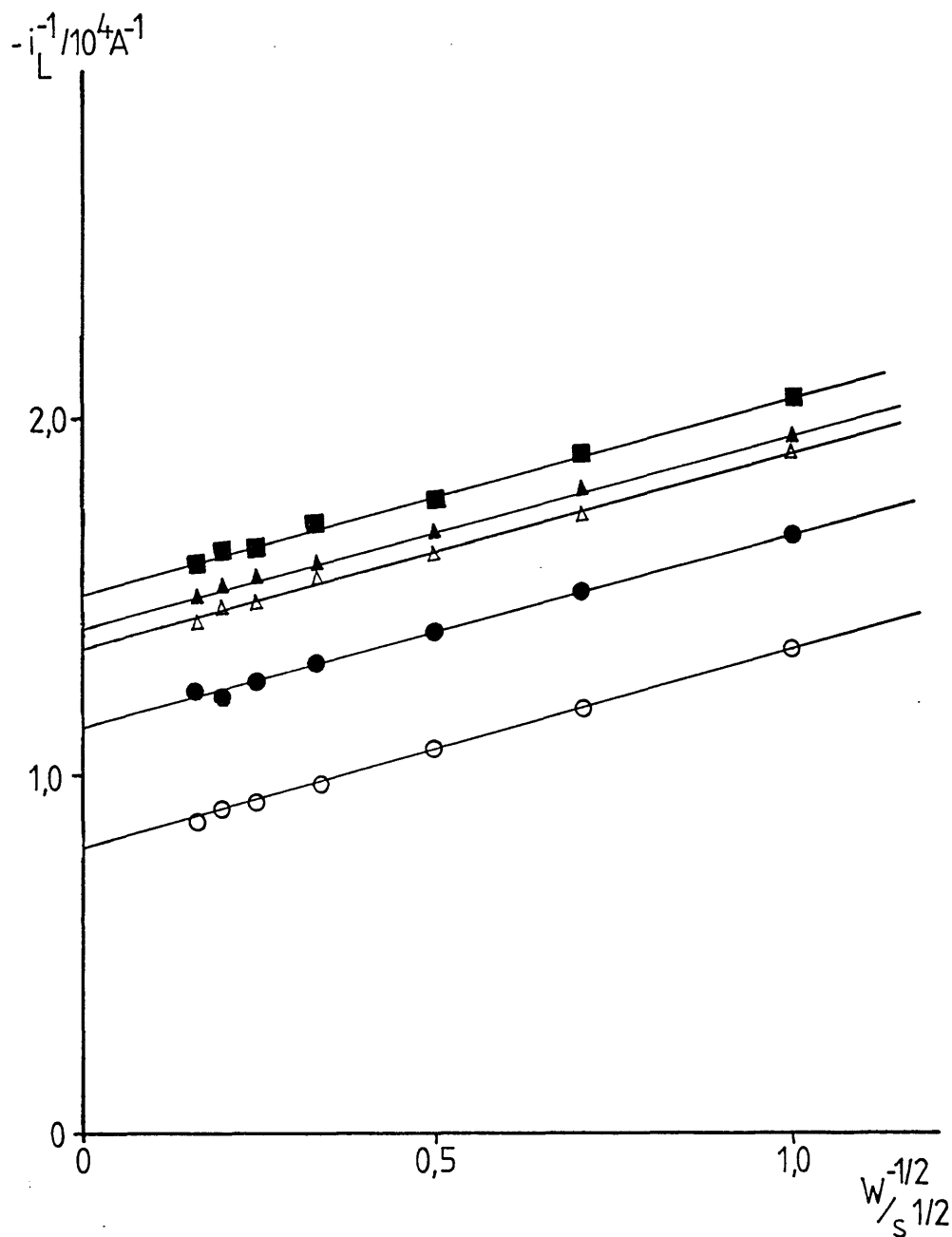
Figure 4.19. Koutecky-Levich plots for the reduction of $Pd(PPh_3)_2Cl_2$ with various concentrations of Cl^-. $[Pd(PPh_3)_2Cl_2]$ = 2.0 mmol dm^{-3}; $[PPh_3]$ = 300 mmol dm^{-3}; $[TEAC]$ = O 20, ● 40, △ 60, ▲ 80, ■ 100 mmol dm^{-3}.

ln((K-L Intercepts)/A^{-1})

$-$ln([PPh$_3$]/mol dm^{-3})
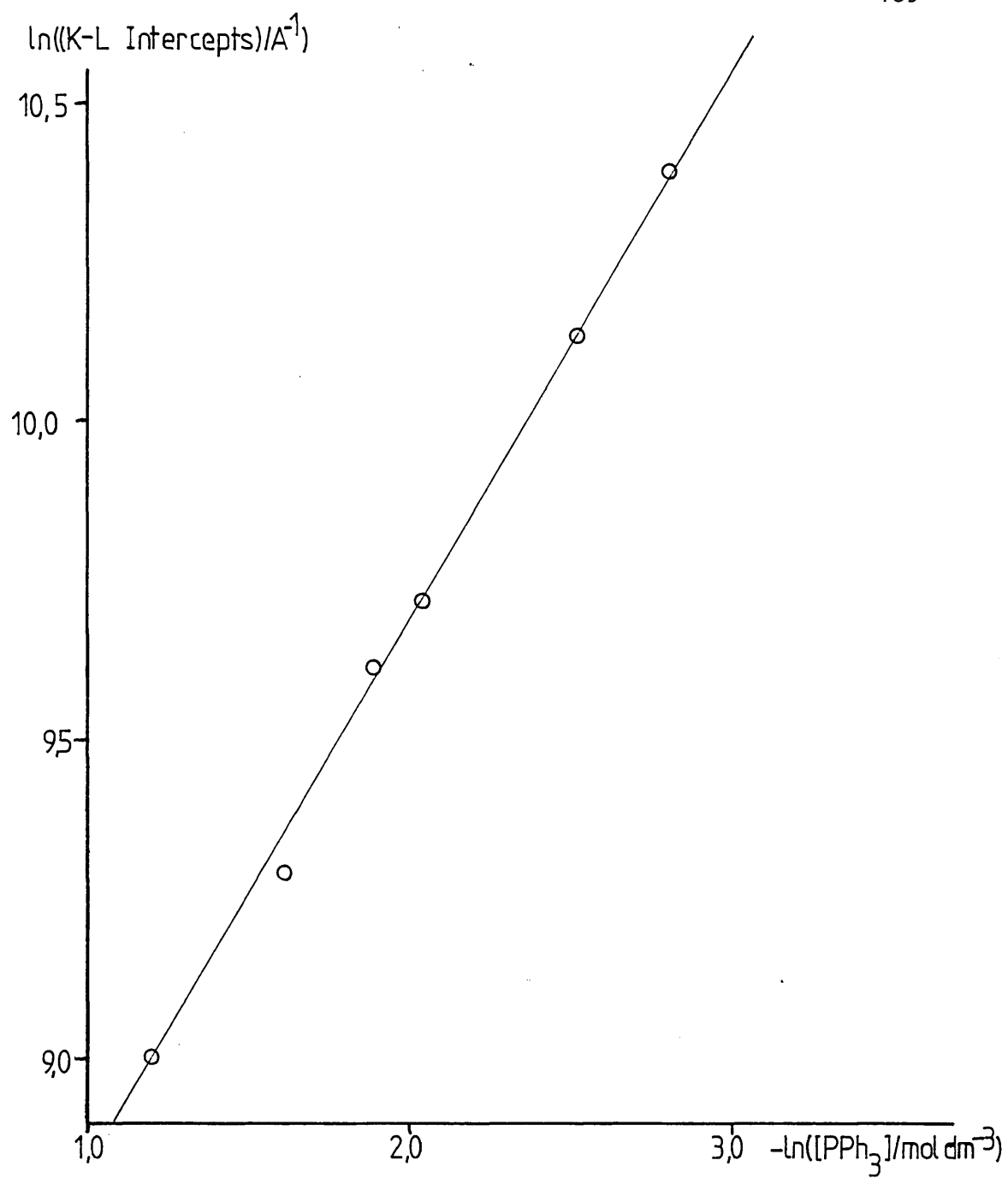
Figure 4.20. A plot of the logarithm of the Koutecky-Levich intercepts from figure 4.18 vs the logarithm of the concentration of PPh$_3$.

ln((K-L Intercepts)/A^{-1})

10,0

9,5

9,0

8,8

2,0   3,0   4,0   - Ln([TEAC]/moldm^{-3})
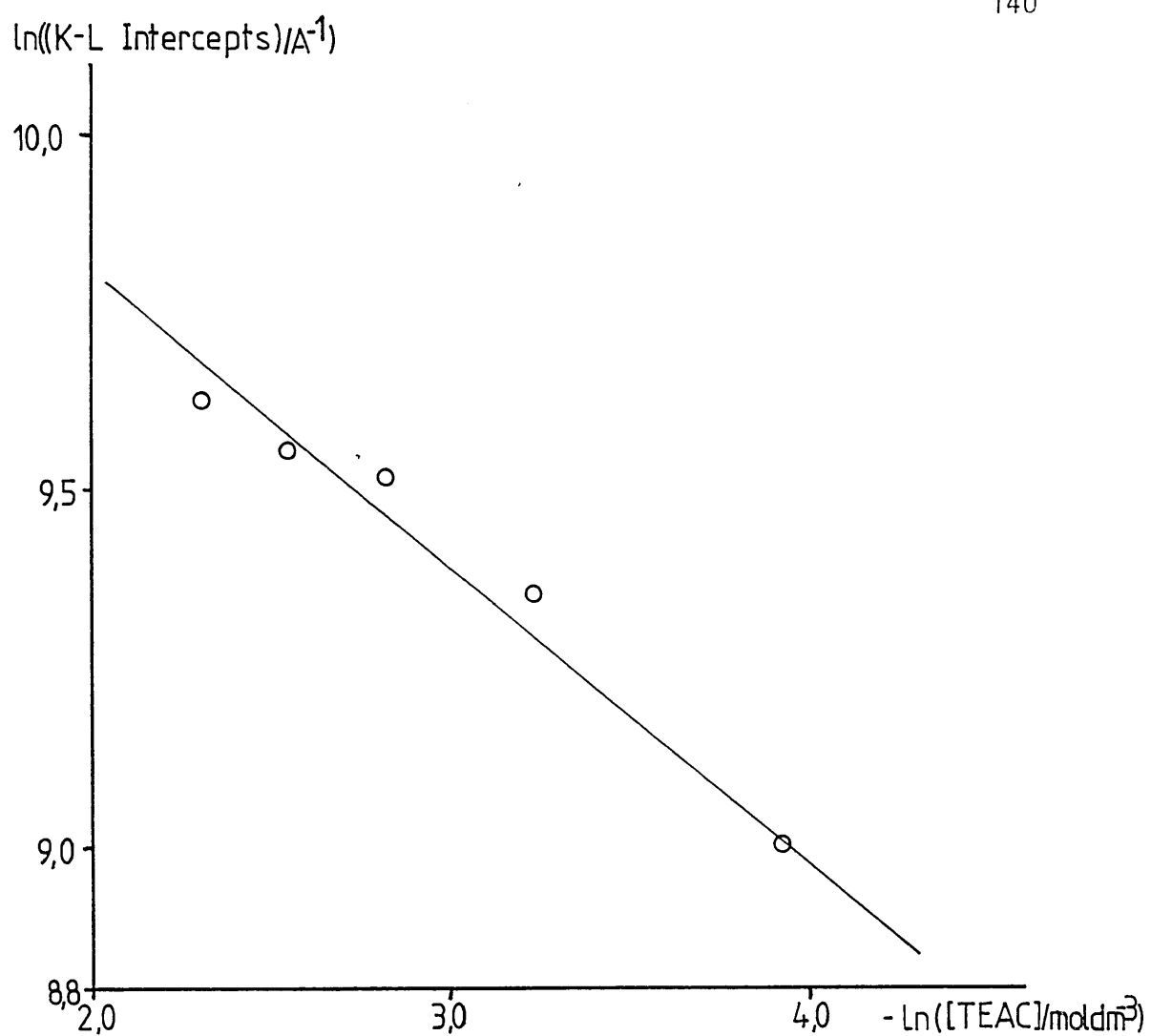
Figure 4.21.   A plot of the logarithm of the Koutecky-Levich
intercepts from figure 4.19 vs the logarithm
of the concentration of TEAC.

due to the TEAC not being totally dissociated and, therefore, there will be an added equilibrium:

$$Et_4NCl \rightleftharpoons Et_4N^+ + Cl^-$$
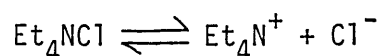
As the supporting electrolyte (TEAP) was present in large excess, the concentration of Et_4N^+ was approximately constant and hence the concentration of Cl^- was proportional to the concentration of TEAC. However, the higher the concentration of TEAC the less accurate this proportionality becomes, and errors are introduced.

From the above results one can propose that point (3), on the scheme of squares (see figure 4.14), is the transition state for the reduction of $Pd(PPh_3)_2Cl_2$ under these conditions.

From the average slope of the Koutecky-Levich plots one can calculate

$$D_{Pd(PPh_3)_2Cl_2} = 5.2 \pm 0.5 \times 10^{-6} \ cm^2 \ s^{-1}$$

and from the slope of a plot of Koutecky-Levich intercepts vs $[PPh_3]^{-1}$, at a constant TEAC concentration (see figure 4.22) one gets

$$\frac{K_B k_B \ D_{(Pd(PPh3)_3Cl)^+}}{[Cl^-]} = 1.2(\pm 0.4) \times 10^{-15} \ m^8 \ mol^{-2} \ s^{-2}$$
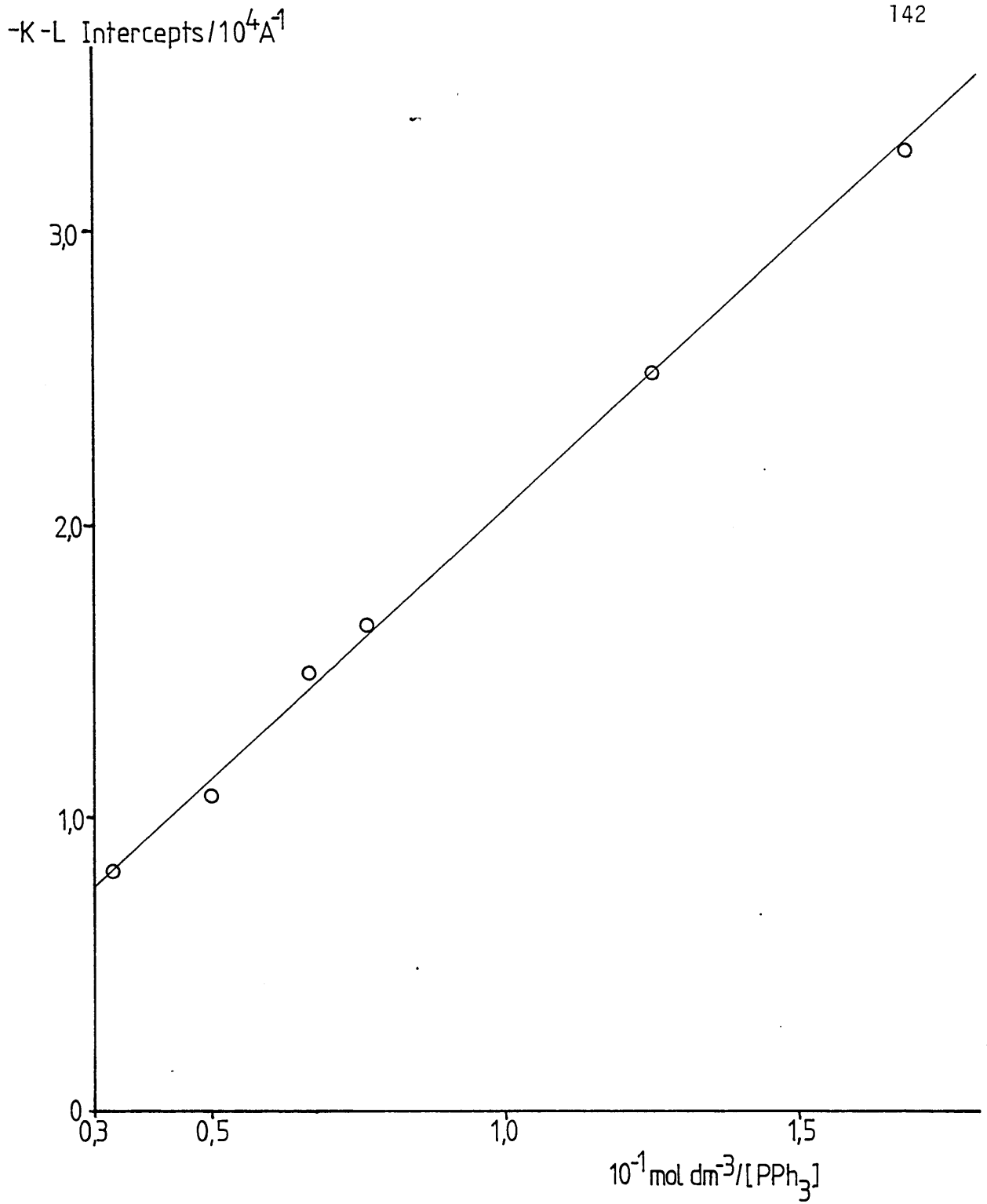
Figure 4.22. A plot of the intercepts of the Koutecky-Levich plots in figure 4.18 vs $[PPh_3]^{-1}$.

Assuming

$$D_{(Pd(PPh_3)_3Cl)^+} \sim D_{(Pd(PPh_3)_2Cl_2)}$$

and

$$[Cl^-] = [TEAC] = 20 \times 10^{-3} \text{ mol dm}^{-3}$$

then

$$K_B k_B = 5 \times 10^{-5} \text{ m}^3 \text{ mol}^{-1} \text{ s}^{-1}$$

As discussed earlier, the phosphine catalysed cis-trans (and trans-cis) isomerisation of square planar PdL_2X_2 complexes (where L = neutral phosphine ligand and X = halide anion) has been studied in the literature[146-149,233,234]. It has been found[149,231,233,234] that the rate-determining step, in this isomerisation, can be the formation of the PdL_3X^+ intermediate. Also, similar (within 5%) rate constants for the isomerisation of the cis and the trans complexes are observed[232]. For these reasons, the rate constant for the isomerisation reaction can be equated to the rate constant for the formation of the cationic PdL_3X^+ intermediate, which is k_B in the above analysis.

The actual rate constant for the isomerisation of cis or trans $Pd(PPh_3)_2Cl_2$ could not be found, but similar isomerisations of PdL_2X_2 complexes have rate constants between 5×10 and 5×10^3 dm^3 mol^{-1} s^{-1} (146-149,232-324).

Assuming k_B is in this range gives

$$K_B \sim 10^{-3} - 10^{-5}$$

and

$$k_{-B} \sim 5 \times 10^4 - 5 \times 10^8 \ dm^3 \ mol^{-1} \ s^{-1}$$

It is reassuring to note that these values for k_B, K_B and k_{-B} are very reasonable. Also, looking back at equation 2.47 one can see that this range of values for k_{-B} will make $Z_R < Z_D$ which indicates that the above treatment of results is valid. It should be noted that if k_{-B} is in the region of $10^8 \ dm^3 \ mol^{-1} \ s^{-1}$ this will be close to a diffusion controlled reaction.

Looking back at the scheme of squares, the above results would support the reaction pathway for the $Pd(PPh_3)_2Cl_2/Pd(PPh_3)_3$ couple, under the stated conditions, being:

$$Pd(PPh_3)_2Cl_2 \xrightleftharpoons{(ax)} Pd(PPh_3)_3Cl_2 \xrightleftharpoons{(bx)} Pd(PPh_3)_3Cl^+$$

$$\Big\updownarrow (3)$$

$$Pd(PPh_3)_3Cl \xrightleftharpoons{(cy)} Pd(PPh_3)_3^+$$

$$\Big\updownarrow (iv)$$
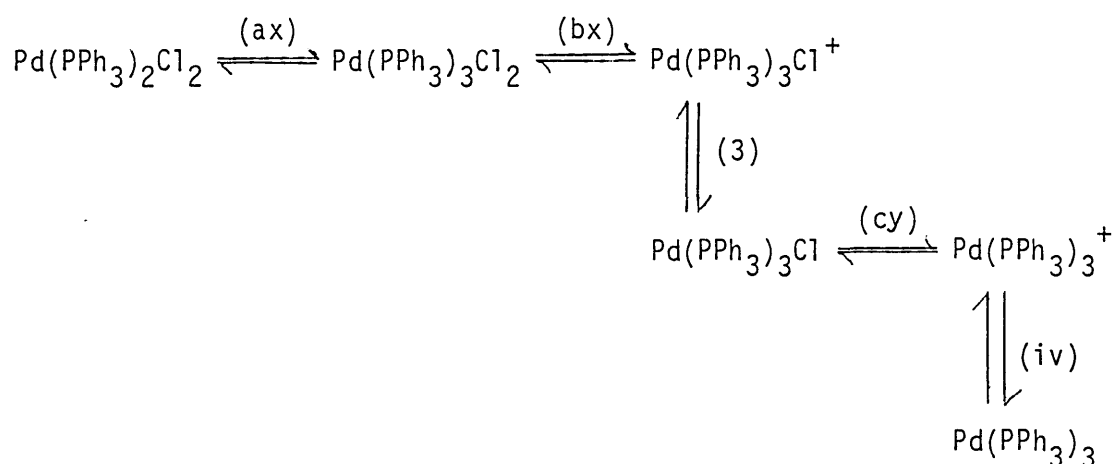
$$Pd(PPh_3)_3$$

where (3) indicates the rate-limiting transition state for the electro-chemical reduction of $Pd(PPh_3)_3Cl^+$ and (iv) indicates the rate-limiting

transition state for the electrochemical oxidation of $Pd(PPh_3)_3$.

As species $Pd(PPh_3)_3Cl^+$ is of higher energy than $Pd(PPh_3)_2Cl_2$ one can assume that the transition state at (bx) will be of higher energy than that at (ax). Therefore (bx) is the probable rate-limiting transition state for the pre-equilibrium to the electrochemical reduction.

4.2.2.6. Electrochemistry of the $Pd(PPh_3)_2Cl_2/Pd(PPh_3)_4$ Couple in Acetonitrile

$Pd(PPh_3)_2Cl_2$ is only slightly soluble in acetonitrile (< 0.2 mM) but it can be reduced electrochemically ($E_{\frac{1}{2}}$ = -1.5 V vs Ag/Ag^+), at a platinum RDE, without the addition of triphenylphosphine being necessary. The limiting reduction current showed Levich dependence on rotation speed, indicating a mass transport limited process.

Using a platinum/platinum rotating ring–disc electrode with the potential of the disc held at -1.7 V vs Ag/Ag^+, where the current is transport limited and hence a fixed flux of product is being generated, the ring's potential was swept anodically. No product of the disc reaction, except for triphenylphosphine, could be detected at the ring. This indicates that the electrochemical reduction of $Pd(PPh_3)_2Cl_2$ is forming palladium metal and releasing free triphenylphosphine.

If excess triphenylphosphine is added to the solution similar behaviour to the chloroform solutions is observed. For this case, the reduction occurs at $E_{\frac{1}{2}}$ = -1.1 V vs Ag/Ag^+ and the reoxidation of $Pd(PPh_3)_3$ (dissociated $Pd(PPh_3)_4$) occurs at $E_{\frac{1}{2}}$ = -0.38 V vs Ag/Ag^+.

$Pd(PPh_3)_4$ is also only slightly soluble in acetonitrile but shows similar behaviour to when in chloroform, with an oxidation wave $E_{\frac{1}{2}}$ = -0.38 V vs Ag/Ag^+ (a re-reduction, in excess triphenylphosphine,

at $E_{\frac{1}{2}}$ = -1.1 V vs Ag/Ag$^+$) with no dependence on triphenylphosphine or chloride ion concentrations.

Therefore, one can conclude that, to form a stable complex by the electrochemical reduction of $Pd(PPh_3)_2Cl_2$ one must have a large excess of triphenylphosphine in solution, while for the electrochemical oxidation of $Pd(PPh_3)_X$ (X = 3 or 4) no added ligands or ions are necessary.

4.2.2.7. Discussion

Considering the above results for a palladium-phosphine polymer modified electrode one can see that if reversible electrochemistry of the form

$$X_2Pd(PPh_2)_{\overline{2}} \textcircled{P} \; \rightleftharpoons \; Pd(PPh_2)_{\overline{4}} \textcircled{P} \; + \; 2X^- \qquad (\text{-}\textcircled{P}= \text{attached to a polymer})$$
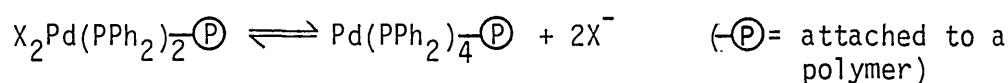
is required, then a large excess of phosphine ligands per palladium in the polymer will be necessary. The palladium complexes should be more stable due to the chelating effect of the polymer and the localisation of ligands.

Using the above results it will be possible to identify this type of reversible electrochemistry in a modified electrode.

However, for regeneration of catalysts from the Wacker process (see section 1.2.1), one is interested in the oxidation of palladium (0) species which, from the above results, is straightforward. One could postulate either a palladium-tetraphosphine complex being formed as a catalyst reaction product where excess phosphine ligands would be necessary

i.e.

$$\underset{\overset{|}{CH_2OH}}{CH_2}\text{-PdX(PPh}_2)_{\overline{2}}\textcircled{P} \xrightarrow{+\textcircled{P}-(PPh_2)_2} Pd(PPh_2)_{\overline{4}}\textcircled{P} + CH_3-C\overset{\overset{O}{\diagup}}{\diagdown_H} + HCl$$
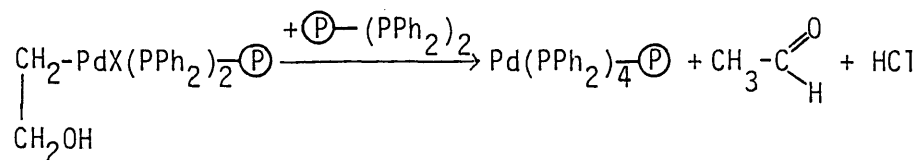
or the palladium (0) being generated by the Wacker reaction could immediately be electrochemically oxidised, as the reaction occurs, thereby never actually making the separate palladium (0)-tetraphosphine species. Again, the above results will help to identify these types of processes in a modified electrode.

4.3. Solution Electrochemistry of Nickel Complexes

4.3.1. Aqueous Solutions

Nickel aqueous electrochemistry is quite widely reported[153] in the literature. The only electrochemistry, at a platinum RDE, seen for nickel ions in aqueous solutions (e.g. $NiSO_4$ (1 mM) with K_2SO_4 (0.1 M) supporting electrolyte) is nickel plating at -1.1 V vs SCE. This plating seems to occur in conjunction with hydrogen evolution. A nickel plated electrode under these conditions is noble, though stripping can occur in acidic conditions or in the presence of high chloride ion concentration.

In aqueous potassium sulphate solution a nickel plated electrode shows oxygen adsorption at +1.1 V vs SCE and oxygen stripping at +0.55 V vs SCE but no nickel stripping (see figure 4.23).

4.3.2. Non-Aqueous Solutions

As with palladium, because it was found necessary to investigate modified electrodes in non-aqueous conditions, so investigation of nickel solution species in non-aqueous conditions was pursued.
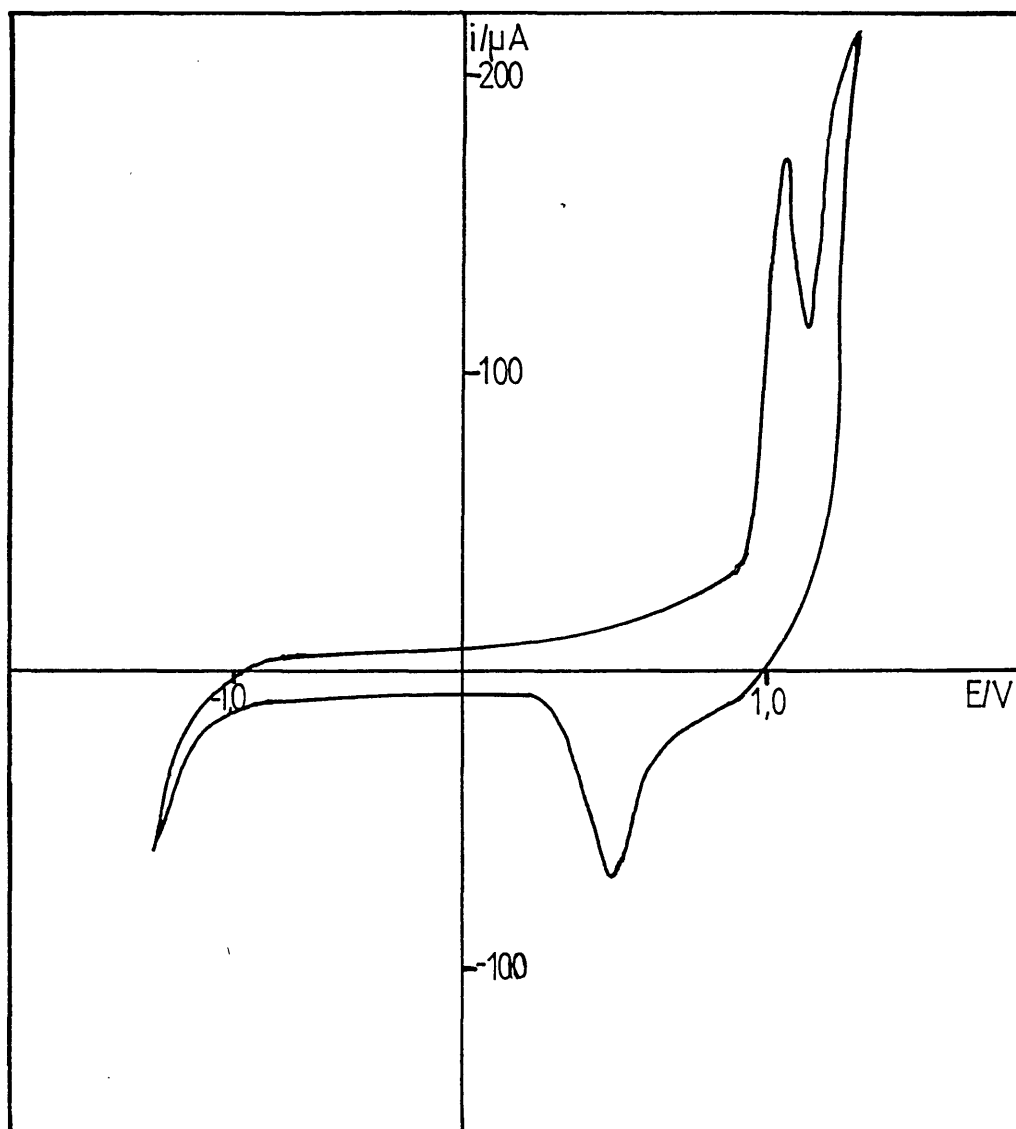
Figure 4.23. Current voltage curve of a nickel plated RDE
(W = 10 Hz, v = 25 mV s^{-1}).

Unlike palladium, some work has been published on the electro-chemistry of nickel complexes in non-aqueous solvents. This includes work by Troupel and coworkers[154-157] on the electrochemistry of $NiBr_2(PPh_3)_2$ in various solvents (tetrahydrofuran, 1,2-dimethoxyethane and ethanol).

The nickel (II) complex can be reduced, at a platinum electrode, by two one-electron transfers. In excess triphenylphosphine, it is predicted that a $NiBr(PPh_3)_3^+$ species is formed[154] which can be reduced to $NiBr(PPh_3)_3$ ($E_{\frac{1}{2}}$ = -1.1 V vs Ag/Ag$^+$ (0.1 M) in tetrahydro-furan) and then further reduced to $Ni(PPh_3)_4 Br^-$ ($E_{\frac{1}{2}}$ = -1.9 V vs Ag/Ag$^+$ (0.1 M)). However, if there is no excess triphenylphosphine $NiBr_2(PPh_3)_2$ is reduced to $NiBr_2(PPh_3)_2^-$ which then loses Br$^-$ to form $NiBr(PPh_3)_2$. $NiBr(PPh_3)_2$ can be further reduced to $NiBr(PPh_3)_2^-$ but this species reacts with the nickel (II) complex to give the nickel (I) complex again.

$$NiBr(PPh_3)_2^- + NiBr_2(PPh_3)_2 \rightarrow 2NiBr(PPh_3)_2 + Br^-$$
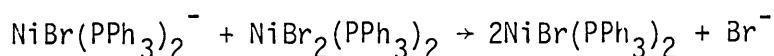
Both $NiBr(PPh_3)_2$ and $NiBr(PPh_3)_3$ can be reoxidised to form nickel (II) complexes and the $Ni(PPh_3)_4$ species can be reoxidised by two one-electron processes giving first nickel (I) and then nickel (II) complexes.

The two-electron reduction of $[Ni(PPh_3)_2(CH_3CN)_4]^{2+}$ in aceto-nitrile, with excess triphenylphosphine, has also been reported[158]. The product was $Ni(PPh_3)_4$, which could be reoxidised by two one-electron oxidations, with $Ni(PPh_3)_4^+$ being the intermediate species and $[Ni(PPh_3)_2(CH_3CN)_4]^{2+}$ being the regenerated, oxidised species.

The simple electrochemical formation of $\underline{Ni}(PPh_3)_4$ from $Ni(PPh_3)_2X_2$,
in the presence of excess triphenylphosphine, was encouraging for the
regeneration of a $Ni(PPh_2)_{\overline{4}}\text{\textcircled{P}}$ species at a modified electrode. However,
one can see that a large excess of phosphine ligands to nickel species
will be necessary.

For the aid of identifying $Ni(PPh_2)_{\overline{4}}\text{\textcircled{P}}$ species, $Ni(PPh_3)_4$ was
synthesised (see section 4.5) and investigated electrochemically. In a
solution of $Ni(PPh_3)_4$ (< 0.5 mM) in acetonitrile (with 0.1 M TBAT as supporting
electrolyte) a very irreversible oxidation wave was observed ($E_{\frac{1}{2}} \sim$ -0.6 V
vs Ag/Ag^+, see figure 4.24) at a platinum RDE. This wave showed Levich
rotation speed dependence (see figure 4.25) indicating a transport
limited process (i.e. no pre-equilibria). The breadth is due to the
wave being two unresolved one-electron transfers.

Cyclic voltammetry, at a platinum electrode, showed two oxidation
peaks (E_p = -0.85 and -0.55 V vs Ag/Ag^+) and one reduction peak (E_p =
-1.1 V vs Ag/Ag^+, see figure 4.26). These are deduced to be two one-
electron oxidations with one two-electron reduction.

From these results identification of both nickel (0) and nickel (II)
phosphine species in a modified electrode will be possible.

4.4. Catalysis Experiments in Solution

Some preliminary experiments were undertaken to investigate catalysis
by palladium and nickel complexes.

4.4.1. Palladium Complexes

The aqueous Wacker process converting ethylene to acetaldehyde
(see section 1.2.1) was attempted. Ethylene was passed through an
aqueous solution of K_2PdCl_4 and an immediate precipitate of palladium
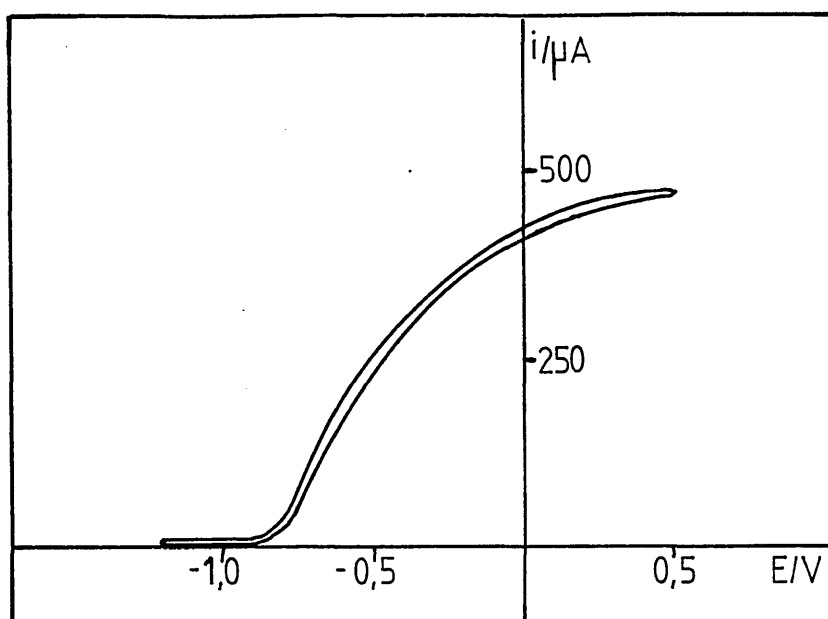
Figure 4.24. Current voltage curve for the oxidation
of $Ni(PPh_3)_4$ (W = 10 Hz, v = 10 mV s^{-1}).

Figure 4.25. Levich plot for the oxidation of $Ni(PPh_3)_4$
(see figure 4.24).
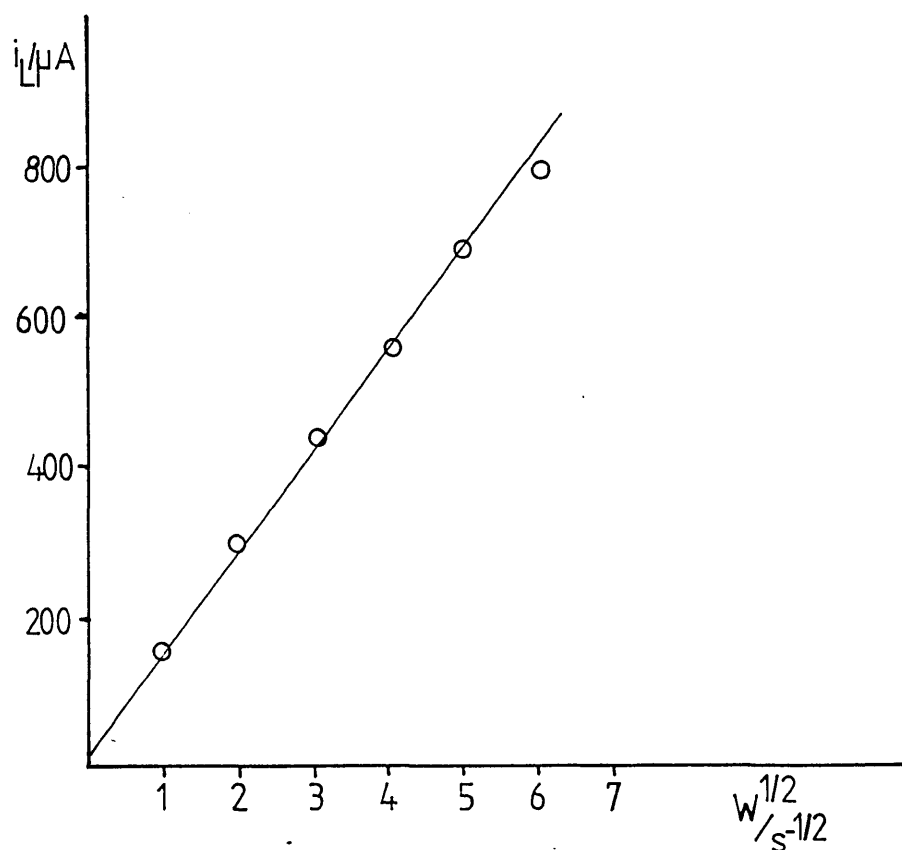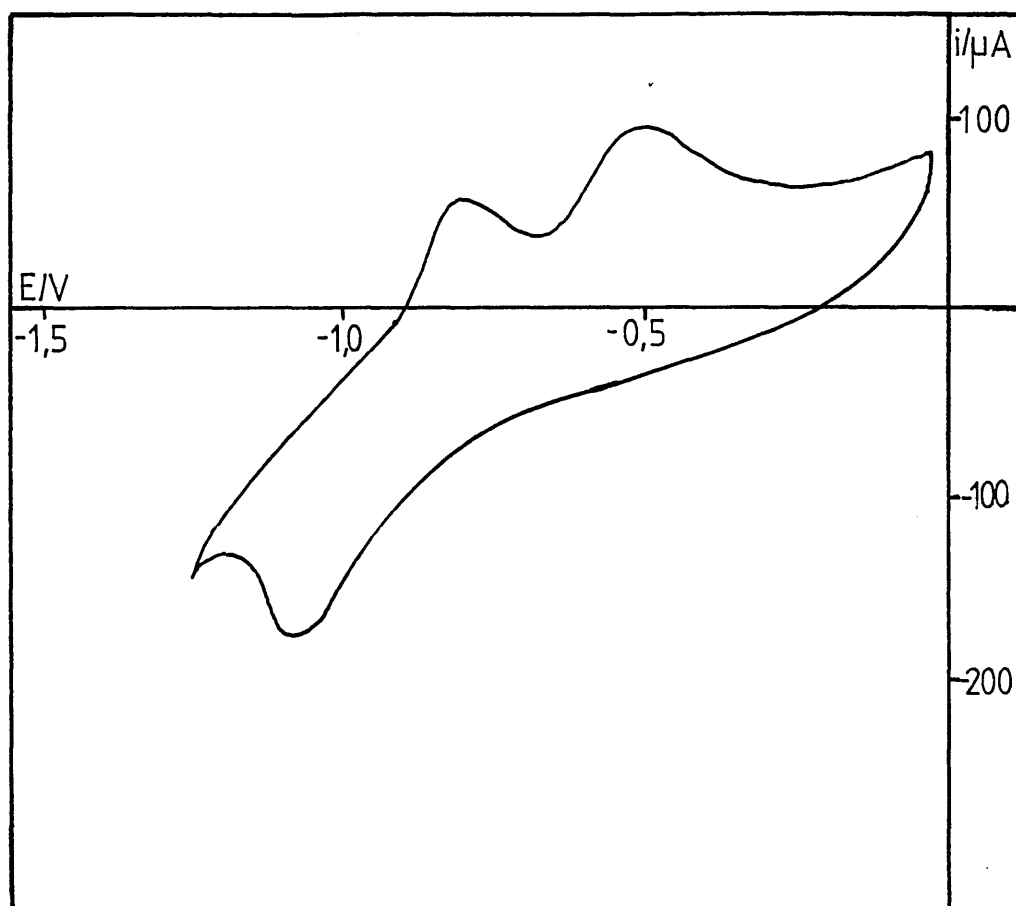
Figure 4.26.   Cyclic voltammetric analysis of $Ni(PPh_3)_4$
(v = 100 mV s^{-1}).

metal was observed, indicating that the reaction had occurred. If copper (II) chloride was added in large excess, palladium precipitation was slower and Cu^I species could be detected electrochemically ($E_{\frac{1}{2}}$ = +0.15 V vs SCE, $Cu^I \rightarrow Cu^{II}$) on a glassy carbon electrode (glassy carbon was used as ethylene adsorbs on platinum[1,2]). This indicated that the Wacker process was occurring.

In acetonitrile, solutions of $Pd(MeCN)_2Cl_2$, with water present in 2 mol dm^{-3} concentration, gave a palladium metal precipitate on passing ethylene. It was found that if water was present in < 1.5 mols dm^{-3} concentration the reaction occurred very slowly. A slower precipitation was observed for $Pd(PPh_3)_2Cl_2$ in dimethylsulphoxide or dimethylformamide, containing 2 mol dm^{-3} water. An even slower precipitation was observed for $Pd(PPh_3)_2Cl_2$ in chloroform. This was probably due to the water solubility, in chloroform, being too low for aqueous reaction to occur significantly and the non-aqueous reaction being much slower.

Therefore, one can conclude that in non-aqueous solvents, for the aqueous Wacker process (acetaldehyde formation) to occur, water must be present in $\sim$ 2 mol dm^{-3} concentration.

4.4.2. Nickel Complexes

$Ni(PPh_3)_4$ catalysis was investigated in a dry box, under argon, due to the oxygen sensitivity of the zero oxidation state complex.

To an acetonitrile solution of $Ni(PPh_3)_4$, with excess triphenylphosphine (and TBAT supporting electrolyte), chlorobenzene was added dropwise and a reduction current was observed at a platinum RDE ($E_{\frac{1}{2}}$ = -1.3 V vs Ag/Ag$^+$). Therefore, this indicates that $Ni(PPh_3)_4$ undergoes an oxidation reaction, to produce a nickel oxidised species. This oxidised species can then be reduced electrochemically regenerating the catalytically active $Ni(PPh_3)_4$.

The overall reaction[94] is

$$2PhCl \rightarrow Ph\text{-}Ph + 2Cl^-$$
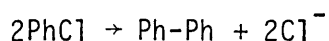
The first stage would be the formation of $PhNi(PPh_3)_2Cl$,

$$PhCl + Ni(PPh_3)_4 \rightarrow PhNi(PPh_3)_2Cl + 2PPh_3$$
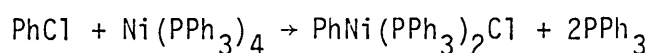
and then $PhNi(PPh_3)_2Cl$ could either react with more PhCl,

$$PhCl + PhNi(PPh_3)_2Cl \rightarrow Ph\text{-}Ph + Ni(PPh_3)_2Cl_2$$
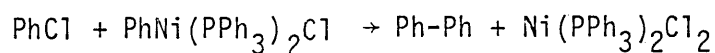
with $Ni(PPh_3)_2Cl_2$ being electrochemically reduced to regenerate $Ni(PPh_3)_4$; or $PhNi(PPh_3)_2Cl$ could itself be electrochemically reduced to regenerate $Ni(PPh_3)_4$ and produce $Ph^- + Cl^-$. This Ph^- can then react with more $PhNi(PPh_3)_2Cl$,

$$Ph^- + PhNi(PPh_3)_2Cl \xrightarrow{\;+2PPh_3\;} Ph\text{-}Ph + Ni(PPh_3)_4 + Cl^-$$
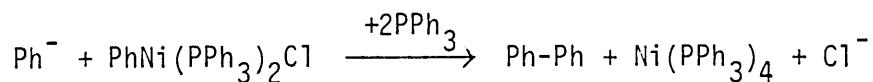
Therefore, the same overall reaction would be observed for both cases.

4.5. Appendix: Synthesis of Complexes

4.5.1. Bis(acetonitrile)palladium dichloride, Pd(MeCN)$_2$Cl$_2$ [159]

Palladium dichloride in acetonitrile was heated to boiling temperature to give a red solution. This solution was filtered hot and petroleum ether (Bp. 30-40°C) added to give a yellow precipitate of Pd(MeCN)$_2$Cl$_2$ which was filtered and washed with more petroleum ether (Bp. 30-40°C).

4.5.2. Bis(triphenylphosphine)palladium dichloride, Pd(PPh$_3$)$_2$Cl$_2$ [160]

This was prepared by slowly adding a solution of K$_2$PdCl$_4$ (1g, 3 mmoles) in water (30 cm^3) plus concentrated hydrochloric acid (0.1 cm^3) to a warm, stirred, ethanolic solution of triphenylphosphine (1.5 g, 5.7 mmoles). The mixture was stirred for 3 hours, at 60°C, as a yellow precipitate formed. This was then filtered, washed with hot water, then ethanol, followed by diethyl ether. The product was then recrystalised from chloroform/petroleum ether (Bp. 40-60°C) and dried under vacuum at 100°C. Overall yield was 1.7 g (88%).

4.5.3. Tetrakis(triphenylphosphine)palladium, Pd(PPh$_3$)$_4$ [161]

Palladium dichloride (1.77 g, 0.01 moles), triphenylphosphine (13.1 g, 0.05 moles) and dimethylsulphoxide (120 cm^3) were placed in a nitrogen purged flask. Under positive nitrogen pressure, the mixture was heated to 140°C to give a yellow solution. This was left for 15 minutes and then hydrazine hydrate (2 g, 0.04 moles) was added rapidly, by syringe. After a rigorous reaction during which nitrogen was evolved, a yellow/ orange precipitate formed. The solution was cooled and filtered under nitrogen. The solid was washed with deoxygenated ethanol, followed by diethyl ether and then dried by passing nitrogen through the funnel

overnight. The product (9 g, 85% yield) was stored under nitrogen, in the dark.

4.5.4. Bis(acetonitrile)nickel dibromide, Ni(MeCN)$_2$Br$_2$[162]

Anhydrous nickel dibromide was dissolved in refluxing acetonitrile using a soxhlet apparatus. On cooling blue/green crystals of Ni(MeCN)$_2$Cl$_2$ precipitated.

4.5.5. Bis(triphenylphosphine)nickel dichloride, Ni(PPh$_3$)$_2$Cl$_2$[163]

Nickel dichloride hexahydrate (2.38 g, 0.01 moles) in 2 cm^3 H$_2$O was diluted with glacial acetic acid (50 cm^3). Triphenylphosphine (5.25 g, 0.02 moles) in glacial acetic acid (25 cm^3) was added and the mixture stirred for 24 hours. The initial green precipitate became dark blue crystals. These were filtered, washed with acetic acid and dried under vacuum. Overall yield was 4.5 g (70%).

4.5.6. Tetrakis(triphenylphosphine)nickel, Ni(PPh$_3$)$_4$[164]

Under nitrogen, sodium borohydride (1.0 g, 25 mmoles) in ethanol (20 cm^3) was added dropwise to a stirred solution of nickel nitrate hexahydrate (2.9 g, 10 mmoles) and triphenylphosphine (15.5 g, 50 m-moles) in ethanol (60 cm^3), at room temperature. A red precipitate formed which, after 15 minutes, was filtered under nitrogen and washed with ethanol followed by ether. The solid was dried by passing nitrogen through the funnel overnight. The resulting product (6.4 g, 58% yield) was stored under nitrogen, in the dark.

5. STYRENE BASED POLYMER COATS

5.1. Introduction

As discussed in chapter 1, the theme of this work is the investigation of polymer coated electrodes containing palladium or nickel complexes which will react with solution species and be regenerated electrochemically, leading to electrocatalysis.

For this purpose the polymer must contain ligands which will bond the metal in both the two and zero oxidation states. This bonding must be strong enough to prevent leaching out or decomposition of the catalyst but not so strong as to inhibit catalysis occurring.

Isocyanide ligands are known[165,166] to form stable complexes with palladium in both oxidation states, though coordinating counter ions (e.g. halide) are needed to stabilise the higher oxidation state complex. Phosphine ligands are also known to form complexes with palladium[160,161,167] and nickel[164,168] in both oxidation states.

Polymers containing phosphine ligands have been widely employed[98,99] as metal supports to give heterogeneous catalysts. Palladium dichloride complexed in a phosphine polymer has been used for hydrogenation of polyenes[99]. Both palladium zero[169] and nickel zero[170] have been complexed in phosphine polymers which were then used to catalyse the dimerisation of butadiene. Phosphine polymer bound nickel dibromide, in the presence of sodium borohydride, has also been used to catalyse this reaction[170,171]. In all these cases the metal does not change oxidation state (i.e. is acting as a true catalyst) but one can see that both oxidation states, of palladium and nickel, are stable in this type of phosphine polymer environment.

Therefore, it was decided that polymers containing isocyanide ligands for the complexing of palladium and polymers containing phosphine ligands

for the complexing of nickel and palladium should be synthesised. These
polymers would have to be sufficiently cross-linked to form insoluble
films but also open enough to allow swelling and diffusion of ions within
the polymer. The polymer would also have to be flexible so that complexa-
tion of the metal species would be unhindered.

The actual polymers used are described in the following section and
the experimental details for their synthesis are given in the appendix to
this chapter (section 5.8). Metal incorporation was done either on bulk
polymers followed by coating the metal containing polymer or by first
coating the unmetallated polymer and incorporating the metal into the
polymer film. The bulk metallated polymers are described in section 5.2
with experimental details of their preparation being given in the appendix
(section 5.8). Metal incorporation into polymer films was done by a
variety of methods from simply soaking the coated electrode in a solution
of the metal ions and waiting for ligand exchange, to cycling the potential
of the coated electrode in a solution of the metal ions required. These
methods will be described in more detail in sections 5.4 and 5.5, when
appropriate.

In section 5.3 the coating procedures used are described and the
electrochemical investigation of these coated electrodes in aqueous and
non-aqueous solvents is presented in sections 5.4 and 5.5 respectively.
The need to move to non-aqueous solvents is discussed at the end of
section 5.4. Section 5.6 describes some catalysis experiments and this
is followed by an overall discussion of the results presented in this
chapter. Finally, in the appendix, the experimental details of the syntheses
discussed in this chapter are given. These have been appended so as not
to interrupt the discussion of results.

5.2. The Polymers Used

As discussed earlier, it was decided to use polymers containing isocyanide or phosphine ligands. To aid flexibility and to enhance accessibility of the coats polymer chain lengths of the order of 100 monomer units were chosen.

Three different types of isocyanide polymer were developed (polymer syntheses are given in section 5.8). Two were based on either styrene or dimethylacrylamide, with hexamethylene diacrylamide cross-linking agent, giving polymers as shown in figures 5.1 and 5.2. These will be referred to as (PS)—NC and (PA)—NC respectively. These two were chosen as (PA)—NC is hydrophilic, thus being swollen by water while (PS)—NC is more hydrophobic, thus being better swollen by non-aqueous solvents.

Palladium dichloride was incorporated into these polymers (see section 5.8.1) in a ratio of five isocyanide ligands to each palladium species. Metal incorporation could be followed by a shift in the infra-red band of the NC bond from 2150 cm^{-1} to 2260 cm^{-1}. Spectroscopic analysis showed the palladium was complexed by two isocyanide ligands[179]. Therefore, these polymers will be referred to as (PS)—$(NC)_2PdCl_2$ and (PA)—$(NC)_2PdCl_2$.

The third type of isocyanide polymer was made by complexing the di-isocyano derivative of m-xylene to give a polymeric species with palladium in its backbone (see figure 5.3a). The ratio of isocyanide ligands to palladium used was 2:1 and this polymer will be referred to as $[(CNRNC)PdCl_2]_n$. This was also reduced chemically in the presence of more CNRNC to give a palladium (0) polymeric species (see figure 5.3b) and this will be referred to as $[(CNRNC)_2Pd]_n$.

Nickel species could not be incorporated into isocyanide polymers as nickel (II) catalyses isocyanide polymerisation[181].

Only one phosphine polymer was synthesised (see section 5.8.3) and this was styrene based (see figure 5.4). This polymer will be referred to as (PS)—PPh_2.
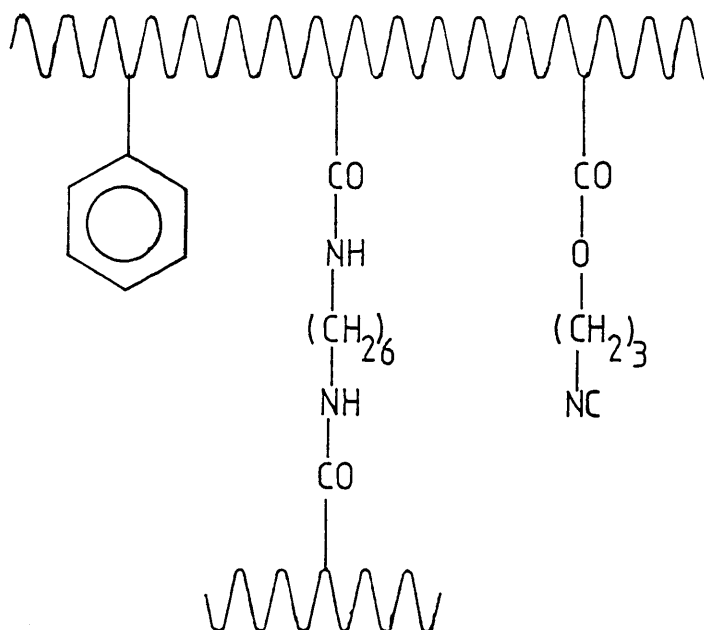
Figure 5.1. Structure of (PS)—NC.
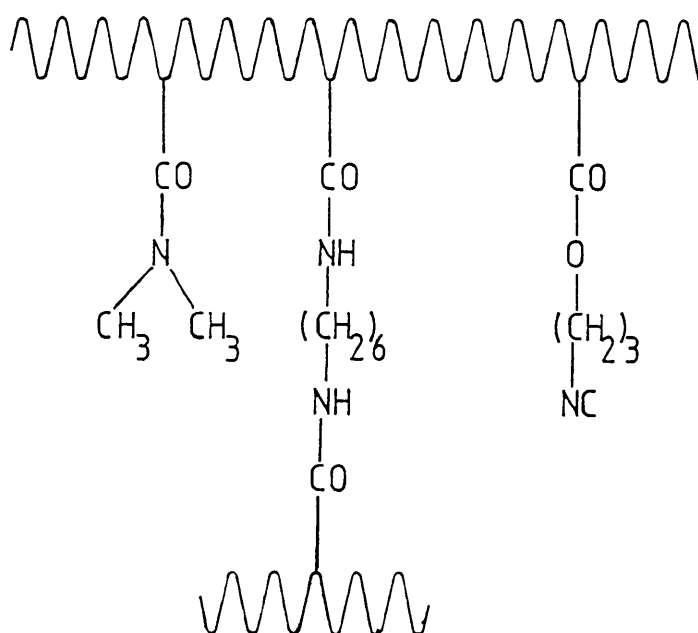
Figure 5.2. Structure of (PA)—NC.
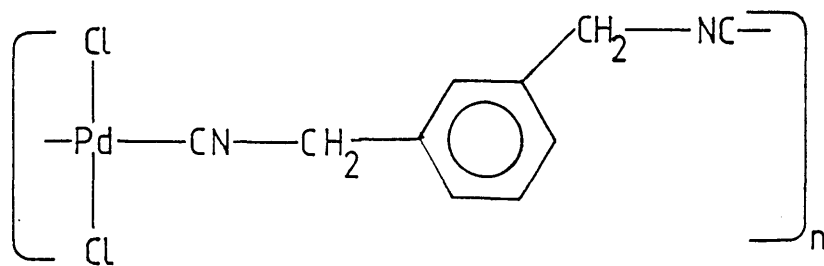
Figure 5.3a. Structure of $[(CNRNC)PdCL_2]_n$.
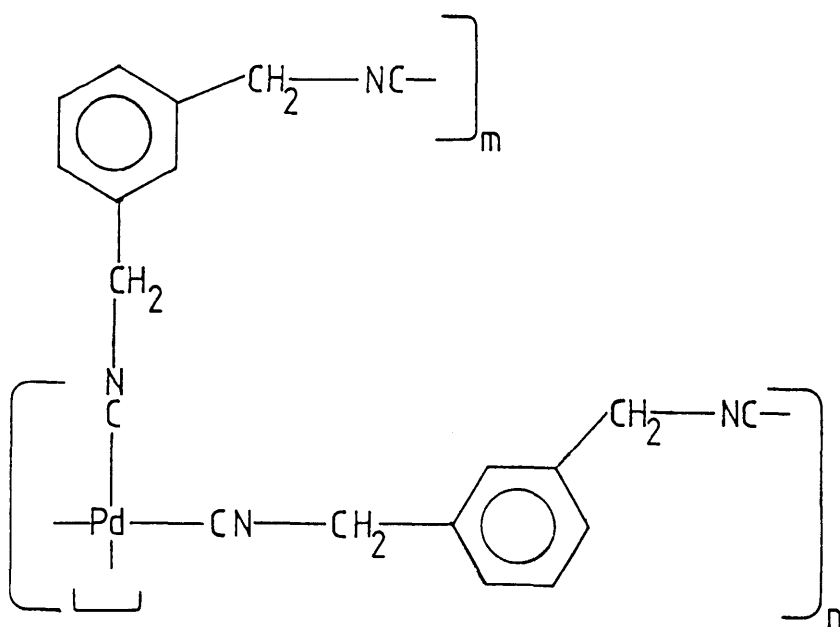
Figure 5.3b. Structure of $[(CNRNC)_2Pd]_n$.
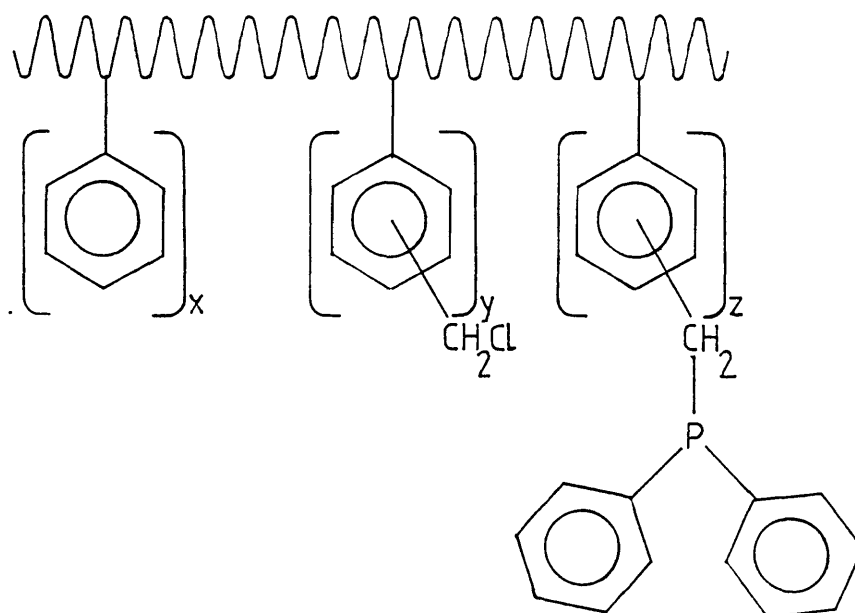
Figure 5.4. Structure of (PS)-PPh₂;
x:y:z = 10:1:9.
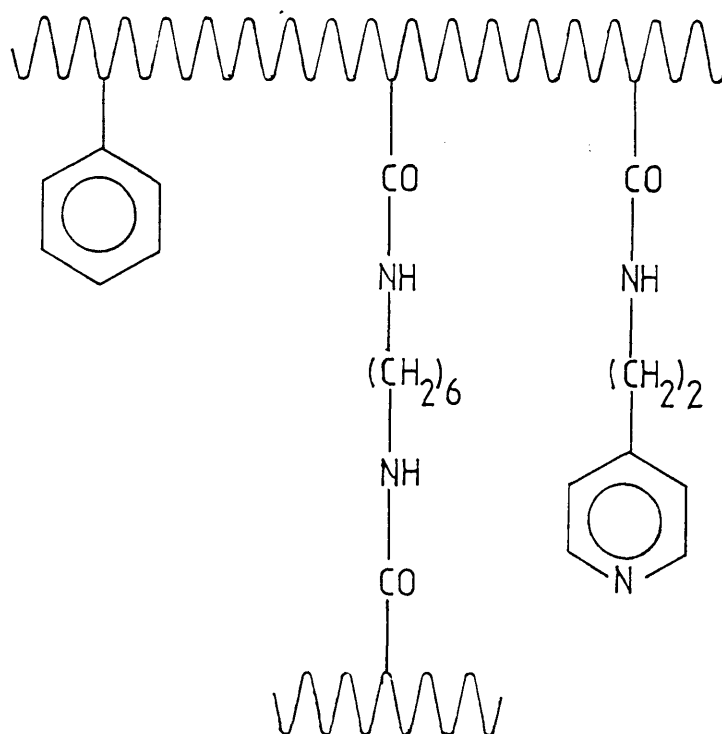
Figure 5.5. Structure of (PS)-Pyn.

Both palladium and nickel dichloride were incorporated into this
polymer with a ratio of ten phosphine ligands to each metal species.
This excess was chosen due to the results presented in chapter 4 which
indicated the need of a high ligand to metal ratio if the zero oxidation
state complex is going to be formed without decomposition. As the majority
of palladium dichloride and nickel dichloride species will be complexed
by two phosphine ligands these polymers will be referred to as $\text{(PS)}-(\text{PPh}_2)_2\text{PdCl}_2$
and $\text{(PS)}-(\text{PPh}_2)_2\text{NiCl}_2$ respectively.

Finally, a styrene based polymer containing pyridine ligands (see
figure 5.5) was also used in some investigations. A similar polymer has
been used to support palladium (II) complexes for the heterogeneous acetoxyla-
tion of aromatic compounds[172]. This polymer will be referred to as
$\text{(PS)}-\text{Pyn}$ and $\text{(PS)}-(\text{Pyn})_2\text{PdCl}_2$ when palladium dichloride is incorporated
(see section 5.8.2).

Solvents which swell or dissolve these polymers are given in table 5.1.
Obviously, electrochemistry must be done in a solvent that swells the
polymer, thus allowing transport of ions into the polymer. However, the
polymer must not be soluble in the electrochemical solvent or else the
coat will dissolve off the electrode surface.

5.3. Coating Procedures

Three techniques for coating the above polymers were investigated.
These were chemical binding, spin coating and drop coating.

Chemical binding of polymers to electrode surfaces via silane linkages
has been reported in the literature[173] and the resulting coats are very
stable.

A platinum flag electrode (a circular disc of platinum welded to a
platinum wire) was cleaned by polishing and electrochemically, as described
in section 3.1.1. This electrode was then oxidised electrochemically by

Table 5.1: The Effect of Various Solvents on the Polymers.

Solvent / Polymer	H_2O	EtOH	CH_2Cl_2	MeCN	DMSO	DMF	Toluene
(PA)–NC	Swells	Swells	Dissolves	Dissolves	Dissolves	Dissolves	Swells
(PS)–NC	Unaffected	Swells Slightly	Dissolves	Swells	Dissolves	Dissolves	Swells
(PS)–PPh$_2$	Unaffected	Swells Slightly	Dissolves	Swells	Dissolves	Dissolves	Swells
(PS)–Pyn	Unaffected	Swells Slightly	Dissolves	Swells	Dissolves	Dissolves	Swells
(PA)–(NC)$_2$ PdCl$_2$	Unaffected	Swells Slightly	Swells	Swells	Dissolves	Dissolves	Swells Slightly
(PS)–(NC)$_2$ PdCl$_2$	Unaffected	Swells Slightly	Swells	Swells	Dissolves	Dissolves	Swells Slightly
(PS)–(PPh$_2$)$_2$ PdCl$_2$	Unaffected	Swells Slightly	Swells	Swells	Dissolves	Dissolves	Swells Slightly
(PS)–(Pyn)$_2$ PdCl$_2$	Unaffected	Swells Slightly	Swells	Swells	Dissolves	Dissolves	Swells Slightly
(PS)–(PPh$_2$)$_2$ NiCl$_2$	Unaffected	Swells Slightly	Swells	Swells	Dissolves	Dissolves	Swells Slightly

holding its potential at +1.1 V vs SCE in 0.1 M aqueous sulphuric acid solution. This formed an oxide layer on the platinum surface which was dried and treated with $(EtO)_3Si(CH_2)_3NH_2$ in toluene to form a monolayer of silane.

$$Pt \quad O{-}{>}Si(CH_2)_3NH_2$$
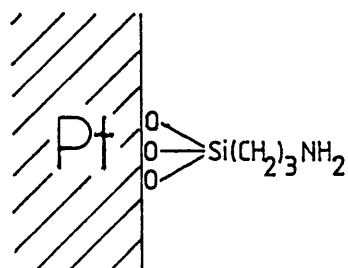
This was then bonded to the polymer (PS)-NC through some of the isocyanide groups by means of a Ugi four centre condensation reaction[174],

$$Pt \quad O{-}{>}Si(CH_2)_3NH_2 + CH_3CO_2H + CH_3CH_2CHO + (PS){-}NC \longrightarrow Pt \quad O{-}{>}Si(CH_2)_3N \overset{COCH_3}{\underset{CHCON}{\diagdown}} \quad CH_3CH_2 \quad (PS){-}NC$$
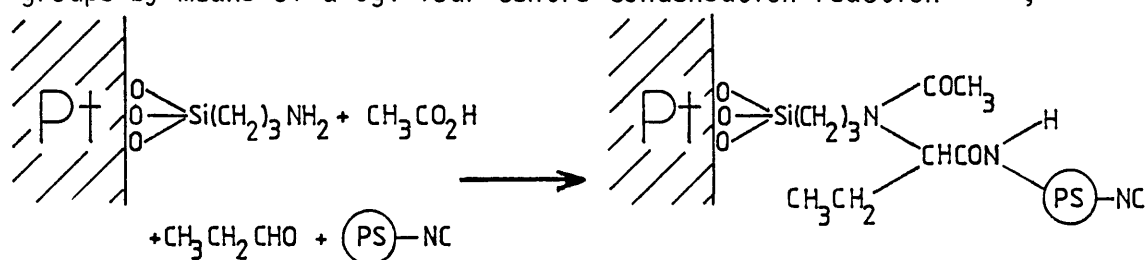
This method was found to be long and complicated giving uneven and irreproducible coats.

Spin coating was performed by dropping a solution of the required polymer on a rapidly rotating RDE, faced upwards. The majority of the solution added is spun off the electrode surface leaving a thin, even film. However, as it is impossible to know how much solution remained on the electrode no real estimation of the coat's thickness can be made.

Drop coating involved dropping a measured amount of polymer solution, of known concentration, onto the electrode and allowing the solvent to evaporate. Films were quite even especially when using volatile solvents. For less volatile solvents, placing the electrode plus solution under

vacuum, resulting in faster solvent evaporation, was found satisfactory. One major advantage of this method was that from the concentration of polymer solution and the amount placed on the electrode an approximate thickness of the coat could be calculated.

Therefore, drop coating was found to be the best method for coating electrodes. It was fast, easy and gave reasonably even and reproducible coats of calculable thickness. In table 5.2 the solvents used for drop coating the various polymers are given. Measured amounts of solution were added using a micro-syringe and solution concentrations were calculated so that between 40 and 100 μlitres would give the required coat thickness. This was to ensure the electrode would be completely covered and that several additions would not be necessary. In general coat thicknesses of the order of 100 monolayer equivalents were used though a range from 10 to 10,000 monolayer equivalents was sometimes required.

5.4. Aqueous Electrochemistry

Due to its hydrophilic nature, (PA)-NC was the main polymer investigated in aqueous solutions. A glassy carbon rotating disc electrode (RDE) was used as this polymer gave better films on glassy carbon than on platinum or gold. Firstly, (PA)-NC drop coated electrodes were investigated to see the effect the polymer film had on simple electrode reactions.

In an aqueous solution of ferrocyanide $(Fe(CN)_6^{4-}$, 1 mM + 0.1 M K_2SO_4 supporting electrolyte) a clean glassy carbon electrode, rotating at 10 Hz, had its potential swept anodically (at 10 mV s^{-1}) to give the expected reversible oxidation wave ($E_{\frac{1}{2}}$ = +0.2 V vs SCE, see figure 5.6a). However, a (PA)-NC coated electrode ($\sim$ 100 layers) completely blocked this couple (see figure 5.6b) and even after six hours of cycling the electrode potential, between +1.2 V and -1.0 V vs SCE at 10 mV s^{-1}, no electrochemical activity was observed. (PS)-NC, (PS)-PPh$_2$ and (PS)-Pyn gave

Table 5.2: Solvents Used for Drop Coating the Polymers

Polymer	Solvent
(PA)—NC	CH_2Cl_2
(PS)—NC	CH_2Cl_2
(PS)—PPh_2	CH_2Cl_2
(PS)—Pyn	CH_2Cl_2
(PA)—$(NC)_2PdCl_2$	DMSO
(PS)—$(NC)_2PdCl_2$	DMF
(PS)—$(PPh_2)_2PdCl_2$	DMF
(PS)—$(Pyn)_2PdCl_2$	DMF
$[(CNRNC)PdCl_2]_n$	DMF
(PS)—$(PPh_2)_2NiCl_2$	DMSO
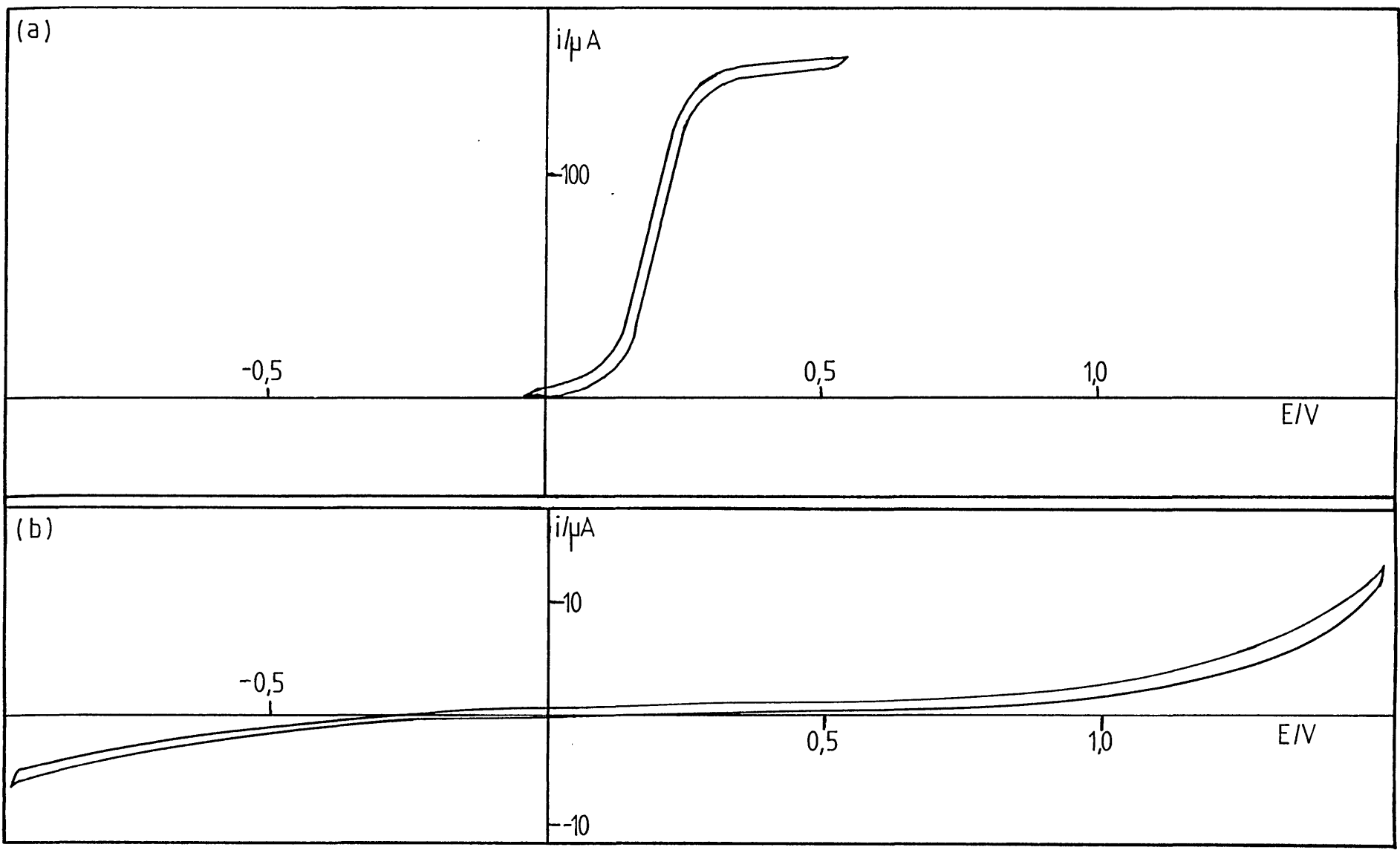
Figure 5.6. (See overleaf).

Figure 5.6. (a) Oxidation of ferrocyanide at a clean glassy carbon RDE; (b) lack of oxidation of

ferrocyanide at a (PA)-NC coated glassy carbon RDE.

similar results, though this was not surprising due to their hydrophobic nature. These results indicate that the polymers are very stable under these conditions and that the coats do not contain large pinholes.

Oxygen reduction at a clean glassy carbon RDE, in oxygenated 0.1 M aqueous K_2SO_4, under similar experimental conditions as above, gave an electrochemical wave at $E_{\frac{1}{2}}$ = -0.35 V vs SCE (see figure 5.7a). A (PA)—NC coated electrode, in a similar solution, also gave a reduction wave ($E_{\frac{1}{2}}$ = -0.35 V vs SCE) but the limiting current was much lower and showed Koutecky-Levich rotation speed dependence (see figure 5.7b and 5.8) rather than Levich dependence which is observed on the clean electrode. This Koutecky-Levich dependence indicates that diffusion of oxygen through the polymer film is slowing the transport of oxygen to the electrode surface.

For this type of behaviour equation 3.32 is applicable with $k'_{ME} = KD_Y/L$. Hence, the intercept of a Koutecky-Levich plot will give $1/nFA[O_2]k'_{ME}$. Therefore, from the intercept of the Koutecky-Levich plot for oxygen reduction at the (PA)—NC coated electrode (see figure 5.8) one gets

$$D_{O_2} \, K/L = 2.2 \times 10^{-5} \, m \, s^{-1}$$

Assuming K = 1 and L $\sim 10^2$ nm (approximate, as the amount the polymer is swelled is unknown), gives the diffusion coefficient of oxygen in the polymer

$$D_{O_2} \sim 2 \times 10^{-8} \, cm^2 \, s^{-1}$$

which is three orders of magnitude lower than in bulk solution.

Figure 5.7. Reduction of oxygen at (a) a clean glassy carbon RDE; (b) a (PA)—NC coated glassy carbon RDE; (W = 10 Hz, v = 10 mV s^{-1}).
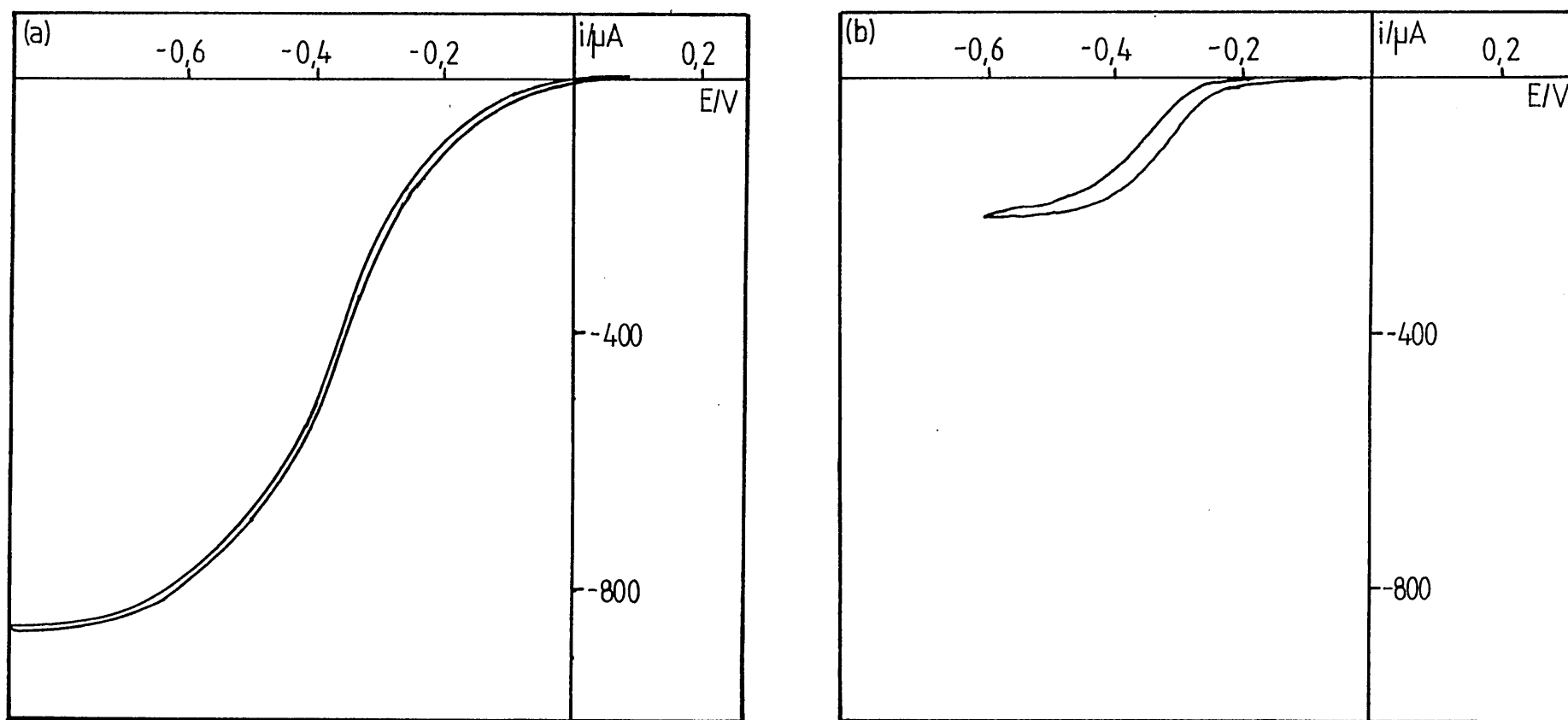
Figure 5.8. (See overleaf).

(a)

(b)

173
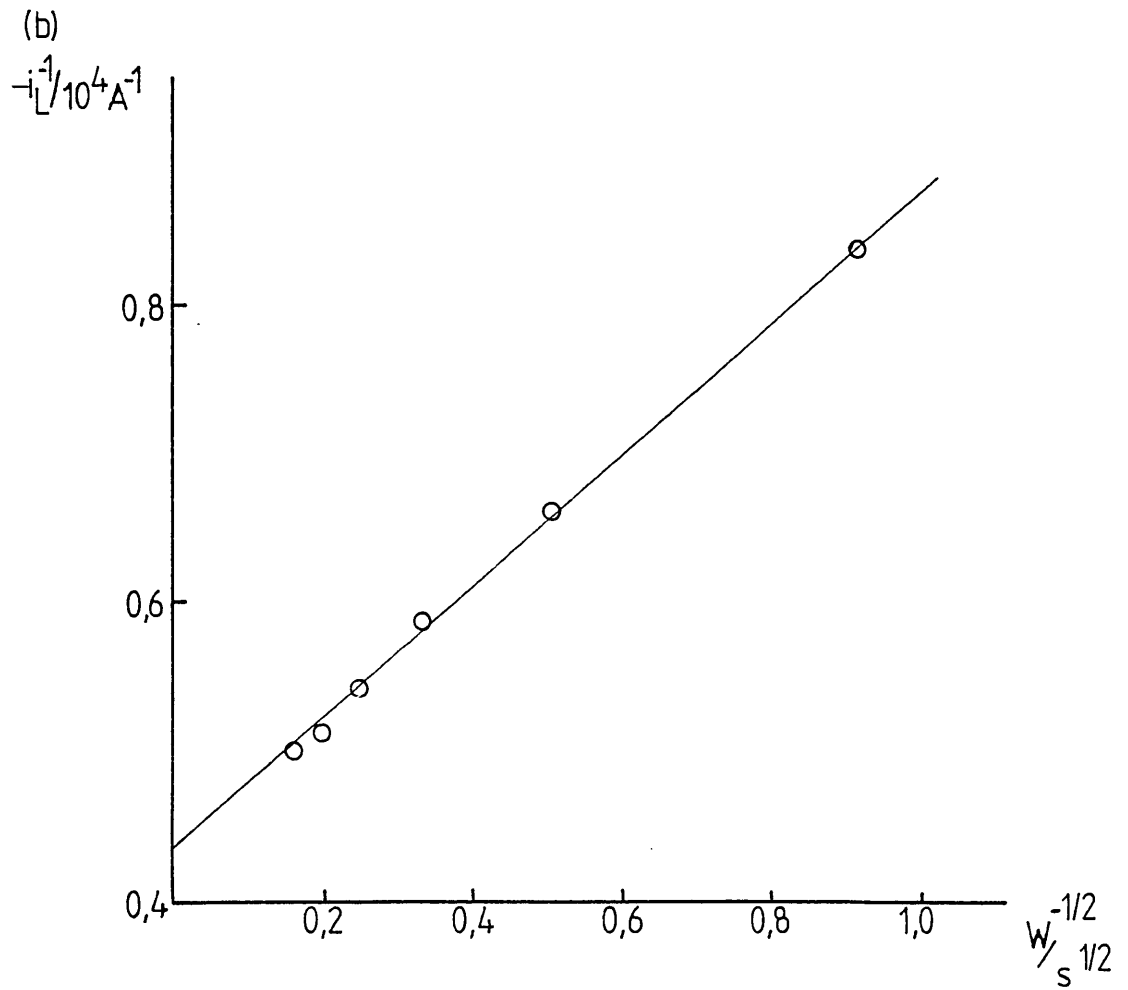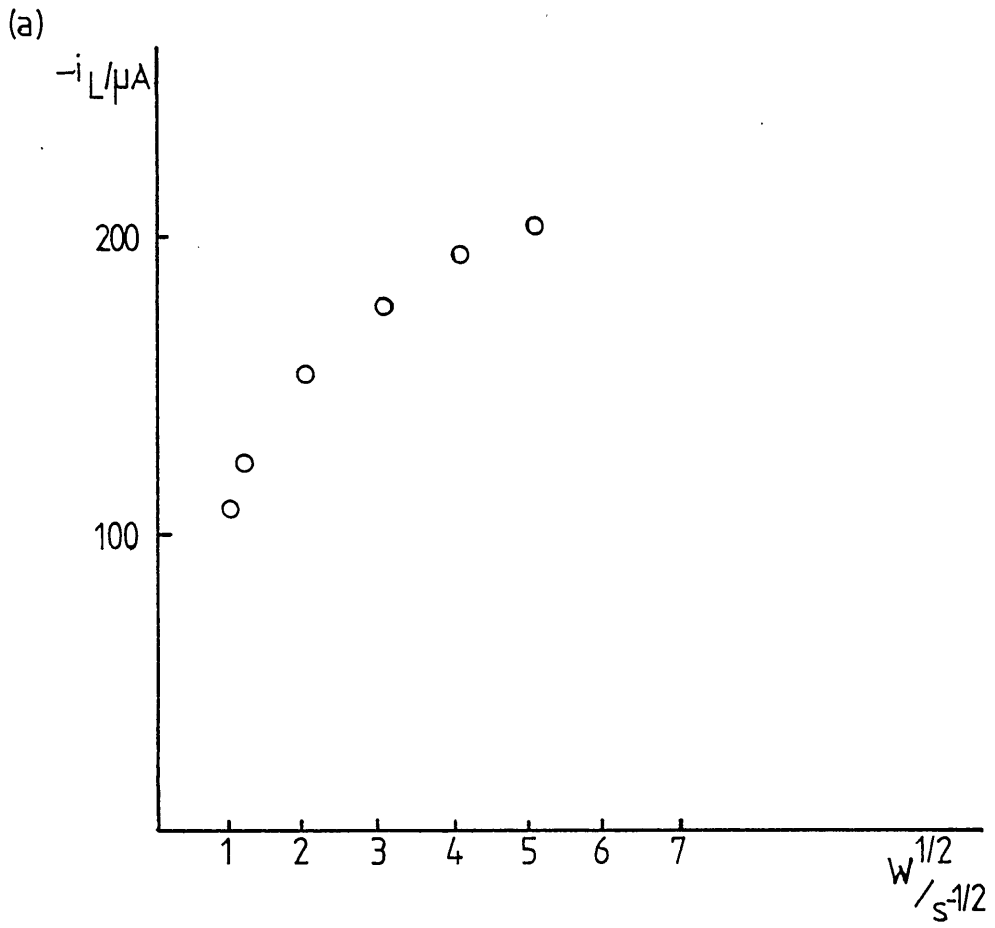
Figure 5.8. (a) Levich and (b) Koutecky-Levich plots for the reduction of oxygen at a (PA)-NC coated RDE (see figure 5.7b).

Metal incorporation into (PA)-NC films, on electrode surfaces, was tried by two methods. Firstly, it was observed that if a dichloromethane solution of (PA)-NC is added to a toluene solution of $Pd(MeCN)_2Cl_2$ a slow precipitate of metal incorporated polymer forms. The $Pd(MeCN)_2Cl_2$ ligands exchange with the polymer's isocyanide ligands and thus the polymer, becoming more cross-linked, precipitates from solution. Expecting similar behaviour, (PA)-NC coated glassy carbon electrodes were soaked in a toluene solution of $Pd(MeCN)_2Cl_2$ for various lengths of time from one hour to one day. The resulting coated electrodes were investigated electrochemically in 0.1 M aqueous K_2SO_4 by cyclic voltammetry (see section 2.3), sweeping the potential at various sweep rates (0.01 - 1 V s^{-1}) for different electrodes. However, no electrochemical activity was observed. Similar experiments were tried on (PS)-NC, (PS)-PPh$_2$ and (PS)-Pyn with the same result of no electrochemical activity. This lack of activity could be due to either palladium not being present in the coat (i.e. ligand exchange not having occurred) or that the palladium species incorporated could not be reduced electrochemically. The first possibility was dismissed because the polymer coats after soaking were insoluble in dichloromethane while non-metallated polymer coats would dissolve. The metallated polymers are only swelled by dichloromethane due to the added cross-linking. Therefore, one can deduce that the polymers were metallated but the incorporated palladium species were electrochemically inactive.

The second method of trying to incorporate palladium species into a polymer coated electrode involved electrochemically reducing palladium (II) in the presence of the polymer's complexing ligands, so that a stable (P)-(L)$_4$Pd species could be formed. Therefore, the potential of a (PA)-NC coated electrode, in 1 mM K_2PdCl_4 aqueous solution (+ 0.1 M KCl supporting electrolyte), was cycled at 10 m V s^{-1}. Unlike with the ferrocyanide solution, electrochemical activity was observed with a reduction wave

($E_{\frac{1}{2}}$ = +0.15 V vs SCE) which grew larger with each cycle (see figure 5.9).

When this electrode was removed from solution, rinsed with distilled water

and then cycled in 0.1 M KCl (see figure 5.10) only two peaks were observed,

one anodic (E_p = -0.3 V vs SCE) and one cathodic (E_p = -0.4 V vs SCE).

Looking back at the aqueous solution electrochemistry of K_2PdCl_4 (see

section 4.2.1) and comparing figures 4.1 and 4.2 with figures 5.9 and

5.10,one can see that these results indicate that palladium is being

reduced electrochemically in the polymer coat, but is forming palladium

metal rather than palladium zero complexes. This palladium metal can

adsorb and strip oxygen and hydrogen, as the plated electrode did, in

plain supporting electrolyte.

Very recently (1984), the electrochemical formation of metal micro-

particles in polymer films has been reported,in the literature,using a

similar method as described here[175,176]. Microparticles (seen by scanning

electron microscopy) are formed as agglomeration is prevented by the polymer

structure. These coated electrodes have been used for catalytic purposes

but are unsatisfactory for the needs of this work. Murray et al[212] have

also used metal deposition, in polymer coated electrodes, to identify where

reactions occur at a modified electrode. Work has also started, in our

laboratories, on the possibility of these palladium microparticles,

dispersed in the polymer, being used as a combined reference counter

micro-electrode[213,214].

Attempts to prevent metal formation by using lower concentrations

of K_2PdCl_4 in solution failed. Similar experiments were tried with

(PS)-NC, (PS)-PPh$_2$ and (PS)-Pyn and, even though these polymers seemed

not to be swelled by water, they surprisingly did give palladium (II)

reduction,forming palladium metal.

Palladium was also incorporated into polymers by bulk reactions

(see section 5.8). The resulting polymers (PA)-(NC)$_2$PdCl$_2$, (PS)-(NC)$_2$PdCl$_2$,

Figure 5.9. Current voltage curves for the reduction of K_2PdCl_4 at a (PA)-NC coated RDE (W = 10 Hz, v = 10 mV s^{-1}).
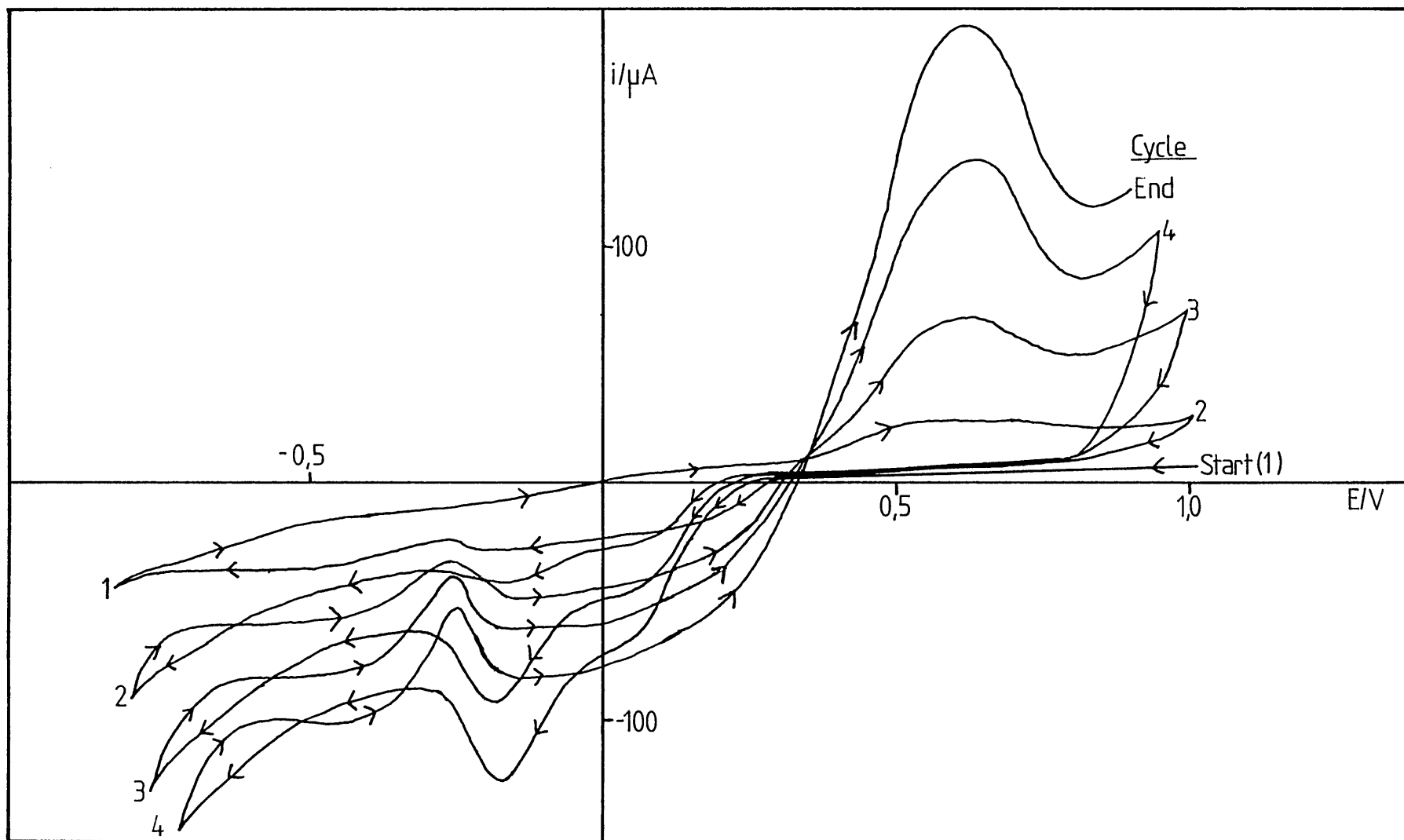
Figure 5.10. Current voltage curve for a palladium metal incorporated (PA)-NC coated RDE. (W = 10 Hz, v = 10 mV s^{-1}).
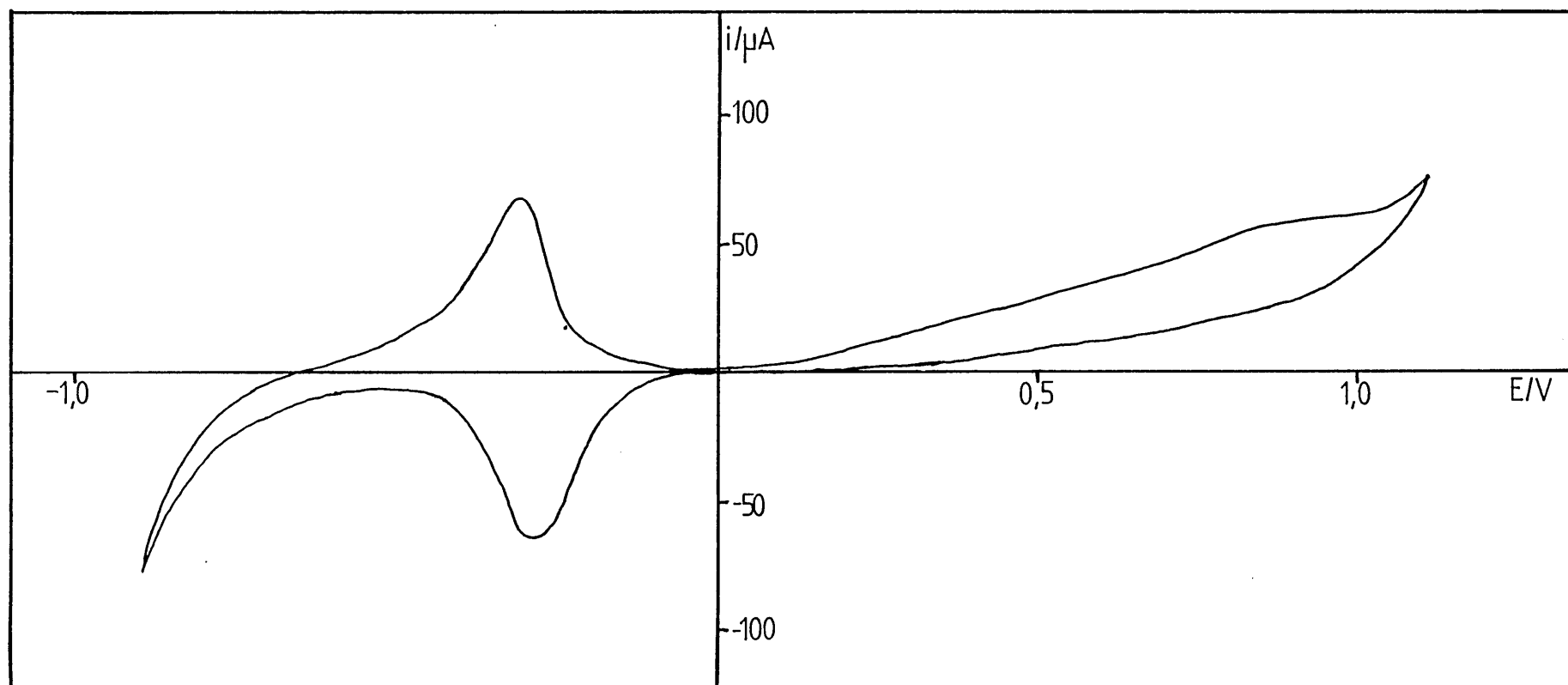
(PS)-$(PPh_2)_2PdCl_2$ and (PS)-$(Pyn)_2PdCl_2$ were drop coated on both platinum and glassy carbon RDEs. These coated electrodes were investigated using cyclic voltammetry with sweep rates from 10 mV s^{-1} to 1 V s^{-1} in 0.1 M aqueous KCl. No electrochemical activity was observed. As $Pd(RNC)_4$ complexes are prepared chemically under alkaline conditions, (PA)-$(NC)_2PdCl_2$ coats were investigated in 0.1 M aqueous KOH, but again no electrochemical activity was seen.

The possibility that the palladium ions were too far apart for electron hopping was considered. Electron hopping is the term used to describe the method of electron diffusion through these types of polymer films[7]. The polymer chains move, bringing two metal species in close proximity so that electron transfer can occur and then polymer motion separates the two species (see figure 5.11). This migration of charge can be dependent on two factors. Firstly, on the site-site collision frequency which, in turn, depends on the number of sites and the flexibility of the polymer chains. Secondly, on the counter ion mobility and this depends on the solvent swelling of the polymer.

Therefore, a polymer (PA)-$(NC)_2PdCl_2$ containing one palladium ion per two isocyanide ligands was synthesised, as was $[(CNRNC)_2PdCl_2]_n$ (see section 5.8.1), but again drop coats of these polymers showed no palladium electrochemistry in aqueous solutions of various pHs.

To see whether palladium (0) oxidation could be observed, (PA)-$(NC)_4Pd$ and $[(CNRNC)_4Pd]_n$ were synthesised (see section 5.8.1) but the resulting polymers were found to be totally insoluble in a wide range of solvents. Therefore, they could not be drop coated or investigated electrochemically. This insolubility of palladium (0) isocyanide complexes is known[166]. Also, the increase in polymer cross-linking by the palladium (0) species, will have only hindered solubilities.
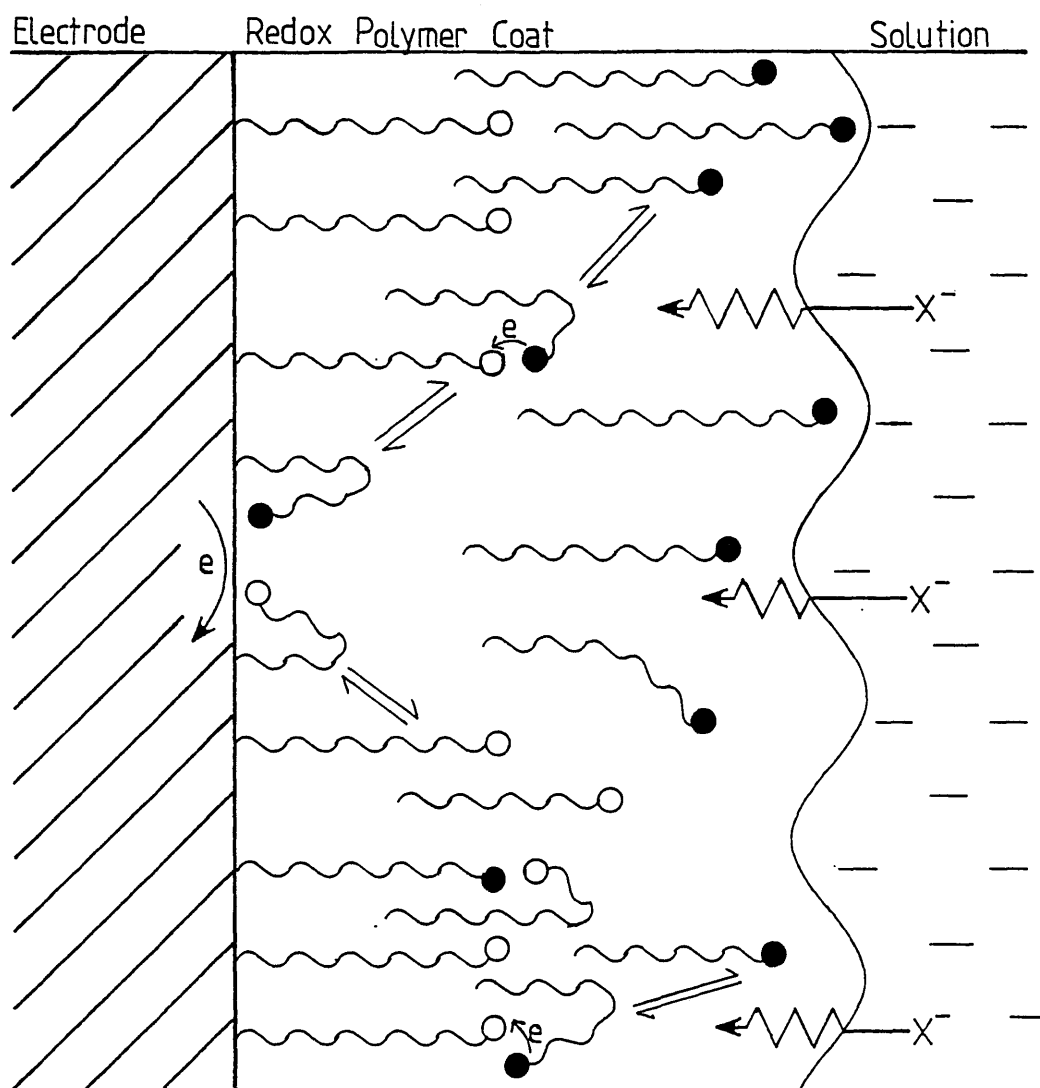
Figure 5.11. Schematic representation of the electron hopping
mechanism for redox-polymer coated electrodes
(O) = oxidised species, ● = reduced species).

Finally a (PS)-(PPh$_2$)$_2$NiBr$_2$ coat was similarly investigated in 0.1 M aqueous KCl and, as with the other polymers, showed no electrochemical activity.

From the above results it was felt the polymers, being hydrophobic in nature, were not being swelled sufficiently by the aqueous supporting electrolyte and hence counter ions were unable to diffuse through the polymer film. Therefore, the metal incorporated coats could not show any electrochemical activity and were just acting as insulators.

However, it is interesting that palladium microparticles could be deposited in all the polymer films, indicating swelling to a limited extent, while the bulk palladium incorporated polymers showed no activity.

From these observations, it was decided to investigate these polymers in non-aqueous solvents which would increase polymer swelling and therefore increase counter ion diffusion through the coat.

5.5. Non-Aqueous Electrochemistry

Considering possible solvents for non-aqueous electrochemical analysis, acetonitrile was chosen due to its swelling of the polymers (PS)-PPh$_2$, (PS)-NC and all the metal incorporated polymers without actually dissolving them (see table 5.1). (PA)-NC was not investigated due to its solubility in acetonitrile.

Investigating the non-metallated polymers, (PS)-PPh$_2$ was drop coated on platinum electrodes giving very even films. The potential of the resulting coated electrode could be cycled, in acetonitrile (plus 0.1 M TEAT supporting electrolyte), at various sweep rates (0.01 → 1 V s^{-1}), between +2 V and -2 V vs Ag/Ag$^+$, for six hours, without any degradation of the polymer film. This stability was also shown on glassy carbon and for (PS)-NC on glassy carbon and platinum.

A clean platinum rotating (at 10 Hz) disc electrode, with its potential being swept anodically (at 10 mV s^{-1}), in a 1 mM ferrocene solution (MeCN + 0.1 M TEAT), gave the expected oxidation wave ($E_{\frac{1}{2}}$ = +0.1 V vs Ag/Ag$^+$, see figure 5.12a) which shows Levich rotation speed dependence (see figure 5.12b) indicating mass transport limited current. When a (PS)–PPh$_2$ coated electrode ($\sim$ 100 layers) was used for a similar experiment, an oxidation wave was again observed but here the limiting current was less than for the clean electrode and showed Koutecky-Levich dependence on rotation speed (see figures 5.13 a and b). This Koutecky-Levich dependence shows that diffusion of ferrocene through the polymer is slowing its transport to the electrode. From the intercept one gets $1/nFA[Ferrocene]k'_{ME}$, where $k'_{ME} = \frac{KD_F}{L}$ (F = Ferrocene). Hence, figure 5.13 gives KD_F/L = 7.9 x 10^{-5} ms^{-1}. Assuming K = 1 and estimating L $\sim 10^2$ nm (approximate, as the amount of swelling of the coat is unknown), the diffusion coefficient of ferrocene in the (PS)–PPh$_2$ coat $D_F \sim 10^{-7}$ cm^2 s^{-1}, which is two orders of magnitude lower than for bulk solution. (PS)–NC coated on glassy carbon gives similar results.

Metal incorporation into (PS)–PPh$_2$ drop coated electrodes was attempted by four different methods. Firstly, as in the previous section, polymer coated platinum electrodes were soaked in Pd(MeCN)$_2$Cl$_2$ aceto-nitrile solutions for various lengths of time from one hour to one week. The resulting metal incorporated (?) polymer coated electrodes were then investigated in plain supporting electrolyte solution (MeCN + 0.1 M TEAT). Cyclic voltammetric analysis of different electrodes at various sweep rates (0.01 $\rightarrow$ 1 V s^{-1}) showed no palladium (II/0) electrochemistry. Similar experiments were tried on (PS)–PPh$_2$ coated platinum electrodes soaked in Ni(MeCN)$_2$Br$_2$ acetonitrile solutions and on (PS)–NC coated glassy carbon electrodes soaked in Pd(MeCN)$_2$Cl$_2$ acetonitrile solutions. Also, (PS)–PPh$_2$ coated platinum electrodes were soaked in Pd(PPh$_3$)$_2$Cl$_2$,

Figure 5.12. The oxidation of ferrocene at a clean platinum RDE; (a) current voltage curve; (b) Levich plot.
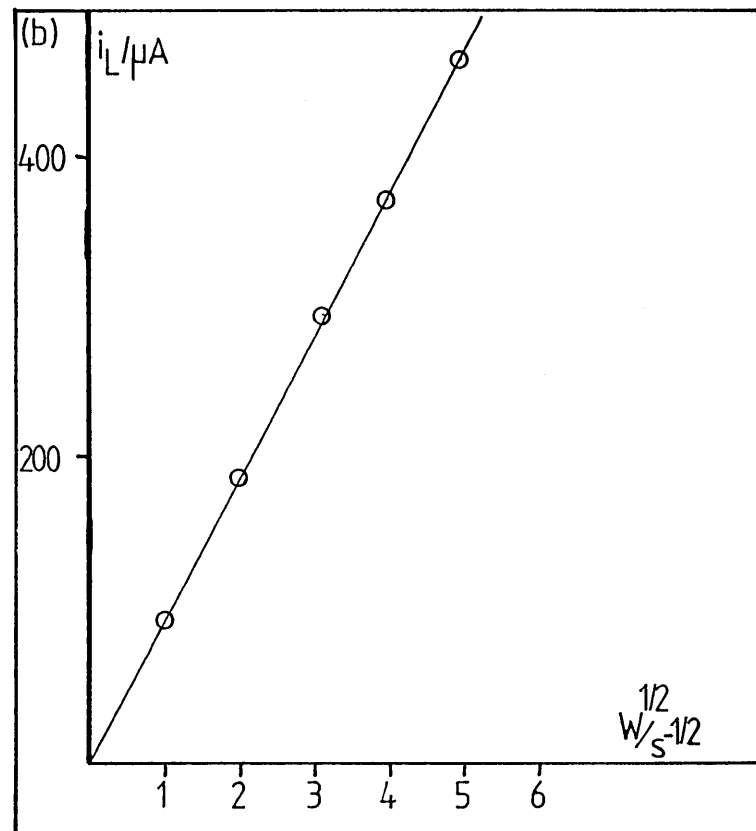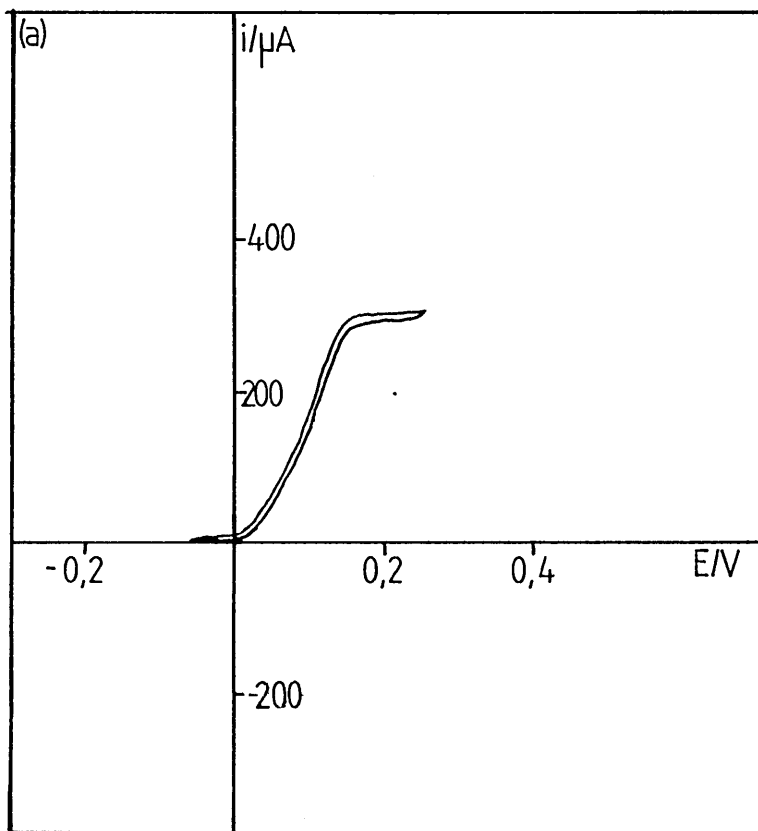
Figure 5.13. Ferrocene oxidation at a (PS)-PPh$_2$ coated platinum RDE; (a) current voltage curve; (b) Koutecky-Levich plot.
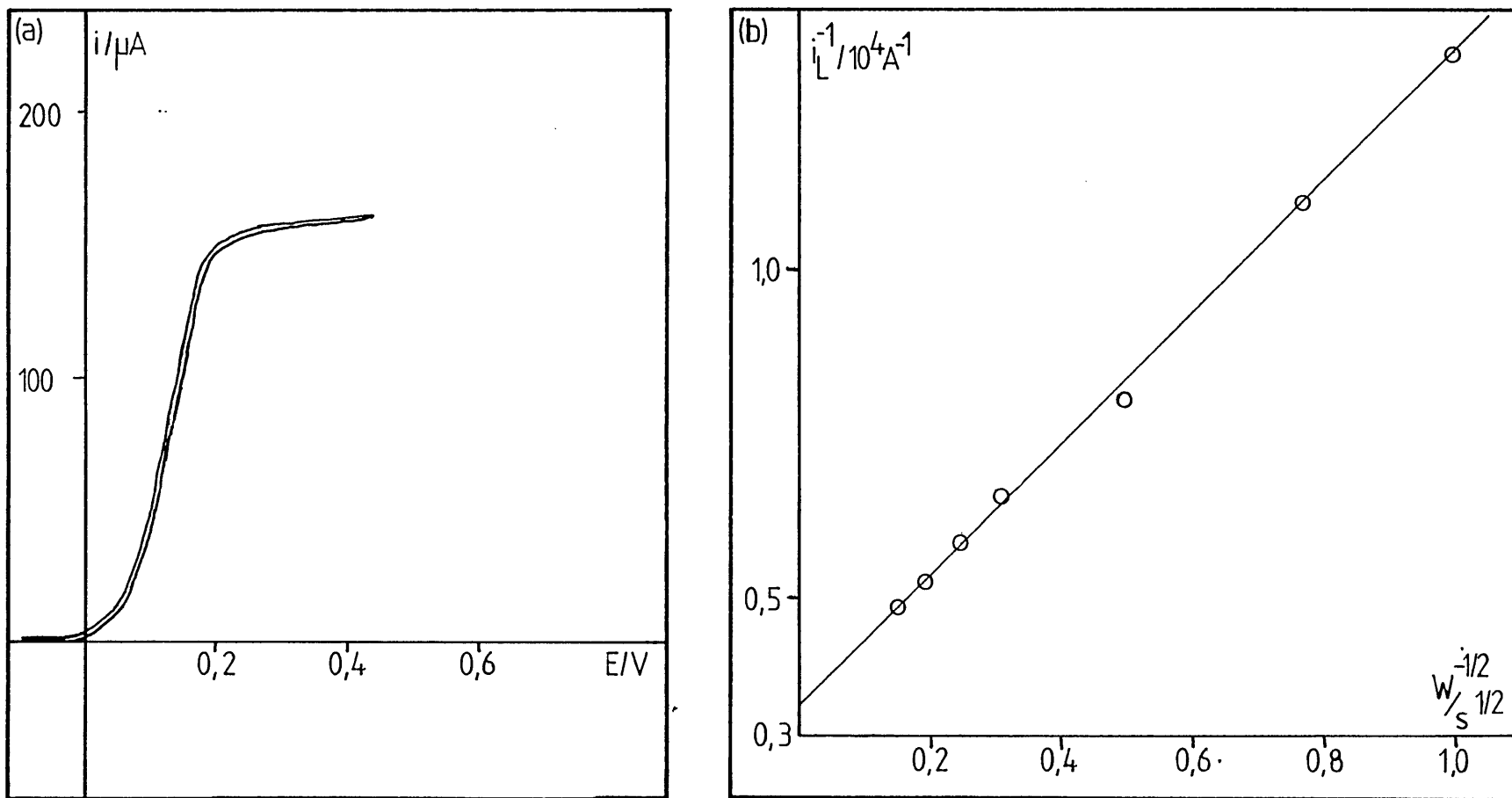
$Pd(PPh_3)_4$, $Ni(PPh_3)_2Cl_2$ and $Ni(PPh_3)_4$ solutions (in acetonitrile),
expecting some phosphine ligand exchange with the polymers. (All
$Pd(PPh_3)_4$ and $Ni(PPh_3)_4$ experiments were done in a glove bag because
of the oxygen sensitivity of the complexes). None of the resulting
coated electrodes showed any metal couple electrochemistry. Metal
incorporation was again tested by the solubility of the polymer in
dichloromethane. Metallation had occurred for the polymers soaked
in $Pd(MeCN)_2Cl_2$ or $Ni(MeCN)_2Br_2$ solutions but seemed not to have oc-
curred for polymers soaked in solutions of the phosphine complexes.
This difference can be explained by the more bulky phosphine complexes
being unable to diffuse through the polymer films and that the $M(MeCN)_2X_2$
complexes may undergo ligand exchange more easily.

The second method of metal incorporation was similar to the first
but during soaking the polymer coated ((PS)-PPh_2 or (PS)-NC) electrodes
were potentiostatted at -0.4 V vs Ag/Ag^+ to see if this would attract
metal ions into the coat. This potential was chosen as it is before
any possible palladium (II) reduction can occur. Cyclic voltammetric
analysis of the resulting electrodes again showed no palladium reduction/
reoxidation electrochemistry. This method was also tried for (PS)-PPh_2
coated electrodes soaking in $Ni(MeCN)_2Br_2$ solutions but the same negative
results were observed.

The third method involved drop coating the polymer (PS)-PPh_2 but
before the solvent evaporated a drop of $Pd(MeCN)_2Cl_2$ dichloromethane
solution was added and a resulting palladium dichloride incorporated
polymer precipitated due to the increased cross-linking in the polymer.
However, the resulting coats were very uneven, leaving bare patches on
the electrode, and showed no electrochemical activity.

The fourth method, as in aqueous electrochemistry, was to reduce
palladium (II) species in the presence of (PS)-PPh_2 coated electrodes

expecting the formation of (PS)–$(PPh_2)_4Pd$ species. Therefore, the potential of a (PS)–PPh_2 coated platinum electrode, rotating at 10 Hz, was cycled at 10 mV s^{-1} in $Pd(MeCN)_2Cl_2$ acetonitrile solution (+ 0.1 M TEAT). A reduction wave was observed ($E_{\frac{1}{2}}$ = -2.0 V vs Ag/Ag$^+$, see figure 5.14) but cyclic voltammetry of the resulting metal incorporated polymer, in plain supporting electrolyte solution, showed no palladium (II/O) electrochemistry (see figure 5.15). Comparing figures 5.14 and 4.4 one can see that the above observed reduction wave is due to palladium metal formation, in the polymer film, rather than a stable (PS)–$(PPh_2)_4Pd$ complex.

As the above gave palladium metal it was thought reduction of $Pd(PPh_3)_2Cl_2$ at a (PS)–PPh_2 coated electrode would have good possibilities of forming a (PS)–$(PPh_2)_2Pd(PPh_3)_2$ complex. Firstly, attempts to find a solvent that swelled (PS)–PPh_2 but dissolved $Pd(PPh_3)_2Cl_2$ failed. All solvents in which $Pd(PPh_3)_2Cl_2$ was reasonably soluble also dissolved the polymer. Acetonitrile was found to be the best solvent, as it swelled the polymer, even though $Pd(PPh_3)_2Cl_2$ was only slightly soluble ($\sim$ 0.2 mM). Therefore, a (PS)–PPh_2 drop coated electrode, rotating at 10 Hz, was cycled (at 10 mV s^{-1}) in a saturated $Pd(PPh_3)_2Cl_2$ acetonitrile solution, for up to six hours, but no palladium (II) reduction was observed. Similar experiments with $Ni(PPh_3)_2Cl_2$ also showed no reduction waves. This lack of electrochemistry is probably due to the very bulky $M(PPh_3)_2Cl_2$ (where M = Ni or Pd) complexes being unable to diffuse easily through even a well swelled polymer.

Due to these negative results it was decided to look at the bulk metallated polymers. Cyclic voltammetric analysis of (PS)–$(PPh_2)_2PdCl_2$ drop coated on a platinum RDE gave, at fast sweep rates (0.5 V s^{-1}), a very slight cathodic peak (E_p = -1.3 V vs Ag/Ag$^+$) on the first sweep, but this was not present on subsequent cycles (see figure 5.16). It

Figure 5.14. Current voltage curve for the reduction of Pd(MeCN)$_2$Cl$_2$ at a (PS)—PPh$_2$ coated RDE.
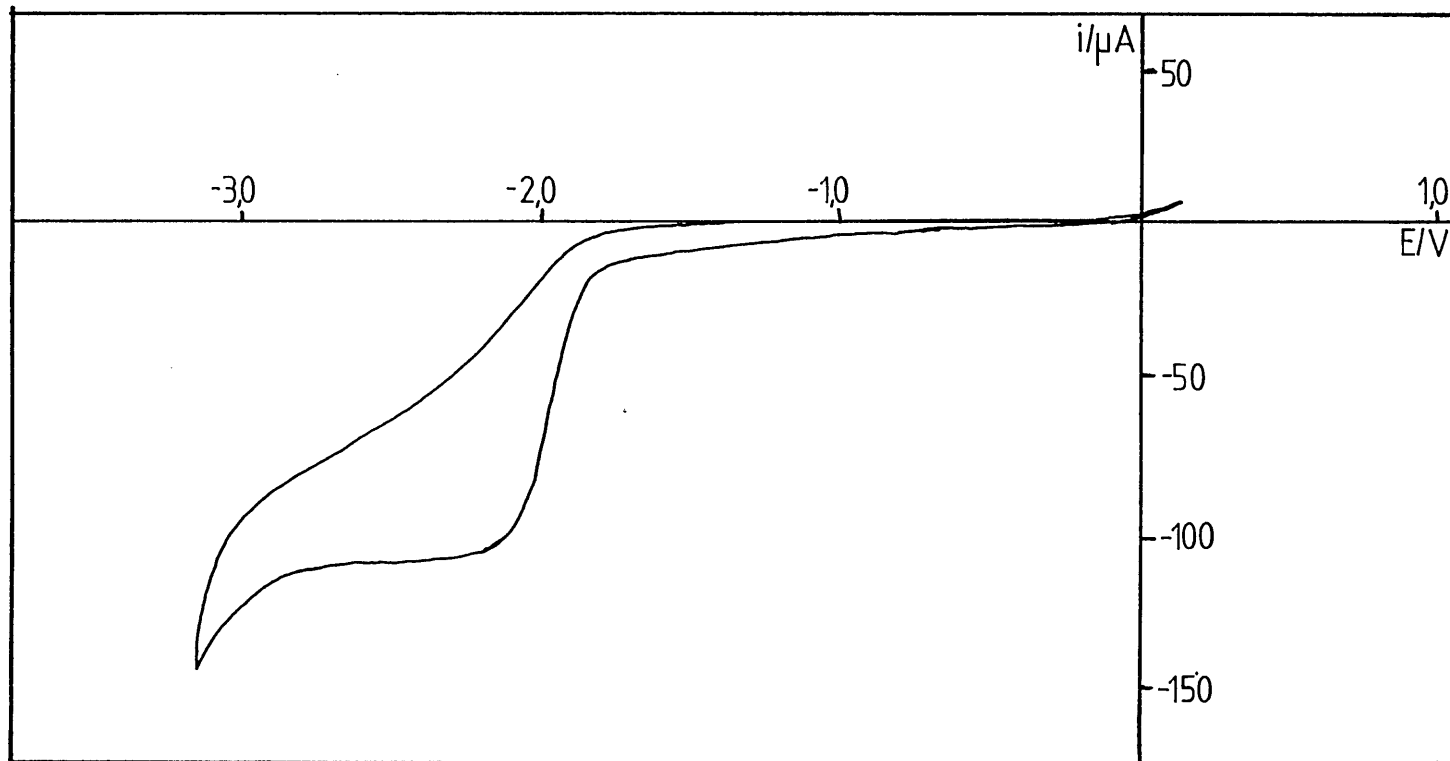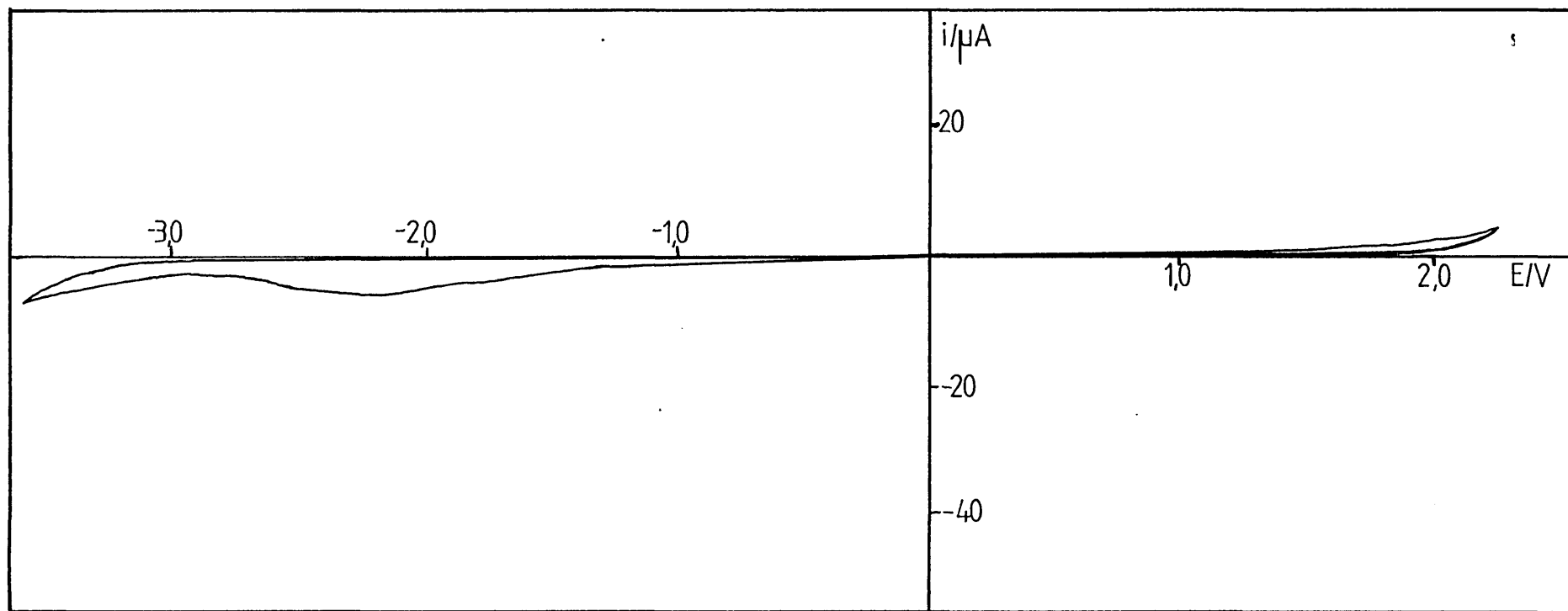
Figure 5.15. Cyclic voltammogram of the (PS)—PPh$_2$ coated electrode after Pd(MeCN)$_2$Cl$_2$ reduction (i.e. after figure 5.14) (v = 100 mV s^{-1}).
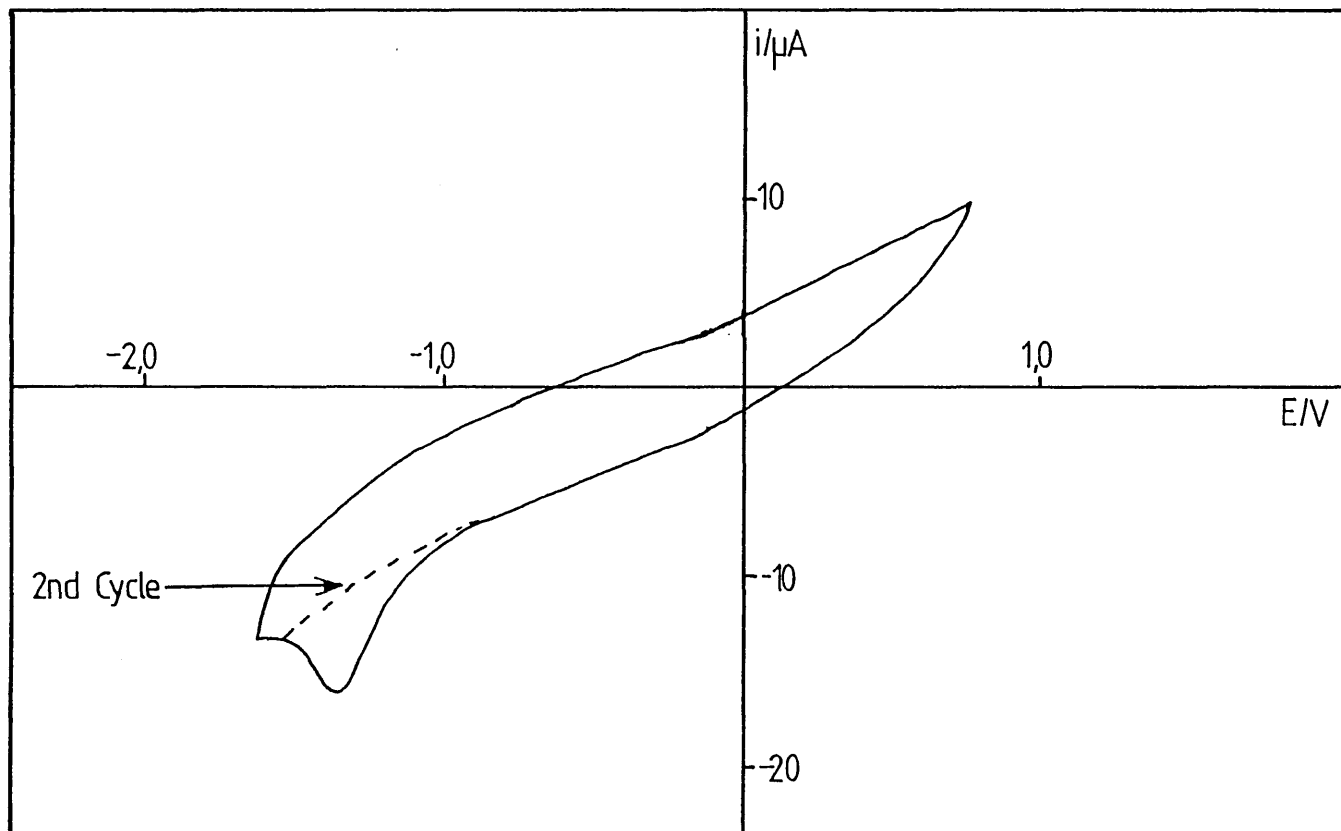
Figure 5.16. Cyclic voltammogram of a (PS)—(PPh$_2$)$_2$PdCl$_2$ coated RDE (v = 500 mV s^{-1}).

was felt that this could be due to a small amount of palladium (II) close to the electrode being reduced to palladium metal by a similar mechanism to $Pd(PPh_3)_2Cl_2$ acetonitrile solution species (see section 4.2.2).

To avoid this metal formation $(PS)-(PPh_2)_2PdCl_2$ coated electrodes were investigated in chloroform (+ 0.1 M TEAP) with added triphenyl-phosphine (0.1 M), as in section 4.2.2. It was hoped that on soaking $(PS)-(PPh_2)_2Pd(PPh_3)Cl^+$ species would be formed. Cyclic voltammetric analysis of the coat in chloroform (+ 0.1 M PPh_3 + 0.1 M TEAT) gave two small peaks, one cathodic (at E_p = -0.55 vs SCE) and one anodic (at E_p = +0.05 vs SCE, see figure 5.17). These peaks decrease on subsequent cycles. However, the peak potentials agree well with the $Pd(PPh_3)_3Cl^+$ reduction ($E_{\frac{1}{2}}$ = -0.52 V vs SCE) and $Pd(PPh_3)_3$ oxidation ($E_{\frac{1}{2}}$ = +0.02 V vs SCE) potentials found in solution electrochemistry (see section 4.2.2). Therefore, one can deduce that a small amount of palladium species close to the electrode were being reduced and re-oxidised. From the area under these peaks one can calculate that less than a monolayer of palladium complexed species were involved.

A $(PS)-(PPh_2)_2NiBr_2$ drop coated electrode showed no electrochemistry when similarly investigated in acetonitrile (+ 0.1 M TEAT), without and with added triphenylphosphine. This lack of activity is probably due to lack of conduction through the coat and the small amount, of Ni(II) close to the electrode which may react, not being detectable. $(PS)-(NC)_2PdCl_2$ and $[(CNRNC)PdCl_2]_n$ drop coated electrodes showed no electrochemical activity in plain acetonitrile (+ 0.1 M TEAT) or with added triphenyl-phosphine (0.1 M) or added CNRNC (0.1 M).

$(PS)-(PPh_2)_4M$ (where M = Ni or Pd) polymers were synthesised (see section 5.8.3) but the resulting products were totally insoluble in a wide range of solvents and therefore could not be investigated. This
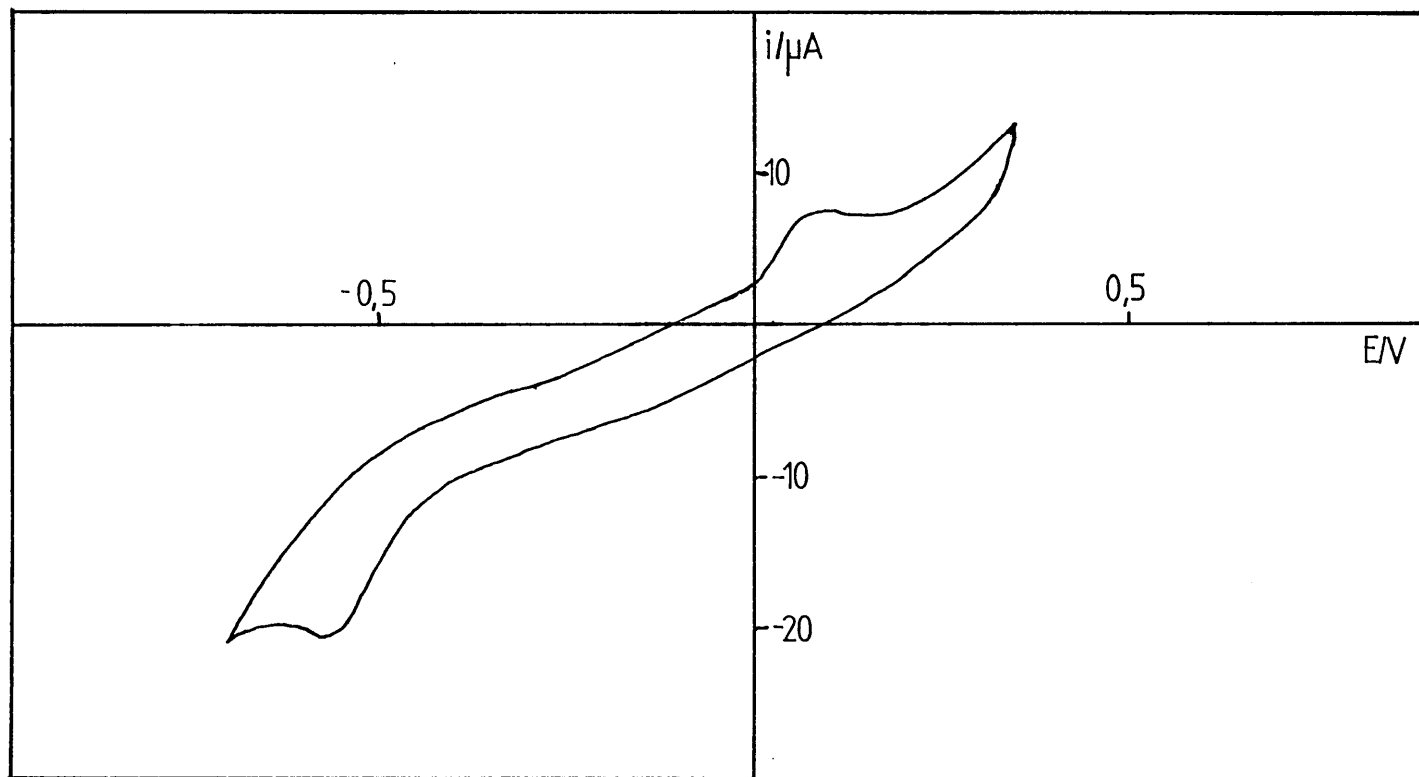
Figure 5.17. Cyclic voltammogram for a (PS)—(PPh$_2$)$_2$PdCl$_2$ coated RDE soaked in a solution containing PPh$_3$ (v = 250 mV s^{-1}).

insolubility is probably due to the increased cross-linking of the polymer by the now, tri- or tetra-coordinated metal species.

From all the above results one can conclude that the lack of electron conduction through the coat seems to be preventing reversible electrochemistry of the metal species incorporated in the layer. This is discussed more fully in section 5.7.

5.6. Catalysis Experiments

From the results in the previous two sections one can see that reversible electrochemistry of palladium incorporated, styrene based polymers was not possible. Zerovalent palladium incorporated polymers could not be investigated as, when made by bulk reactions, they were totally insoluble. It was therefore decided to attempt the aqueous Wacker reaction (see section 1.2.1) with palladium (II) incorporated polymers, coated on electrodes. Thus, one could see if reaction occurs and if the palladium (II) species can be regenerated. As discussed in section 4.2.2 it is possible that regeneration of the palladium (II) species will occur during the Wacker process rather than via a generated (P)-$(L)_4Pd$ product.

Therefore, (PA)-$(NC)_2PdCl_2$ was drop coated on a glassy carbon RDE (glassy carbon was used as ethylene adsorbs on platinum[1,2]) and the electrode was rotated (at 10 Hz) in aqueous KCl (0.1 M). The electrode potential was potentiostatically held at +1.1 V vs SCE which is as far positive as one can go before oxygen evolution. The reason for this is to give the electrode the best possibility to perform the palladium (0 → II) oxidation reaction. Ethylene was then passed through the solution for up to one hour. No oxidation current was observed but looking at coated electrodes one could visually see palladium metal particles in the polymer layer. This indicates that the Wacker reaction occurred but the palladium (II) regeneration did not.

It was decided to try investigations in non-aqueous solvents where larger voltage limits are possible and the palladium (II/0) couple is known (see section 4.2.2). (PS)—$(PPh_2)_2PdCl_2$, (PS)—$(NC)_2PdCl_2$ and $[(CNRNC)PdCl_2]_n$ drop coated glassy carbon electrodes were rotated (at 10 Hz) in acetonitrile (+ 0.1 M TEAT) plus ~2 mols dm^{-3} water. This concentration of water was found necessary in section 4.4.1. The electrode was potentiostatically held at +0.6 V vs Ag/Ag^+ which is well above the $Pd(PPh_3)_4 \rightleftharpoons Pd(PPh_3)_2X_2$ solution oxidation potential. Ethylene was passed through the solution for up to one hour. Again, no oxidation current was observed but on removal one could see metallic particles dispersed in the polymer coat. Similar experiments with triphenylphosphine in solution (0.1 M), attempting to stabilise a palladium (0) complex, gave the same result. These results show that the Wacker process had occurred but again palladium (II) electrochemical regeneration had failed. An interesting deduction, that can be made, is that as the Wacker process has occurred water must diffuse through the polymers. Therefore, these polymers must be slightly swelled by water.

The catalysis of nickel incorporated polymers could not be investigated as it is the nickel (0) species which is catalytically active and as the (PS)—$(PPh_2)_4Ni$ polymer was totally insoluble, it could not be drop coated.

5.7. Discussion

A summary of the electrochemical analyses on the metallation of polymer films and on bulk metallated polymer films are given in tables 5.3 and 5.4 respectively.

Looking at the results of this chapter, one can see that catalysis by palladium (II) species incorporated in a polymer does occur.

Table 5.3: Summary of the Electrochemical Results for Metal Incorporation into Polymer Films on Electrode Surfaces.

Method of metallation of polymer films	Polymers → Electrochemical Solvent ↓	(PA)-NC	(PS)-NC	(PS)-PPh$_2$	(PS)-Pyn
Soaking in a toluene solution of Pd(MeCN)$_2$Cl$_2$	Aqueous + 0.1 M KCl	Metal was incorporated but the resulting polymer showed no electrochemical activity			
Cycle potential of polymer coated electrode in aqueous K$_2$PdCl$_4$ (1 mM) + 0.1 M KCl	Aqueous + 0.1 M KCl	Deposition of Pd microparticles, in the polymer coat, was observed. These microparticles could adsorb and strip oxygen and hydrogen			
Soaking in an acetonitrile soln. of M(MeCN)$_2$X$_2$ (M = Ni, Pd; X = Cl$^-$, Br$^-$)	Acetonitrile + 0.1 M TEAT	——	Metallation occurred but the polymer showed no electrochemical activity		
Soaking in an acetonitrile soln. of M(PPh$_3$)$_2$Cl$_2$ or M(PPh$_3$)$_4$ (M = Ni, Pd)	Acetonitrile + 0.1 M TEAT	——	——	Showed no metallation of the polymer	——
Soaking in an acetonitrile soln. (+ 0.1 M TEAT) of Pd(MeCN)$_2$Cl$_2$ at a potential of + 0.4 V vs Ag/Ag$^+$	Acetonitrile + 0.1 M TEAT	——	Metallation occurred but the resulting polymer showed no electrochemical activity		——
As above except Ni(MeCN)$_2$Br$_2$ soln.		——	——	same as above	——
Drop coating the polymer and adding Pd(MeCN)$_2$Cl$_2$ before evaporation	Acetonitrile + 0.1 M TEAT	——	Coats (very uneven) showed no electrochemical activity		——
Cycling potential of polymer coated electrode in MeCN (+ 0.1 M TEAT) soln. of Pd(MeCN)$_2$Cl$_2$	Acetonitrile + 0.1 M TEAT	——	——	Formation of Pd metal in the polymer film	——
As above in M(PPh$_3$)$_2$Cl$_2$ soln.		——	——	no electrochem	——

Table 5.4: Summary of the Electrochemical Analysis on Bulk Metallated Polymers Coated on Electrodes (Polymers (PS)-$(NC)_4Pd$, $[(CNRNC)_2Pd]_n$, (PS)-$(PPh_2)_4Pd$ and (PS)-$(PPh_2)_4Ni$ were also Synthesised but Found Insoluble in a Wide Range of Solvents).

Polymer / Solution	(PA)-$(NC)_2PdCl_2$	(PS)-$(NC)_2PdCl_2$	$[(CNRNC)PdCl_2]_n$	(PS)-$(Pyn)PdCl_2$	(PS)-$(PPh_2)_2PdCl_2$	(PS)-$(PPh_2)NiCl_2$
Aqueous (+ 0.1 M KCl or +0.1 M KOH)	Showed no electrochemical activity	Showed no electrochemical activity	Showed no electrochemical activity	Showed no electrochemical activity	Showed no electrochemical activity	Showed no electrochemical activity
Acetonitrile + 0.1 M TEAT		Showed no electrochemical activity	Showed no electrochemical activity	Showed no electrochemical activity	Showed Pd(II) reduction on first cycle (< monolayer)	Showed no electrochemical activity
Acetonitrile + 0.1 M TEAT + 0.1 M PPh_3		Showed no electrochemical activity				Showed no electrochemical activity
Acetonitrile + 0.1 M TEAT + 0.05 M CNRNC		Showed no electrochemical activity	Showed no electrochemical activity			
Chloroform + 0.1 M TEAP + 0.1 M PPh_3					Showed reversible Pd(II/0) couple for few cycles (again, < monolayer)	

However, electrochemical regeneration of the catalytically active species fails and palladium metal is generated. This palladium metal could be formed by the decomposition of a zerovalent complex produced by the catalytic reaction or palladium metal itself could be the direct product of the catalytic reaction. In both cases, fast electrochemical oxidation could regenerate the palladium (II) species either from the zerovalent complex before it decomposed, or from the catalytic complex as the products were generated.

Some reversible palladium (II/O) electrochemistry did occur at a (PS)-$(PPh_2)_2PdCl_2$ coated electrode. This amounted to less than a monolayer next to the electrode surface reacting, but this does show that the polymer was well swelled and counter ions (and triphenyl-phosphine) could diffuse through the polymer. Therefore, results indicate that it is the lack of electron conduction through the polymer layer which is preventing electrochemical reductions/oxidations. This is probably due to poor electron exchange between the palladium or nickel species because they are two-electron couples.

To try to overcome this poor electron conduction the incorporation of quinone groups in the polymer was considered. Work on styrene based polymers with attached quinone groups showed very good reversible electro-chemistry in aqueous base (see figures 5.18 and 5.19). Also work published by Arai and Yashiro[100] shows quinone groups can be used to regenerate palladium (II) during the Wacker process (discussed in section 1.2.1). Therefore, in this situation the electrode must only regenerate the quinone from the hydroquinone produced. However, the synthesis of a styrene based polymer with attached phosphine and quinone groups was not possible in the time available to the polymer chemists[177] (see section 5.8).
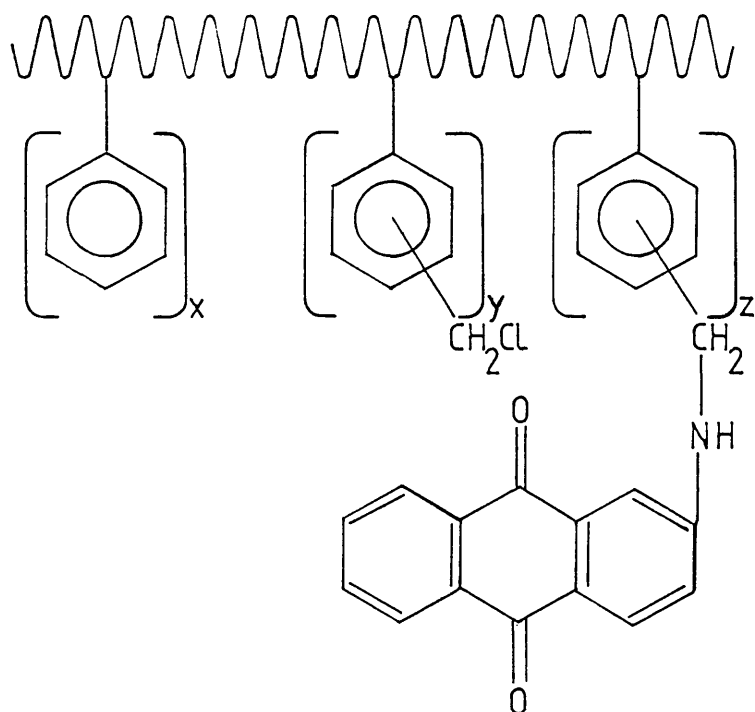
Figure 5.18. Structure of the styrene based polymer with attached quinone groups ((PS)—Q); x:y:z = 10:1:9.
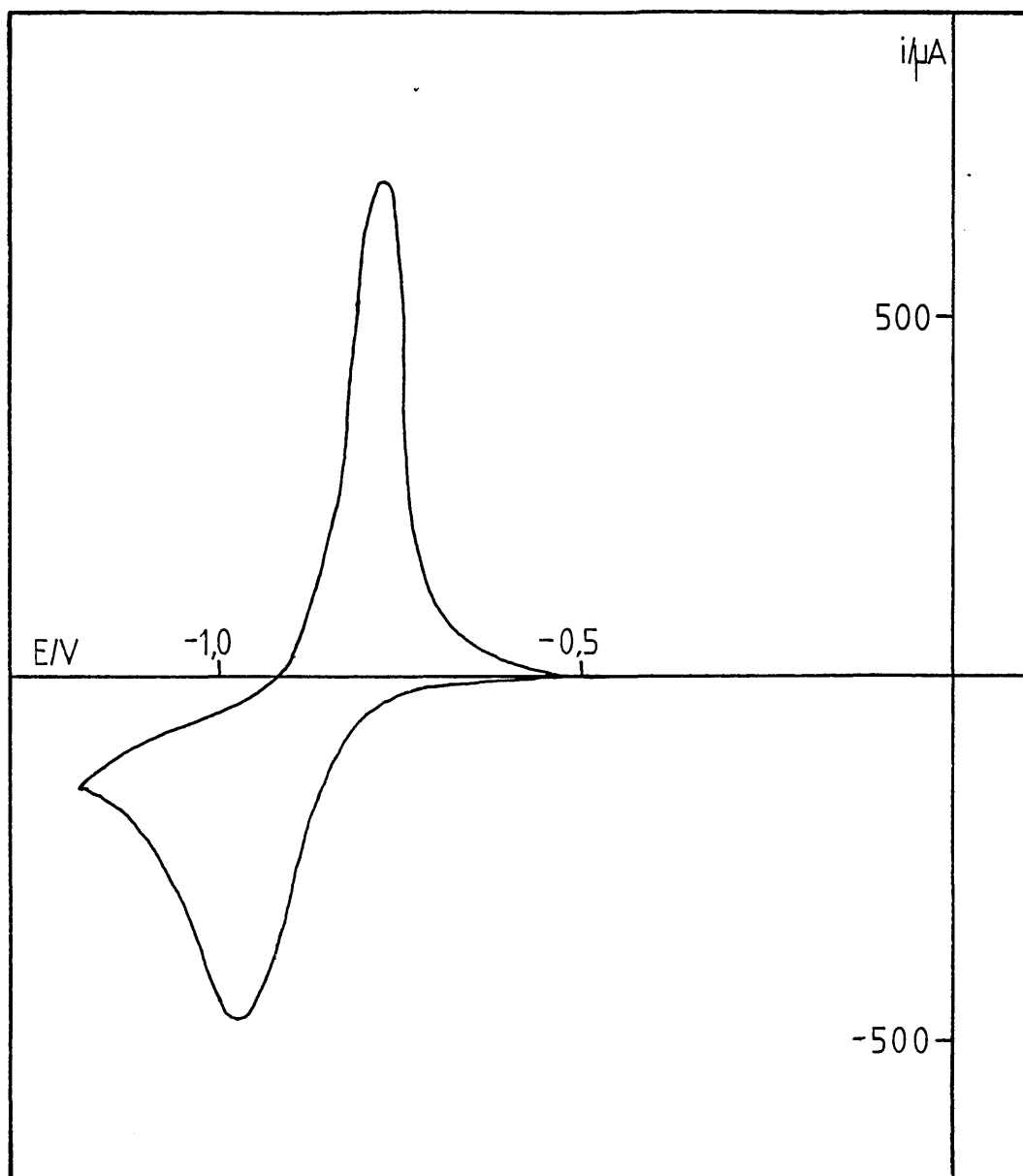
Figure 5.19. Cyclic voltammogram of a (PS)—Q coated platinum
RDE (v = 100 mV s^{-1}).

Due to these factors, the use of conducting polymers with attached phosphine ligands for metal complexation, was envisaged. With this type of system the conducting polymer backbone would transport electrons directly to the metal sites and hence regenerate the catalytically active metal species. Thus, electron exchange between the metal species would be by-passed. This is the topic of work discussed in the following chapter.

5.8. Appendix: Polymer Syntheses

In this section the syntheses of the polymers investigated in this chapter are discussed. The majority of these polymers were synthesised by R. Arshady and B.S.R. Reddy, whilst members of the Wolfson Unit for Modified Electrodes at Imperial College, though some metal incorporations and reductions were performed by myself.

The strategy of the polymer section was to functionalise monomers with labile groups. Then these monomers would be copolymerised with non-functionalised monomers. The labile group in the resulting polymer could then be displaced to give the required ligand attached polymer. Metal incorporation can follow to give the polymer supported catalyst. The advantages of this method are that the degree of cross-linking and the separation of functional groups are variable and controllable. Also, a single polymer precursor can be used to produce a variety of ligand attached polymers, and ligands sensitive to the polymerisation conditions can be safely introduced at a later stage.

All polymers were characterised by ^{1}H NMR, ^{13}C NMR, infra-red and gel permeation chromatography (for molecular weight determination).

5.8.1. Isocyanide Polymers

The isocyanide ligand containing polymers were synthesised by

methods published in the literature[178,179]. 2,4,5-trichlorophenyl acrylate and dimethylacrylamide (or styrene) were copolymerised, with hexamethylene diacrylamide cross-linking agent, by azo-bis-isobutyronitrile (AIBN) radical initiator (see figures 5.20 and 5.21). Exchange of the trichlorophenoxy group with 3-hydroxypropylformamide followed by elimination of water gave the required (PA)-NC and (PS)-NC polymers.

Metal incorporation was achieved by adding a solution (aqueous K_2PdCl_4 for (PA)-NC, $Pd(PhCN)_2Cl_2$ in dichloromethane for (PS)-NC) of the required palladium species to the polymers, swelled/dissolved in the same solvent. The mixture was shaken for one hour, filtered and the solid palladium (II) incorporated polymers washed several times with clean solvent.

$[(CNRNC)PdCl_2]_n$ was synthesised by simple ligand exchange of CNRNC with $Pd(PhCN)_2Cl_2$, which gave the polymer as a precipitate.

Palladium reduction to give palladium (0) incorporated isocyanide polymers was performed by Malatesta's method[165] using strong base:

$$(RNC)_2PdX_2 + 2RNC + 2KOH \rightarrow [(RNC)_4Pd](OH)_2 + 2KX$$

$$[(RNC)_4Pd](OH)_2 + RNC \rightarrow (RNC)_4Pd + RNCO + H_2O$$
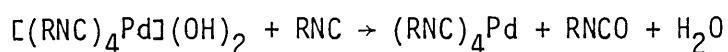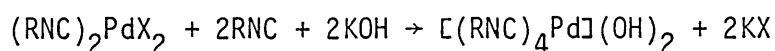
5.8.2. Pyridine Polymer

This was synthesised by reacting the same trichlorophenyl acrylate/styrene copolymer as above (see figure 5.21) with 4-(2-aminoethyl)pyridine, eliminating the trichlorophenoxy group, to give the polymer (PS)-Pyn.

Figure 5.20. Synthesis of the precursor to (PA)-NC.
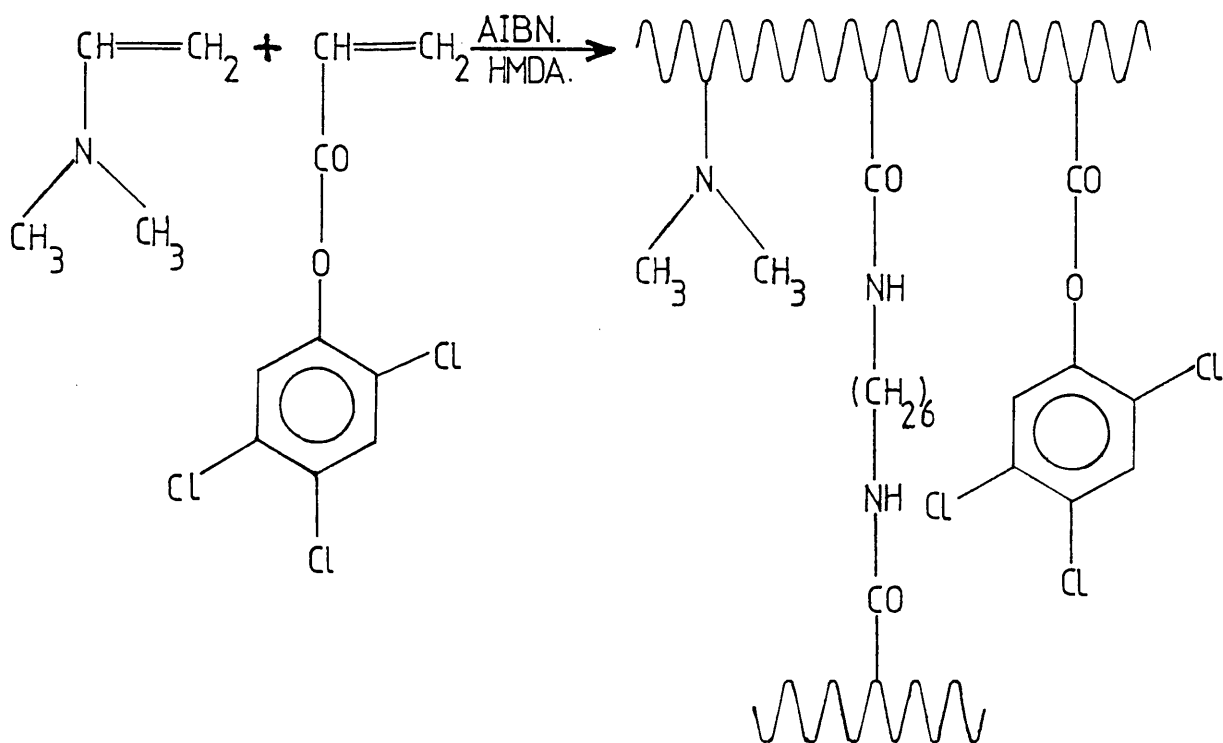
Figure 5.21. Synthesis of the precursor to (PS)-NC and (PS)-Pyn.
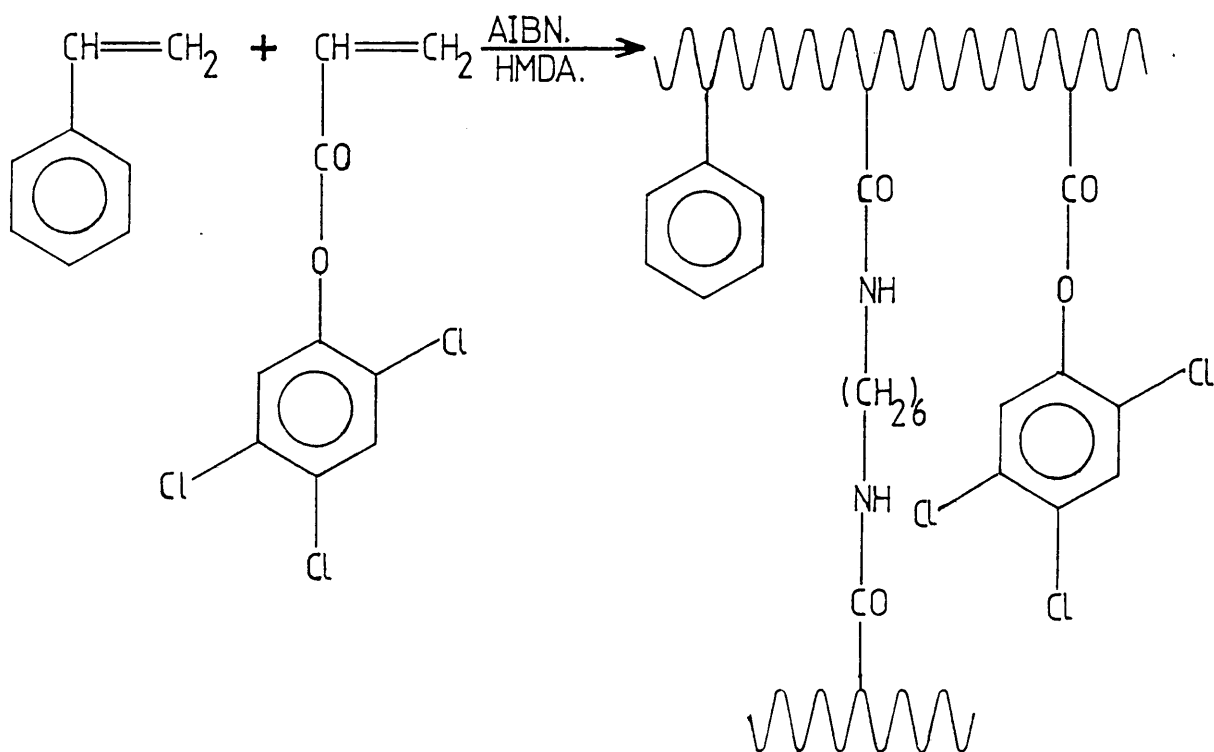
Palladium dichloride incorporation was achieved by mixing di-chloromethane solutions of the polymer and $Pd(PhCN)_2Cl_2$. The metallated polymer slowly precipitated.

5.8.3. Phosphine Polymers

The precursor polymer was prepared by the copolymerisation of chloromethylated styrene with styrene[180] in the presence of azo-bis-isobutyronitrile radical initiator (see figure 5.22). This polymer was then reacted with lithium diphenylphosphide, eliminating lithium chloride, to give the polymer $(PS)\!-\!PPh_2$.

Metal incorporation was achieved by mixing polymer and metal complex $(Pd(PhCN)_2Cl_2$ or $Ni(MeCN)_2Br_2)$ dichloromethane solutions. The solvent was then evaporated under reduced pressure. The resulting solid was dissolved in dimethylformamide, filtered and $(PS)\!-\!(PPh_2)_2MX_2$ (where M = Ni or Pd) precipitated from solution by the addition of ethyl acetate.

Metal reduction to give $(PS)\!-\!(PPh_2)_4$ M polymers was performed using hydrazine hydrate reducing agent as discussed in section 4.5.3. The resulting polymers were kept under argon due to the air sensitivity of the zerovalent complexes.

5.8.4. Quinone Polymer

This was prepared by reacting the above chloromethylated styrene/styrene copolymer (see figure 5.22) with 2-aminoanthraquinone[180] to give the required $(PS)\!-\!Q$ polymer, with the elimination of HCl.
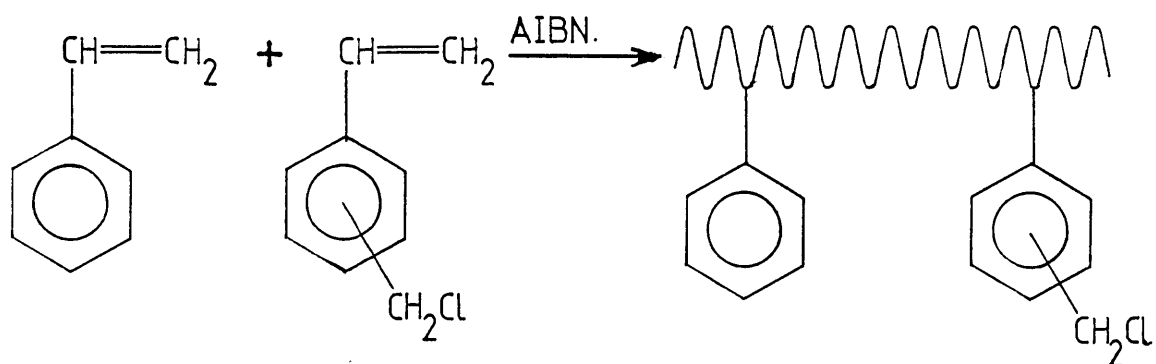
Figure 5.22. Synthesis of the precursor to (PS)–PPh$_2$ and (PS)–Q.

6. CONDUCTING POLYMER COATS

6.1. Introduction

In the previous chapter electrocatalysis by palladium incorporated, styrene based, polymer films was prevented by the lack of conduction of electrons through the film. As discussed in chapter 5, conduction in these redox polymers occurs by an electron 'hopping' mechanism between the metal sites in the polymer. For the palladium and nickel incorporated polymers, investigated in chapter 5, this was shown not to occur.

Therefore, it was decided to develop a conducting polymer backbone with ligands attached which would complex metal species. In this system, electrons would be transported through the delocalised band structure of the polymer to each metal site independently. Therefore, the need for the metal site/metal site redox reaction is unnecessary.

Since 1977 interest in the field of conducting polymers has increased dramatically. These polymers can be either chemically synthesised as polyacetylene[182] and polyphenylene[183,184] or electrochemically generated as polypyrrole[27,185,187], polythiophene[29,186] and polyfuran[29]. It is the second type which is of interest to this work.

Electrochemical generation is achieved by oxidation of monomeric species at the electrode and results in the electrode being coated by the polymer. During the coating the polymer is automatically doped with counter ions and hence is conducting, in this oxidised state, without any external doping being necessary. Electrochemical generation is a quick and easy method for making modified electrodes and by controlling the number of coulombs passed at the electrode, one can accurately control the thickness of the coat.

Polypyrrole, polythiophene and polyfuran coats are adhering, very even and pinholes are unlikely as any exposed surface reacts quickly with the monomer to accentuate polymer growth. Looking at these facts polypyrrole type coated electrodes seem ideal to act as a conducting polymer backbone.

However, these coats can be electrochemically reduced and reoxidised but are only conducting in the oxidised form. This means that the polymer coat can only be electrochemically active when in its oxidised state, which will put limitations on its uses.

6.1.1. The Structure of this Chapter

The aim of the work presented in this chapter was to produce a polymer coated electrode, with a conducting polymer backbone and attached ligands for the complexation of metal species.

Polypyrrole type polymers were considered ideal for the conducting polymer backbone (see above) and phosphine ligands have already been shown (see chapters 4 and 5) to be ideal for the complexation of palladium (II/0) and nickel (II/0) species.

In section 6.2 electrogeneration and analysis of polypyrrole coated electrodes is presented. Plain polypyrrole coats were investigated to gain information about these type of modified electrodes. The strategy for the synthesis of phosphine substituted pyrroles and their electro-chemical analysis are presented in sections 6.3 and 6.4 respectively. Palladium complexation of the phosphine pyrrole monomer and the electro-chemistry of the resulting complex is also presented.

Similar investigation of thiophene and furan is performed, with results for plain thiophene and furan in section 6.5 and the synthesis of phosphine substituted thiophenes and furans, with their electro-chemistry, in section 6.6.

In addition to synthesising phosphine substituted monomers, phosphine substitution of conducting polymer coated electrodes was attempted. These results are presented in section 6.7, There is an overall discussion of this chapter in section 6.8 and finally, in the appendix (section 6.9), the experimental conditions of all the syntheses are given. These have been appended so as not to interrupt the rest of the chapter.

6.2. Electropolymerisation of Pyrrole and Investigation of Polypyrrole Coated Electrodes

6.2.1. Coating Procedure

Initially, the potential of a platinum stationary electrode was swept anodically in a 0.05 M pyrrole solution (in acetonitrile + 0.1 M TEAT) and a steep rise in current was observed at +0.75 V vs Ag/Ag$^+$ (see figure 6.1). After this the electrode was removed and a black coat could be seen on the platinum surface.

Cyclic voltammetric analysis of this coated electrode, in supporting electrolyte (acetonitrile + 0.1 M TEAT), gave a broad anodic peak at E_p = -0.02 V vs Ag/Ag$^+$ and a very broad cathodic peak at E_p = -0.1 V vs Ag/Ag$^+$ (see figure 6.2). These peaks are characteristic of a polypyrrole coat[188]. Estimation of coat thicknesses by analyses of these cyclic voltammograms is not possible due to the peaks being both very broad and superimposed on large background currents. The background currents are due to resistance and capacitance effects. It has been suggested[188] that the breadth of the peaks could be due to repulsive interactions between the electroactive sites and/or the electrochemical non-equivalence of these sites.

More controlled coating could be achieved by stepping the potential to +0.72 V (the base of the oxidation wave) and following the current

Figure 6.1. Current voltage curve for the electropolymerisation of pyrrole (W = 0 Hz, v = 10 mV s^{-1}).
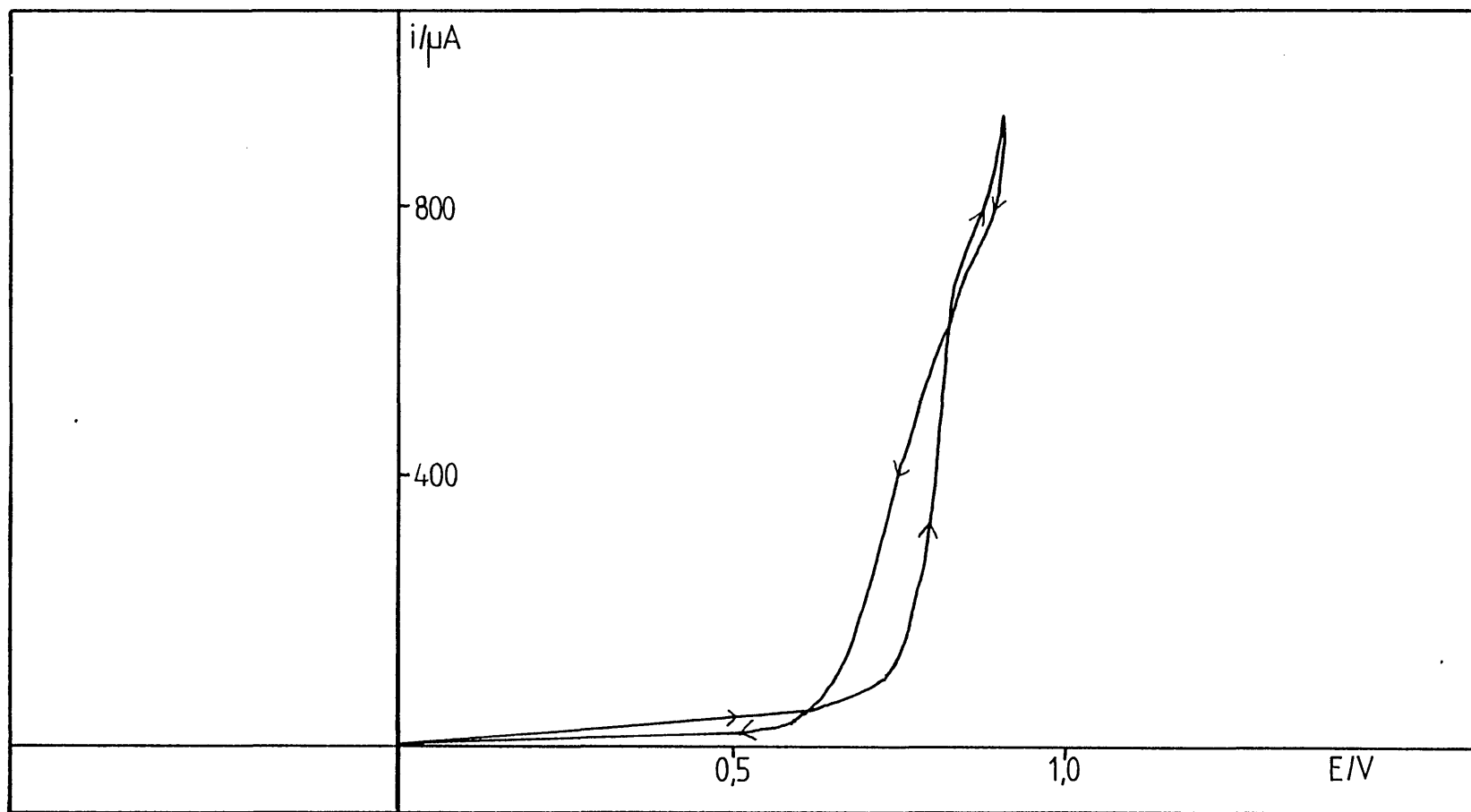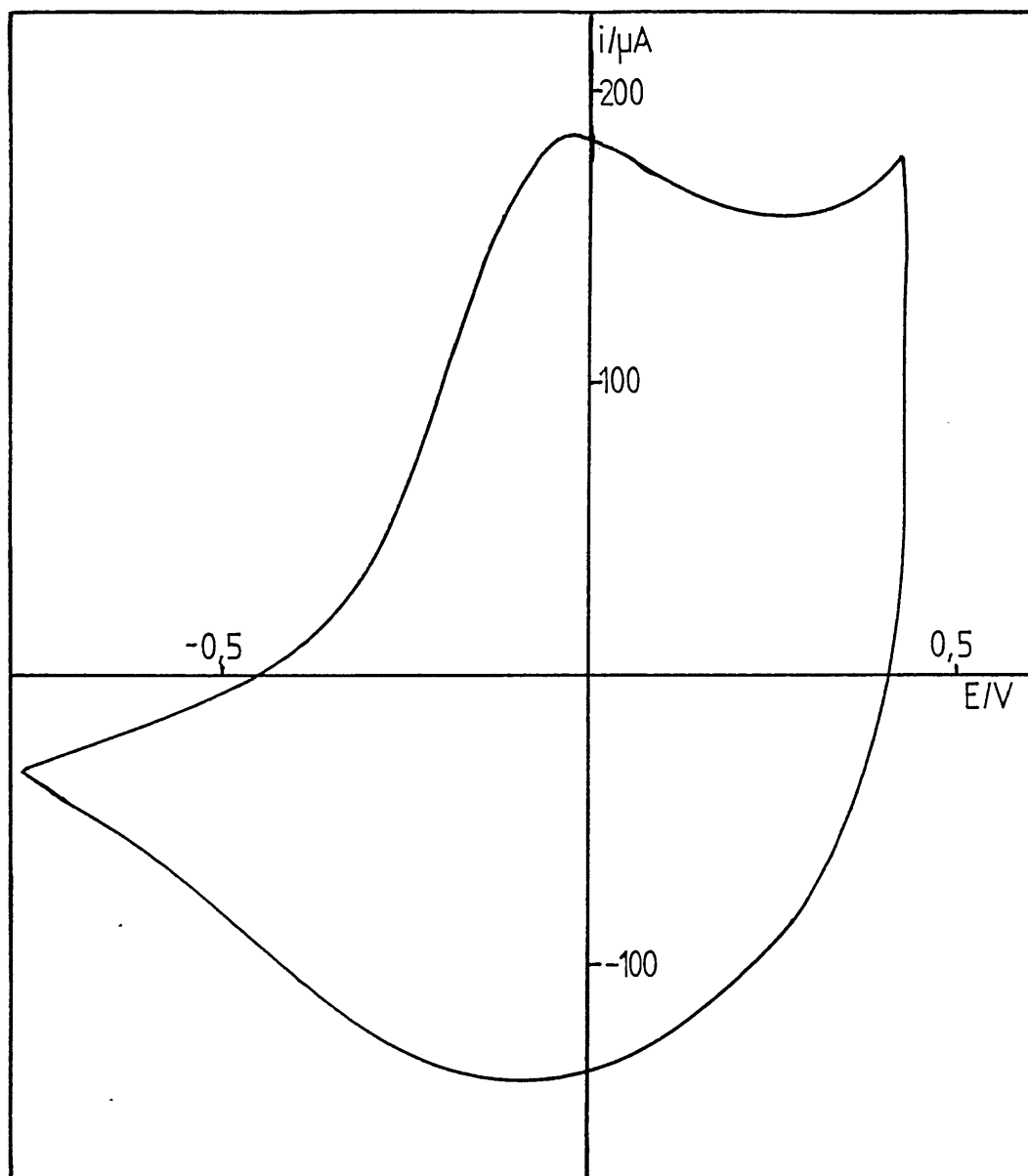
Figure 6.2. Cyclic voltammogram of a polypyrrole coated platinum
RDE (v = 100 mV s⁻¹).

with respect to time. Therefore one can calculate the number of coulombs passed during the coating process. It has been calculated[185,188] that 2.25 electrons, per pyrrole unit, are used in the coating process. Two electrons per pyrrole unit are used in the coupling reaction (i.e. in the formation of the polymer) and one electron per four pyrrole units oxidise the pyrrole coat. Therefore, one can estimate that cyclic voltammograms should show 1/9th of the charge passed during coating. From this n value of 2.25 and density measurements of coats it has been calculated that a charge density of 40 mC cm^{-2} gives a coat thickness of 100 nm[188]. Thus, from the current time plots for coating experiments, coat thicknesses can be estimated.

As α-substituted pyrroles do not electropolymerise, while β-substituted ones do, it can be deduced that the polymer coat is made up of α-α coupled pyrrole monomer units (see figure 6.3). The actual mechanism of coating has been under recent investigation, in the literature[189,190], and a radical initiation, as shown in figure 6.4, is presently favoured.

The above method of polymerisation required 0.05 M pyrrole solutions and it was felt lower concentrations could be used at a rotating disc electrode. Therefore, electropolymerisation in pyrrole solutions of various concentrations was investigated. In this investigation low rotation speeds (2-4 Hz) were found to give better coats and concentrations as low as 5 mM could be used. A typical current-time curve for a platinum RDE, held at +0.72 V vs Ag/Ag^{+}, rotating at 4 Hz in 5 mM pyrrole solution (acetonitrile + 0.1 M TEAT) is given in figure 6.5. The resulting coat is even and reproducible. The cyclic voltammogram of this coated electrode ($\sim$ 130 nm thick), in supporting electrolyte, is shown in figure 6.6.
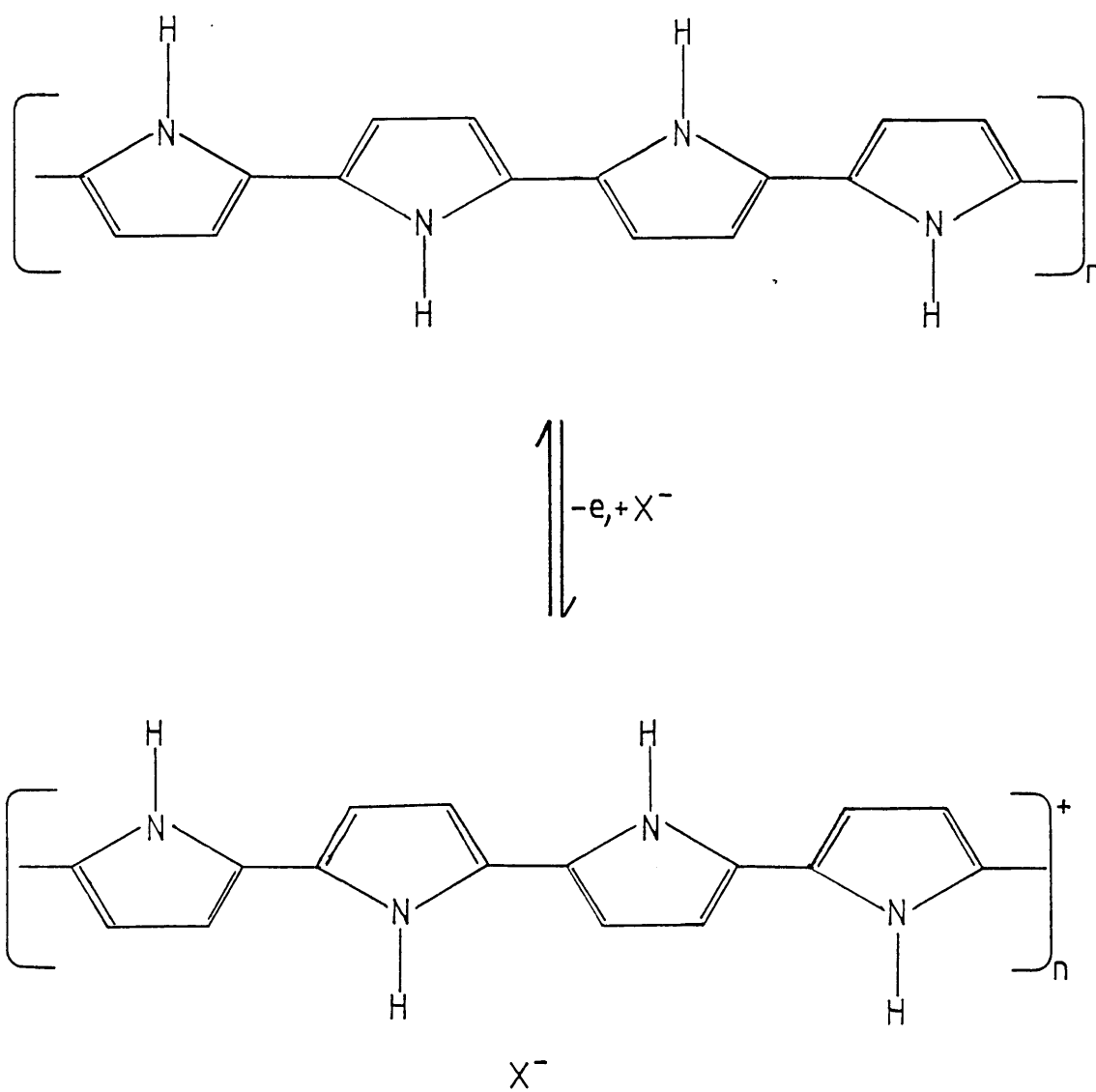
Figure 6.3. Structure of polypyrrole in reduced and oxidised form.

$$(1)$$

$$(2)$$

$$(3)$$

$$(4)$$

$$(5)$$
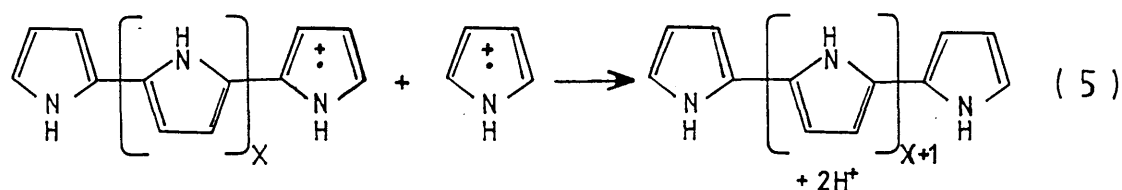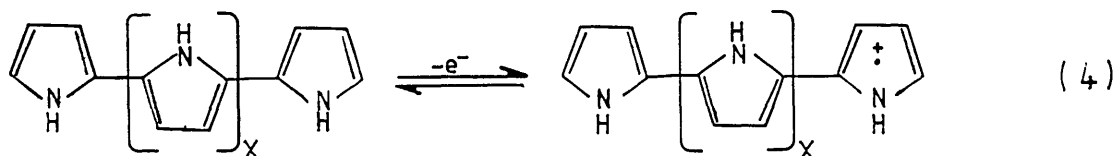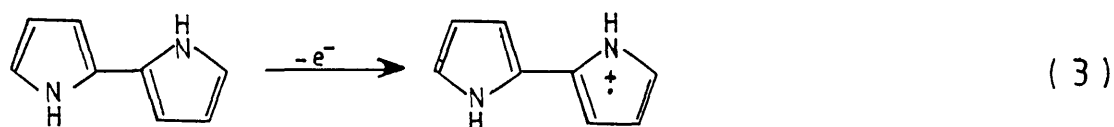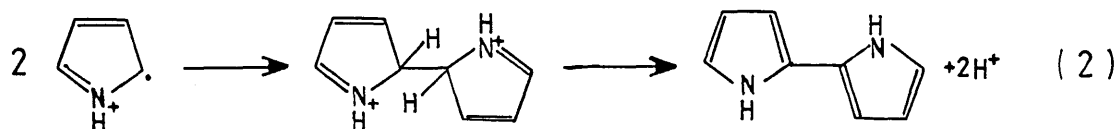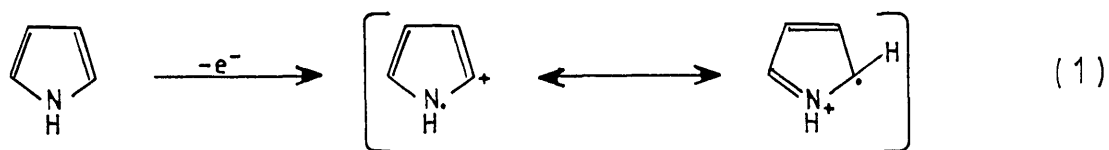
Figure 6.4. Mechanism for the electropolymerisation of pyrrole. (The oxidation of the polypyrrole unit to give the oxidised conducting polymer (see figure 6.3) has been omitted for simplicity). Step (3) has been included because the aromatic dimer and the higher oligomers oxidise more easily than the monomer. By extension steps (4) and (5) describe the polymerisation reaction.
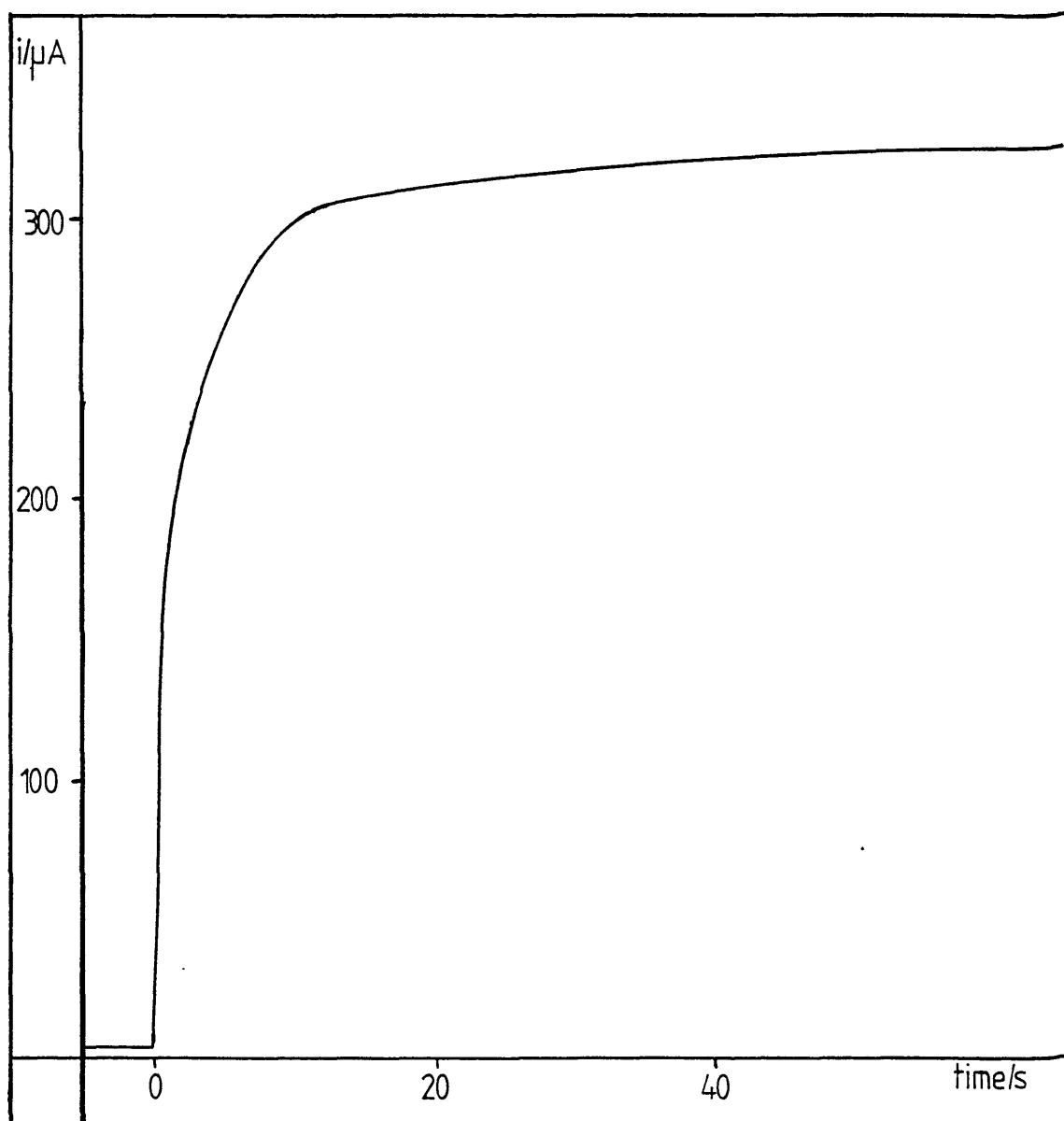
Figure 6.5. Current-time plot for the electropolymerisation of pyrrole (At time = 0s the potential of the RDE was stepped to +0.72 V vs Ag/Ag$^+$).
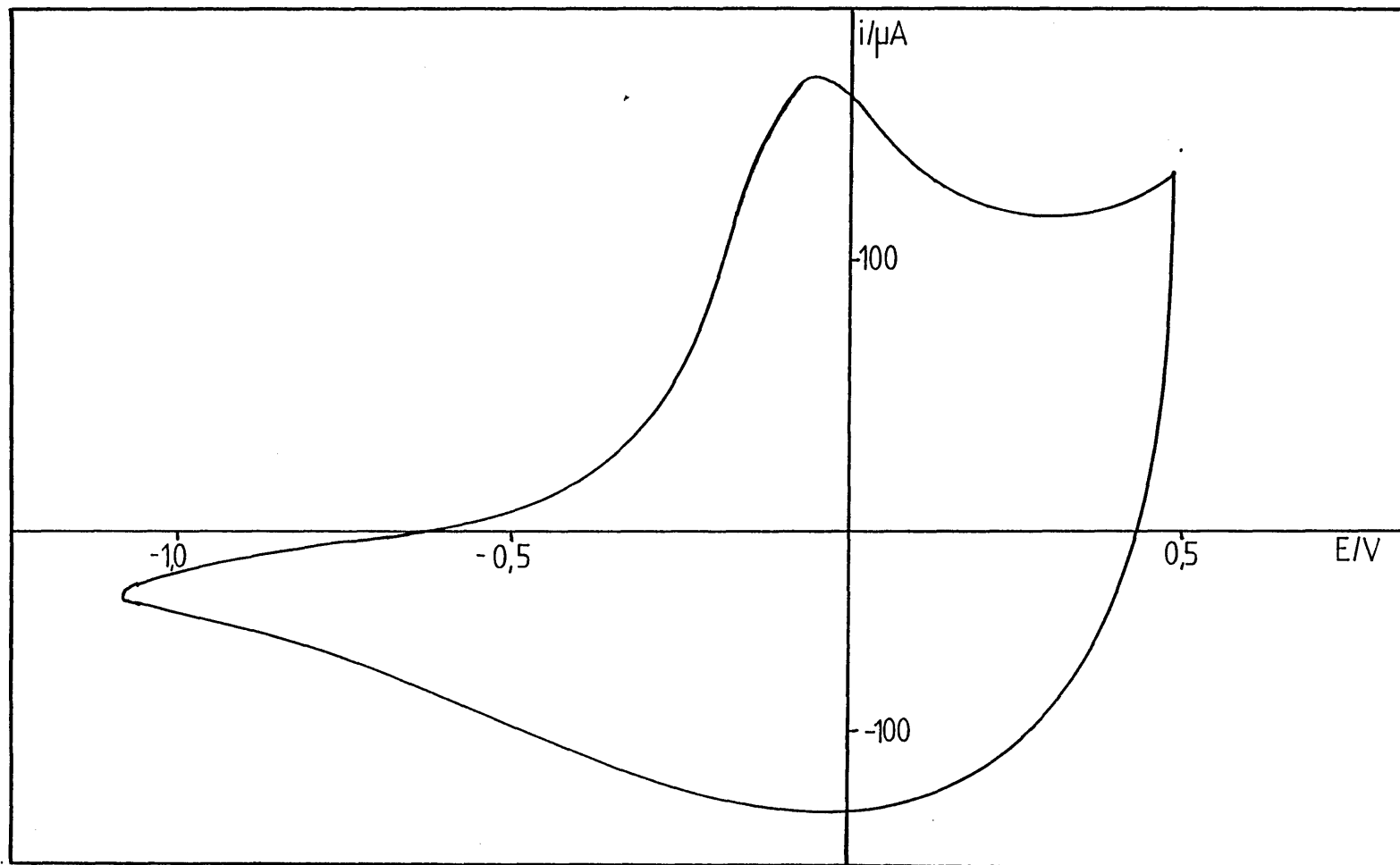
Figure 6.6.   Cyclic voltammogram of a polypyrrole coated electrode (coated by method in figure 6.5; v = 100 mV s⁻¹).

However, if one used a 1 mM pyrrole solution, holding the potential of the disc between +0.7 and 1 V vs Ag/Ag^+, a current was passed but no coating was observed. This was probably due to the formation of oligomers which then dissolved in solution. For the formation of a polymer coat a higher current density was needed. This is supported by the observation that if, in this 1 mM pyrrole solution, the potential of the disc was held at +1.2 V (the top of the oxidation wave where the current is transport controlled) a higher current density was obtained and a coat was observed.

From these results, the general method employed for coating polypyrrole, on electrodes, was to use a platinum RDE, rotating at 4 Hz, with its potential held at +0.72 V vs Ag/Ag^+ in a 5 mM pyrrole solution. Varying the length of time for coating gives an easy method for controlling the thickness of the coat.

6.2.2. Investigation of a Polypyrrole Coated Electrode

Polypyrrole coated electrodes were investigated in supporting electrolyte, ferrocene and $Pd(PPh_3)_4$ solutions.

6.2.2.1. In Supporting Electrolyte

A typical cyclic voltammogram for a polypyrrole coated electrode is shown in figure 6.6. In the oxidised state, above -0.02 V vs Ag/Ag^+, the coat is either black (thick coats) or dark blue (thin coats) while in the reduced state, below -0.1 V vs Ag/Ag^+, the coat is golden in colour. This colour difference is due to electrons being removed from/ injected into the extended π-system of the polymer.

Cyclic voltammetric analysis of coated electrodes, with various film thicknesses, was carried out at various sweep rates. The results

show that, for thin films (< 70 nm) the peak current varies linearly with sweep rate (see figure 6.7), which indicates that the kinetics of charge transfer are fast enough for complete reduction/oxidation of the coat, in each cycle. However, for thicker coats this linear dependence was only observed at low sweep rates and changed to peak current being proportional to the square root of the sweep rate at higher values (see figures 6.8 a + b). This indicates that the kinetics of charge transfer, in these thicker coats, was too slow for complete conversion of the coat, at these faster sweep rates. The diffusion of counter ions was considered likely to be the rate-limiting process for this oxidation/reduction of the coat. Potential step experiments on polypyrrole coated electrodes, in various supporting electrolytes, supports this idea[189,191].

Looking at the stabilities of these polypyrrole films it was observed that if, while investigating the coat in supporting electrolyte, one sweeps the voltage, of the coated electrode, above +0.65 V vs Ag/Ag^+, the coat degrades. This was indicated by less activity on the subsequent sweep of the cyclic voltammogram (see figure 6.9). This degradation increased on subsequent sweeps, above +0.65 V vs Ag/Ag^+, or was total if the potential, of the electrode, was kept above this voltage for a short period of time ($\sim$ 15 seconds). However, if one does not reach this oxidation potential the coated electrode could be cycled for hours without any degradation being observed (see figure 6.10).

After being reduced, polypyrrole coats become totally insulating and no electrochemistry was seen when the potential of the coated electrode was swept cathodically.

This lack of activity when reduced (i.e. below -0.1 V vs Ag/Ag^+) and instability above +0.65 V vs Ag/Ag^+ will limit the usefulness of polypyrrole coated electrodes.
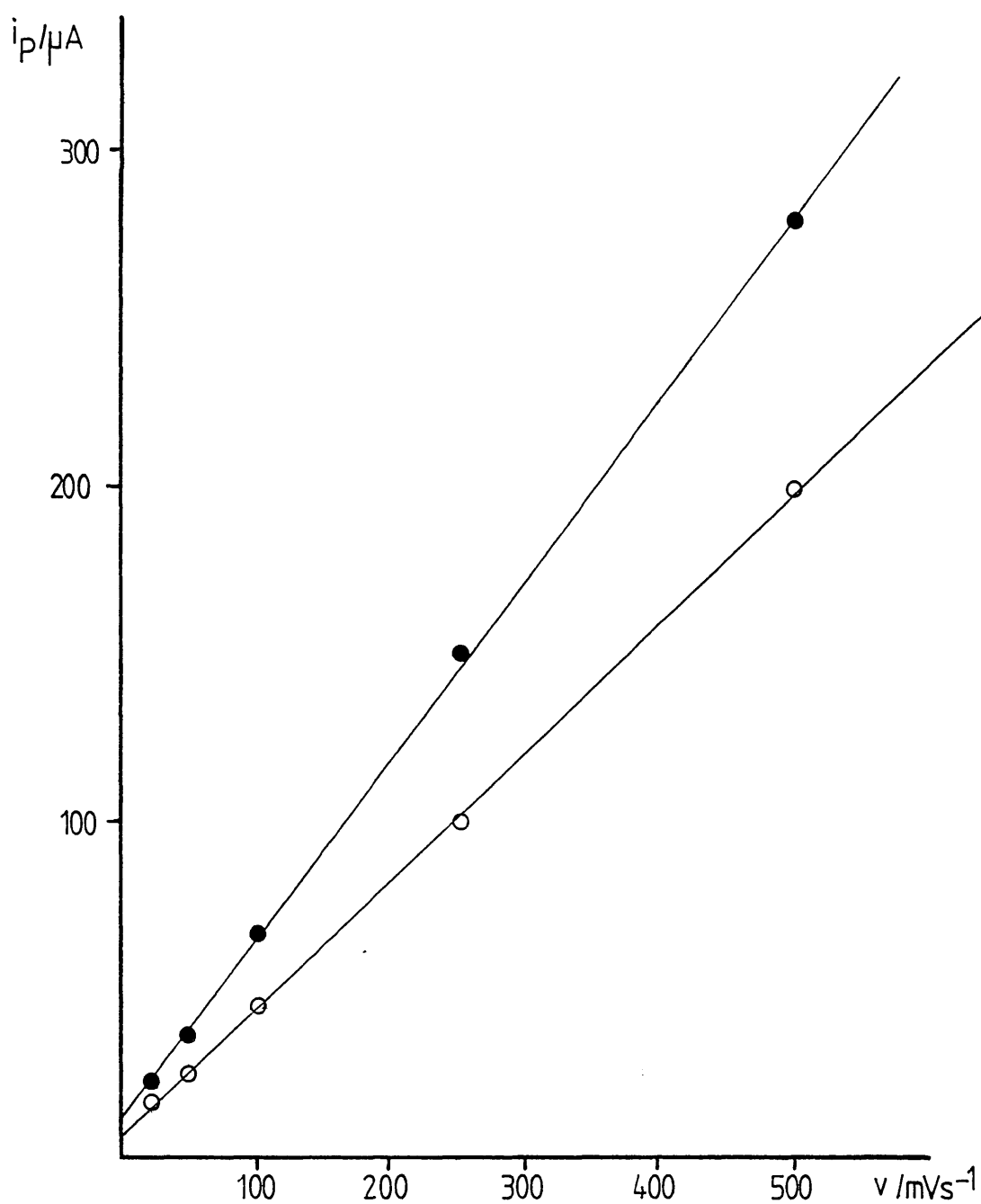
Figure 6.7. A typical plot of peak current vs sweep rate for polypyrrole thinly-coated platinum electrodes (O = cathodic peak, ● = anodic peak).

Figure 6.8. Typical plots of peak current vs (a) sweep rate and (b) the square root of sweep rate for thicker polypyrrole coated electrodes (O = cathodic peak, ● = anodic peak).
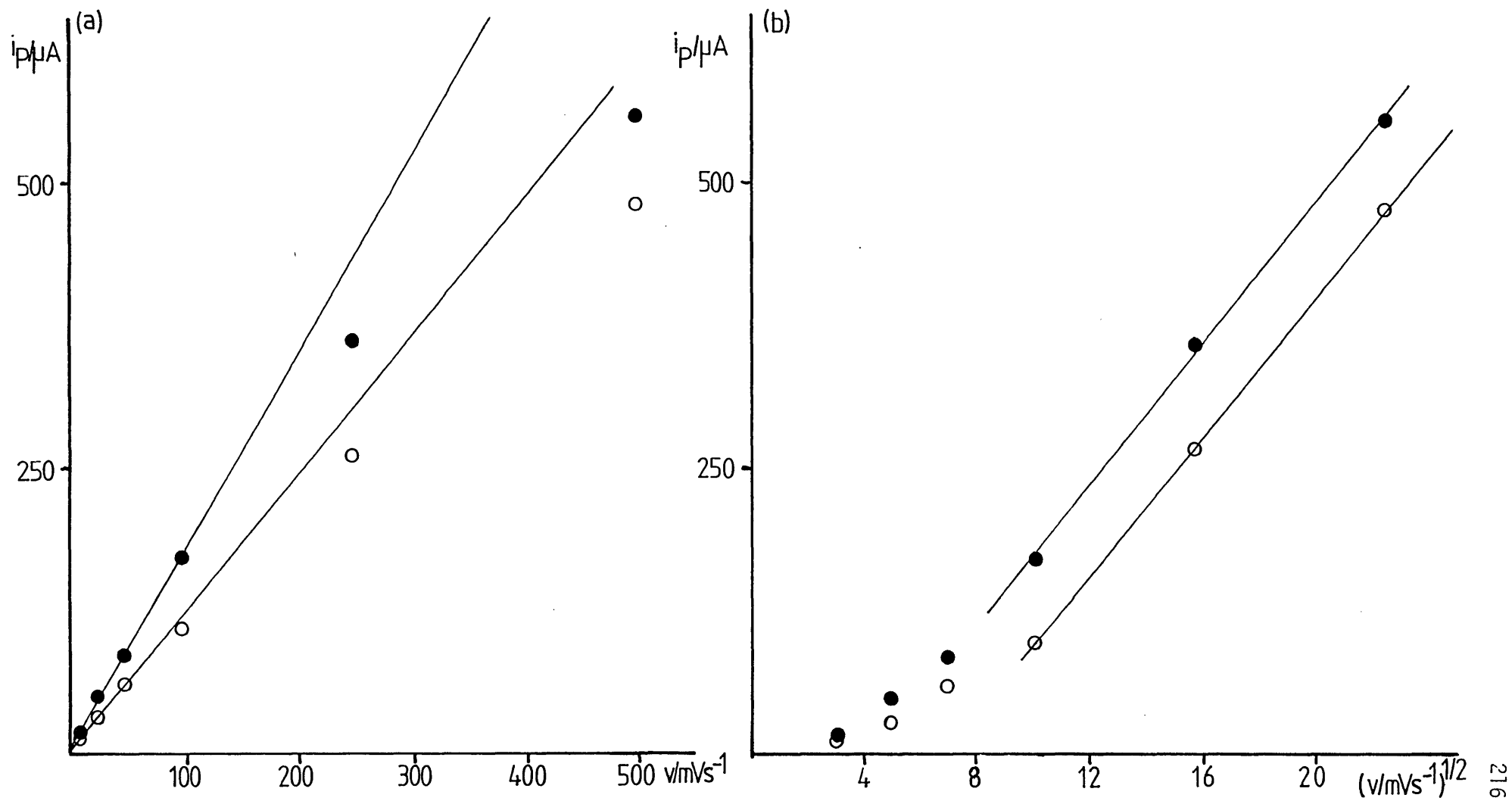
Figure 6.9. Cyclic voltammogram of a polypyrrole coated electrode after being swept past +0.65 V vs Ag/Ag$^+$ (figure 6.6 shows original activity; $v = 100$ mV s^{-1}).
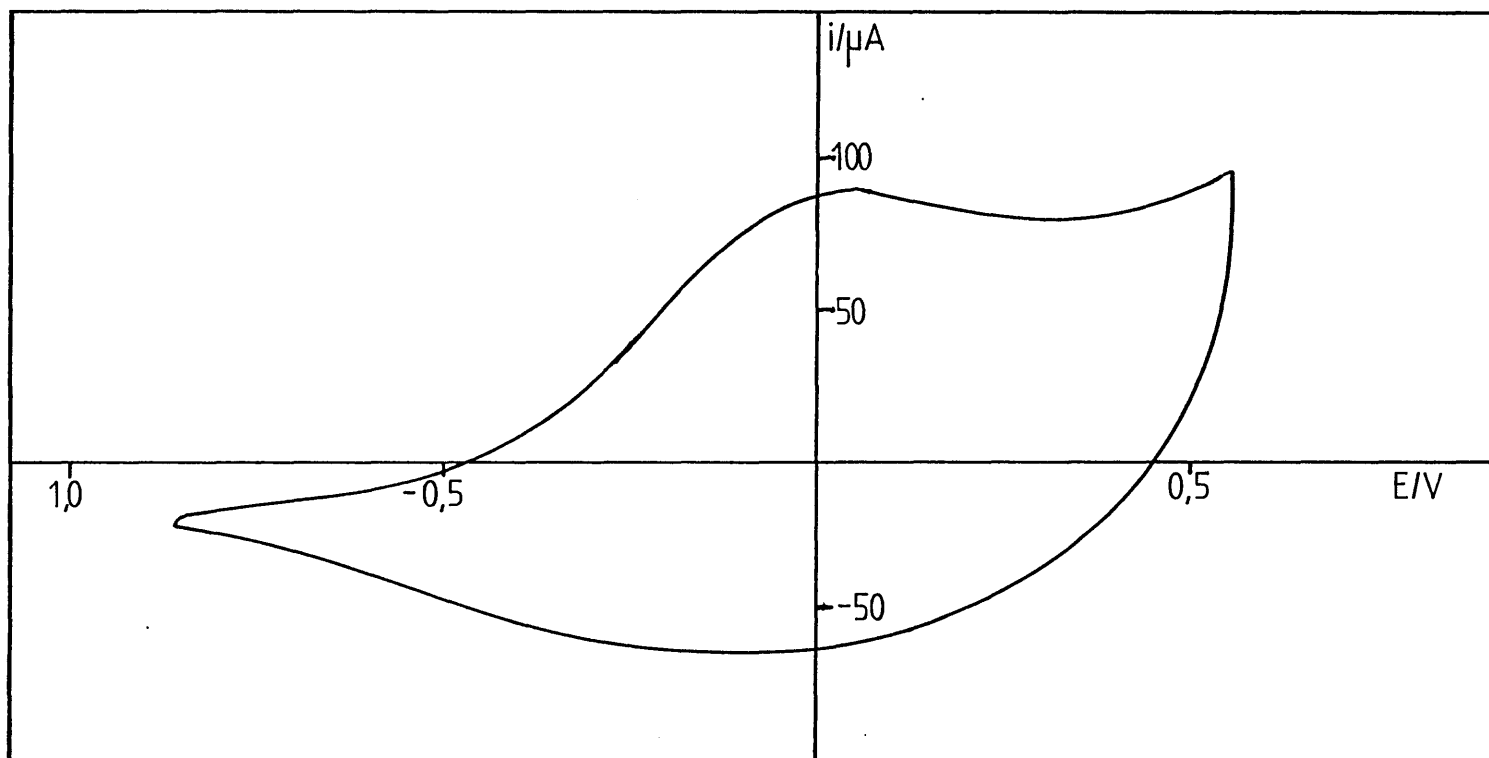
Figure 6.10. Cyclic voltammogram of a polypyrrole coated electrode ($v = 100$ mV s^{-1}; $---$ shows cyclic voltammogram after 2 hours cycling between +0.5 and -1.0 V vs Ag/Ag$^+$).
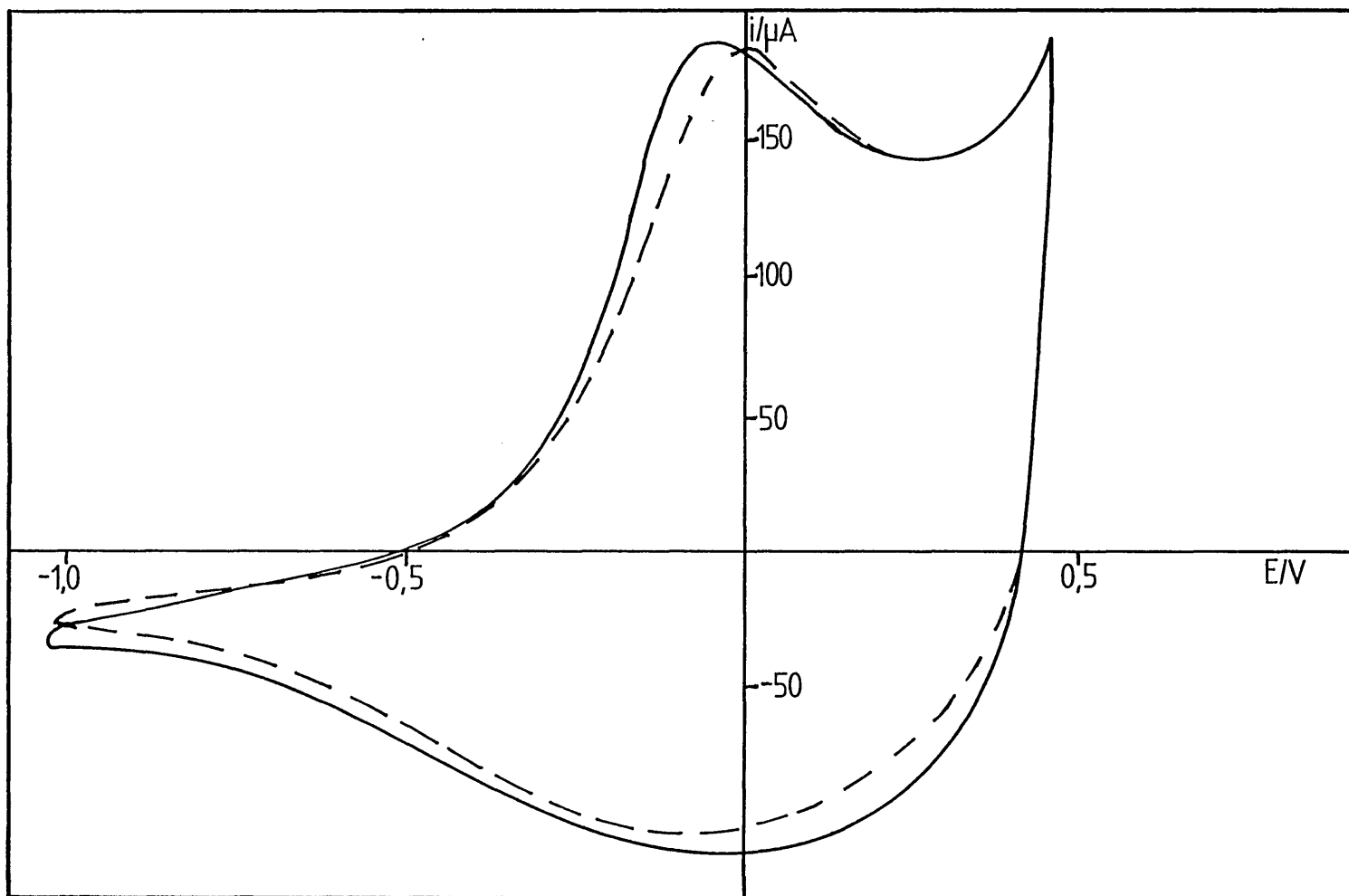
Considering its applications to this work one can see that a
polypyrrole coated electrode will not reduce Ni(II) phosphine complexes
to Ni(0) phosphines or Pd(II) phosphines to Pd(0) phosphine complexes.
However, it should oxidise Pd(0) phosphines to Pd(II) phosphines
($E_{\frac{1}{2}}$ = -0.38 V vs Ag/Ag$^+$ in acetonitrile, see section 4.2.2.6), which
is the requirement for the regeneration of a Pd(II) catalyst. The
oxidation of Pd(PPh$_3$)$_4$ by a polypyrrole coated electrode is verified
in section 6.2.2.3.

Finally, there have been contradictory reports in the literature
on the stability of polypyrrole coated electrodes when exposed to air.
In this work it was found that coated electrodes, both in the oxidised
and reduced states, could only be handled in air for very short periods
of time, and exposure to air for longer than a few minutes resulted in
degradation of the coat.

6.2.2.2. In Ferrocene Solutions

Platinum RDEs coated with polypyrrole were investigated in 1 mM
ferrocene solution (in acetonitrile + 0.1 M TEAT). A clean platinum RDE
shows an oxidation wave ($E_{\frac{1}{2}}$ = +0.1 V vs Ag/Ag$^+$) and its limiting current
shows Levich dependence which indicates mass transport is current limiting
(see figure 5.12).

Exactly the same behaviour is seen for polypyrrole coated electrodes
up to coat thicknesses of the order of 700 nm (see table 6.1). As, at
the limiting current, the coated electrode shows Levich dependence on
rotation speed indicates the current is solely dependent on the mass
transport of ferrocene to the electrode. Results discussed later, on
Ph(PPh$_3$)$_4$ oxidation at polypyrrole coated electrodes and ferrocene
oxidation at polythiophene coated electrodes, show that these oxidations

Table 6.1: Values of the Half Wave Potential ($E_{\frac{1}{2}}$), Limiting Current at 10 Hz (i_L) and Levich Slope for Ferrocene Oxidation at Polypyrrole ·Coated Electrodes.

Coat Thickness /nm	$E_{\frac{1}{2}}$ /V vs Ag/Ag$^+$	i_L /μA	Levich Slope /μ A s$^{\frac{1}{2}}$
Uncoated	0.10	300	94
24	0.11	300	94
50	0.09	295	94
100	0.11	295	95
200	0.10	300	94
320	0.10	295	94
650	0.11	300	95

are completely blocked until the coat is oxidised (i.e. becomes con-
ducting). This indicates that these oxidations are being mediated
by the coat and not occurring at the electrode surface. Therefore,
for the oxidation of ferrocene at the polypyrrole coated electrode,
one can deduce that the reaction is also mediated by the coat. Also,
as ferrocene seems reluctant to diffuse through these coats and react
at the electrode surface (polythiophene and polyfuran results), one
can postulate that the mediated reaction is occurring at the coat
surface (i.e. S) or just inside the coat/solution interface (i.e. L/S).
However, as the limiting current is only dependent on the diffusion of
ferrocene (i.e. k_D') and not the modified electrode reaction (k_{ME}'), no
more information on the mediated reaction can be obtained. The fact
that k_{ME}' is so rapid that k_D' becomes limiting is encouraging for the
use of these types of electrodes for electrocatalysis.

For thicker coats (> 1000 nm), which due to their thickness show
very broad, if any, cyclic voltammetric behaviour in supporting electro-
lyte (see figure 6.11 and 6.12), Koutecky-Levich dependence, of limiting
current on rotation speed, is observed (see figures 6.13 a, b + c). The
slope of this Koutecky-Levich plot (8.3 ($\pm$ 0.3) x 10^3 A^{-1} $s^{-\frac{1}{2}}$) is less
than the inverse Levich slope for ferrocene oxidation, at a clean
platinum electrode, in the same solution (Slope = 94 ($\pm$ 1) μA $s^{\frac{1}{2}}$,
inverse slope = 10.6 ($\pm$ 0.2) x 10^3 A^{-1} $s^{-\frac{1}{2}}$). Looking at the table 2.3
(the diagnosis of the mechanism for a modified electrode), one can see
that this indicates the L/RZ - $t_e t_y$ case where the reaction occurs in
a reaction zone somewhere in the middle of the layer and

$$k_{ME}' = \frac{D_e b_o}{L \, y_s} + \frac{KD_y}{L}$$

Figure 6.11. Cyclic voltammogram of a thick polypyrrole coated electrode ($v = 100$ mV s^{-1}).
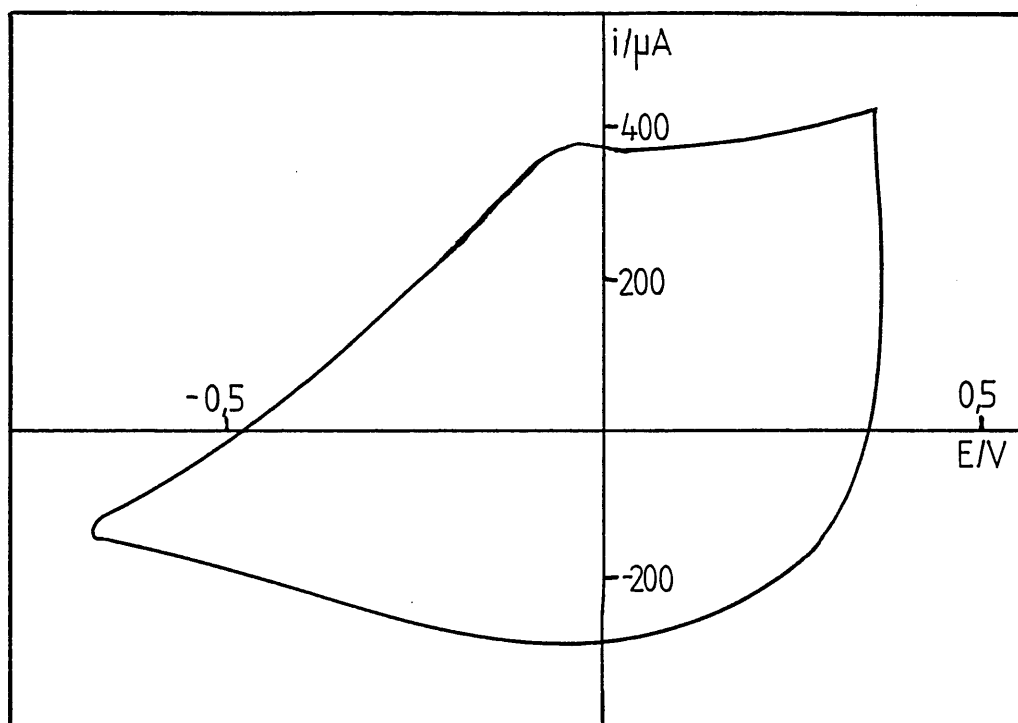
Figure 6.12. Cyclic voltammogram of a very thick (~ 1 μm) polypyrrole coated electrode ($v = 50$ mV s^{-1}).
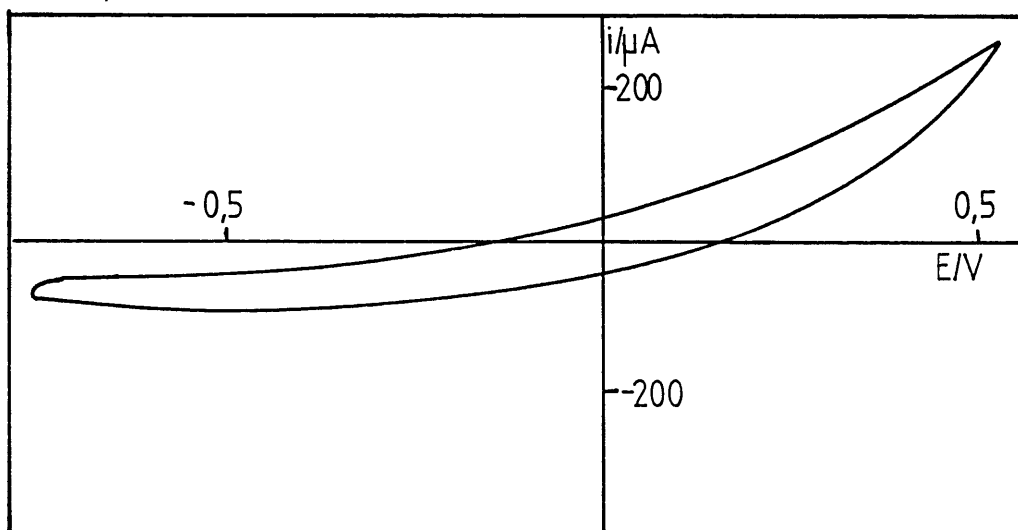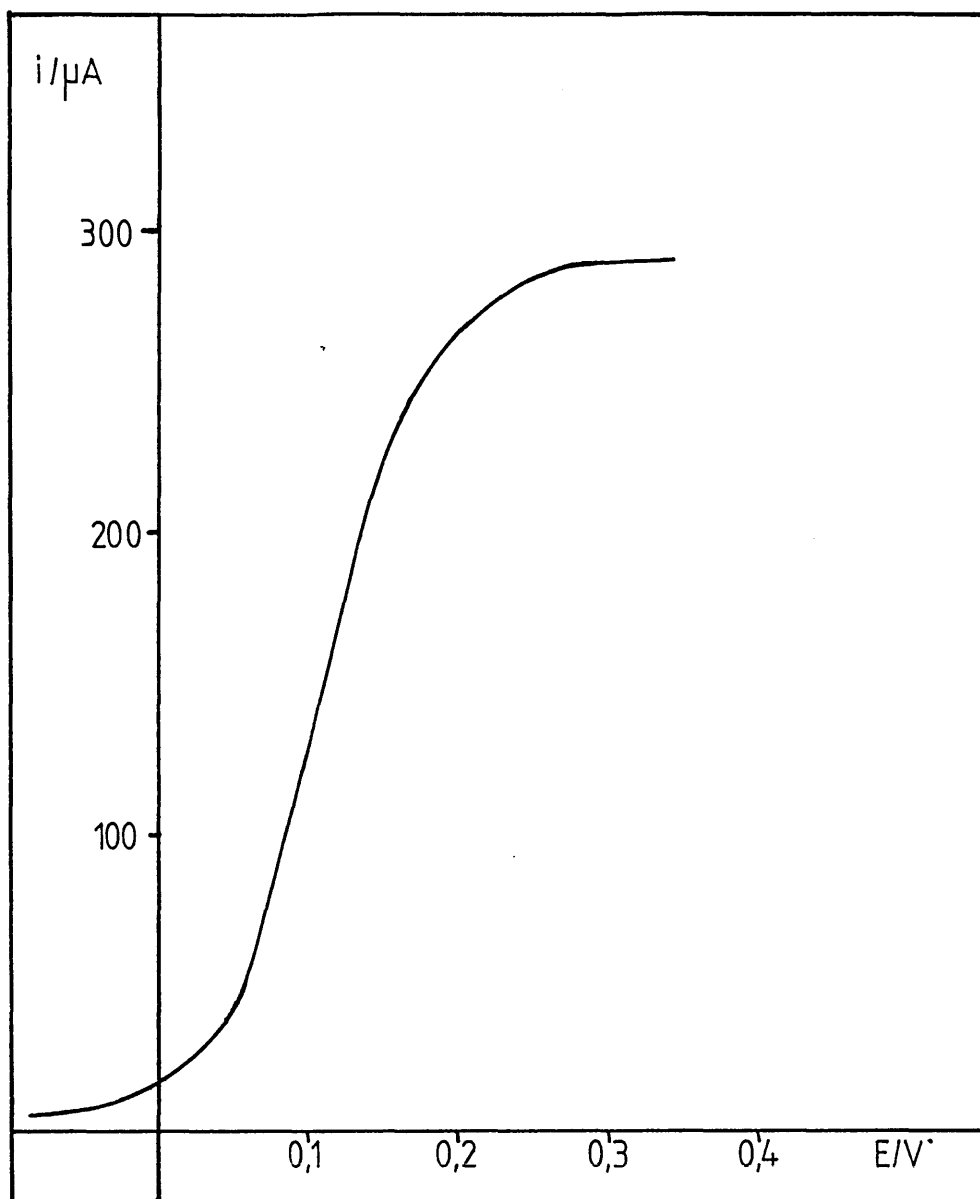
Figure 6.13a. Current voltage curve for the oxidation of ferro-
cene at a very thickly polypyrrole coated RDE
(W = 10 Hz, v = 10 mV s^{-1}).

Figure 6.13. (b) Levich and (c) Koutecky-Levich plots for the oxidation of ferrocene at thickly polypyrrole coated electrodes (see figure 6.13 a).
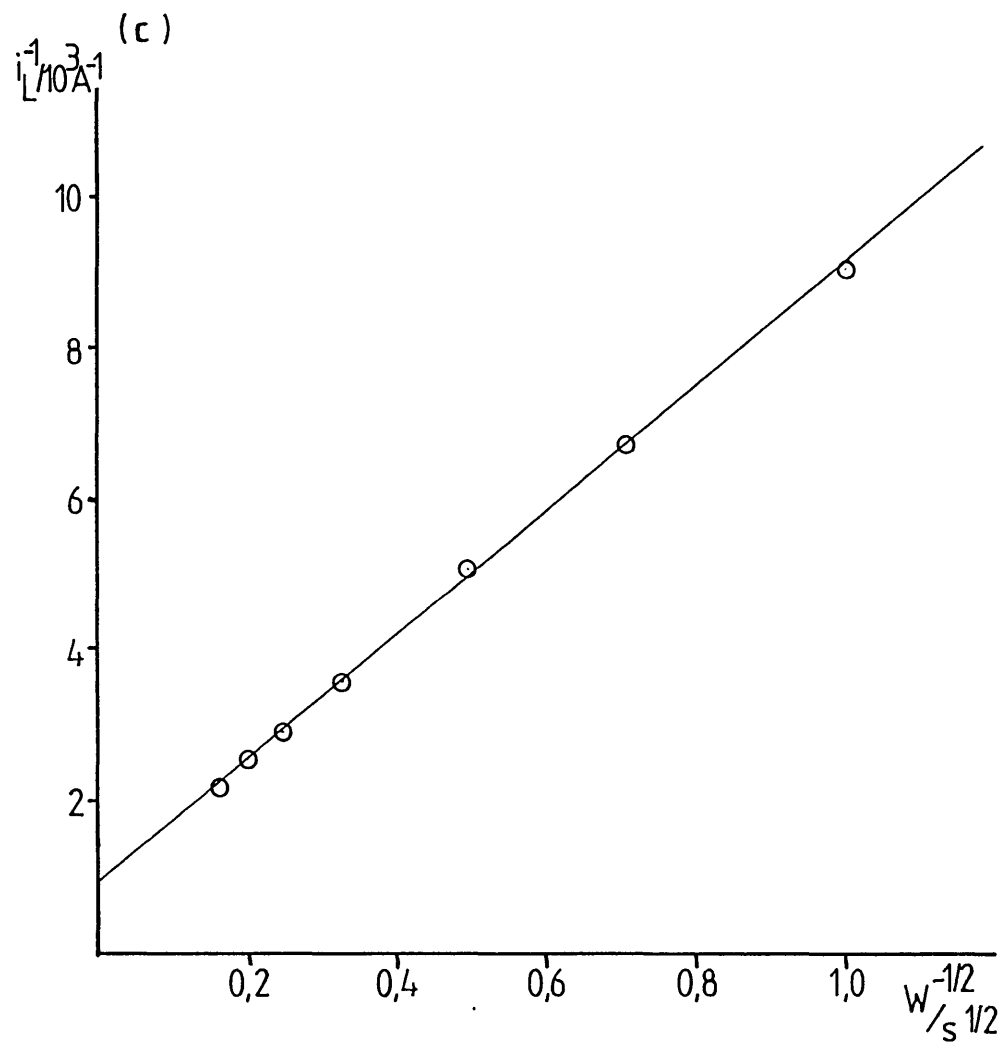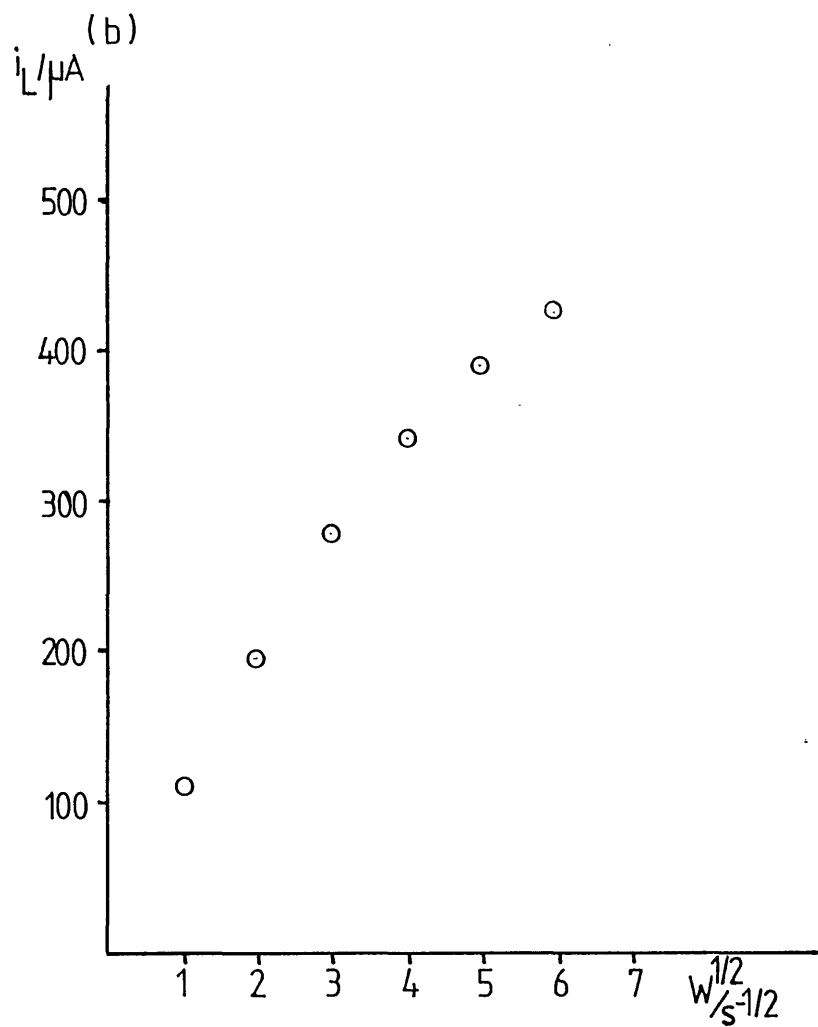
which means the transport of electrons from the electrode or the transport of Y from the electrolyte can be rate-limiting.

Looking at a diagram showing the eight possible cases for a mediated reaction at a modified electrode (see section 4.2, figure 6.14 and figure 10 of the Albery-Hillman review[9]), lowering L (the thickness of the coat) moves one from the left, bottom, front corner diagonally to the right, top, back corner of the cube. Above, it has been shown that for the oxidation of ferrocene, at a thickly polypyrrole coated electrode, one is in the L/RZ - $t_e t_y$ zone of the diagram. For thinner coats it is not known if the reaction occurs at the surface (S) or the layer/surface interface (L/S). However, from the L/RZ - $t_e t_y$ zone of the diagram, if L is lowered (i.e. a thinner coat) one cannot move into the L/S zone but can move into the S zone (see figure 6.14). Therefore, one can propose that for the oxidation of ferrocene at a thinly polypyrrole coated electrode the reaction occurs at the surface of the coat (i.e. S) with a large k'_{ME} and hence, the current is limited by the diffusion of ferrocene to the coat's surface.

6.2.2.3. In $Pd(PPh_3)_4$ Solutions

Polypyrrole coated (< 600 nm thick) platinum RDEs were investigated in saturated $Pd(PPh_3)_4$ solution (in acetonitrile +0.1 M TEAT).

At a clean platinum RDE, rotating at 10 Hz, the oxidation of $Pd(PPh_3)_3$ in acetonitrile is observed at $E_{\frac{1}{2}}$ = -0.38 V vs Ag/Ag$^+$ (see section 4.2.2.6). On a polypyrrole coated electrode, sweeping the potential anodically (at 10 mV s^{-1}) from -0.5 V, one observes the oxidation of pyrrole, at -0.3 V vs Ag/Ag$^+$, with the oxidation of $Pd(PPh_3)_3$ superimposed (see figure 6.15). Holding the potential at +0.1 V vs Ag/Ag$^+$ one observes a steady current which shows Levich dependence on rotation

Figure 6.14. Block diagram showing how the five different locations for a mediated reaction at a modified electrode depend on the three parameters (X_0/L), (X_L/L) and ℓ/KL and are related to each other. This is a simplification of the figure in the Albery and Hillman article[9] (their figure 10) as here the lines separating the different rate limiting processes have been omitted.
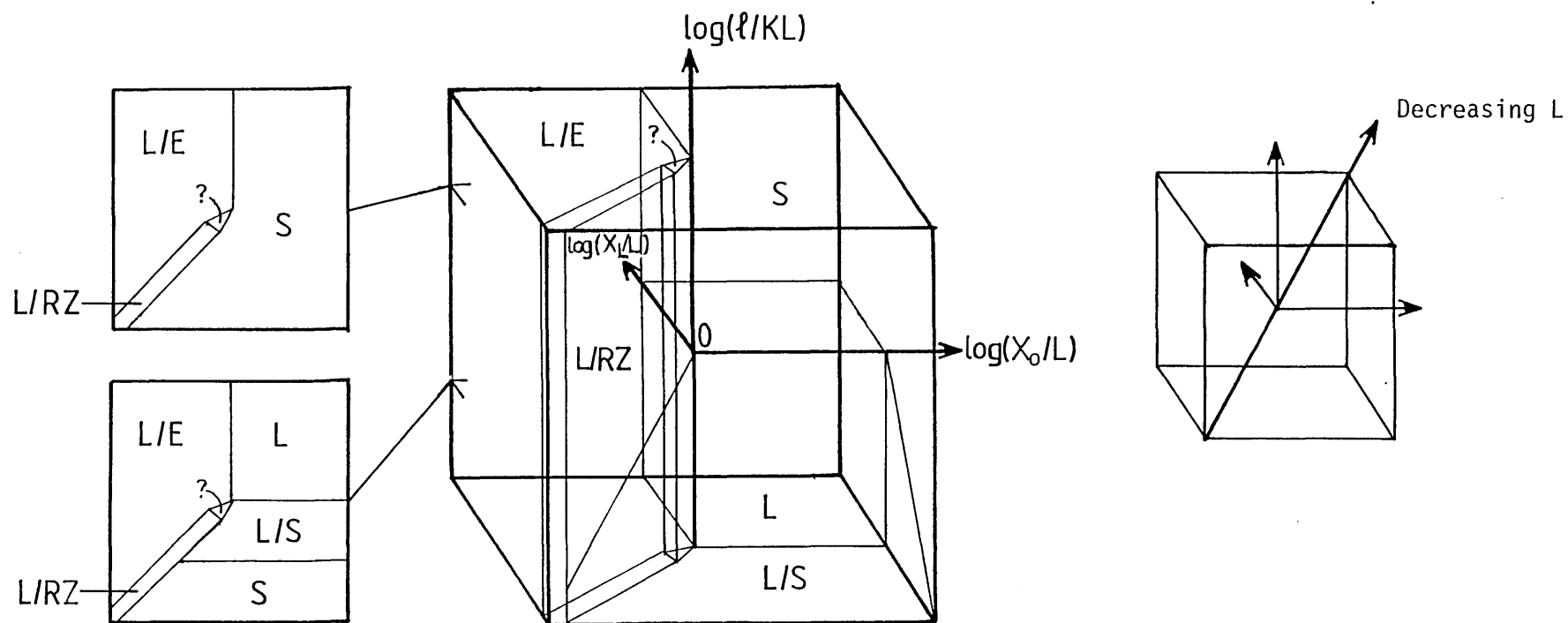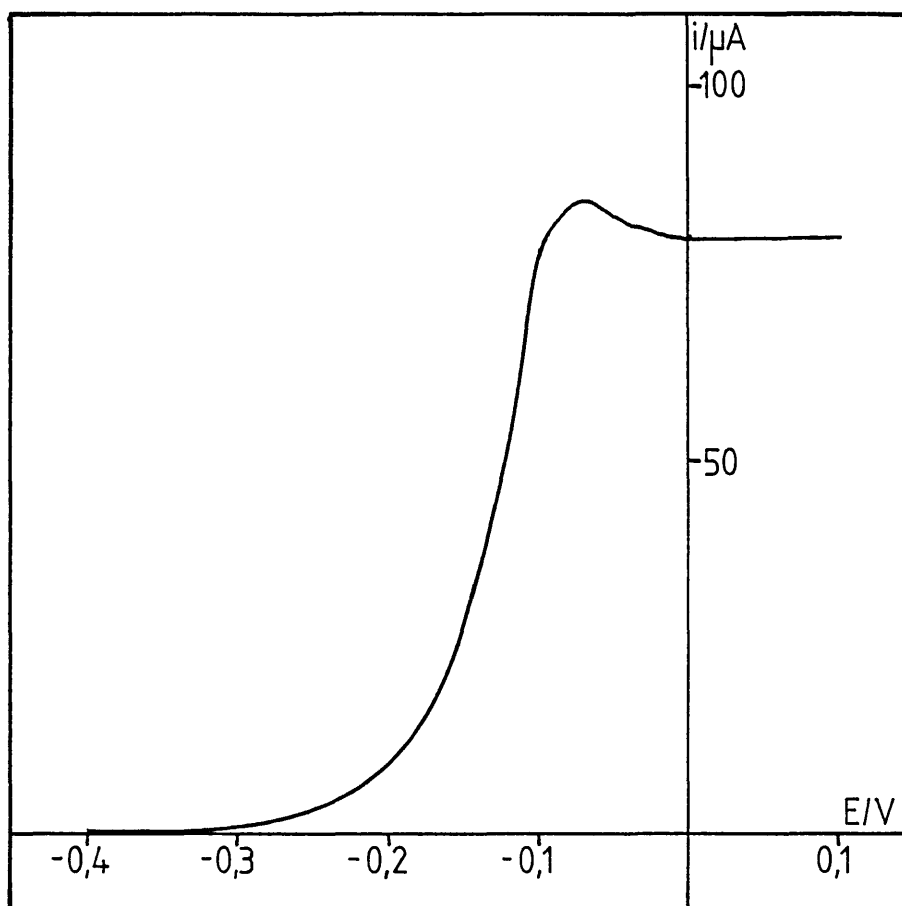
Figure 6.15. Current voltage curve for the oxidation of $Pd(PPh_3)_4$ at a polypyrrole coated RDE. The curve also includes the oxidation of the polypyrrole coat.

speed. This Levich dependence gives an identical slope to the Levich slope for the clean electrode, in the same solution (on the polypyrrole coated electrode the Levich slope = 13.5 ($\pm$ 1.5) $\mu A \ s^{\frac{1}{2}}$ while on the clean electrode the Levich slope = 14.1 ($\pm$ 1.0) $\mu A \ s^{\frac{1}{2}}$). Therefore, as with ferrocene, the polypyrrole coat mediated oxidation of $Pd(PPh_3)_3$ is very rapid (i.e. k'_{ME} is again very large and k'_D is limiting).

It was interesting to note that no current was observed between -0.4 V vs Ag/Ag^+ and the oxidation of the coat at -0.3 V vs Ag/Ag^+. This indicates that $Pd(PPh_3)_3$ was unable to diffuse through the poly-pyrrole coat, to react at the electrode. This is probably due to the phosphine complex being very bulky.

The above results are encouraging as they show that any $Pd(PPh_3)_3$ species, formed in a polypyrrole type coat, can be rapidly oxidised, by the coat, to regenerate the Pd(II), catalytically active, species. This is exactly the requirement needed for the use of polypyrrole type coated electrodes in this work.

6.3. Strategy for the Synthesis of Phosphine Substituted Pyrroles

As discussed in the previous section electrochemical polymerisation of pyrroles occurs through the coupling of α-positions in the monomer.
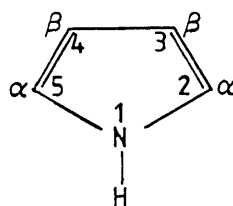
Hence, α-substituted pyrroles do not polymerise[188]. Therefore, for this work, where a polypyrrole coated electrode containing phosphine ligands is required, the phosphine ligands will have to be attached either in the β-positions or at the nitrogen.

Pyrroles are much more reactive through the α-positions than the β, and this is why polymerisation occurs through α couplings. This obviously causes a problem when wanting to substitute pyrroles in the β-position.

One method of preventing α-substitution is to attach protecting groups, to this position, which can later be removed. This strategy has been employed in the synthesis of 3,4-dihalopyrroles[192]. This method used carboxylate protecting groups, in the α-position, which could later be removed by reaction with strong base. However, protecting the α-position prevents reaction occurring there but does not increase the reactivity of the β-position which is relatively unreactive. Also, the use of protecting groups does involve two extra preparative steps. Thus, for example, the overall literature yield for the preparation of 3,4-dichloropyrrole, by this method, is less than 5%. This indicates the disadvantages of using this approach.

Therefore, it was decided that the best approach to the synthesis was to actually prepare the pyrrole ring by a ring closure reaction rather than trying to substitute already formed pyrroles.

The method published by A.M. van Leusen and co-workers[193] for the synthesis of a range of β-substituted pyrroles seemed ideal for this approach. In this method an α,β unsaturated ketone, ester or nitrile (i.e. a Michael acceptor) is reacted with tosylmethylisocyanide (Tos-MIC), in the presence of base, to give the 3,4 substituted pyrrole.

$Tos-CH_2-NC$

+

$R^1-CH = CH-\overset{O}{\overset{\|}{C}}-R^2$

$\xrightarrow[-TosH]{\text{Base}}$
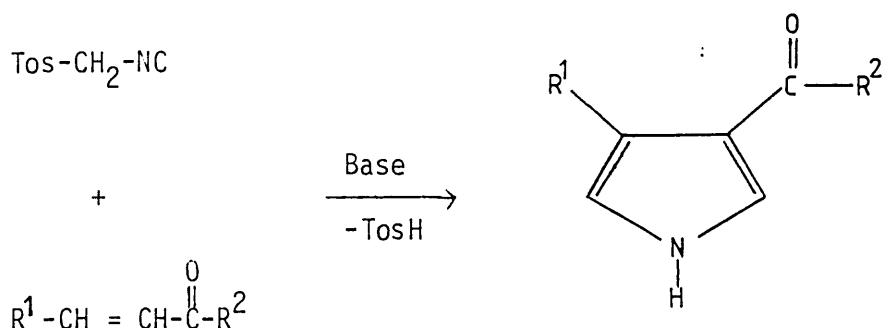
(where Tos indicates the tosyl group, i.e.

$$CH_3$$
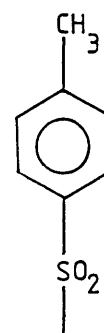
and TosH is p-toluenesulph:nic acid).

$$SO_2$$

Although the mechanism of this reaction has not been fully investigated (see literature proposed mechanism in figure 6.16) it seems likely that an enolate anionic intermediate of the type

$$R^1-CH-CH = \overset{\overset{\displaystyle O^\ominus}{|}}{C}-R^2$$

$$\underset{\underset{H}{|}}{Tos-C}\diagdown_{NC}$$
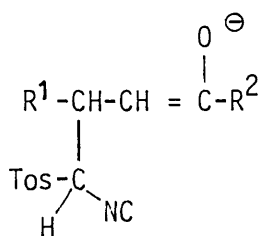
is formed.   This shows the necessity for the α,β unsaturated starting material.

6.3.1.   Attempts to Synthesise 3-Diphenylphosphinopyrroles

For this work, the target molecule was the 3-diphenylphosphino-pyrrole.
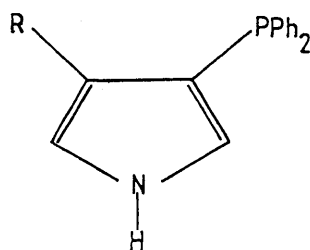
where R = H or alkyl

Figure 6.16. The published[193] mechanism of the TosMIC reaction.
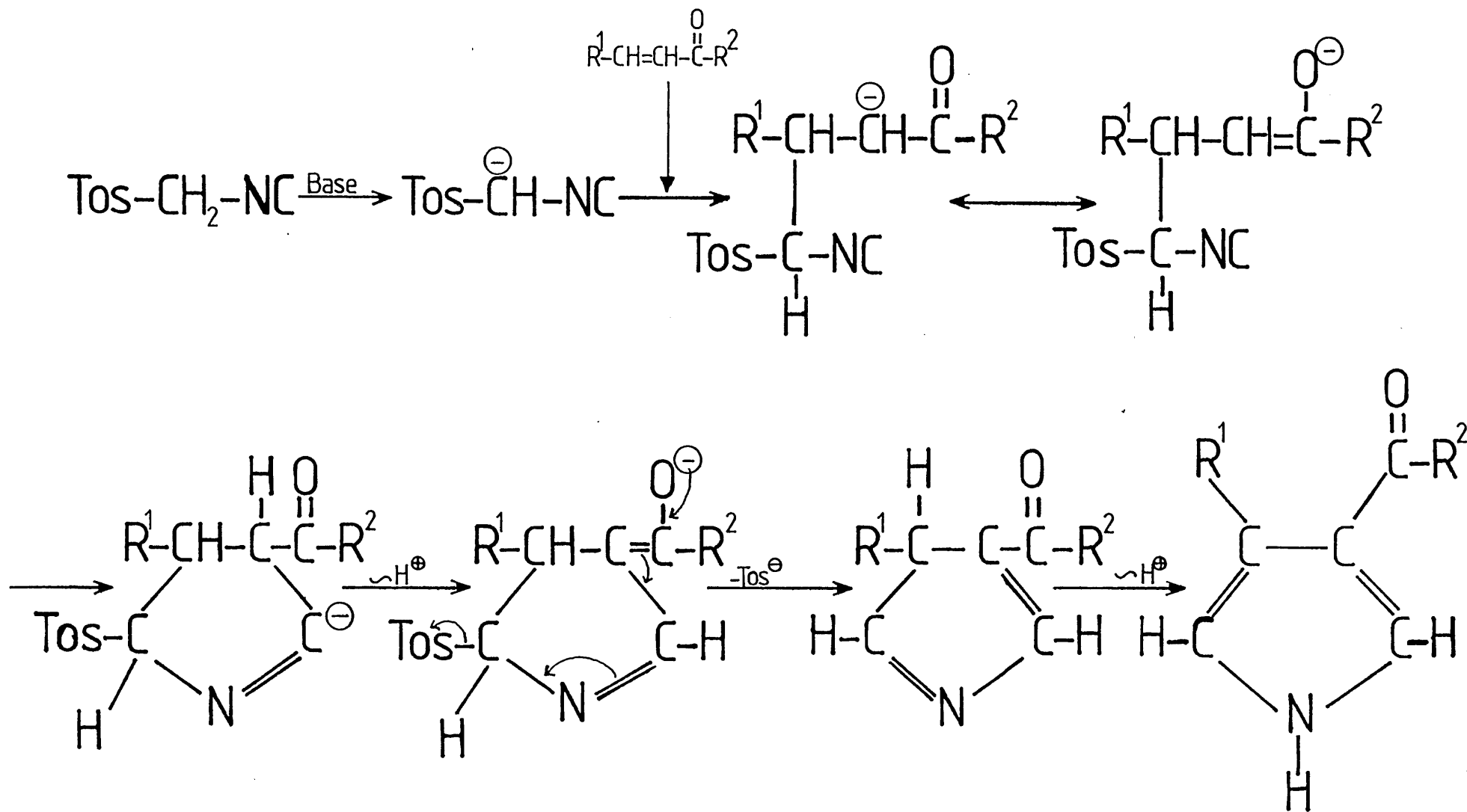
The 3,4-bis(diphenylphosphino) pyrrole was also considered but polymerisation of this molecule would not be possible due to steric effects between the phosphine groups (see figure 6.17).

It has been reported[194] that trivalent phosphine groups can stabilise α-carbanions by delocalisation of charge into the vacant 3-d orbitals. Therefore, it was thought that the above TosMIC reaction could occur with a simple vinylphosphine. An intermediate of the type

$$
\begin{array}{c}
H \\
\diagdown \quad \ominus \\
\mathrm{Tos\text{-}C\text{-}CH_2\text{-}CH\text{-}PPh_2} \\
| \\
\mathrm{NC}
\end{array}
$$
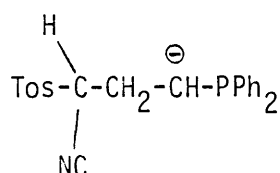
was envisaged with stabilisation of the carbanion by the phosphine's 3-d orbitals.

Diphenylvinylphosphine can be prepared from chlorodiphenylphosphine and vinyl Grignard reagent by the method of Berlin and Butler[195] (see section 6.9.1) though it is also available from Fluorochem (British agents for Strem Chemicals of the USA).

The reaction between diphenylvinylphosphine and TosMIC was attempted by several methods (see section 6.9.2) but no pyrrole type products were detected. The products isolated were either unreacted or decomposed starting materials.

Diphenylvinylphosphine oxide was synthesised (see section 6.9.3) by oxidation, with hydrogen peroxide, of the diphenylvinylphosphine. This was also tried in the TosMIC reaction but again no formation of pyrroles resulted.
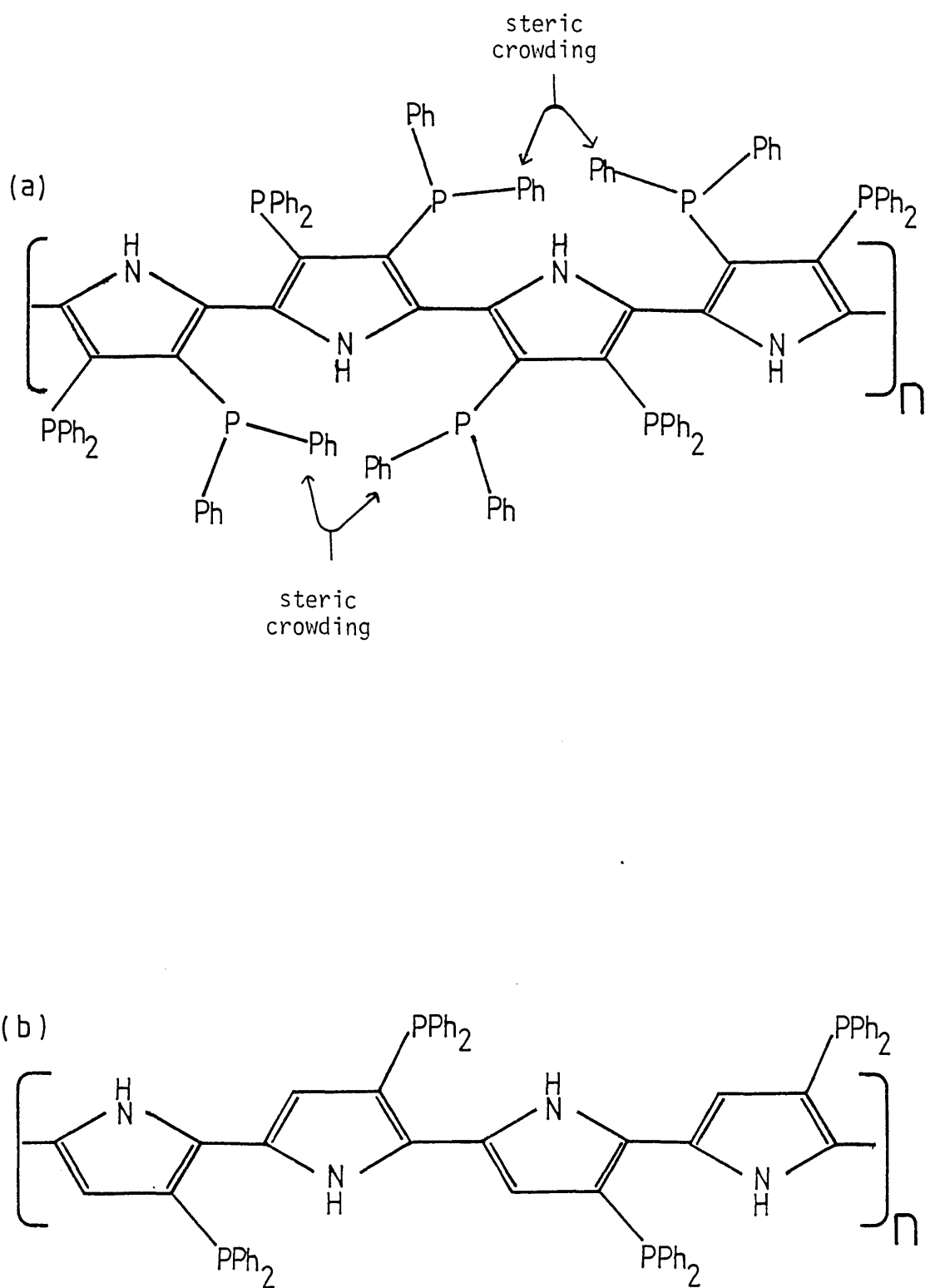
Figure 6.17. Steric interactions would prevent the polymerisation of 3,4-bis(diphenylphosphine)pyrrole (see (a)) but this would not occur with the mono-substituted pyrrole 3-diphenylphosphinopyrrole (see (b)).

Selective methods for the reduction of phosphine oxides to phosphines by chlorosilanes are well known[196,197,198]. Therefore, if a phosphine oxide pyrrole could be·synthesised its reduction to the equivalent phosphine would be a standard reaction.

As the above vinylphosphine/TosMIC reaction failed to produce the required product it was felt that α,β -unsaturated compounds are definitely necessary for the above TosMIC reaction to occur. Therefore the synthesis of an α,β-unsaturated phosphine such as methyl β-(diphenylphosphino)vinylketone

$$
\underset{CH_3}{}\overset{\overset{\textstyle O}{\parallel}}{C} \diagdown \underset{H}{\overset{}{C}} = \underset{PPh_2}{\overset{H}{C}}
$$
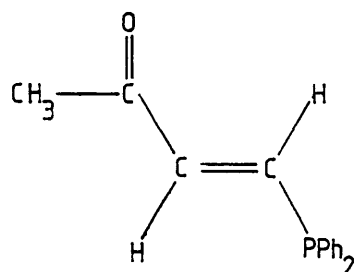
was considered. This would give a 3-phosphino-4-acetyl pyrrole

$$
CH_3(O)C \diagup \diagdown PPh_2
$$
N
H
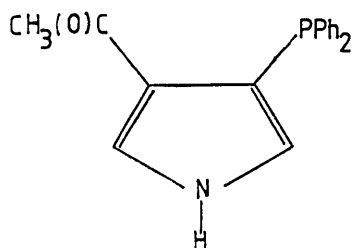
which could then be reduced to give the 3-phosphino-4-ethyl pyrrole

$$
CH_3CH_2 \diagup \diagdown PPh_2
$$
N
H
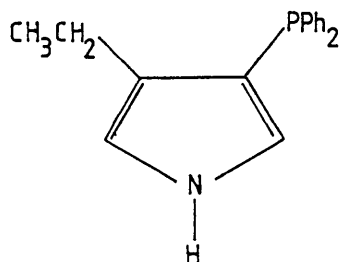
The first method tried for the synthesis of the α,β-unsaturated phosphine was the acylation of diphenylvinylphosphine. Acylation of alkenes, using Lewis acids (e.g. $SnCl_4$, $AlCl_3$ and $ZnCl_2$) with acetyl chloride or acetic anhydride, is well known in the literature[199,200]. However, similar reactions with diphenylvinylphosphine led to immediate, uncontrolled, polymerisation of the reactant (see section 6.9.4). Use of milder Lewis acids, more dilute solutions and lower temperatures failed to prevent this rapid polymerisation.

As vinylphosphine oxides are more stable to polymerisation, diphenyl-vinylphosphine oxide was synthesised (see earlier) and acylation was attempted (see section 6.9.5). However, extraction of products showed that no reaction had occurred.

Due to the difficulty found in acylating vinylphosphines, it was decided that perhaps the α,β-unsaturated phosphine could be synthesised by phosphine substitution of another α,β-unsaturated compound. It is known[201,202,203] that lithium diphenylphosphide reacts with vinyl-chlorides to give vinylphosphines. Therefore, a reaction of the form
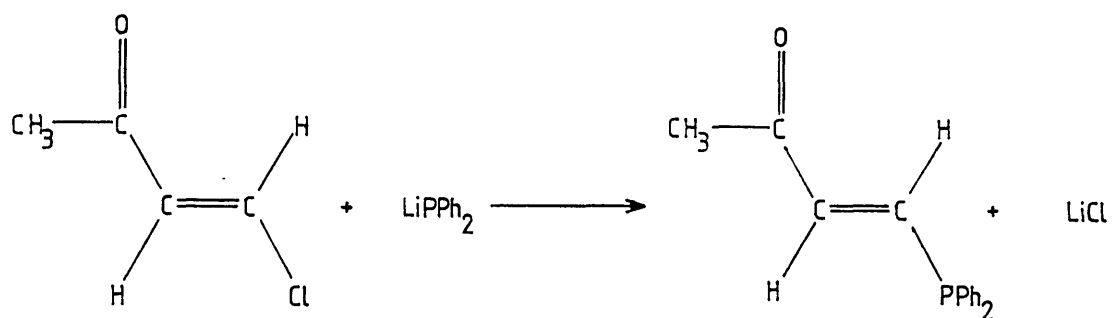
was proposed.

The synthesis of methyl β-chlorovinyl ketone has been published[204, 205] but it must be handled with great care as it is intensely lachrymatory and causes severe blisters. It is also unstable at room temperature but can be kept when frozen at less than 5°C. Due to these reasons methyl

β-chlorovinyl ketone was synthesised (see section 6.9.6a), isolated and used in a special toxic laboratory.

Lithium diphenylphosphide was synthesised (see section 6.9.6b) from lithium metal and chlorodiphenylphosphine[206].

The reaction between lithium diphenylphosphide and methyl β-chloro-vinyl ketone was attempted several times (see section 6.9.6c) but the products isolated were diphenylphosphine and diphenylphosphinic acid. Therefore, one can see that the reaction resulted in the decomposition of the methyl β-chlorovinyl ketone.

Due to the lack of success in the synthesis of 3-phosphine sub-stituted pyrroles it was decided to synthesise the 1-phosphine substituted pyrrole (see below). It was also decided to investigate thiophenes and furans. This was because the 3-bromothiophene and 3-bromofuran are easy to make, or commercially available (see section 6.5 and 6.6), and when used as starting materials give the 3-phosphine substituted thiophene and furan in a two step reaction (see section 6.6).

6.3.2. Synthesis of 1-Diphenylphosphinopyrrole

1-Diphenylphosphinopyrrole

(Ph$_2$P-1-py)
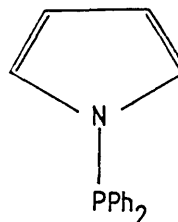
was synthesised from potassium pyrrolide[207] and chlorodiphenylphosphine as published in the literature[208,209,210]. This was carried out suc-cessfully (see section 6.9.7a) with the resulting product being purified and stored under argon.

For later needs in this work, the 1-diphenylphosphinatopyrrole was synthesised by the oxidation, with hydrogen peroxide, of the 1-diphenylphosphinopyrrole (see section 6.9.7 (i)). Also, the bis(1-diphenylphosphinopyrrole) palladium dichloride complex was synthesised by a ligand exchange reaction (see section 6.9.7 (ii)).

1-diphenylphosphinatopyrrole

$(Ph_2P(O)-1-py)$
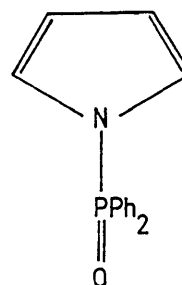
Bis(1-diphenylphosphinopyrrole)palladium dichloride

$(Pd(Ph_2P-1-py)_2Cl_2)$
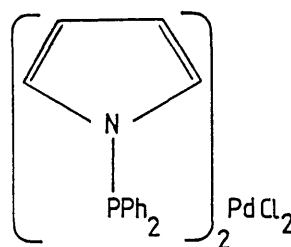
6.4. The Electrochemistry of 1-Diphenylphosphinopyrrole and Related Compounds

Electrochemical investigation of 1-diphenylphosphinopyrrole $(Ph_2P-1-py)$ involved several different approaches. Initially, its dilute solution electrochemistry was investigated. This was followed by attempts to electropolymerise the compound, from various solutions, to give a polymer coat as shown in figure 6.18a. Copolymerisation of 1-diphenylphosphinopyrrole and pyrrole, to give a polymer as shown in figure 6.18b, and the electropolymerisation of 1-diphenylphosphinopyrrole

(a)

(b)

Figure 6.18. Structure of (a) poly-1-diphenylphosphinopyrrole and
              (b) copolymer of pyrrole and 1-diphenylphosphinopyrrole.
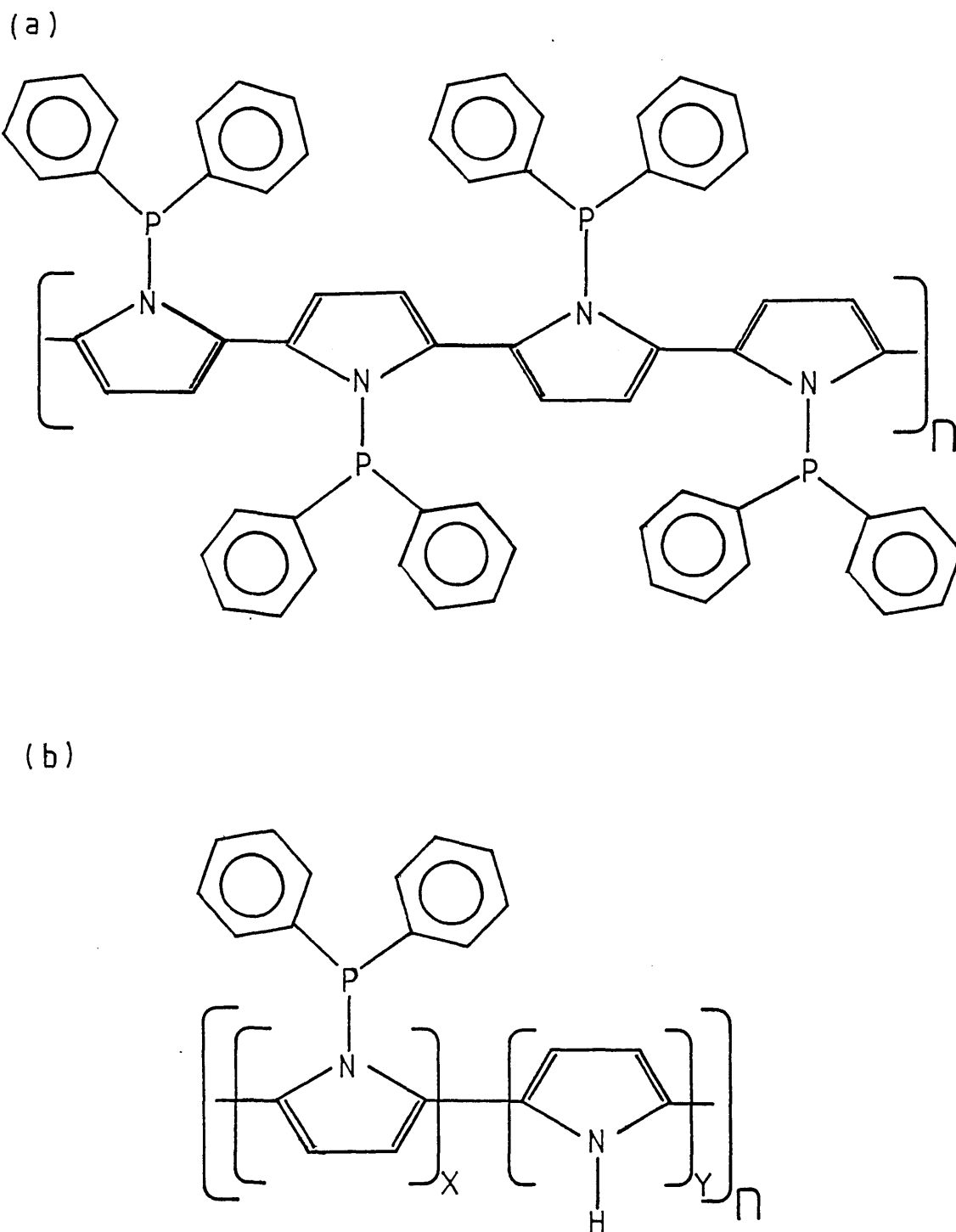
at a thinly polypyrrole-coated electrode were also tried. Finally, bis(1-diphenylphosphinopyrrole) palladium dichloride ($Pd(Ph_2P-1-py)_2Cl_2$) and 1-diphenylphosphinatopyrrole ($Ph_2P(O)-1-py$) were synthesised and investigated electrochemically.

6.4.1. The Electrochemistry and Attempted Electropolymerisation of 1-Diphenylphosphinopyrrole

Initially, a 5 mM Ph_2P-1-py acetonitrile solution (+ 0.1 M TBAP) was investigated electrochemically, using a platinum RDE. The electrode was rotated at 4 Hz and swept anodically at 10 mV s^{-1}. Sweeping the potential up to +2.0 V vs Ag/Ag$^+$ the only electrochemical activity was a peak, not a wave as would be expected, at E_p = +1.1 V vs Ag/Ag$^+$ (see figure 6.19a). This peak was not present in plain supporting electrolyte (see figure 6.19b).

If one held the potential at +1.1 V vs Ag/Ag$^+$ (i.e. the peak potential) the current fell to zero over the period of a few seconds.

Increasing the concentration of Ph_2P-1-py to 0.05 M increased the peak height for the same rotation speed and sweep rate (see figure 6.20a). It was also noted that on subsequent sweeps the peak height was reduced (see figure 6.20b). No other electrochemical activity was detected between -2.8 V and +2.0 V vs Ag/Ag$^+$.

Cyclic voltammetric analysis of this solution gave an oxidation peak at E_p = +1.1 V vs Ag/Ag$^+$ with a reduction on the return cycle at E_p = -0.5 V vs Ag/Ag$^+$, which in turn gave rise to an oxidation peak at E_p = -0.25 V vs Ag/Ag$^+$. These extra reduction (at -0.5 V) and re-oxidation (at -0.25 V) peaks were not present if the first oxidation (at +1.1 V) was not performed (see figure 6.21). This activity is very similar to that discussed for triphenylphosphine electrochemical oxidation
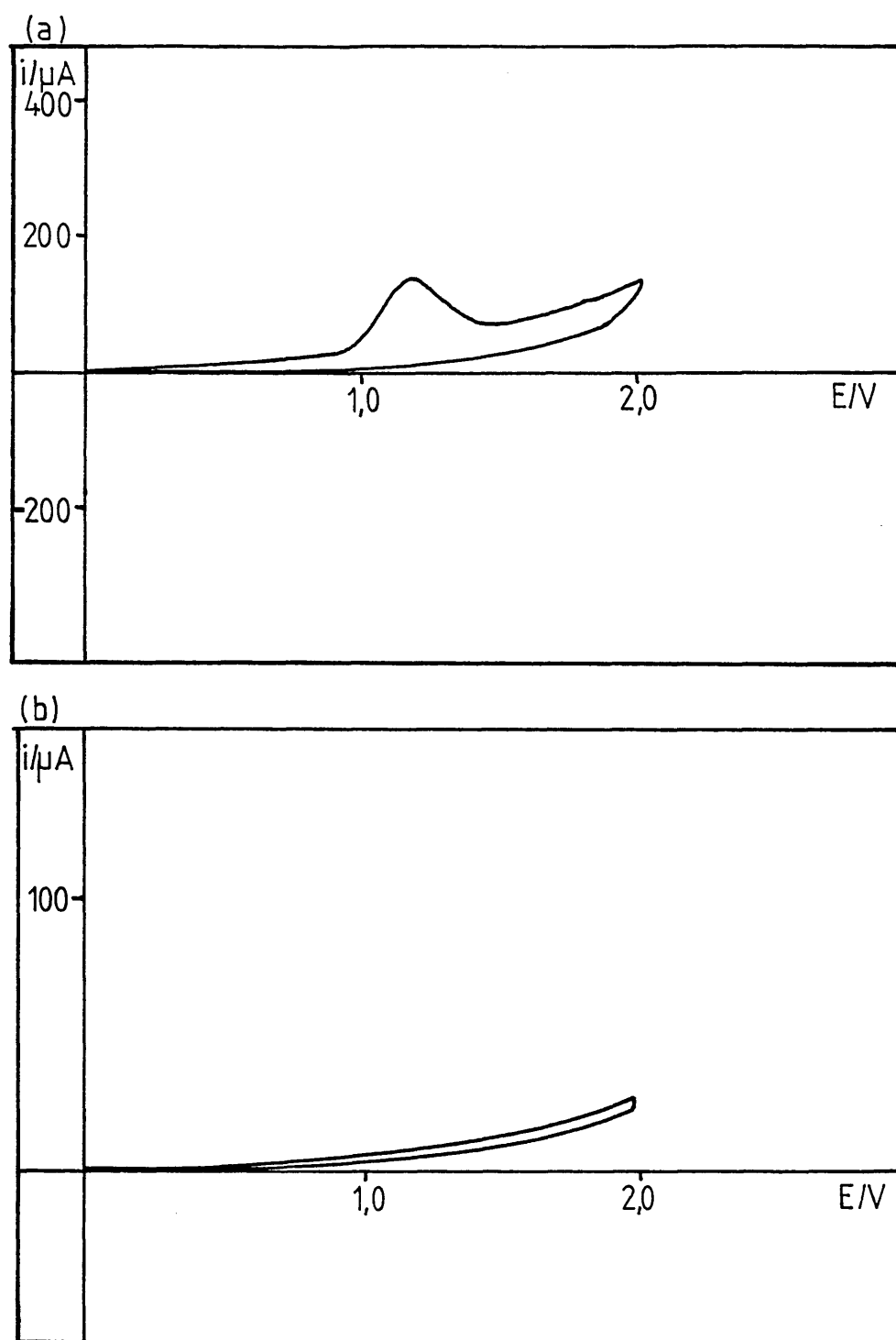
Figure 6.19. (a) Current voltage curve for 1-diphenylphosphino-
pyrrole in acetonitrile (+0.1 M TBAP); (b) current
voltage curve for plain supporting electrolyte.

(a)

(b)
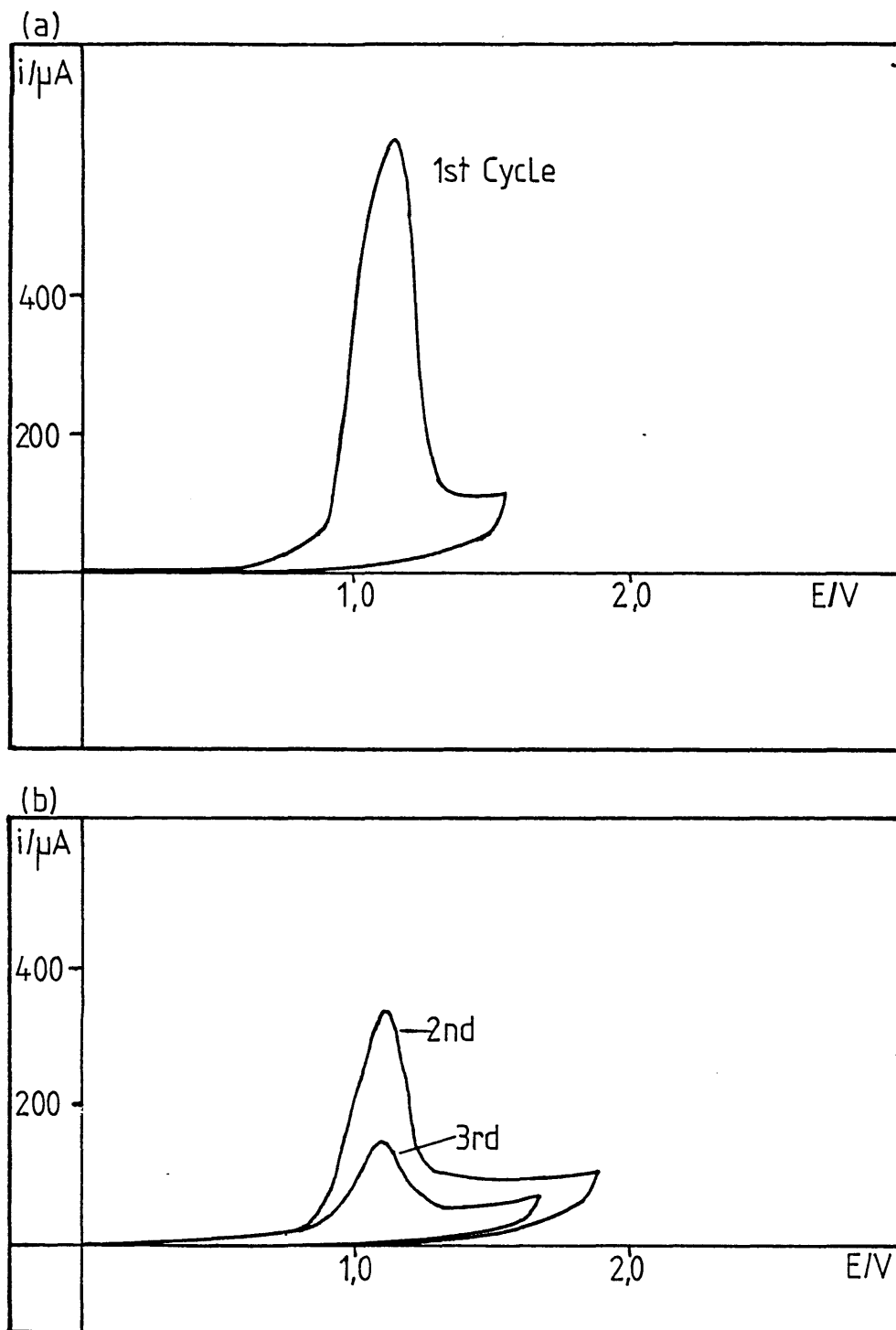
Figure 6.20. Current voltage curve for 1-diphenylphosphino-
pyrrole as in figure 6.19, but with a larger
concentration of 1-diphenylphosphinopyrrole in
solution.
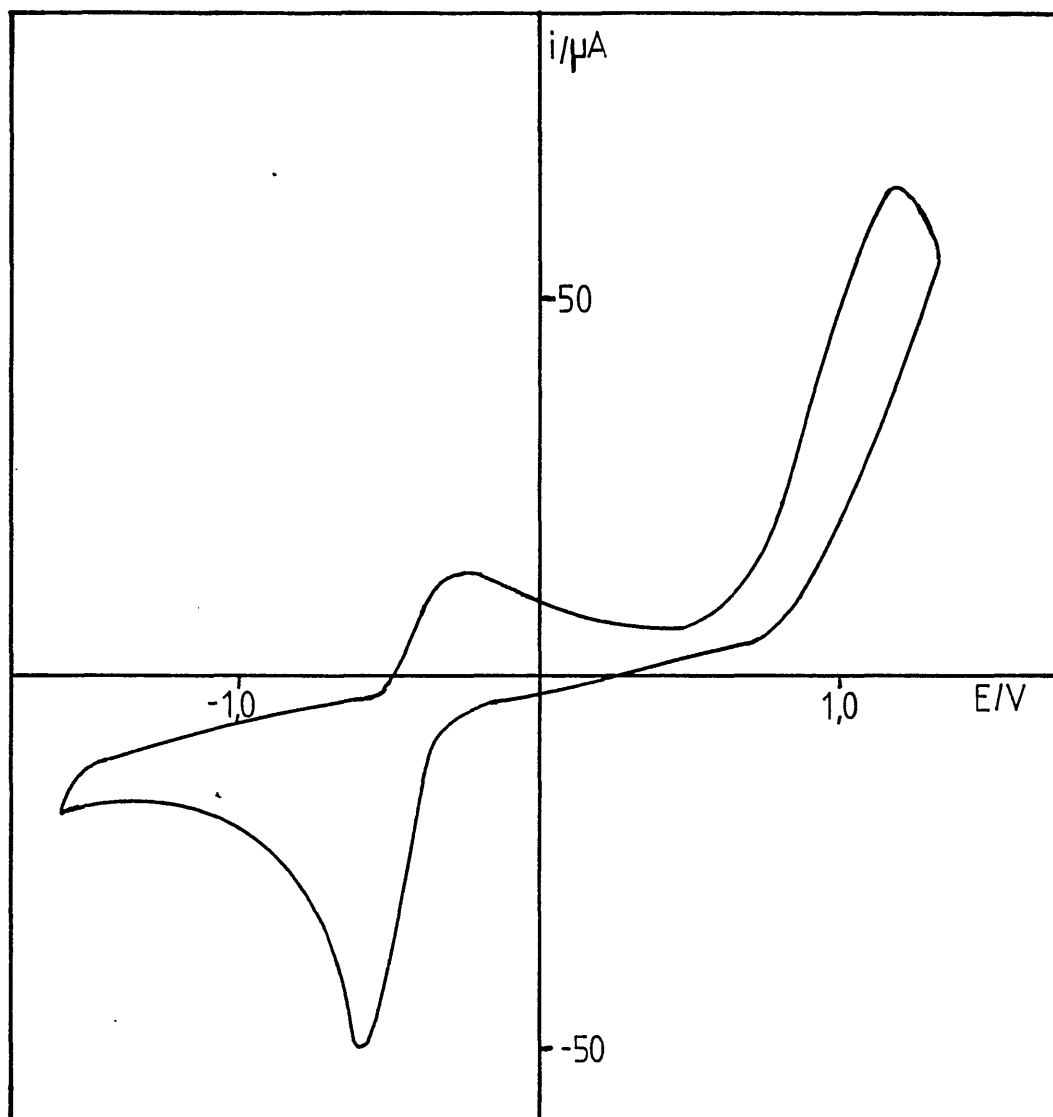
Figure 6.21. Cyclic voltammetric analysis of 1-diphenylphosphino-
pyrrole (v = 100 mV s^{-1}).

(see section 4.2.2.3). Therefore, one can deduce that the activity at +1.1 V is the oxidation of the phosphine group of 1-diphenylphosphino-pyrrole.

Similar results were found for glassy carbon electrodes and when using dimethylsulphoxide solutions.

However, in acetonitrile solutions, if one extended the anodic limit, a wave was observed just before solvent decomposition ($E_{\frac{1}{2}}$ = +2.4 V vs Ag/Ag$^+$, see figure 6.22). Holding the potential at the limiting current, of this wave, one observes a gradual drop in current and the formation of a grey-black coat on the electrode surface. However, the coat is electroinactive and completely blocks ferrocene oxidation.

As a control experiment, a platinum RDE was held at +2.5 V vs Ag/Ag$^+$ in plain supporting electrolyte and no current or coat were observed. The potential was also paused at +2.7 V vs Ag/Ag$^+$, where solvent decomposition occurs, and a current was observed but no coat formed. Therefore, one can conclude that the coat is connected with Ph$_2$P-1-py, but the inactivity and appearance of the coat tends to suggest some adsorbed, decomposed product rather than electropolymerised pyrrole.

From these results one can see that Ph$_2$P-1-py does not electro-polymerise under these conditions. The peak at +1.1 V vs Ag/Ag$^+$ on a rotating electrode tends to indicate some poisoning of the electrode by the oxidation product. This poisoning could be preventing the electro-polymerisation. However, it does not alter solvent limits and as peaks are observed on subsequent sweeps, it seems the adsorbed species (which poisons the electrode) is not firmly attached.

Due to these results it was decided to investigate the possible electropolymerisation of Ph$_2$P-1-py in the presence of pyrrole initiator This is discussed in the following section.
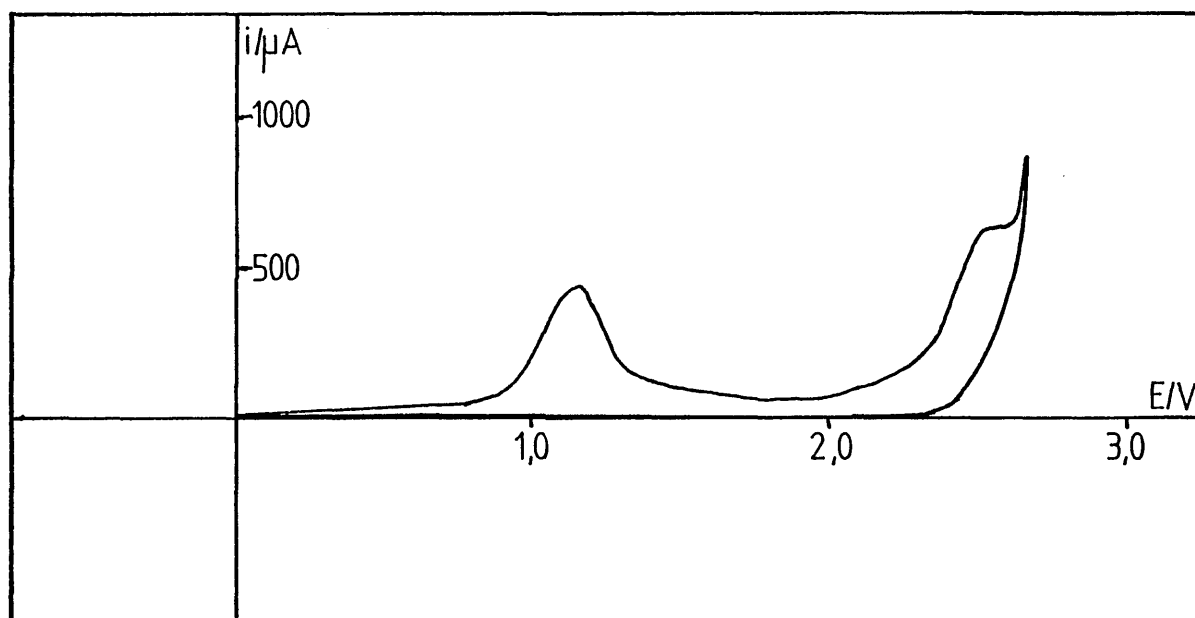
Figure 6.22. Current voltage curve for 1-diphenylphosphinopyrrole as in figure 6.20 (a), but with an extended positive limit.

6.4.2. <u>Copolymerisation of Ph$_2$P-1-py and Pyrrole</u>

The copolymerisation of Ph$_2$P-1-py with pyrrole was investigated by three different methods. Two involve pyrrole as an initiator while the third is an attempted copolymerisation.

The first method involved adding a small concentration of pyrrole, which would not electropolymerise on its own, to a solution containing a large concentration of Ph$_2$P-1-py. Thus, the small amount of pyrrole could be oxidised electrochemically and may initiate the polymerisation of Ph$_2$P-1-py. Therefore, a 0.5 mM pyrrole + 0.05 M Ph$_2$P-1-py solution (in acetonitrile + 0.1 M TBAP) was used. A platinum RDE, rotating at various speeds (from 0 to 10 Hz) was stepped to +0.8 V vs Ag/Ag$^+$. This resulted in a small oxidation current being observed but no coating. This means that the pyrrole was being oxidised but did not react with Ph$_2$P-1-py.

Secondly, it was decided to try and electropolymerise Ph$_2$P-1-py on a polypyrrole coated electrode. Therefore, the potential of a platinum RDE thinly coated with polypyrrole, rotating at 4 Hz, in a 0.05 M Ph$_2$P-1-py acetonitrile solution (+ 0.1 M TBAP) was stepped to +0.60 V vs Ag/Ag$^+$. However, no growth of the coat was observed. This was checked by cyclic voltammetry, of the coated electrode, before and after seeing the Ph$_2$P-1-py solution. If the potential of the polypyrrole coated electrode was stepped above +0.65 V vs Ag/Ag$^+$ decomposition of the polypyrrole coat was observed.

Finally, copolymerisation of Ph$_2$P-1-py and pyrrole was attempted. This was tried from an acetonitrile (+ 0.1 M TBAP) solution containing 0.01 M Ph$_2$P-1-py and 0.01 M pyrrole. The potential of a platinum RDE (rotating at 4 Hz) was stepped to +0.72 V vs Ag/Ag$^+$. A constant current resulting in a coat was observed. However, the coating current was identical to 0.01 M pyrrole and investigation of the resulting coat gave

identical results to a plain polypyrrole coat. If Ph_2P-1-py had been present in the coat, then one would expect either a shift in peak potentials or extra peaks/shoulders due to Ph_2P-1-py oxidation/ reduction. This would be expected due to the electronic effect of the phosphine groups on the pyrrole unit.

From these results, one can see that the electropolymerisation of Ph_2P-1-py with pyrrole in solution or at a polypyrrole coated electrode was unsuccessful.

6.4.3. Electrochemical Analysis of Bis(1-Diphenylphosphinopyrrole) Palladium Dichloride

Electrochemical investigation of $Pd(Ph_2P$-1-py$)_2Cl_2$, at a platinum RDE in chloroform solution (+ 0.1 M TEAP), showed no electrochemical activity between solvent limits. However, on the addition of excess Ph_2P-1-py a reduction wave was observed at $E_{\frac{1}{2}}$ = -1.15 V vs SCE (see figure 6.23). Cyclic voltammetry, at a stationary electrode, showed a reduction wave at $E_{\frac{1}{2}}$ = -1.2 V vs SCE and a reoxidation peak at +0.5 V vs SCE (see figure 6.24). Thus, similar activity to $Pd(PPh_3)_2Cl_2$ (see section 4.2) was observed.

Though not surprising, this is encouraging as it indicates that similar activity is observed for 1-diphenylphosphinopyrrole complexes as for triphenylphosphine complexes.

6.4.4. Electrochemical Analysis of Diphenylphosphinatopyrrole

Electrochemical investigation in acetonitrile solutions (+ 0.1 M TBAP) of diphenylphosphinatopyrrole (5 mM and 50 mM) showed no electro-chemical activity between solvent limits of -2.8 V and +2.5 V vs Ag/Ag^+ (see figure 6.25).
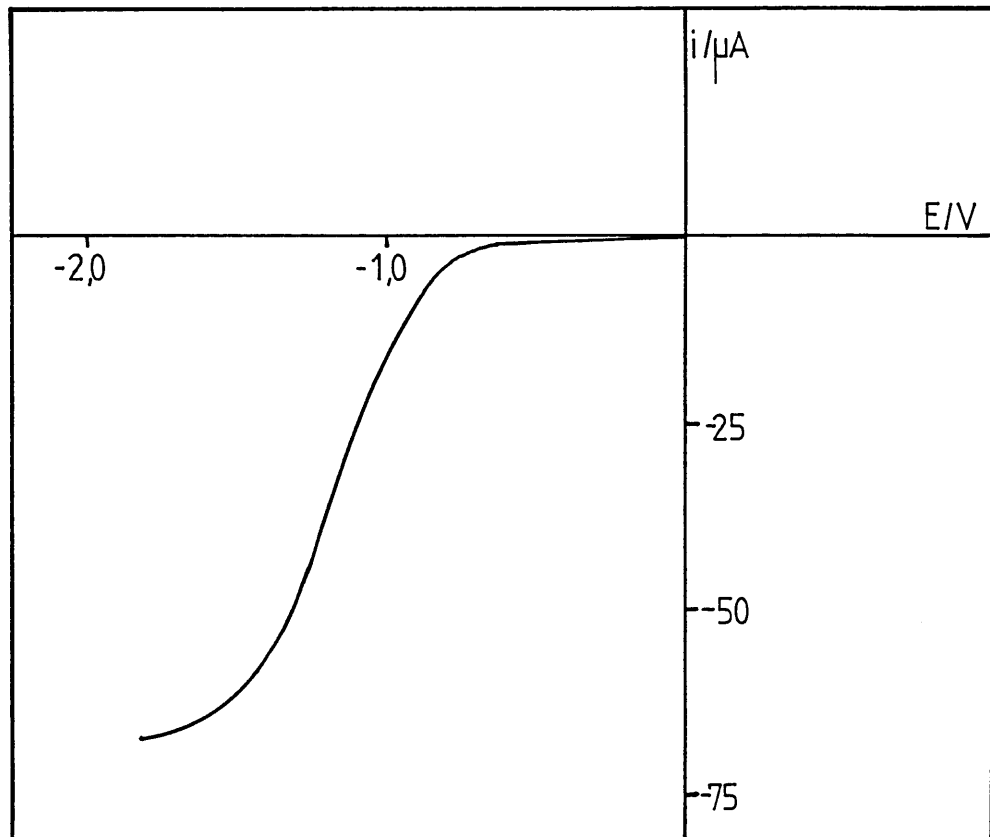
Figure 6.23. Current voltage curve for the reduction of
$Pd(Ph_2P-1-py)_2Cl_2$ in the presence of excess
$Ph_2P-1-py$ (W = 10 Hz, v = 10 mV s^{-1}).
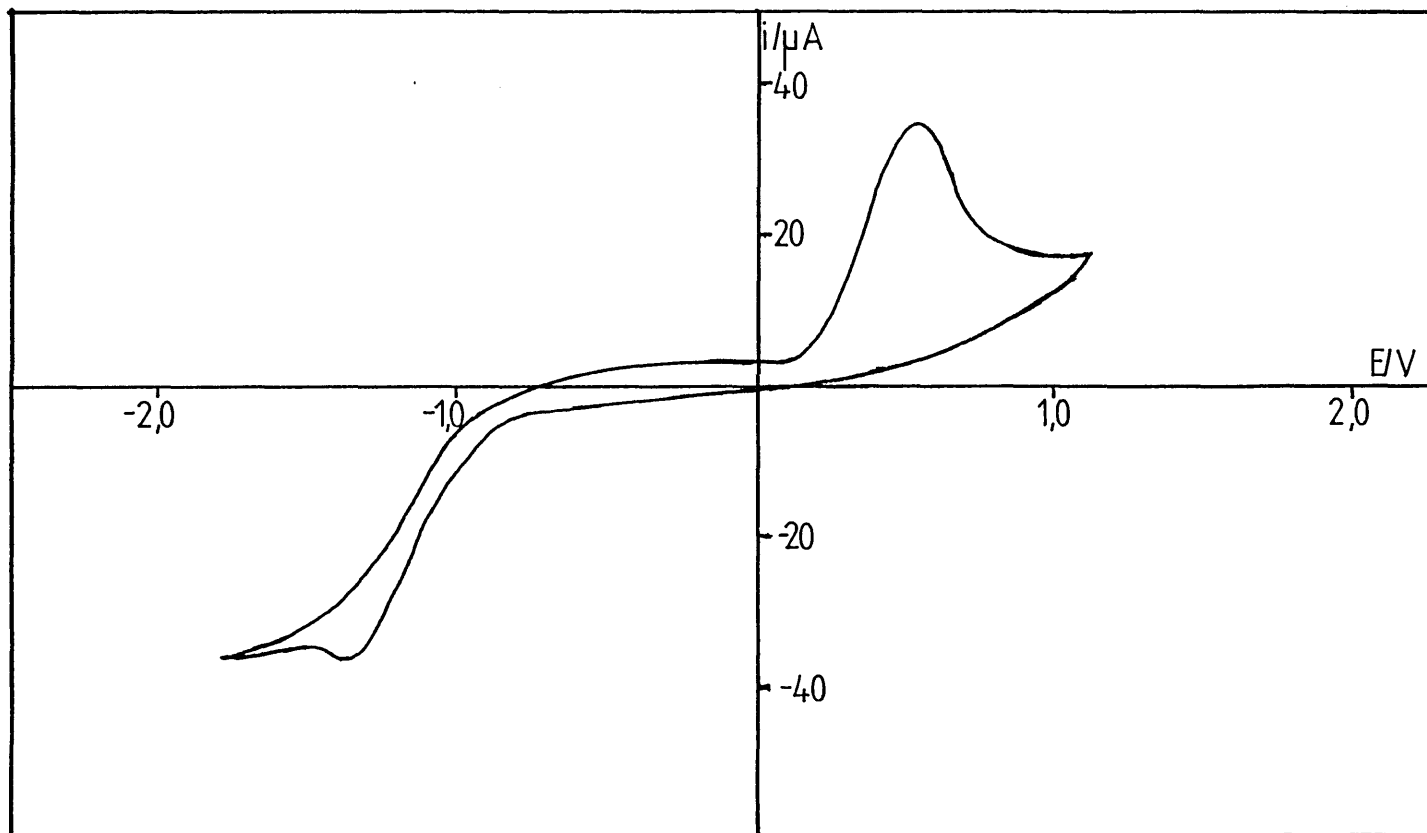
Figure 6.24. Cyclic voltammogram for $Pd(Ph_2P-1-py)_2Cl_2$ in the presence of excess $Ph_2P-1-py$ ($v = 100$ mV s^{-1}).
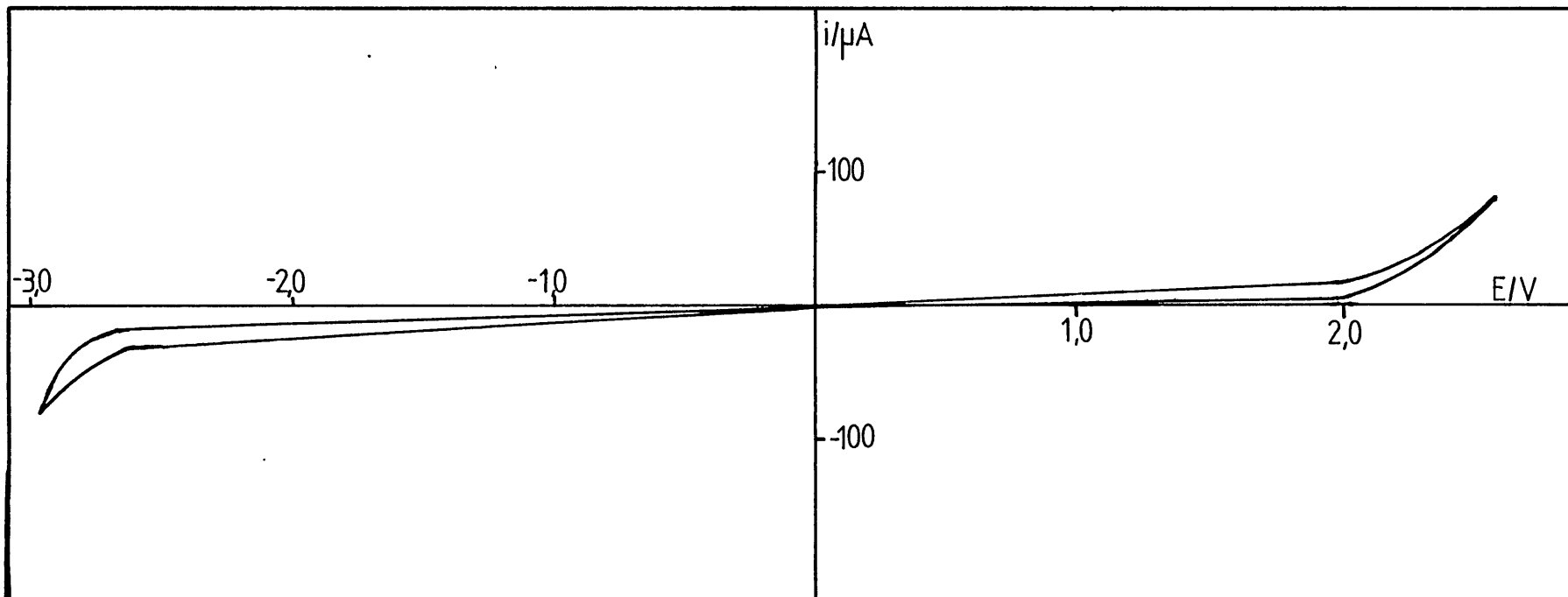
Figure 6.25. Current voltage curve for 1-diphenylphosphinatopyrrole in acetonitrile (+0.1 M TBAP) (W = 4Hz, v = 10 mV s^{-1}) - shows no electrochemical activity between solvent limits.

This means that electropolymerisation of $Ph_2P(O)$-1-py does not occur and also tends to indicate that the electropolymerisation of Ph_2P-1-py will also fail to occur within solvent limits.

6.4.5. Discussion

N-Alkyl and N-aryl pyrroles have been investigated in the literature[215,216,217,218]. Both electronic and steric factors influence the coating process.

Electronic effects can be seen by looking at N-phenylpyrrole which electropolymerises at a potential 0.6 V more positive than pyrrole. This has been explained[215] in terms of the enhancement the phenyl group produces in the π-dipole moment of the pyrrole molecule.

Steric effects have been shown[217] by looking at N-(ortho-substituted phenyl) pyrroles where o-OMe, o-F, o-Cl and o-Br all electropolymerise to give coated electrodes. However, if bulkier groups are used (e.g. $o-NO_2$ and $o-CF_3$) then electro-oxidation is observed, but no polymerisation occurs and hence no coats are formed. Dimers are perhaps made but higher oligomers are prevented by the steric hindrance from these larger ortho-groups.

Considering the results of this section, no electrochemical oxidation of the pyrrole group (of the N-phosphine substituted pyrrole) was observed. This indicates an electronic effect is preventing electropolymerisation by pushing the potential needed for electropolymerisation beyond the positive solvent limit. If only steric effects were the reason, then an electro-oxidation of the pyrrole would have been observed.

This electronic effect is probably due to π-electrons, from the pyrrole, being in some way influenced by the PPh_2 group and being made

more stable, hence resulting in a greater energy needed (i.e. higher potential) to oxidise the pyrrole.

6.5. Electropolymerisation of Thiophene and Furan and Investigation of the Resulting Polymer Coats

Due to the lack of success in electropolymerising 1-diphenylphosphino-pyrrole it was decided to look for other conducting polymers which could be used. As discussed in the next section, it was found possible to synthesise the 3-diphenylphosphinothiophene and the 3-diphenylphosphino-furan.

It was felt that investigation of the electropolymerisation of plain thiophene and furan would be helpful. The resulting coats were also analysed by cyclic voltammetry.

6.5.1. Thiophene

The potential of a platinum RDE, rotating at 4 Hz, was swept anodically (at 10 mV s^{-1}) in an acetonitrile solution (+ 0.1 M LiClO$_4$) of 0.01 M thiophene. An oxidation wave began at +1.4 V vs Ag/Ag$^+$ and rose to give a maximum current greater than the electronics could cope with (i.e. > 1.2 mA, see figure 6.26a). The oxidation wave was due to the electropolymerisation of thiophene and resulted in the electrode being coated with polythiophene.

Stepping the potential of a platinum RDE, rotating at 4 Hz, to +1.5 V vs Ag/Ag$^+$ gave a constant coating current and by varying the length of time, at this potential, one could vary the thickness of the coat. As with pyrrole, analysis[221] has shown that 40 mC cm^{-2} gives approximately a 100 nm thick film.

Figure 6.26. (a) Current voltage curve for the electropolymerisation of thiophene; (b) cyclic voltammogram of the resulting polythiophene coated electrode ($v = 100$ mV s^{-1}).
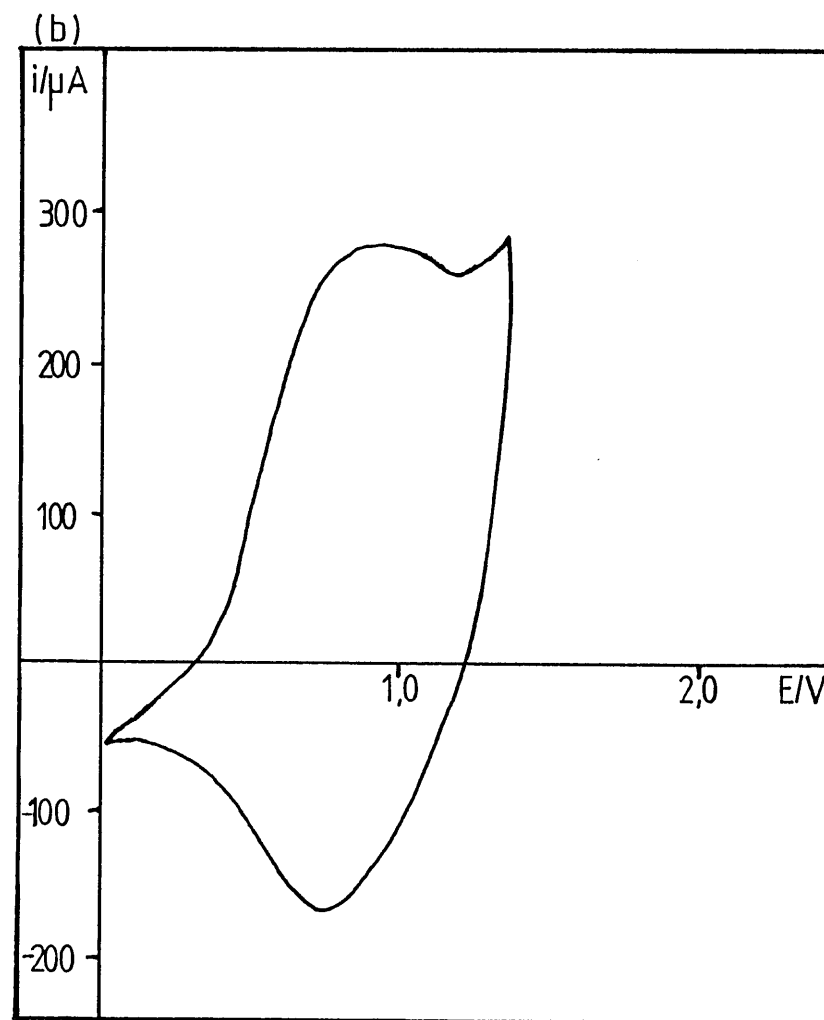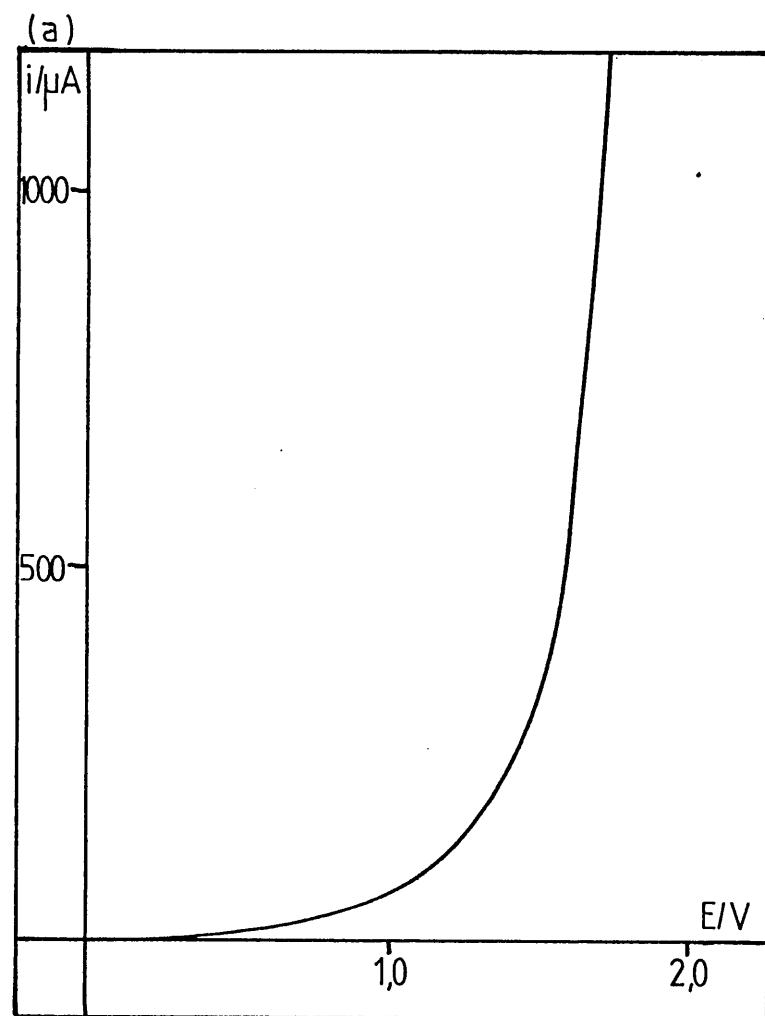
Cyclic voltammetric analysis of a coated electrode showed an anodic peak at +0.9 V vs Ag/Ag$^+$ and a cathodic peak at +0.75 V vs Ag/Ag$^+$ (see figure 6.26b). The peaks, as with polypyrrole films, are very broad. In the oxidised, conducting state the polythiophene coat is dark blue while in the reduced state it is a reddish/brown colour. As with pyrrole, analysis of polythiophene coats has shown[187] that in the oxidised state there is one electron removed per four thiophene units (see figure 6.27).

A polythiophene coated electrode ($\sim$ 100 nm) completely blocked the ferrocene oxidation wave until the coat was oxidised at +0.9 V vs Ag/Ag$^+$. This indicates that ferrocene does not easily diffuse through the polymer coat and that the polymer coat did not contain any pinholes. At +0.9 V vs Ag/Ag$^+$ the oxidation of ferrocene was seen superimposed on the coat oxidation peak. When the potential of the coated electrode was held at +1.0 V vs Ag/Ag$^+$ the ferrocene oxidation showed Levich dependence on rotation speed. This is similar to the results for pyrrole discussed in section 6.2.2.2.

The polythiophene coat was stable in plain supporting electrolyte (0.1 M LiClO$_4$ in acetonitrile) up to +1.4 V vs Ag/Ag$^+$ but if this potential was passed then the electrochemical activity of the coat was lost. The stability of polythiophene coats in air/oxygen is debated in the literature[219,220,221]. Work done here indicated that polythiophene coats are much more stable to air and oxygen than polypyrrole coats. In their oxidised state the polythiophene coated electrodes could be exposed to air for several hours without any degradation being observed. However, the coat is less stable in its reduced form showing considerable loss of activity after 1 hour's exposure.
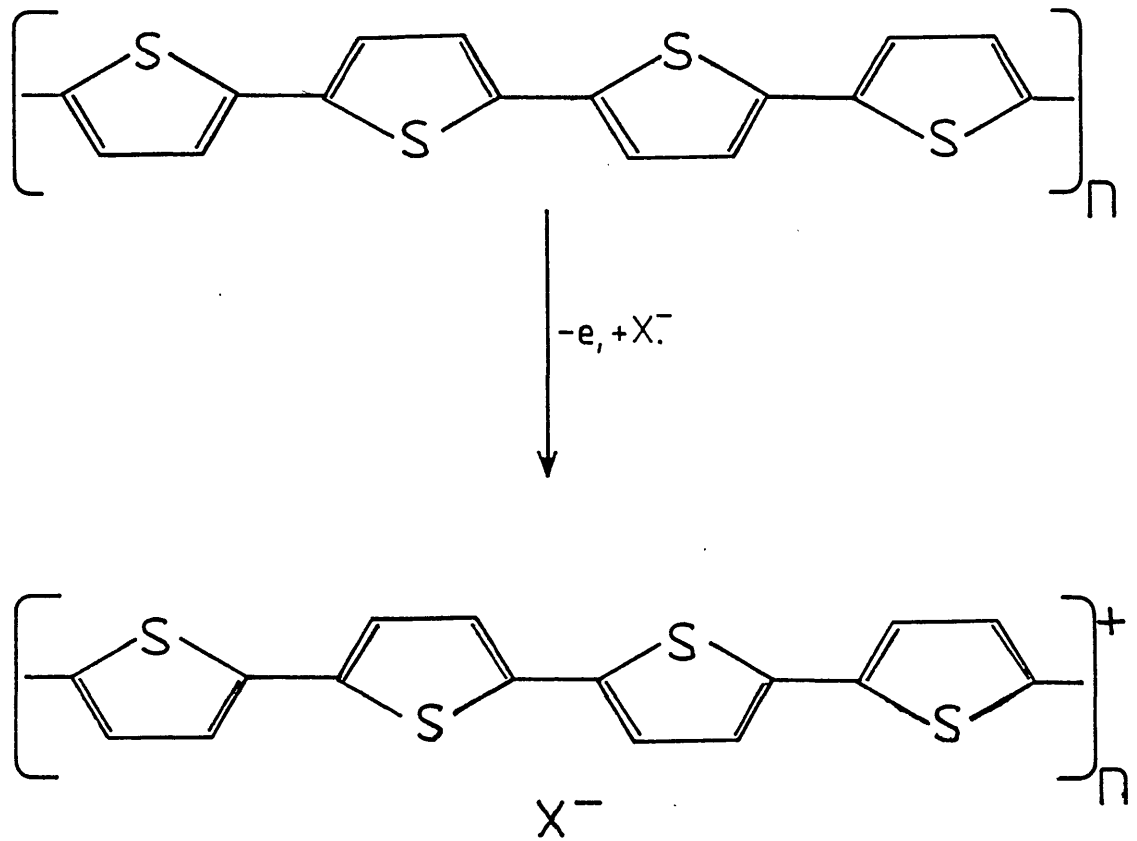
Figure 6.27.   Structure of polythiophene in the reduced and oxidised (conducting) form.

6.5.2. Furan

A furan solution (0.01 M in acetonitrile + 0.1 M LiClO$_4$) was electrochemically investigated as thiophene above. Electropolymerisation occurred at +1.8 V vs Ag/Ag$^+$ and resulted in a polyfuran coat. Cyclic voltammetric analysis of the coat gave a broad anodic peak at +1.2 V vs Ag/Ag$^+$ and a broad cathodic peak at +1.0 V vs Ag/Ag$^+$ (see figure 6.28 a + b). The coat was stable in supporting electrolyte (0.1 M LiClO$_4$ in acetonitrile) up to +1.7 V vs Ag/Ag$^+$ and showed similar stability in air and electrochemical properties to polythiophene coats.

Therefore, one can see that both thiophene and furan can electropolymerise, as does pyrrole, to give conducting polymer coats. The polymerisation potentials for pyrrole, thiophene and furan, the oxidation and reduction potentials of their coats and the potential region in which the coats are useful are given in table 6.2.

6.6. The Preparation and Electrochemical Investigation of 3-Diphenyl-phosphino-Thiophene and Furan

6.6.1. Preparations

For reasons already discussed in section 6.3 it was necessary to make the 3-diphenylphosphino-thiophene and furan.

(X=S or O)
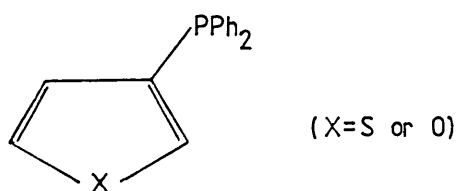
It was found that, unlike pyrrole, 3-bromothiophene and 3-bromofuran are both literature preparations[224,225,226] and commercially available (Aldrich Chemicals).

Figure 6.28.   (a) Current voltage curve for the electropolymerisation of furan $(W = 4$ Hz, $v = 10$ mV s$^{-1})$;

(b) Cyclic voltammogram of the resulting polyfuran coated electrode $(v = 100$ mV s$^{-1})$.
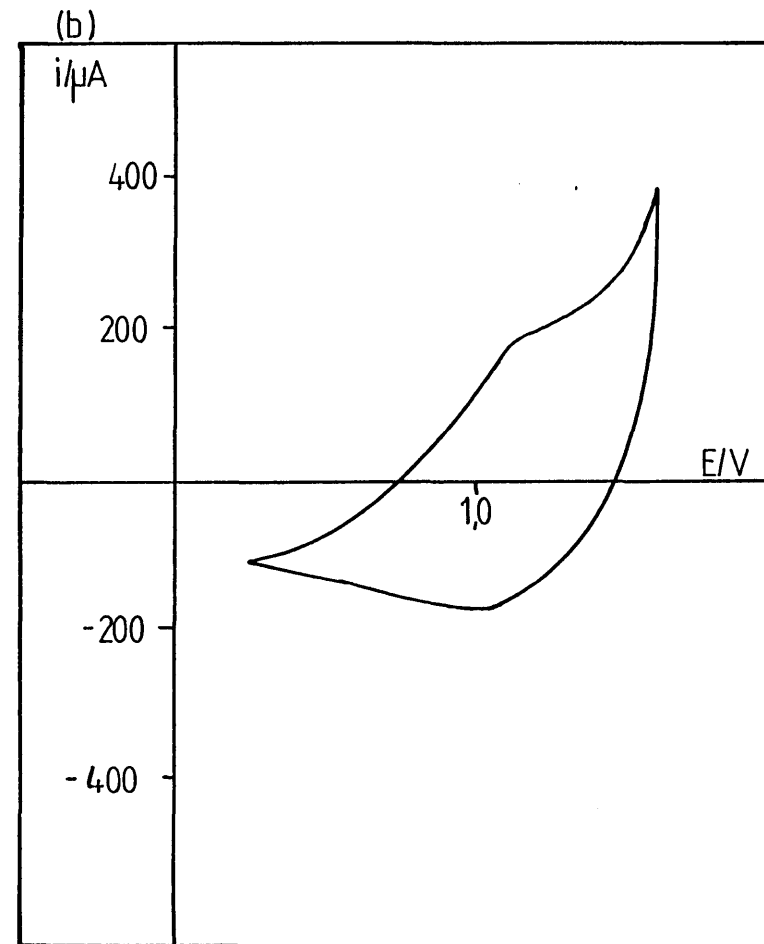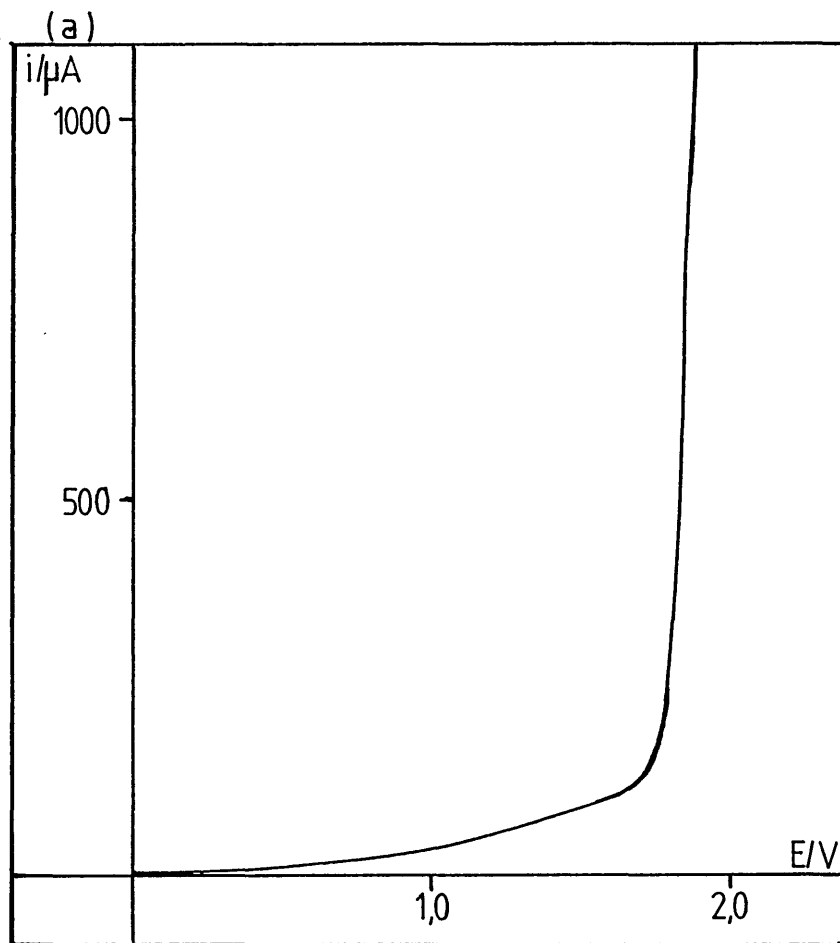
Table 6.2:   Characteristics of Conducting Polymer Coats.

Monomer	Monomer's polymerisation potential/ V vs Ag/Ag$^+$	Polymer's oxidation potential/ V vs Ag/Ag$^+$	Polymer's reduction potential/ V vs Ag/Ag$^+$	Potential region in which polymer would be conducting and stable/ V vs Ag/Ag$^+$
Pyrrole	+0.72	-0.02	-0.1	-0.02 → +0.65
Thiophene	+1.5	+0.90	+0.75	+0.9 → +1.4
Furan	+1.8	+1.2	+1.0	+1.2 → +1.7

These 3-bromo derivatives were reacted with butyllithium at -70°C. This low temperature was needed to prevent migration of the lithium to the preferred 2-position. Chlorodiphenylphosphine was then added to give the required products. The exact experimental details are given in section 6.9.8.

6.6.2. Attempted Electropolymerisations

Sweeping the potential (10 mV s^{-1}) of a platinum RDE (rotating at 4 Hz) in a 0.01 M 3-diphenylphosphinothiophene solution (acetonitrile + 0.1 M LiClO$_4$) gave a peak at +0.9 V vs Ag/Ag$^+$ (see figure 6.29). Cyclic voltammetric analysis showed three peaks (see figure 6.30). The first anodic peak at +0.9 V vs Ag/Ag$^+$ followed by a reduction peak at -0.45 V vs Ag/Ag$^+$ which gave rise to another anodic peak at -0.25 V vs Ag/Ag$^+$. This was similar to the behaviour shown by Ph$_2$P-1-py (see section 6.4.1). Therefore, it can be deduced that it is the phosphine group which is being oxidised at +0.9 V vs Ag/Ag$^+$.

No other electrochemical activity was seen up to the solvent limit and hence no coating was observed.

Similar results were obtained for 3-diphenylphosphinofuran.

6.6.3. Electrochemistry of 3-diphenylphosphinatothiophene

3-Diphenylphosphinothiophene was oxidised by the same method as 1-diphenylphosphinopyrrole (see section 6.9.7b). The product was investigated electrochemically, as 3-diphenylphosphinothiophene above, but showed no electrochemical activity up to the anodic solvent limit (see figure 6.31).

Therefore, one can see the electropolymerisation of 3-diphenylphosphinatothiophene does not occur under these conditions.
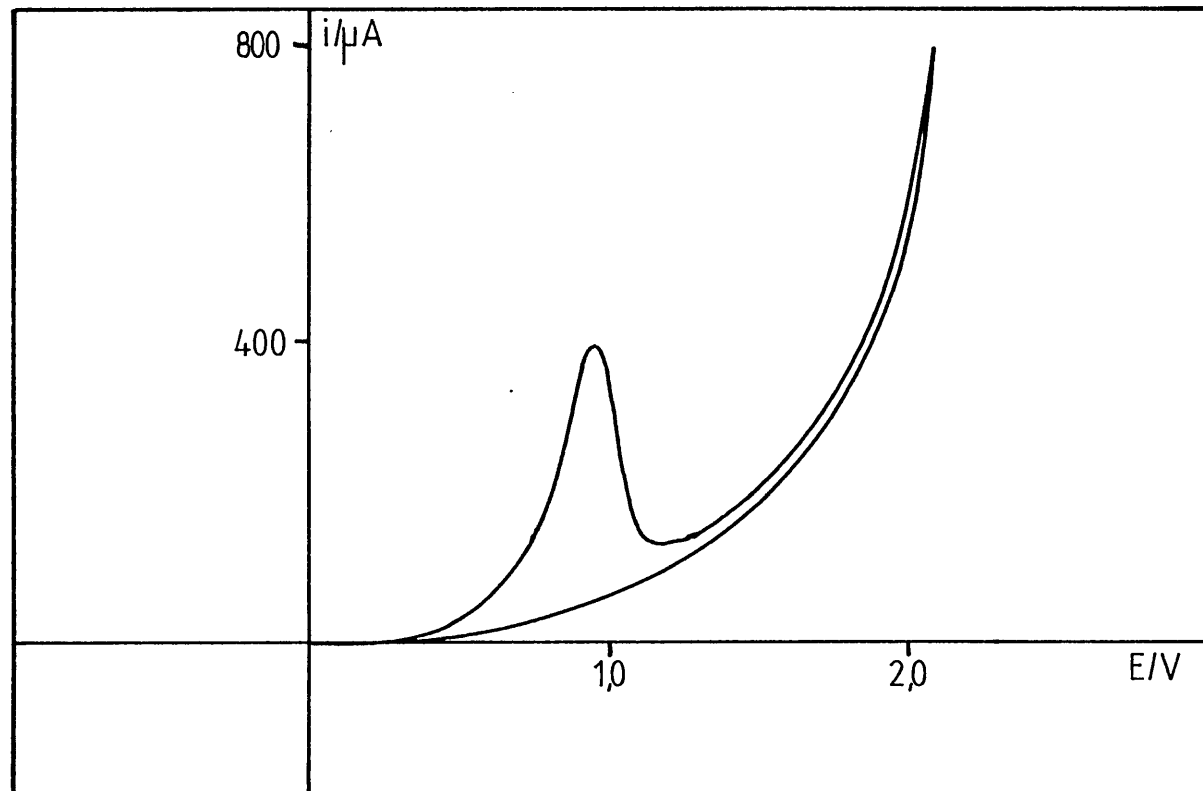
Figure 6.29. Current voltage curve for 3-diphenylphosphinothiophene in acetonitrile (+0.1 M $LiClO_4$).
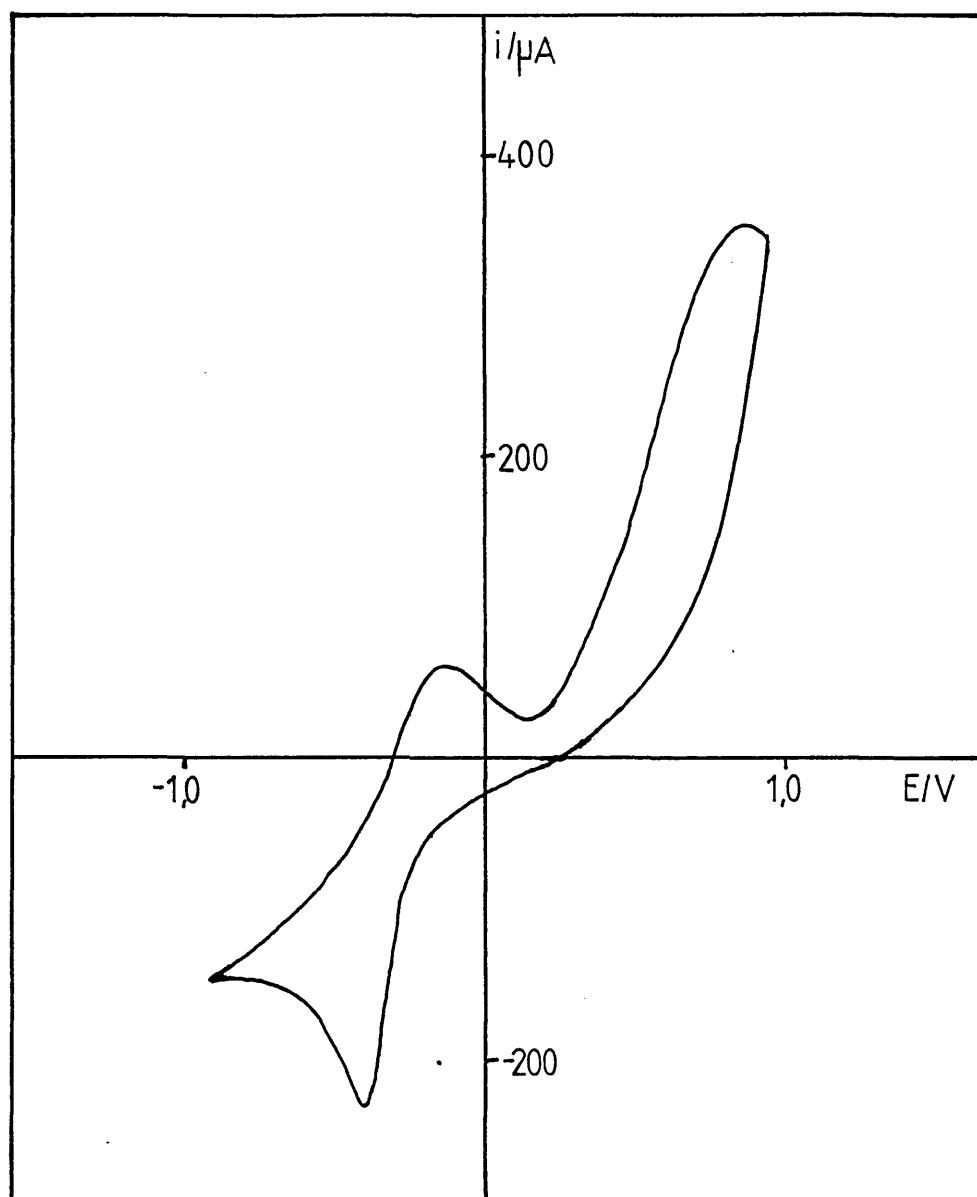
Figure 6.30. Cyclic voltammogram of 3-diphenylphosphino-
thiophene in acetonitrile (+0.1 M $LiClO_4$),
(v = 100 mV s^{-1}).

Figure 6.31. Current voltage curve for 3-diphenylphosphinatothiophene (W = 4 Hz, v = 10 mV s^{-1}) - shows no electrochemical activity within solvent limits.
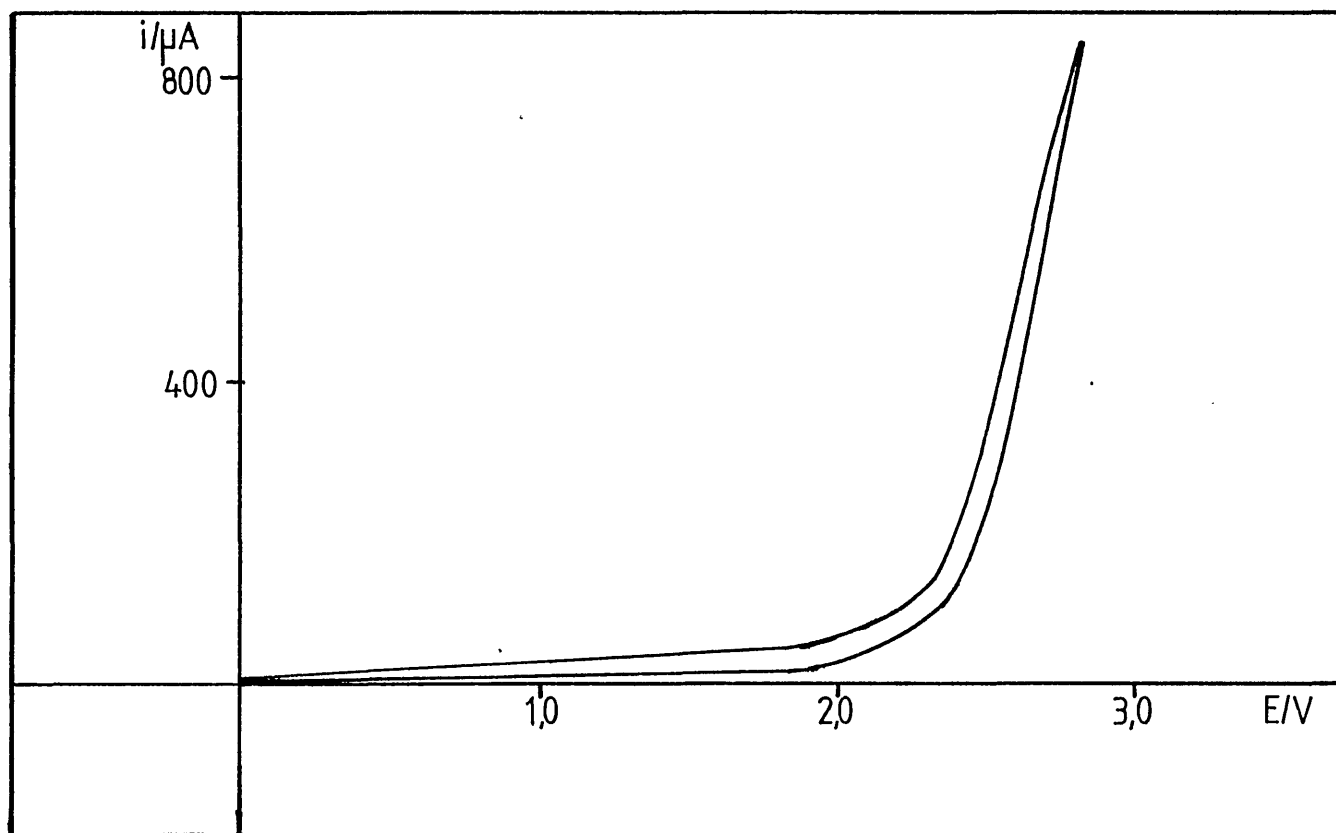
⌐ 6.6.4. Discussion

From the above results one can see that the electrochemical polymerisation of 3-diphenylphosphinothiophene, 3-diphenylphosphinofuran and 3-diphenylphosphinatothiophene does not occur under the conditions given.

The electropolymerisation of various 3-substituted thiophenes has been reported in the literature[186,221,222,223]. These have mainly been 3-alkyl or 3-halogeno-thiophenes where both electronic and steric effects have been investigated.

It is found that[221-223] a plot of the oxidation potential for the monomers versus the oxidation potential of the resulting polymers gives an approximate straight line. This linear dependence indicates that the substituent group has a similar electronic effect on the polymer as on the monomer. However, the 3,4-dialkyl substituted thiophenes seem to deviate from this linear dependence[222]. This has been explained by steric effects in the polymer. It is suggested that due to steric hindrance, in the polymer, the polymer chain twists in the neutral state. However, when oxidised the polymer must become planar to give the conducting, delocalised π-system. This alignment will require energy and hence the observed oxidation potential for the polymer is higher than would be expected from the monomer's oxidation potential (i.e. one gets the observed deviation from the above linear plot).

A plot of the monomers' oxidation potentials versus the Hammett substituent constant[221,223] also gives an approximate linear correlation. This indicates that the more electrophilic the substituent (i.e. electron withdrawing) the more difficult it will be to oxidise the corresponding thiophene.

It has also been noted[223] that 3-cyano, 3-nitro and 3-carboxylate thiophenes can be electrochemically oxidised but they do not give polymers. It has been suggested that, for these cases, the radical cation may under-go side reactions with solvent, or other nucleophilic species, rather than coupling to give the polymer. Steric effects could influence this by making the coupling reaction less favourable. There is also the pos-sibility that at the higher potentials needed for these groups, due to their electronegativity, that solvent breakdown may interfere.

Steric factors do not effect the monomers' oxidation potential but, as discussed above, they can effect polymerisation and the oxida-tion potentials in polymers.

Considering these effects and the above results, one can see that as the electrochemical oxidation, as well as polymerisation, of 3-di-phenylphosphinothiophene, 3-diphenylphosphinofuran and 3-diphenylphosphinato-thiophene were not observed, it seems that it is the electronic effect of the phosphine group which is moving the oxidation potentials above the solvent's limit. The Hammett substituent constant for diphenyl-phosphine could not be found in the literature and hence a prediction of the monomers' electrochemical oxidation potential could not be made. Also comparisons with other groups of known Hammett substituent co-efficients (e.g. amines) is not possible due to the added $p\pi - d\pi$ bonding exhibited by phosphorus (due to its 3-d orbitals).

Steric effects of diphenylphosphine groups in a polythiophene coat can also be envisaged (see sections 6.7 and 6.8).

6.7. <u>Phosphine Substitution of Coated Electrodes</u>

As 3-diphenylphosphinothiophene would not electropolymerise, it was decided to electropolymerise 3-bromothiophene and attempt to substitute the bromine groups with diphenylphosphine, in the coated electrode.

3-Bromothiophene was electropolymerised on a platinum flag (a disc of platinum with a platinum wire welded to the edge) by sweeping the potential of the electrode to +1.75 V vs Ag/Ag$^+$ (see figure 6.32a). Cyclic voltammetry on the resulting coated electrode showed an anodic peak at +1.2 V vs Ag/Ag$^+$. This peak had a shoulder at +0.6 V vs Ag/Ag$^+$. The cathodic peak was much broader (E_p ~ +1.0 V vs Ag/Ag$^+$) and had another small peak superimposed at +0.5 V vs Ag/Ag$^+$ (see figure 6.32b).

Similar behaviour has been observed for 3-methylthiophene[222] where the smaller peaks were explained as the formation of a stable partially doped (i.e. oxidised polymer).

The poly-3-bromothiophene coated platinum flag was then suspended in tetrahydrofuran (15 cm^3) under argon. Butyllithium in hexane (1 cm^3 of 1.6 M solution) was added dropwise and the solution stirred for half an hour. Chlorodiphenylphosphine (3 mmoles, 0.66 g) in tetrahydrofuran (15 cm^3) was added dropwise and the solution stirred for 3 hours. A precipitate was observed, probably due to lithium chloride formation, indicating reaction occurred in solution. The reaction expected on the electrode is shown in figure 6.33.

The resulting electrode was removed and rinsed with tetrahydrofuran and kept under argon at all times. Visually, the electrode was still coated with a grey/black polymer but when investigated electrochemically, in plain supporting electrolyte (acetonitrile + 0.1 M LiClO$_4$), no activity was observed. When investigated in ferrocene solution (1 mM in acetonitrile + 0.1 M TBAP), the ferrocene oxidation was completely blocked indicating a completely insulating film.

This lack of activity could be due to several reasons. Firstly, the poly-3-bromothiophene could have substituted its bromines for diphenylphosphine giving the poly-3-diphenylphosphinothiophene. The

Figure 6.32. (a) Current voltage curve for the electropolymerisation of 3-bromothiophene $(v = 10 \ mV \ s^{-1})$.

(b) Cyclic voltammogram of the resulting poly-3-bromothiophene coated electrode $(v = 100 \ mV \ s^{-1})$.
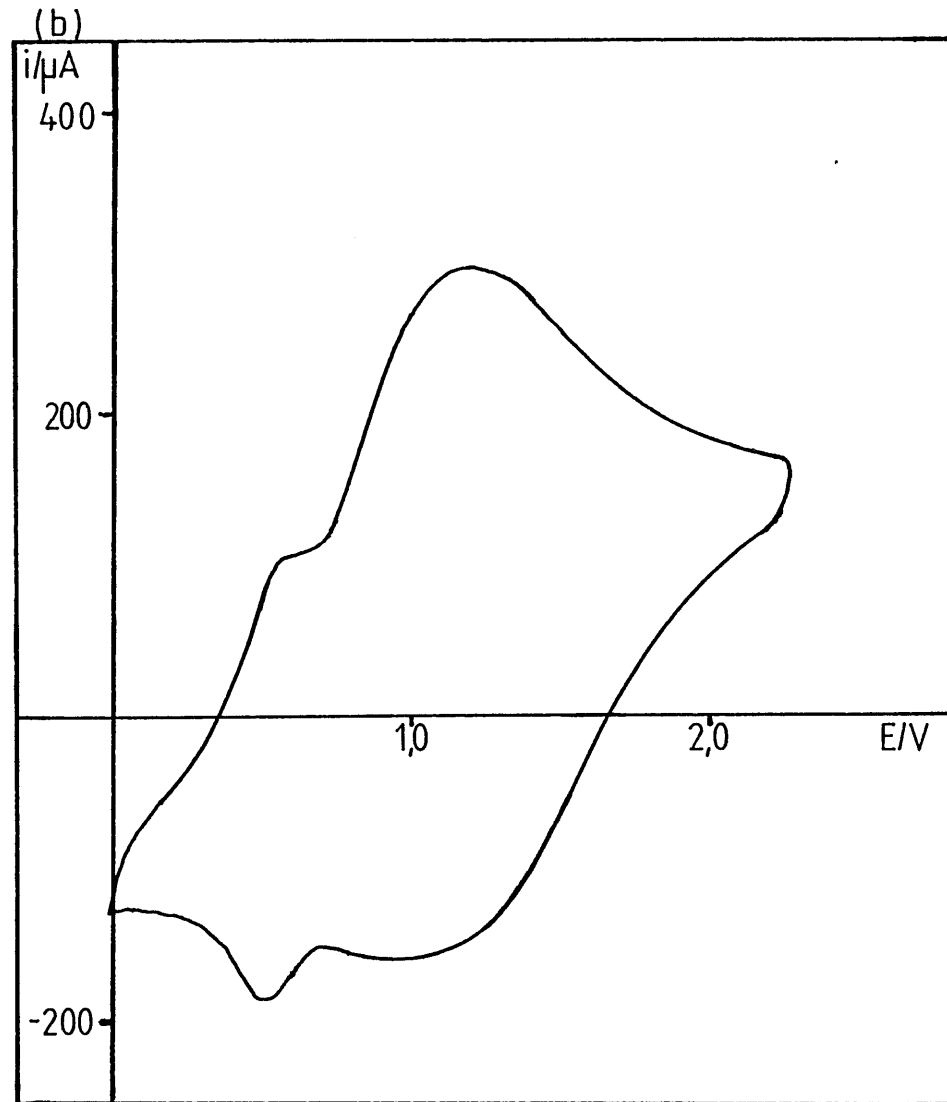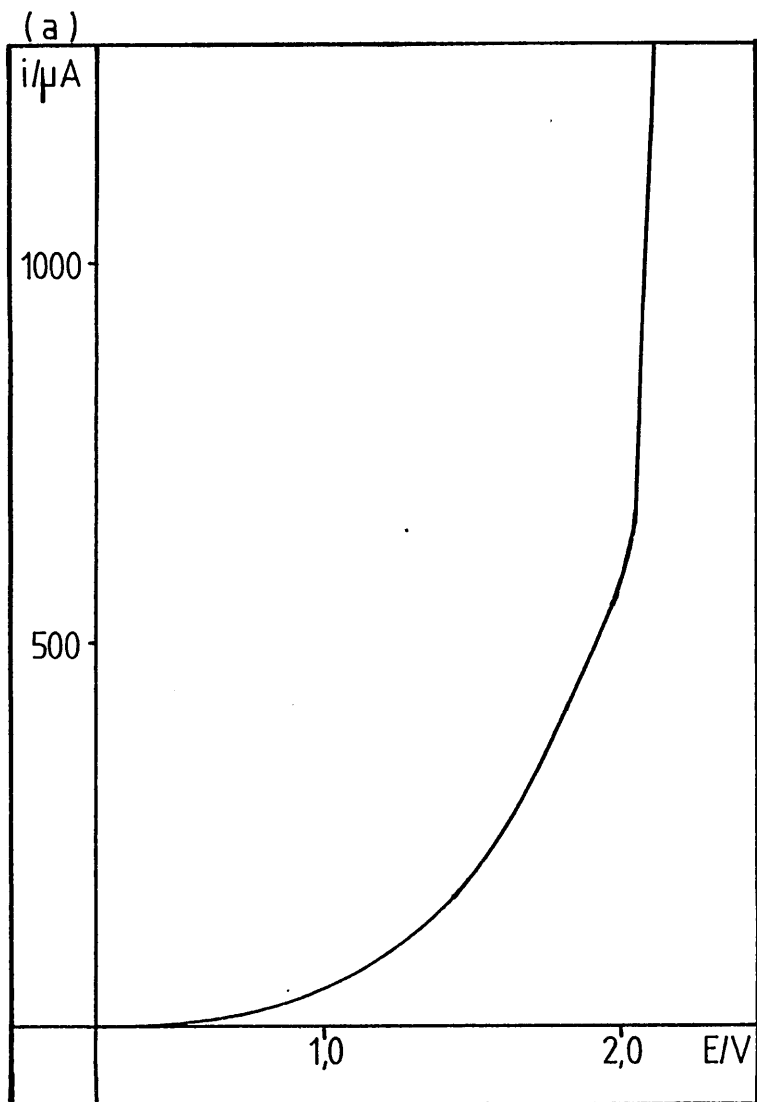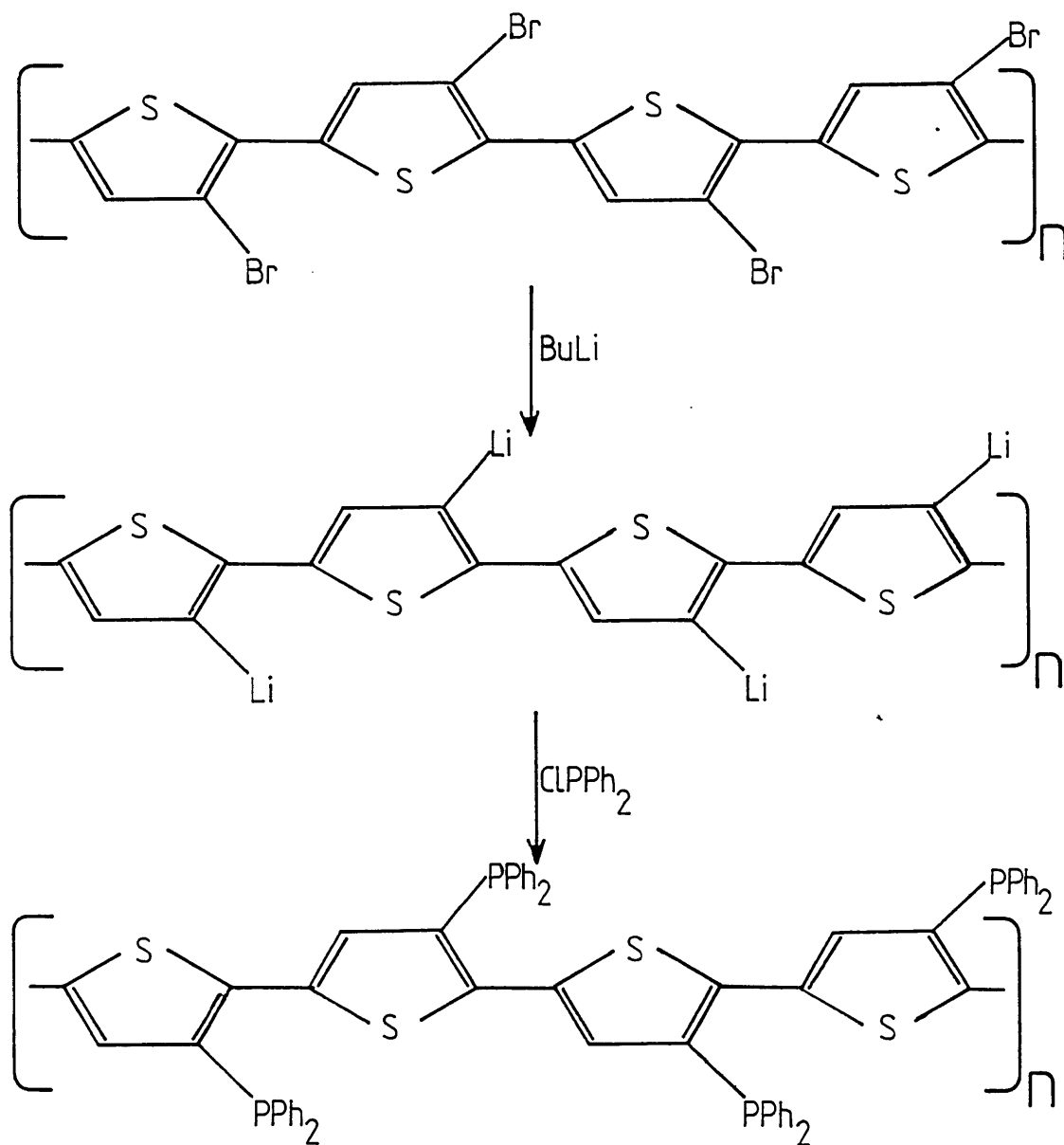
Figure 6.33. Phosphine substitution reaction attempted on a
poly-3-bromothiophene coated electrode.

oxidation potential of the poly-3-diphenylphosphinothiophene could be so high, due to electronic effects, that it is not attainable in this solvent and hence the coat does not become conducting.

There is the possibility that on forming the 3-diphenylphosphine substituted polymer, the polymer chain has to twist due to the steric effects of the large phosphine groups. This twisting would destroy the π-delocalisation along the polymer chain, thereby resulting in an insulating, rather than a conducting, polymer film.

Finally, there is also the possibility of some synthetic mis-adventure, during the substitution reaction, resulting in the polymer coat decomposing and hence becoming inactive.

Spectroscopic analysis of these coats (e.g. ESCA) would enable identification of which of these possibilities is correct. However, time was not available for this analysis to be undertaken.

If it was found that the 3-diphenylphosphine substituted polymer had been formed, steric effects could be minimised by using a less bulky phosphine (e.g. dimethylphosphine). Also, copolymers of thio-phene and 3-bromothiophene could have their bromines substituted with phosphines to give polymers as in figure 5.34a and poly-3-bromothio-phene could be only partially substituted to give a polymer as shown in figure 6.34b. These types of polymers may show lower oxidation potentials and hence become conducting. Finally, there is the possi-bility of reacting the poly(3-lithiothiophene) (formed by the reaction of poly(3-bromothiophene) with butyllithium) with phosphorus tri-chloride (PCl_3) to give a polyphosphinothiophene with each phosphorus attached to three thiophene units (i.e. a tri-3-thienylphosphine species). This would overcome the steric problem of phosphine groups but would highly cross-link the polymer. Also the formation of the poly(tri-3-thienylphosphine) species will depend on the relative

Figure 6.34.

(a)

A possible thiophene/3-diphenylphosphino-
thiophene copolymer.

(b)

A possible 3-bromothiophene/3-diphenylphosphino-
thiophene copolymer.
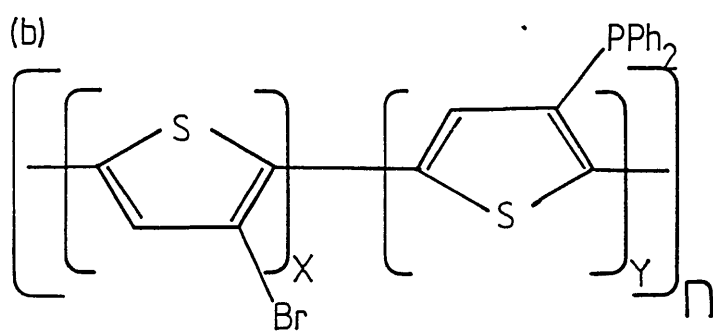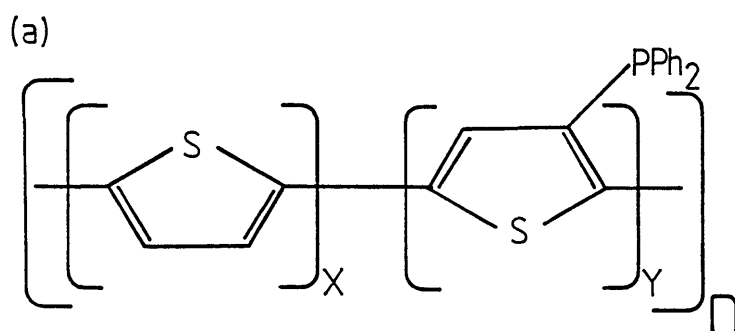
reactivities of the mono and di-substituted species with respect to PCl_3.

6.8. Overall Discussion

In this chapter the need for conducting polymers for transporting electrons to each metal site, independently, was introduced. The use of polypyrrole, polythiophene and polyfuran coated electrodes for electrochemical oxidations proved successful. Coats of reasonable thickness (< 500 nm) oxidised ferrocene and $Pd(PPh_3)_4$ by a mediated electron transfer mechanism which was rapid enough to make the transport of solution species to the electrode the rate (i.e. current)-limiting process.

This was encouraging for the development of a phosphine substituted conducting polymer modified electrode containing bound palladium species. One can predict that, in such a modified electrode, electrochemical oxidation of zerovalent palladium, in the coat, would be very rapid. Therefore, from an electrocatalytic point of view, one can envisage reactions of Pd(II) with solution species (e.g. the Wacker process) generating Pd(O) which would then be rapidly turned back, by the electrode/conducting polymer backbone, to Pd(II). As this regeneration would be rapid the rate of reaction would be limited by the actual reaction and not the regeneration of the catalyst.

It was found possible to synthesise several phosphine substituted monomers; 1-diphenylphosphinopyrrole, 3-diphenylphosphinothiophene and 3-diphenylphosphinofuran. A method for the synthesis of 3-diphenylphosphinopyrrole could not be developed.

Electrochemical investigation of these monomers proved disappointing as they would not electropolymerise to give the required phosphine substituted conducting polymers. An approach to avoid the

necessity of electropolymerising the phosphine substituted monomers was to electropolymerise a monomer which can then easily be modified to give the phosphine substituted polymer coat. This was tried with 3-bromothiophene and resulted in a coated electrode but the coat was insulating. As discussed earlier this could be due to several reasons which may be overcome by different approaches (see section 6.7).

The development of a modified electrode, containing the palladium (II/0) couple, for electrocatalysis, was an ambitious project which has not been achieved. However, several approaches, leading on from each other, have been investigated and with each a greater understanding of the processes occurring and that are necessary in such a system, has been achieved. The solution electrochemistry of palladium-phosphine complexes has been fairly well characterised. The necessity for conducting polymers was introduced and several were analysed and found suitable. It has been shown that 1-diphenylphosphinopyrrole and 3-diphenylphosphinothiophene palladium complexes show similar electrochemistry to the equivalent triphenylphosphine complexes. Due to the lack of success in electropolymerising 1-diphenylphosphinopyrrole and 3-diphenylphosphinothiophene it was found necessary to electropolymerise a precursor (e.g. 3-bromothiophene) and then perform a substitution reaction on the polymer coat.

From this work others may find a basis from which further investigations can stem. These could include continuing work on substituting conducting polymer precursors (e.g. 3-bromothiophene, see section 6.7) or moving into new areas to investigate other ligands, other conducting polymers/copolymers, and other methods of incorporating palladium complexes into conducting polymer coats (e.g. electrostatic rather than covalent binding).

6.9. Appendix: Synthesis

In these syntheses, unless otherwise stated, reagent grade chemicals were used without any further purification. Products were analysed by microanalysis, mass spectroscopy, infra-red spectroscopy and NMR (60 MHz, unless otherwise stated).

6.9.1. Diphenylvinylphosphine[195]

Vinyl Grignard reagent (0.2 moles; i.e. 200 cm^3 of a 1 M tetrahydrofuran solution available from Aldrich Chemicals) was placed in a flask under dried argon. Chlorodiphenylphosphine (0.12 moles, 26.5 g) in dry benzene (50 cm^3) was added dropwise with cooling and stirring. The addition took one hour and was regulated to maintain a gentle reflux. This reflux was continued for a further 22 hours after which, the reaction mixture was chilled and 10% aqueous ammonium chloride (100 cm^3) was added. The aqueous phase was extracted with ether (3 x 50 cm^3) and then by hot benzene (200 cm^3). The combined organic phases were dried over sodium sulphate, filtered and fractionally distilled. The diphenylvinylphosphine distilled over, as a colourless oil, at 100°C (0.2 mm Hg) and was stored under argon (yield = 12.5 g, 49%).

Microanalysis for $C_{14}H_{13}P$ Calcd.   C 79.24; H 6.17

Found   C 79.36; H 6.20

NMR (in $CDCl_3$) gave two overlapping sets of multiplets centred at ∂ = 7.2 ppm and 7.5 ppm due to the phenyl protons and another multiplet centred at ∂ = 6.1 ppm due to the vinyl protons.

6.9.2. Reaction of Diphenylvinylphosphine with TosMIC[193]

Sodium hydride (6 mmoles, 0.24 g of a 60% dispersion in mineral oil, Aldrich Chemicals) was placed in a flask under dried argon. To

remove the mineral oil, the solid was washed with petroleum ether (Bp. 30-40°C, 3 x 10 cm^3). Sodium dried ether (10 cm^3) was then added and the mixture stirred to give a suspension. To this suspension, a solution of tosylmethylisocyanide (TosMIC; 5 mmoles, 0.98 g) and diphenylvinylphosphine (5 mmoles, 1.06 g) in a mixture of sodium dried diethyl ether (16 cm^3) and dried/distilled dimethylsulphoxide (8 cm^3) was added dropwise. No refluxing of the ether was observed. The mixture was stirred for half an hour and then distilled water was added. The addition of water caused severe effervescence as the sodium hydride was neutralised. The water fraction was extracted with ether and dichloromethane and the organic phases were dried over sodium sulphate. However, isolation of products gave unreacted diphenylvinylphosphine and other decomposed starting materials.

The preparation was repeated with several variations. These included leaving the reaction mixture for 24 hours before quenching with water and refluxing the reaction mixture, after the addition of TosMIC/diphenylvinylphosphine mixture, for one hour to one day. Other reducing agents (e.g. t-BuOK in THF and K$_2$CO$_3$ in refluxing methanol[193]) were also tried. However, none of these variations gave the required pyrrole product.

6.9.3. Diphenylvinylphosphine Oxide[195]

Diphenylvinylphosphine (0.04 moles, 8.5 g) in dried benzene (40 cm^3) was treated dropwise with hydrogen peroxide (5.7 cm^3 of 30% solution). The addition took one hour, keeping the reaction mixture gently boiling. The mixture was refluxed for a further four hours and then allowed to cool. It was then poured onto water (20 cm^3) and the water fraction extracted with diethyl ether. The organic extracts were dried over magnesium sulphate, filtered and the solvent volume reduced. With this

evaporation of the solvent a white precipitate of diphenylvinylphosphine

oxide formed. This was filtered and the product was recrystallised from

benzene/petroleum ether (Bp. 40-60°C). The yield of product was 4.5 g

(50%).

Microanalysis for $C_{14}H_{13}PO$ Calcd.   C 73.68; H 5.74

Found   C 73.58; H 5.70

NMR (in $CDCl_3$) gave two overlapping multiplets at ∂ = 7.5 ppm

and 7.7 ppm, due to the phenyl protons, and another multiplet at

∂ = 6.4 ppm, due to the vinyl protons.

Infra-red showed P = O deformations in the 1150-1200 cm^{-1}

region.

This product was used in similar TosMIC reactions, as discussed

in section 6.9.2, but again no pyrrole type products were observed.

6.9.4. Attempted Acylation of Diphenylvinylphosphine

The methods for the acylation of alkenes[199,200], by the reaction

with acetic anhydride in the presence of a Lewis acid, were employed.

However, when tin (IV) chloride (gold label from Aldrich Chemicals,

0.01 moles, 2.5 g) was added dropwise, under dry argon, to diphenyl-

vinylphosphine (0.01 moles, 3.0 g) a violent reaction, resulting in

the polymerisation of diphenylvinylphosphine, occurred.

It was decided to try milder Lewis acids (e.g. $AlCl_3$ and $ZnCl_2$)

but polymerisation again resulted. Other variations were also tried.

These included using dilute solutions, lowering the temperature, adding

the Lewis acid and the acetic anhydride together as a mixture, and

adding the acetic anhydride first followed by the Lewis acid. However,

in all these cases the required methyl β-(diphenylphosphino)vinyl ketone

was not produced and the majority of reactions resulted in the polymerisation of the diphenylvinylphosphine.

6.9.5. Attempted Acylation of Diphenylvinylphosphine Oxide

Tin (IV) chloride (gold label; 1.7 mmoles, 0.44 g) was added dropwise to an ice cold, stirred dichloromethane (10 cm^3) solution of diphenylvinylphosphine oxide (2.5 mmoles, 0.57 g) and no polymerisation reaction was observed. Acetic anhydride (1.7 mmoles, 0.17 g) was then added dropwise. The mixture was stirred for two hours, at 0°C, and then allowed to warm to room temperature. The mixture was then poured onto ice and the aqueous phase extracted with dichloromethane. The organic extracts were dried over magnesium sulphate, filtered and the solvent evaporated under reduced pressure. The isolated product was unreacted diphenylvinylphosphine oxide.

This method was repeated with refluxing of the reaction mixture after the addition of acetic anhydride. However, again, unreacted starting material was isolated.

6.9.6. Alternative Attempted Preparation of Methyl β-(Diphenylphosphino) Vinyl Ketone

The scheme of this preparation was

$$CH_3COCl + CHCH \xrightarrow{(a)} CH_3COCHCHCl$$

$$Li + PPh_2Cl \xrightarrow{(b)} LiPPh_2$$

$$\xrightarrow{(c)} CH_3COCHCHPPh_2$$
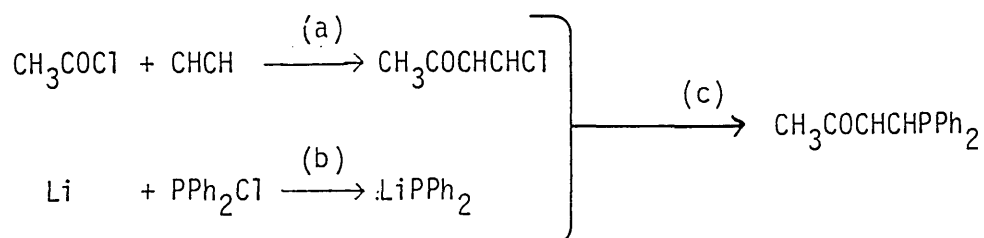
(a) <u>Preparation of Methyl β-Chlorovinyl Ketone</u>[205]

In a system sealed from moisture, acetyl chloride (0.60 moles, 47.6 g) was added dropwise to a well stirred ice cold suspension of $AlCl_3$ (0.66 moles, 88 g) in dried/distilled carbon tetrachloride (200 cm^3). Acetylene, dried by bubbling through concentrated sulphuric acid, was passed in a rapid stream through the well stirred suspension, which was maintained below 5°C, for 14 hours. The reaction mixture was poured onto ice/saturated salt solution and the aqueous layer was extracted with diethyl ether. The combined extracts were dried over magnesium sulphate and filtered. The solution was then distilled under reduced pressure to give the required product at 40°C (20 mm Hg) as a colourless oil. Methyl β-chlorovinyl ketone was stored in its frozen state (below 5°C) under argon. (Yield = 21g, 34%).

It should be stressed that due to the very lachrymatory and corrosive nature of methyl β-chlorovinyl ketone, it was only handled in a special toxic laboratory with the required precautions being taken.

Due to the product's hostile nature the only analysis done was NMR (in $CDCl_3$), which gave a singlet at ∂ = 2.3 ppm, due to the methyl protons, and multiplets, due to the vinyl protons, centred at ∂ = 6.7 ppm and 7.25 ppm, and refractive index n_D^{22} = 1.4657, which agrees well with the literature n_D^{20} = 1.4654[205].

(b) <u>Preparation of Lithium Diphenylphosphide</u>[206]

In a system under dry argon, freshly distilled chlorodiphenyl-phosphine (0.23 moles, 50 g) was added dropwise to a stirred, ice cooled, suspension of lithium wire (1 mole, 6.94 g) in dry/distilled tetrahydro-furan (200 cm^3). The mixture was allowed to warm to room temperature and was stirred for a further three hours. The solution turned deep

red indicating that the reaction had occurred. The mixture was kept under argon and aliquots were removed by syringe as required. The literature reports yields in excess of 98%[206].

(c) <u>Reaction of (a) + (b)</u>

Under dried argon, methyl β-chlorovinylketone (0.1 moles, 10 g) in tetrahydrofuran (50 cm^3) was added dropwise to lithium diphenyl-phosphide (100 cm^3 of the above solution). The mixture was stirred and disappearance of the dark red lithium phosphide colour was observed. Also, formation of a white precipitate (presumed to be lithium chloride) was noted. The reaction mixture was stirred for a further one hour, poured onto distilled water and extracted with diethyl ether. The organic extracts were dried over sodium sulphate, filtered and the solvent evaporated under reduced pressure. Dichloromethane was used, after diethyl ether, for further extraction of the water fraction. These extracts were also dried over sodium sulphate, filtered and the solvent evaporated under reduced pressure.

Analysis of the products showed that they were diphenylphosphine and diphenylphosphinic acid. Several attempts, varying temperatures and reaction times, always gave similar products.

6.9.7. 1-Diphenylphosphinopyrrole[208-210]

This was made by the reaction of potassium pyrrolide with chloro-diphenylphosphine

$$py + K \longrightarrow K^+(py^-) \xrightarrow{ClPPh_2} Ph_2P\text{-}1\text{-}py + KCl$$

(a)   (b)
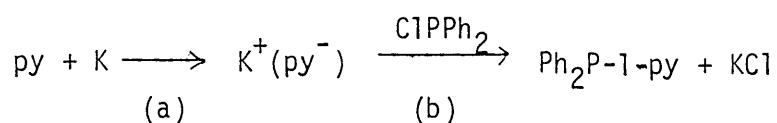
(where py = pyrrole)

(a) Potassium Pyrrolide[(207)]

In a system sealed from moisture, potassium (0.2 moles, 8 g) was shaken with boiling xylene (100 cm^3). The mixture was cooled and absolute alcohol (2 drops) was added. Freshly distilled pyrrole (0.2 moles, 13.4 g) was added in small amounts with reaction being allowed to cease after each addition. More pyrrole (0.08 moles, 5 g) was then added to dissolve any remaining potassium. The solution was heated, on a water bath, for one hour and then the xylene was removed, under reduced pressure. This gave potassium pyrrolide (Yield = 21 g, 100%) as a white, highly deliquescent powder which was used immediately.

(b) 1-Diphenylphosphinopyrrole[(208-210)]

The above potassium pyrrolide (0.2 moles, 21 g) was suspended in sodium dried ether (100 cm^3) and ice cooled, under dried argon. To this suspension chlorodiphenylphosphine (0.17 moles, 37 g), in sodium dried ether (50 cm^3), was added dropwise. The stirred mixture was allowed to warm to room temperature, overnight. The mixture was filtered and the ether removed under reduced pressure. The product was twice vacuum distilled to give a colourless oil ($123^{o}C$ at 1 mm Hg) which froze at approximately $17^{o}C$ (Yield = 25 g, 59%).

Anal. $C_{16}H_{14}NP$ Calcd. C 76.48; H 5.62; N 5.57

Found C 76.56; H 5.66; N 5.62

Mass spectroscopy gave the parent ion at 251.

NMR, in $CDCl_3$, gave two overlapping multiplets centred at ∂ = 7.3 ppm and 7.5 ppm due to the phenyl protons, a multiplet centred at ∂ = 6.8 ppm due to the pyrrole's α-protons and a multiplet centred at 6.3 ppm due to the pyrrole's β-protons.

(i) 1-Diphenylphosphinatopyrrole

This was prepared by the oxidation of the above 1-diphenyl-phosphinopyrrole. The method used was as discussed in section 6.9.3 and gave a white crystalline product (Yield = 3.5 g, 65%).

Anal. $C_{16}H_{14}NOP$ Calcd. C 71.90; H 5.24; N 5.24

Found C 71.99; H 5.27; N 5.20

I.R. showed increased activity in the 1150-1200 cm^{-1} region due to P = O vibrations.

(ii) Bis(1-diphenylphosphinopyrrole) Palladium Dichloride

A mixture of 1-diphenylphosphinopyrrole and bis(benzonitrile) palladium dichloride (see section 4.5.1), in benzene, was stirred for several hours to give an orange precipitate of the required product (Yield = 6.8 g, 95%).

Anal. $C_{32}H_{28}Cl_2N_2P_2Pd$ Calcd. C 56.53; H 4.15; N 4.12

Found C 56.81; H 4.20; N 4.07

6.9.8. 3-Diphenylphosphinothiophene

Butyllithium (0.16 moles, 100 cm^3 of 1.6 M hexane solution; Aldrich Chemicals) was transferred to a flask under dry argon. The temperature was reduced to -70°C and 3-bromothiophene (0.15 moles, 25 g), in tetrahydrofuran (25 cm^3), was added dropwise with stirring. After the addition was complete stirring was continued for a further 30 minutes, at -70°C. Then, chlorodiphenylphosphine (0.15 moles, 33.8 g) in tetrahydrofuran (40 cm^3) was added dropwise, maintaining the temperature at -70°C. After the addition, the mixture was stirred for a further one hour and then was allowed to warm to room temperature, overnight. The solution gradually turned brown and gave a white precipitate. The reaction mixture was poured onto distilled water and

extracted with diethyl ether. The combined extracts were dried over magnesium sulphate, filtered and the solvent removed under reduced pressure. The product was vacuum distilled to give the product (150°C at 0.5 mm Hg) as a colourless oil (Yield = 26 g, 65%).

Anal. $C_{16}H_{13}PS$ Calcd. C 71,62; H 4.88; S 11.95

Found C 71.59; H 4.89; S 11.90

Mass spectroscopy gave the parent ion at 268.

NMR (250 MHz), in $CDCl_3$, gave a multiplet centred at ∂ = 6.95 ppm due to the 4-thiophene proton, a multiplet at ∂ = 7.13 ppm due to the 2-thiophene proton and two sets of overlapping multiplets centred at ∂ = 7.22 ppm and 7.31 ppm due to the phenyl protons and also containing the 5-thiophene proton. The NMR proves that the phosphine group is in the thiophene 3-position[227,228].

(i)   3-Diphenylphosphinatothiophene

The 3-diphenylphosphinatothiophene was synthesised by the oxidation of the above 3-diphenylphosphinothiophene using the same method as described in section 6.9.3. The product was a white crystalline solid (Yield = 3.1 g, 55%).

Anal. $C_{16}H_{13}OPS$ Calcd. C 67.59; H 4.61; S 11.28

Found C 67.63; H 4.63; S 11.24

I.R. showed increased activity in the 1150-1200 cm^{-1} region due to P = O vibrations.

6.9.9.   3-Diphenylphosphinofuran

A similar preparation as described for 3-diphenylphosphinothiophene was performed, using 3-bromofuran (0.017 moles, 2.5 g). Vacuum distillation gave the product (130°C at 0.4 mm Hg) as a colourless oil (Yield = 2.5 g, 60%).

Anal. $C_{16}H_{13}OP$ Calcd. C 76.18; H 5.19

Found C 76.24; H 5.19

Mass spectroscopy gave the parent ion at 252.

NMR (250 MHz), in $CDCl_3$, gave a multiplet centred at ∂ = 6.29 ppm due to the 4-furan proton, and two sets of overlapping multiplets centred at ∂ = 7.25 ppm and 7.38 ppm due to the phenyl protons and also containing the 2- and 5-furan protons. This NMR proves the phosphine group is in the furan 3-position[228,229].

REFERENCES

1. R.F. Lane and A.T. Hubbard, *J. Phys. Chem.*, 1973, 77, 1401.

2. R.F. Lane and A.T. Hubbard, *J. Phys. Chem.*, 1973, 77, 1411.

3. P.R. Moses, L. Wier and R.W. Murray, *Anal. Chem.*, 1975, 47, 1882.

4. B.F. Watkins, J.R. Behling, E. Kariv and L.L. Miller, *J. Am. Chem. Soc.*, 1975, 97, 3549.

5. W.R. Heineman and P.T. Kissinger, *Anal. Chem.*, 1978, 50, 166R.

6. K.D. Snell and A.G. Keenan, *Chem. Soc. Rev.*, 1979, 8, 259.

7. R.W. Murray, *Acc. Chem. Res.*, 1980, 13, 135.

8. A.F. Diaz, *Midl. Macromol. Monogr.*, 1980, 7, 137.

9. W.J. Albery and A.R. Hillman, *Annu. Rep.C*, 1981, 78, 377.

10. R.W. Murray, *Electroanal. Chem.*, 1984, 13, 191.

11. P.R. Moses and R.W. Murray, *J. Electroanal. Chem.*, 1977, 77, 393.

12. D.C.S. Tse and T. Kuwana, *Anal. Chem.*, 1978, 50, 1315.

13. C.A. Koval and F.C. Anson, *Anal. Chem.*, 1978, 50, 223.

14. N. Oyama, A.P. Brown and F.C. Anson, *J. Electroanal. Chem.*, 1978, 87, 435.

15. M.F. Dautartas, J.F. Evans and T. Kuwana, *Anal. Chem.*, 1979, 51, 104.

16. C.M. Elliot and R.W. Murray, *Anal. Chem.*, 1976, 48, 1247.

17. N. Oyama and F.C. Anson, *J. Am. Chem. Soc.*, 1979, 101, 739.

18. A. Merz and A.J. Bard, *J. Am. Chem. Soc.*, 1978, 100, 3222.

19. P. Daum and R.W. Murray, *J. Phys. Chem.*, 1981, 85, 389.

20. J.B. Kerr, L.L. Miller and M.R. Van De Mark, *J. Am. Chem. Soc.*, 1980, 102, 3383.

21. A.H. Schroeder and F.B. Kaufman, *J. Electroanal. Chem.*, 1980, 113, 209.

22. A.P. Brown, C. Koval and F.C. Anson, *J. Electroanal. Chem.*, 1976, <u>72</u>, 379.

23. A. Bettelheim, R.J.H. Chan and T. Kuwana, *J. Electroanal. Chem.*, 1979, <u>99</u>, 391.

24. J. Zagal, R.K. Sen and E. Yeager, *J. Electroanal. Chem.*, 1977, <u>83</u>, 207.

25. J.P. Collman, M. Marrocco, P. Denisevich, C. Koval and F.A. Anson, *J. Electroanal. Chem.*, 1979, <u>101</u>, 117.

26. A.F. Diaz and J.A. Logan, *J. Electroanal. Chem.*, 1980, <u>111</u>, 111.

27. A.F. Diaz and J.A. Logan, *J. Electroanal. Chem.*, 1980, <u>108</u>, 377.

28. R.J. Waltman, J. Bargon and A.F. Diaz, *J. Phys. Chem.*, 1983, <u>87</u>, 1459.

29. G. Tourillon and F. Garnier, *J. Electroanal. Chem.*, 1982, <u>135</u>, 173.

30. R. Nowak, F.A. Schultz, M. Umana, H. Abruna and R.W. Murray, *J. Electroanal. Chem.*, 1978, <u>94</u>, 219.

31. J. Facci and R.W. Murray, *Anal. Chem.*, 1982, <u>54</u>, 772.

32. P.J. Peerce and A.J. Bard, *J. Electroanal. Chem.*, 1980, <u>114</u>, 89.

33. A.P. Brown and F.C. Anson, *Anal. Chem.*, 1977, <u>49</u>, 1589.

34. A.F. Diaz and K.K. Kanazawa, *J. Electroanal. Chem.*, 1978, <u>86</u>, 441.

35. P.J. Peerce and A.J. Bard, *J. Electroanal. Chem.*, 1980, <u>112</u>, 97.

36. A. Akahoshi, S. Toshima and K. Itaya, *J. Phys. Chem.*, 1981, <u>85</u>, 818.

37. W.J. Albery, M.G. Boutelle, P.J. Colby and A.R. Hillman, *J. Electroanal. Chem.*, 1982, <u>133</u>, 135.

38. G. Tourillon, J.-E. Dubois and P.-C. Lacaze, *J. Chim. Phys. Phys.-Chim. Biol.*, 1979, <u>76</u>, 369.

39. P.-C. Lacaze and G. Tourillon, *J. Chim, Phys. Phys.-Chim. Biol.*,
    1976, 76, 371.

40. A. Volkov, G. Tourillon, P.-C. Lacaze and J.-E. Dubois,
    J. Electroanal. Chem., 1980, 115, 279.

41. J.-E. Dubois, P.-C. Lacaze and M.-C. Pham, *J. Electroanal. Chem.*,
    1981, 117, 233.

42. C.A. Melendres and F.A. Cafasso, *J. Electrochem. Soc.*, 1981, 129,
    755.

43. V.S. Srinivasen and W.J. Lamb, *Anal. Chem.*, 1977, 49, 1639.

44. M.F. Dautartas and J.F. Evans, *J. Electroanal. Chem.*, 1980, 109,
    301.

45. H.D. Abruna, T.J. Meyer and R.W. Murray, *Inorg. Chem.*, 1979, 18,
    3233.

46. J.A. Bruce and M.S. Wrighton, *J. Electroanal. Chem.*, 1981, 122,
    93.

47. M.S. Wrighton, *Acc. Chem. Res.*, 1979, 12, 303.

48. A.B. Bocarsly, E.G. Walton and M.S. Wrighton, *J. Am. Chem. Soc.*,
    1980, 102, 3390.

49. G. Horowitz, G. Tourillon and F. Garnier, *J. Electrochem. Soc.*,
    1984, 131, 151.

50. W.J. Albery, A.W. Foulds, K.J. Hall and A.R. Hillman, *J. Electrochem.
    Soc.*, 1980, 127, 654.

51. W.J. Albery, W.R. Bowen, F.S. Fisher, A.W. Foulds, K.J. Hall,
    A.R. Hillman, R.G. Egdell and A.F. Orchard, *J. Electroanal. Chem.*,
    1980, 107, 37.

52. M. Fujihira, A. Jamura and T. Osa, *Chem. Lett.*, 1977, 361.

53. S. Abe and T. Nonaka, *Chem. Lett.*, 1983, 1541.

54. R.A. Kamin and G.S. Wilson, *Anal. Chem.*, 1980, 52, 1198.

55. R.M. Ianniello and A.M. Yacynych, *Anal. Chem.*, 1981, 53, 2090.

56. N.K. Cenas, A.K. Pocius and J.J. Kulys, *J. Electroanal. Chem.*, 1984, 161, 103.

57. D.C. Bookbinder and M.S. Wrighton, *J. Electrochem. Soc.*, 1983, 130, 1080.

58. A. Desbene-Monvernay, P.-C. Lacaze, J.E. Dubois and P.L. Desbene, *J. Electroanal. Chem.*, 1983, 152, 87.

59. H.D. Abruna, P. Denisevich, M. Umana, T.J. Meyer and R.W. Murray, *J. Am. Chem. Soc.*, 1981, 103, 1.

60. P.G. Pickup, C.R. Leidner, P. Denisevich and R.W. Murray, *J. Electroanal. Chem.*, 1984, 164, 39.

61. C.R. Leidner, P. Denisevich, K.W. Willman and R.W. Murray, *J. Electroanal. Chem.*, 1984, 164, 63.

62. R.W. Murray, *Phil. Trans. R. Soc. Lond.*, 1981, A302, 253.

63. J. Zak and T. Kuwana, *J. Electroanal. Chem.*, 1983, 150, 645.

64. A. Bettelheim, R.J.H. Chan and T. Kuwana, *J. Electroanal. Chem.*, 1980, 110, 93.

65. A. Bettelheim, R. Parash and D. Ozer, *J. Electrochem. Soc.*, 1982, 129, 2247.

66. H. Behret, H. Binder, G. Sandstede and G.G. Scherer, *J. Electroanal. Chem.*, 1981, 117, 29.

67. C. Paliteiro, A. Hamnet and J.B. Goodenough, *J. Electroanal. Chem.*, 1984, 160, 359.

68. G.S. Calabrese, R.M. Buchanan and M.S. Wrighton, *J. Am. Chem. Soc.*, 1983, 105, 5594.

69. N. Oyama, N. Oki, H. Ohno, Y. Ohnuki, M. Matsuda and E. Tsuchida, *J. Phys. Chem.*, 1983, 87, 3642.

70. P. Martigny and F.C. Anson, *J. Electroanal. Chem.*, 1982, 139, 383.

71. J.P. Collman, P. Denisevich, T. Konai, M. Marrocco, C. Koval and F.C. Anson, *J. Am. Chem. Soc.*, 1980, 102, 6027.

72. R.R. Durand Jr., J.P. Collman and F.C. Anson, *J. Electroanal. Chem.*, 1983, 151, 289.

73. C. Ueda, D.C.S. Tse and T. Kuwana, *Anal. Chem.*, 1982, 54, 850.

74. A. Torstensson and L. Gorton, *J. Electroanal. Chem.*, 1981, 130, 199.

75. R.D. Rocklin and R.W. Murray, *J. Phys. Chem.*, 1981, 85, 2104.

76. C.M. Elliot and C.A. Marrese, *J. Electroanal. Chem.*, 1981, 119, 395.

77. G.J. Samuels and T.J. Meyer, *J. Am. Chem. Soc.*, 1981, 103, 307.

78. M. Fujihira, S. Tasaki, T. Osa and T. Kuwana, *J. Electroanal. Chem.*, 1983, 150, 665.

79. C.P. Andrieux, J.M. Dumas-Bouchiat and J.M. Savéant, *J. Electroanal. Chem.*, 1982, 131, 1.

80. J.B. Davison, P.J. Peerce-Landers and R.J. Jasinski, *J. Electrochem. Soc.*, 1983, 130, 1862.

81. P.M. Maitlis, *'The Organic Chemistry of Palladium'*, Vol. II, *'Catalytic Reactions'*, Academic Press, 1971.

82. B.M. Trost, *Tetrahedron*, 1977, 33, 2615.

83. T.H. Black, *Aldrichimica Acta*, 1982, 15, 13.

84. J.K. Stille and R. Divakaruni, *J. Organometal. Chem.*, 1979, 169, 239.

85. J.E. Bäckvall, B. Åkermark and S.O. Ljunggren, *J. Am. Chem. Soc.*, 1979, 101, 2411.

86. A. Aguilö, *Advan. Organometal. Chem.*, 1967, 5, 321.

87. E.W. Stern and M.L. Spector, *Proc. Chem. Soc. (London)*, 1961, 370.

88. G.W. Godin and J.W. Williamson, *Brit. Pat.* 928 739, 1963; *Chem. Abst.*, 1963, <u>59</u>, 12647e.

89. Union Oil of California, *Brit. Pat.* 1032 325, 1966; *Chem. Abst.*, 1966, <u>65</u>, 5372h.

90. H.A. Tayim, *Chem. Ind. (London)*, 1970, 1468.

91. C.W. Capp, G.W. Godin, R.F. Neale, J.B. Williamson and B.W. Harris, *Brit. Pat.* 918 062, 1963; *Chem. Abst.*, 1963, <u>59</u>, 5021g.

92. R.F. Heck, *J. Am. Chem. Soc.*, 1968, <u>90</u>, 5531.

93. R.F. Heck, *J. Am. Chem. Soc.*, 1968, <u>90</u>, 5538.

94. P.W. Jolly, '*Comprehensive Organometallic Chemistry*', Vol. 8, Chapt. 56, Pergamon Press, 1982.

95. S. Takahashi, Y. Suzuki and N. Hagihara, *Chem. Lett.*, 1974, 1363.

96. B. Hipler and B. Uhling, *J. Organometal. Chem.*, 1980, <u>199</u>, C27.

97. A.S. Kende, L.S. Liebeskind and D.M. Braitsch, *Tetrahedron Letts.*, 1975, 3375.

98. B.C. Gates, *Nato Adv. Study Inst. Ser. Ser. E*, 1980, <u>39</u>, 437.

99. C.U. Pittman Jr., '*Comprehensive Organometallic Chemistry*', Vol. 8, Chapt. 55, Pergamon Press, 1982.

100. H. Arai and M. Yashiro, *J. Mol. Catal.*, 1977-78, <u>3</u>, 427.

101. W.J. Albery and C.C. Jones, *Faraday Trans.*, to be published.

102. G. Inzelt, J.Q. Chambers and F.B. Kaufman, *J. Electroanal. Chem.*, 1983, <u>159</u>, 443.

103. J.A. Bruce and M.S. Wrighton, *J. Am. Chem. Soc.*, 1982, <u>104</u>, 74.

104. V.G. Levich, '*Physicochemical Hydrodynamics*', Prentice Hall, 1962.

105. J. Koutecky and V.G. Levich, *Zh. Fiz. Khim.*, 1956, <u>32</u>, 1565.

106. A.N. Frumkin and L.I. Nekrasov, *Dokl. Akad. Nauk. SSSR*, 1959, <u>126</u>, 115.

107. W.J. Albery and M.L. Hitchman, '*Ring Disc Electrodes*', Oxford University Press, 1971.

108. W.J. Albery, *Trans. Faraday Soc.*, 1966, 62, 1915.

109. W.J. Albery and S. Bruckenstein, *Trans. Faraday Soc.*, 1966, 62, 1920.

110. F. Decker and B.A. Parkinson, *J. Electrochem. Soc.*, 1980, 127, 2370.

111. W.J. Albery and P.N. Bartlett, *J. Electrochem. Soc.*, 1982, 129, 2254.

112. W.J. Albery, P.N. Bartlett, W.R. Bowen, F.S. Fisher and A.W. Foulds, *J. Electroanal. Chem.*, 1980, 107, 23.

113. W.J. Albery, P.N. Bartlett, A.W. Foulds, F.A. Souto-Bachiller and R. Whiteside, *J. Chem. Soc. Perkin II*, 1981, 794.

114. Y. Matsumato, H. Yoneyama and H. Tamura, *Bull. Chem. Soc. Jpn.*, 1978, 51, 1927.

115. W.J. Albery, E. Calvo-Sotelo and M. Lyons, to be published.

116. T. Ikeda, C.R. Leidner and R.W. Murray, *J. Am. Chem. Soc.*, 1981, 103, 7422.

117. R.S. Nicholson and I. Shain, *Anal. Chem.*, 1964, 36, 706.

118. R.S. Nicholson and I. Shain, *Anal. Chem.*, 1965, 37, 178.

119. E. Laviron, *J. Electroanal. Chem.*, 1979, 100, 263.

120. E. Laviron, *J. Electroanal. Chem.*, 1981, 122, 37.

121. F.C. Anson, *J. Phys. Chem.*, 1980, 84, 3336.

122. C.P. Andrieux, J.M. Dumas-Bouchiat and J.M. Savéant, *J. Electroanal. Chem.*, 1980, 114, 159.

123. N. Oyama and F.C. Anson, *Anal. Chem.*, 1980, 52, 1192.

124. D.M. Oglesby, S.H. Omang and C.N. Reilley, *Anal. Chem.*, 1965, 37, 1312.

125. P. Daum, J.R. Lenhard, D. Rolison and R.W. Murray, *J. Am. Chem. Soc.*, 1980, 102, 4649.

126. J. Facci and R.W. Murray, *J. Electroanal. Chem.*, 1981, <u>124</u>, 339.

127. A.H. Schroeder, F.B. Kaufman, V. Patel and E.M. Engler, *J. Electroanal. Chem.*, 1980, <u>113</u>, 193.

128. R.W. Murray, *Electrochemical Society, 161st Meeting,* Montreal, 1982.

129. R.C. Engstrom, *Anal. Chem.*, 1982, <u>54</u>, 2310.

130. R. Jasinski, G. Brilmyer and L. Helland, *J. Electrochem. Soc.* 1983, <u>130</u> 1634.

131. R.C. Engstrom, and V.A. Strasser, *Anal. Chem.*, 1984, <u>56</u>, 136.

132. D.T. Sawyer and J.L. Roberts, '*Experimental Electrochemistry for Chemists*', Wiley-Interscience, 1974.

133. A.R. Hillman, D. Phil. Thesis, Oxford, 1979.

134. P.J. Colby, Ph.D. Thesis, London, 1983.

135. D.R. Burfield, K.H. Lee and R.H. Smithers, *J. Org. Chem.*, 1977, <u>42</u>, 3060.

136. M. Walter and L. Ramaley, *Anal. Chem.*, 1973, <u>45</u>, 165.

137. C.K. Mann, *J. Electroanal. Chem.*, 1969, <u>4</u>, 57.

138. D.R. Burfield and R.H. Smithers, *J. Org. Chem.*, <u>43</u>, 1978, 3966.

139. G. Schiavon, S. Zecchin, G. Cogoni and G. Bontempelli, *J. Electroanal. Chem.*, 1973, <u>48</u>, 425.

140. A.J. Bard, '*Encyclopedia of Electrochemistry of the Elements*', Dekker, New York, 1976, <u>6</u>, 254.

141. K.K. Gazizov, D.M. Yukhnovich, G.K. Budnikov, V.K. Polovnyak and N.S. Akhmetov, *Russian J. Inorg. Chem.*, 1982, <u>27</u>, 1623.

142. K.K. Gazizov, D.M. Yukhnovich, G.K. Budnikov, V.K. Polovnyak and N.S. Akhmetov, *Russian J. Inorg. Chem.*, 1982, <u>27</u>, 1690.

143. C.A. Tolman, W.C. Seidel and D.H. Gerlach, *J. Am. Chem. Soc.*, 1972, <u>94</u>, 2669.

144. R. Ugo, *Coordin. Chem. Rev.*, 1968, <u>3</u>, 319.

145. F. Cariati, R. Ugo and F. Bonati, *Inorg. Chem.*, 1966, <u>5</u>, 1128.

146. W.J. Louw, D.J.A. de Waal and G.J. Kruger, *J. Chem. Soc. Dalton*, 1976, 2364.

147. D.A. Redfield and J.H. Nelson, *Inorg. Chem.*, 1973, <u>12</u>, 15.

148. D.R. Eaton, *J. Am. Chem. Soc.*, 1968, <u>90</u>, 4272.

149. G.K. Anderson and R.J. Cross, *Chem. Soc. Rev.*, 1980, <u>9</u>, 185.

150. D.G. Cooper and J. Powell, *J. Am. Chem. Soc.*, 1973, <u>95</u>, 1102.

151. D.G. Cooper and J. Powell, *Canad. J. Chem.*, 1973, <u>51</u>, 1634.

152. W.J. Louw, *Inorg. Chem.*, 1977, <u>16</u>, 2147.

153. A.J. Bard, '*Encyclopedia of Electrochemistry of the Elements*', Dekker, New York, 1975, <u>3</u>, 212.

154. M. Troupel, Y. Rollin, C. Chevrot, F. Pfluger and J.-F. Fauvarque, *J. Chem. Research* (S), 1979, 50.

155. M. Troupel, Y. Rollin, S. Sibille, J.-F. Fauvarque and J. Perichon, *J. Chem. Research* (S), 1980, 24.

156. S. Sibille, M. Troupel, J.-F. Fauvarque and J. Perichon, *J. Chem. Research* (S), 1980, 147.

157. M. Troupel, Y. Rollin, S. Stibille, J.-F. Fauvarque and J. Perichon, *J. Chem. Research* (S), 1980, 26.

158. G. Bontempelli, F. Magno, G. Schiavon and B. Corain, *Inorg. Chem.*, 1981, <u>20</u>, 2579.

159. J.R. Doyle, P.E. Slade and H.B. Jonassen, *Inorg. Synth.*, 1960, <u>6</u>, 218.

160. G. Booth, *Advan. Inorg. Chem. Radiochem.*, 1964, <u>6</u>, 1.

161. D.R. Coulson, *Inorg. Synth.*, 1972, <u>13</u>, 121.

162. B.J. Hathaway and D.G. Holah, *J. Chem. Soc.*, 1964, 2400.

163. L. Venanzi, *J. Chem. Soc.*, 1958, 719.

290

164. J.J. Levison and S.D. Robinson, *J. Chem. Soc. A*, 1970, 96.

165. L. Malatesta, *J, Chem. Soc.*, 1955, 3924.

166. L. Malatesta and S. Cenini, '*Zerovalent Compounds of Metals*', Academic Press, 1974.

167. P.M. Maitlis, P. Espinet and M.J.H. Russell, '*Comprehensive Organometallic Chemistry*', Vol. 6, Chapt. 38, Pergamon Press, 1982.

168. P.W. Jolly, '*Comprehensive Organometallic Chemistry*', Vol. 6, Chapt 37, Pergamon Press, 1982.

169. C.U. Pittman Jr. and Q. Ng, *J. Organometal. Chem.*, 1978, 153, 85.

170. C.U. Pittman Jr. and L.R. Smith, *J. Am. Chem. Soc.*, 1975, 97, 341.

171. H.S. Bruner and J.C. Bailar, *Inorg. Chem.*, 1973, 12, 1465.

172. L. Eberson and L. Jonsson, *Acta, Chem. Scand. B*, 1976, 30, 579.

173. K. Itaya and A.J. Bard, *Anal. Chem.*, 1978, 100, 1487.

174. I. Ugi, *Angew. Chem. Int. Ed. Engl.*, 1962, 1, 8.

175. D.E. Weisshaar and T. Kuwana, *J. Electroanal. Chem.*, 1984, 163, 395.

176. W.-H. Kao and T. Kuwana, *J. Am. Chem. Soc.*, 1984, 106, 473.

177. R. Arshady and B.S.R. Reddy, private communication.

178. R. Arshady and I. Ugi, *Angew. Chem. Int. Ed. Engl.*, 1982, 21, 374.

179. B.S.R. Reddy, R. Arshady and M.H. George, *Macromolecules*, 1983, 16, 1813.

180. B.S.R. Reddy, R. Arshady and M.H. George, *Polymer*, 1984, 25, 716.

181. W. Drenth and R.J.M. Nolte, *Acc. Chem. Res.*, 1979, 12, 30.

182. K. Kaneto, M. Maxfield, D.P. Nairns, A.G. MacDiarmid and H.J. Heeger, *J. Chem. Soc. Faraday Trans. I*, 1982, 78, 3417.

183. D.G.H. Ballard, A. Courtis, I.M. Shirley and S.C. Taylor,
     J. Chem. Soc. Chem. Commun., 1983, 954.

184. D.M. Ivory, G.G. Miller, J.M. Sowa, L.W. Shacklette, R.R. Chance
     and R.H. Baughman, *J. Chem. Phys.*, 1979, 71, 1506.

185. A.F. Diaz and K.K. Kanazawa, *J. Chem. Soc. Chem. Commun.*, 1979,
     635.

186. F. Garnier, G. Tourillon, M. Gazard and J.C. Dubois, *J. Electro-
     anal. Chem.*, 1983, 148, 299.

187. A.F. Diaz and J. I. Castillo, *J. Chem. Soc. Chem. Commun.*, 1980,
     397.

188. A.F. Diaz, J.I. Castillo, J.A. Logan and W.-Y. Lee, *J. Electro-
     anal. Chem.*, 1981, 129, 115.

189. E.M. Genies, G. Bidan and A.F. Diaz, *J. Electroanal. Chem.*,
     1983, 149, 101.

190. R.N. O'Brien and K.S.V. Santhanam, *J. Electrochem. Soc.*, 1983,
     130, 1114.

191. J. Mulligan, '*Third Year Research Project Report*', Imperial
     College of Science and Technology, Chem. Dept., 1984.

192. R.J. Motekaitis, D.H. Heinert and A.E. Martell, *J. Org. Chem.*,
     1970, 35, 2504.

193. A.M. Van Leusen, H. Siderius, B.E. Hoogenboom and D. Van Leusen,
     Tetrahedron Letts., 1972, 52, 5337.

194. D.J. Peterson, *J. Org. Chem.*, 1966, 31, 950.

195. K.D. Berlin and G.B. Butler, *J. Org. Chem.*, 1961, 26, 2537.

196. K. Naumann, G. Zon and K. Mislow, *J. Am. Chem. Soc.*, 1969, 91,
     7012.

197. Y. Segall, I. Granoth and A. Kalir, *J. Chem. Soc. Chem. Commun.*,
     1974, 501.

198.   K.L. Marsi, *J. Org. Chem.*, 1974, <u>39</u>, 265.

199.   C.D. Nenitzescu and A.T. Balaban, '*Friedel Crafts and Related Reactions*', Vol. 3, Pt. 2, Wiley-Interscience, 1964, 1033.

200.   E.E. Royals and C.M. Hendry, *J. Org. Chem.*, 1950, <u>15</u>, 1147.

201.   A.M. Aguiar and T. Archibald, *Tetrahedron Letts.*, 1966, <u>45</u>, 5541.

202.   A.M. Aguiar and D. Daigle, *J. Org. Chem.*, 1965, <u>30</u>, 2826.

203.   A.M. Aguiar and D. Daigle, *J. Am. Chem. Soc.*, 1964, <u>86</u>, 2299.

204.   D. Dabrowski and J. Terpiñski, *J. Org. Chem.*, 1966, <u>31</u>, 2159.

205.   C.C. Price and J.A. Pappalardo, *J. Am. Chem. Soc.*, 1950, <u>72</u>, 2613.

206.   E. Vedejs and P.L. Fuchs, *J. Am. Chem. Soc.*, 1973, <u>95</u>, 822.

207.   G.R. Clemo and G.R. Ramage, *J. Chem. Soc.*, 1931, 49.

208.   S. Fischer, L.K. Peterson and J.F. Nixon, *Canad. J. Chem.*, 1974, <u>52</u>, 3981.

209.   S. Fischer, J.K. Hoyano, I.W. Johnson and L.K. Peterson, *Can. J. Chem.*, 1976, <u>54</u>, 2706.

210.   L.K. Peterson, I.W. Johnson, J.K. Hoyano, S. Au-Yeung and B. Gour, *J. Inorg. Nucl. Chem.*, 1981, <u>43</u>, 935.

211.   W.J. Albery, '*Electrode Kinetics*', Clarendon Press, Oxford, 1975.

212.   P.G. Pickup, K.N. Kuo and R.W. Murray, *J. Electrochem. Soc.*, 1983, <u>130</u>, 2205.

213.   M. Fleischmann and J.N. Hiddleston, *J. Sci. Instrum.* 2, 1968, <u>1</u>, 667.

214.   K.P. Parsons, private communication.

215.   A.F. Diaz, A. Martinez, K.K. Kanazawa and M. Salmón, *J. Electroanal. Chem.*, 1981, <u>130</u>, 181.

216.   A.F. Diaz, J. Castillo, K.K. Kanazawa, J.A. Logan, M. Salmón and O. Fajardo, *J. Electroanal. Chem.*, 1982, <u>133</u>, 233.

217. M. Salmón, M.E. Carbajal, M. Aguilar, M. Saloma and J.C. Juárez, *J. Chem. Soc. Chem. Commun.*, 1983, 1532.

218. M. Salmón, M. Aguilar and M, Saloma, *J. Chem. Soc. Chem. Commun.*, 1983, 570.

219. G. Tourillon and F. Garnier, *J. Electrochem. Soc.*, 1983, 130, 2043.

220. K. Kaneto, K. Yoshino and Y. Inuishi, *Jpn. J. Appl. Phys.*, 1982, 21, L567.

221. R.J. Waltman, J. Bargon and A.F. Diaz, *J. Phys. Chem.*, 1983, 87, 1459.

222. G. Tourillon and F. Garnier, *J. Electroanal. Chem.*, 1984, 161, 51.

223. R.J. Waltman, A.F. Diaz and J. Bargon, *J. Electrochem. Soc.*, 1984, 131, 740.

224. S. Gronowictz and T. Raznikiewicz, *Org. Synth.*, Coll. Vol. 5, 149.

225. D.W. Slocum and D.L. Gierer, *J. Org. Chem.*, 1976, 41, 3668.

226. R. Sornay, J.M. Meunier and P. Fournari, *Bull. Soc. Chim. Fr.*, 1971, 990,

227. J.-P. Lampin and F. Mathey, *J. Organometal. Chem.*, 1974, 71, 239.

228. H.J. Jakobsen and J.A. Nielsen, *J. Mol. Spectry.*, 1970, 33, 474.

229. H.J. Jakobsen, *J. Mol. Spectry.*, 1971, 38, 243.

230. W.J. Albery and A.R. Hillman, *J. Electroanal. Chem.*, 1984, 170, 27.

231. L. Cattalini and M. Martelli, *J. Am. Chem. Soc.*, 1969, 91, 312.

232. D.G. Cooper and J. Powell, *Can. J. Chem.*, 1973, 51, 1634.

233. F. Basolo and R.G. Pearson, 'Mechanisms of Inorganic Reactions', 2nd Ed., Wiley, New York, 1967.

234. C.H. Langford and H.B. Gray, 'Ligand Substitution Processes', W.A. Benjamin, New York, 1966.

* * * * * *